



**This electronic thesis or dissertation has been
downloaded from Explore Bristol Research,
<http://research-information.bristol.ac.uk>**

Author:

Lee, Winnie W Y

Title:

Optimising antimicrobial therapy through local genomic surveillance of resistance patterns among bacteria from bloodstream and urinary tract infections

General rights

Access to the thesis is subject to the Creative Commons Attribution - NonCommercial-No Derivatives 4.0 International Public License. A copy of this may be found at <https://creativecommons.org/licenses/by-nc-nd/4.0/legalcode> This license sets out your rights and the restrictions that apply to your access to the thesis so it is important you read this before proceeding.

Take down policy

Some pages of this thesis may have been removed for copyright restrictions prior to having it been deposited in Explore Bristol Research. However, if you have discovered material within the thesis that you consider to be unlawful e.g. breaches of copyright (either yours or that of a third party) or any other law, including but not limited to those relating to patent, trademark, confidentiality, data protection, obscenity, defamation, libel, then please contact collections-metadata@bristol.ac.uk and include the following information in your message:

- Your contact details
- Bibliographic details for the item, including a URL
- An outline nature of the complaint

Your claim will be investigated and, where appropriate, the item in question will be removed from public view as soon as possible.



**This electronic thesis or dissertation has been
downloaded from Explore Bristol Research,
<http://research-information.bristol.ac.uk>**

Author:

Lee, Winnie W Y

Title:

Optimising antimicrobial therapy through local genomic surveillance of resistance patterns among bacteria from bloodstream and urinary tract infections

General rights

Access to the thesis is subject to the Creative Commons Attribution - NonCommercial-No Derivatives 4.0 International Public License. A copy of this may be found at <https://creativecommons.org/licenses/by-nc-nd/4.0/legalcode> This license sets out your rights and the restrictions that apply to your access to the thesis so it is important you read this before proceeding.

Take down policy

Some pages of this thesis may have been removed for copyright restrictions prior to having it been deposited in Explore Bristol Research. However, if you have discovered material within the thesis that you consider to be unlawful e.g. breaches of copyright (either yours or that of a third party) or any other law, including but not limited to those relating to patent, trademark, confidentiality, data protection, obscenity, defamation, libel, then please contact collections-metadata@bristol.ac.uk and include the following information in your message:

- Your contact details
- Bibliographic details for the item, including a URL
- An outline nature of the complaint

Your claim will be investigated and, where appropriate, the item in question will be removed from public view as soon as possible.

Optimising antimicrobial therapy through local genomic surveillance of resistance patterns among bacteria from bloodstream and urinary tract infections

Winnie Wing Yee Lee

A dissertation submitted to the University of Bristol in
accordance with the requirements for award of the degree of
Doctor of Philosophy in the Faculty of Life Sciences School of
Cellular and Molecular Medicine

October 2023

Word count: 37,206

Abstract

Bloodstream infections (BSIs) and urinary tract infections (UTIs), predominantly caused by *Escherichia coli* and *Klebsiella* spp., are an increasing clinical challenge. Rapid empiric antimicrobial therapy is vital to prevent UTIs from progressing to BSIs and BSIs progressing to sepsis. This study aims to improve empiric antimicrobial prescribing, which in the UK is currently based on historic phenotypic data collected at regional level.

This study investigates the diversity and molecular epidemiology of deduplicated, sequential *E. coli* from BSIs (n=669) and UTIs (n=199), as well as *Klebsiella* spp. from BSIs (n=210), isolated at a regional diagnostic laboratory serving a population of 1.5 million people including Bristol, Bath, North Somerset and South Gloucestershire. All isolates were subjected to whole genome sequencing (WGS) and data were interrogated for antimicrobial resistance (AMR) determinants and phylogenetic relationships. Genotypic data were compared with phenotypic antimicrobial susceptibility data provided by the diagnostic laboratory, and the concordance with predictions from commonly used methods for AMR prediction based on WGS was evaluated.

There was a significant rise in *E. coli* BSIs in the summer of 2020, however this was not due to any particular source of infection or *E. coli* sequence type (ST). It was found that *E. coli* ST131 BSIs were significantly biased towards a urinary tract source of infection, and that carriage of TEM genes by BSI *E. coli* was more common if the infection came from a urinary source. Phylogenetic analysis showed resistance mechanisms were dispersed and intermixed among isolates from different phylogroups. Comparison between BSI 2018 and 2020 show significant increases in TEM, OXA and *ampC* genes. Significant increases were observed with genes associated with resistance to fluoroquinolones in UTIs between 2018 and 2020. Analysis of highly resistant ST15 *K. pneumoniae* containing *bla*_{NDM-1} indicated transmission in the same hospital ward. *K. pneumoniae* BSI isolates from two different patients showed 100% identity for AMR and virulence regions on plasmids having IncFIB, IncR and Col440 replicons. Concordance for genomic AMR prediction varied across bioinformatics tools for both *E. coli* and *Klebsiella* spp. Lowest critical errors were detected across all bioinformatics tools for cefotaxime. No critical errors were observed with Kleborate for ciprofloxacin.

In silico detection and characterisation of AMR via WGS to inform empiric therapy is still in its infancy and requires further optimisation before utilisation alone in clinical settings. However, characterisation of infection source, AMR and virulence genes in BSIs and UTIs will be important factors in optimising empiric therapy.

Acknowledgements

I would like to express my heartfelt thank you to my supervisor, Professor Matthew Avison, who has been exceptionally patient and understanding throughout my PhD studies. I have learnt so much and developed new ways of thinking which I will take forwards in my career. Your advice and guidance has been absolutely invaluable. Thank you for passing on your wisdom and for your time in helping me improve academically as well as personally; I am forever grateful. Moreover, there are no words that can describe how thankful I am for the opportunity to do a PhD with you; I really appreciate it. Many thanks for absolutely everything and for your promised smile (finally!) upon the completion of this PhD!

Many thanks to Dr Philip Williams for the UTI and BSI isolates and his support. Furthermore, thank you so much to the Medical Research Foundation for funding this PhD and giving me the opportunity to undertake a 3-month placement at Quadram Institute to learn long read sequencing. Thank you to Dr Gemma Langridge, Dr Marie Chattaway and Langridge lab for teaching me long read sequencing from DNA extraction to analysis. Thank you to Dr Claire Spreadbury and Pei Hayes for all their support and both cohort one and two from my PhD programme for their support and laughs. Thank you to Dr Carlos Reding Roman for their guidance on de-bugging scripts.

Many thanks also to former members of Avison lab, especially Dr Jacqueline Findlay, for their support. Thank you so much to all the current members of Avison Lab for their motivation, encouragement and laughs. In particular, a special thank you to Dr Oliver Mounsey and his wife, Shona Mounsey for their amazing help, patience, support, humour and efforts in taking care me during my entire PhD; I am really grateful. Additionally, special thanks to Dr Beatriz Llamazares for being there for me and her support. Thank you to Dr Carlos Reding Roman and Emily Syvret for their support and being my work buddy in cafés. Thank you also to Dr Jordan Sealey for her words of encouragement and being a great office and exercise buddy.

A very special thank you goes to my parents and family, who have always believed in me and for their love and support throughout this PhD, before and beyond. Special thank you also to my partner Danny Ward and his family for their support and encouragement. Lastly, thank you to all my friends for their friendship and support.

Author's declaration

I declare that the work in this dissertation was carried out in accordance with the requirements of the University's *Regulations and Code of Practice for Research Degree Programmes* and that it has not been submitted for any other academic award. Except where indicated by specific reference in the text, the work is the candidate's own work. Work done in collaboration with, or with the assistance of, others, is indicated as such. Any views expressed in the dissertation are those of the author.



SIGNED: DATE:.....05.10.2023.....

Publications and pre-prints

Bhamber R., Sullivan, B., **Lee, WWY.**, Avison, MB., Dowsey, AW., & Williams, P. 2023. Rational Antibiotic Escalation Applied to Specific Patient Groups. Preprint found here: <https://www.medrxiv.org/content/10.1101/2023.11.03.23298025v2>

Dulyayangkul, P., Beavis, T., **Lee, WWY.**, Ardagh, R., Edwards, F., Hamilton, F., Head I., Heesom, K., Mounsey, O., Muraik, M., Reding, C., Satapoomin, N., Shaw, J., Takebayashi, Y., Tooke, C., Spencer, J., Williams, P., & Avison, MB. 2023. Harvesting and amplifying gene cassettes confers cross-resistance to critically important antibiotics. Preprint found here: <https://www.biorxiv.org/content/10.1101/2023.12.02.569715v1>

Brignoli, T., Recker, M., **Lee, WWY.**, Dong, T., Bhamber, R., Albur M., Williams, P., Dowsey AW., & Massey, RC. 2022, 'Diagnostic MALDI-TOF MS can differentiate between high and low toxic Staphylococcus aureus bacteraemia isolates as predictor of patient outcome', *Microbiology*, vol 168, no. 8. DOI: [10.1099/mic.0.001223](https://doi.org/10.1099/mic.0.001223)

Findlay, J., Mounsey, O., **Lee, WWY.**, Newbold, N., Morely, K., Schubert, H., Gould, V., Cogan, TA., Reyher, KK., & Avison, MB. 2021, 'Molecular Epidemiology of Escherichia coli Producing CTX-M and pAmpC β -Lactamases from Dairy Farms Identifies a Dominant Plasmid Encoding CTX-M-32 but No Evidence for Transmission to Humans in the Same Geographical Region', *Applied and Environmental Microbiology*, vol. 87, no. 1, e01842-20, pp. 1-9. <https://doi.org/10.1128/AEM.01842-20>

Presentations

- June 2023 **Invited talk** at EPFL, Switzerland – Chapters 1 and 3
- March 2023 **Invited talk** at University of Oxford, UK – Chapters 1 and 3
- April 2023 **Poster presentation** at European Congress of Clinical Microbiology and Infectious Diseases (ECCMID) 2023, Copenhagen, Denmark – Chapter 1
- November 2023 **Oral presentation** at International Congress on Infectious Diseases, Kuala Lumpur, Malaysia, Chapters 1 and 3
- June 2022 **Poster presentation** at ASM 2022, Washington DC, USA – Chapters 1 and 3

As part of my PhD programme (National PhD Programme in Antimicrobial Research), I undertook a 3 month placement at Quadram Institute, Norwich UK conducting a research project involving characterizing large chromosomal rearrangements in *Salmonella* using Nanopore sequencing and analysis to investigate the physical structure of these genomes. This work was presented as talks or posters detailed below:

- November 2023 **Oral presentation** at International Congress on Infectious Diseases, Kuala Lumpur, Malaysia
- June 2022 **Poster presentation** at ASM 2022, Washington DC, USA
- March 2022 **Flash talk** at HPRU GI Annual Scientific Conference, Warwick, UK

Table of Contents

Abstract	2
Acknowledgements	3
1.0 Introduction	17
1.1 General Overview	17
1.2 UTIs	18
1.3 BSIs	22
1.4 E. coli	25
1.4.1 Characteristics of pathogenic <i>E. coli</i>	25
1.4.2 <i>E. coli</i> population structure	29
1.5 Klebsiella spp.	32
1.5.1 Characteristics of pathogenic <i>Klebsiella</i> spp.	32
1.5.2 <i>Klebsiella</i> spp. population structure.....	33
1.6 Typing and WGS of E. coli and Klebsiella spp.	38
1.7 AMR in BSI and UTI pathogens:	39
1.7.1 Burden of AMR	39
1.8 Phenotypic and genotypic AMR detection	41
1.9 Cephalosporins and the associated mechanisms of resistance	44
1.10 Quinolones, FQs and associated mechanisms of resistance	50
1.11 Transmission of AMR bacteria and genes	54
1.12 Impact of WGS, bioinformatics and surveillance on improving antimicrobial therapy and better targeted infection control	57
1.13 PhD aims	60
2.0 Methods	62
2.1 Study area	62
2.2 Provision of clinical data	62
2.3 Bacterial isolates from BSI in 2020, identification and demographics	62
2.3.1 <i>E. coli</i> bacterial isolates from BSI	62
2.3.2 <i>Klebsiella</i> spp. isolates from BSIs	63
2.4 Bacterial isolates from UTI in 2020, identification and demographics	63
2.4.1 <i>E. coli</i> bacterial isolates from UTIs	63
2.5 3GC-R E. coli BSI and UTI in 2020	63
2.6 3GC-R E. coli BSI and UTI in 2018, identification, molecular screening and antimicrobial susceptibility	64
2.7 WGS with Illumina and long read sequencing	64
2.8 Long read sequencing and data processing for selected NDM-positive K. pneumoniae isolates from BSIs	65
2.9 Genotyping and detection of plasmid, AMR and virulence genes	65

2.10	Genome visualisation, annotation and pairwise alignment comparisons for MDR <i>E. coli</i> ST15 of <i>K. pneumoniae</i>	66
2.10.1	Characterisation of regions encoding AMR genes	66
2.10.2	Detection of virulence and AMR genes on plasmid associated contigs from short-read assemblies for <i>E. coli</i> and <i>K. pneumoniae</i> , as well as long read assemblies for <i>K. pneumoniae</i>	66
2.11	Phylogenetic analysis	67
2.12	Antimicrobial susceptibility	67
2.13	Polymerase Chain Reaction	68
2.13.1	Sample preparation for polymerase chain reactions	68
2.13.2	Screening for β -lactamase genes with polymerase chain reactions	70
2.13.3	Gel electrophoresis.....	70
2.14	Comparison of variation in AMR detection with R to analyse true positive (TP), true negative (TN), false positive (FP) and false negative (FN) rates	70
2.15	Statistical analysis	72
2.15.1	Associations between source, phylogroups, AMR and virulence	72
2.15.2	Statistical comparison of precision and recall for the prediction of phenotypic AMR using several bioinformatics tools.....	72
3.0	Results Chapter 1	74
3.1	Introduction	74
3.2	Results	78
3.2.1	Temporal trend in Gram-negative BSI isolates cultured by Severn Pathology in 2020 with a focus on <i>E. coli</i>	78
3.2.2	Urinary source <i>E. coli</i> BSI was not associated with the observed increase of <i>E. coli</i> BSI in the summer months	81
3.2.3	ST131 was not responsible for the increase of <i>E. coli</i> BSI in the summer of 2020	83
3.2.4	Association between phylogroups, AMR and source of infection	88
3.2.5	Phylogenetic relationships showed AMR mechanisms found in 2020 BSI isolates are dispersed and intermixed with isolates from different phylogroups	90
3.2.6	Phylogenetic analysis reveals ST131 and ST1193 clades within the UTI population in 2020 conferring MDR including and resistance to ciprofloxacin	92
3.2.7	Sequenced genomes of 2018 3GC-R <i>E. coli</i> from BSI and UTI showed a clonal spread in the community.....	94
3.2.8	Diversity of AMR genes among 3GC-R <i>E. coli</i> has stayed consistent, with an increase of resistance to aminoglycosides observed between 2018 and 2020 within BSIs	100
3.2.9	ST131 within the 3GC-R UTI populations in 2018 and 2020 were divided into two clusters, with one cluster harbouring CTX-M-14 and mutations associated with resistance to FQs	103
3.3	Discussion and Conclusion	106
4.0	Results Chapter 2	113
4.1	Introduction	113
4.2	Results	118
4.2.1	Temporal trend in <i>Klebsiella</i> spp. in BSIs received by Severn Pathology in 2020	118
4.2.2	Source of infection for <i>Klebsiella</i> spp. collected in 2020 is not associated with seasonality	119
4.2.3	<i>K. pneumoniae</i> displayed higher resistance and virulence score in comparison to <i>K. quasipneumoniae</i>	122
4.2.4	Phylogenetic relationships reveal the majority of AMR mechanisms identified in <i>K. pneumoniae</i> , with MDR are detected in both ST307 and ST15.....	125
4.2.5	Characterisation of the genetic environments of 1 MDR ST147 and 3 MDR ST15 harbouring NDM-1 reveal the same resistance genes present in 5 separate genomic regions, with all ST15 identified from the same hospital ward	128

4.3	Discussion and Conclusion.....	134
5.0	Results Chapter 3.....	140
5.1	Introduction.....	140
5.2	Results.....	145
5.2.1	Dominance of a small number of virulence factors including yersiniabactin, aerobactin, salmochelin and serum resistance were found among <i>E. coli</i> causing BSIs.....	145
5.2.2	Understanding the distribution of AMR, virulence and plasmid replicons in the BSI <i>E. coli</i> population	147
5.2.3	In MDR <i>E. coli</i> isolates, most virulence and AMR genes were not detected on plasmid associated contigs	156
5.2.4	Phylogenetic analysis shows the presence of only yersiniabactin and invasins in MDR ST307 and NDM producing ST15 <i>K. pneumoniae</i>	160
5.2.5	No virulence genes were detected on plasmid associated contigs in NDM-positive <i>K. pneumoniae</i> , however AMR genes were detected	162
5.2.6	Localisation and detection of AMR and virulence genes on plasmids from NDM-positive <i>K. pneumoniae</i> using Nanopore sequencing.....	165
5.2.7	Plasmid annotations and comparisons all in MDR NDM carrying <i>K. pneumoniae</i> , show identical plasmids present in 2 different patients.....	171
5.3	Discussion and Conclusion.....	178
6.0	Results Chapter 4.....	183
6.1	Introduction.....	183
6.2	Results.....	187
6.2.1	Overall genotypic-phenotypic concordance ranged from 65% to 99% across the antimicrobial panel for <i>E. coli</i>	187
6.2.2	Concordance varied across bioinformatics tools, with ABRicate and ResFinder with PointFinder displaying the least accuracy for AMR detection of resistance in <i>E. coli</i> associated with amoxicillin/clavulanate acid. F1 score was greatest for detection of resistance in <i>E. coli</i> associated with cefotaxime	189
6.2.3	Concordance varied across bioinformatics tools (ABRicate, ResFinder with PointFinder, ARIBA and Kleborate) in all <i>Klebsiella</i> spp. F1 score was greatest for detection of resistance in <i>K. pneumoniae</i> associated with gentamicin	191
6.2.4	Critical errors detected in all antimicrobial classes for <i>K. pneumoniae</i> , however for other species critical errors were only detected for amoxicillin/clavulanate	195
6.2.5	Investigation reasons for critical errors between 3GC-R phenotype and genotype in <i>E. coli</i> and <i>Klebsiella</i> spp.	201
6.3	Discussion and Conclusion.....	206
7.0	General Discussion and Conclusion.....	212
7.1	Discussion.....	212
7.2	Conclusion	218
8.0	References.....	219

List of Figures

Figure 1. Summary of the different pathotypes of pathogenic <i>E. coli</i> created using biorender.com	25
Figure 2. A timed-scale phylogeny displaying all clades of ST131, the associated AMR mechanisms and global transmission from geographical information. Taken from Stoesser et al, 2016.....	30
Figure 3. Phylogeny showing the relationships between KpSC, (red branches) and the other <i>Klebsiella</i> spp., <i>E. coli</i> and <i>Salmonella</i> spp. Taken from Wyres et al, 2020.....	34
Figure 4. Phylogenetic lineages of <i>K. pneumoniae</i> establishing different clonal groups and the association with AMR. Taken from Wyres et al, 2020.....	35
Figure 5. Global distribution detailing most resistant and hypervirulent STs of <i>K. pneumoniae</i> revealing regional differences.....	37
Figure 6. Summary of the different methods utilised for antimicrobial susceptibility testing and the associated turnover time. Taken from Gajic et al, 2022).....	41
Figure 7. Primary mechanisms involved in resistance to cephalosporins.....	45
Figure 8. An illustration of the components of efflux pumps and the process by which drugs or antimicrobials are transported out of the cell in Gram-negative bacteria. IM and OM stands for inner and outer membrane respectively. Taken from (Li, Plésiat & Nikaido, 2015).....	49
Figure 9. A schematic displaying an overview of the main factors contributing towards the spread of resistance. Taken from Prestinaci et al, 2015.....	54
Figure 10. Overview of the characteristics of IS26 taken from (Varani et al, 2021). A) Displays the structure of IS26 and the 8bp repeats are represented with black arrows. B) Displays the structure of a pseudo-compound transposon. Ab ^r represents any AMR gene.....	56
Figure 11. Overview of CTX-M variants in different time periods within Europe (a,b,c) and the rest of the continents in the world (d,e,f). Taken from Bevan <i>et al.</i> (2017).....	75
Figure 12. Total number of bacterial isolates most commonly found from different bacterial species in 2020.....	79
Figure 13. Number of <i>E. coli</i> collected per month broken up by source of infection or unknown source.....	82
Figure 14. Number of <i>E. coli</i> sequenced per month displaying broken down by predicted source of infection.....	83
Figure 15. A stacked bar chart containing the most common STs found per month, amongst 696 <i>E. coli</i> isolated from BSIs between January 2020 and December 2020.....	84
Figure 16. Monthly number of <i>E. coli</i> BSI per month from Severn Pathology displaying the number of urine source of infection in 2021.....	86
Figure 17. Monthly number of total <i>E. coli</i> BSIs per month from Severn Pathology also displaying the number of urine source of infection in 2022.....	86
Figure 18. Average monthly temperature in Bristol, Southwest UK in 2020, 2021 and 2022.....	87
Figure 19. A core genome SNP tree consisting of 667 <i>E. coli</i> (n=11 isolates with bad quality assemblies that are not present in the tree) displaying the distribution of phylogroups and its associated AMR mechanisms.....	91
Figure 20. A core genome SNP tree consisting of 3GC-R <i>E. coli</i> from UTI from 2020 displaying the distribution of phylogroups and its associated resistance profiles.....	93
Figure 21. Maximum likelihood tree containing 145 3GC-R ST131 <i>E. coli</i> core Illumina genomes from BSIs and UTIs in 2018 displaying the presence of AMR resistant genes present within this <i>E. coli</i> population.....	95

Figure 22. A maximum likelihood tree of consisting of 20 ST73 <i>E. coli</i> and their associated AMR, plasmid type and point mutations profiles. The coloured branches represent clusters of isolates which are most likely genetically similar.....	97
Figure 23. A maximum likelihood tree of consisting of 16 <i>E. coli</i> of ST38 and its associated resistance, plasmid and point mutations profiles. The coloured branches represent clusters of isolates which are most genetically similar.....	98
Figure 24. A core genome SNP tree consisting of 3GC <i>E. coli</i> from BSI from 2018 and 2020 displaying the distribution of phylogroups and its associated AMR mechanism profiles. Isolates from 2018 have shorter name labels than those isolates from 2020.....	101
Figure 25. Trends in AMR mechanisms carried in 3GC-R isolates conferring resistance to 3GCs, aminoglycosides and FQs in BSI <i>E. coli</i> in 2018 and 2020.....	102
Figure 26. A core genome SNP tree consisting of 3GC-R <i>E. coli</i> from UTI from September and October in both 2018 and 2020 displaying the distribution of phylogroups and its associated AMR profiles.....	104
Figure 27. Trends in AMR determinants among 3GC-R <i>E. coli</i> associated with 3GCs, aminoglycosides and FQs in UTI <i>E. coli</i> in September and October of 2018 and 2020.....	105
Figure 28. Global distribution detailing the resistance associated with a range of STs of <i>K. pneumoniae</i> to carbapenems and 3GCs. Taken from Wyres et al, 2020.....	114
Figure 29. Total number of BSI isolates of the species most commonly found in 2020 . Reprinted from Chapter 1.....	118
Figure 30. Monthly number of <i>Klebsiella</i> spp. collected divided by source of infection.....	119
Figure 31. Resistance and virulence scores for <i>Klebsiella</i> spp.....	123
Figure 32. Graph showing most common STs detected in BSI <i>Klebsiella</i> spp.....	123
Figure 33. A heatmap displaying the different virulence factors and AMR mechanisms within the ST307 population. The red bars show the presence of resistance to specific antimicrobials and the blue bar shows the presence of specific virulence factors. No bars represent the absence of virulence factors and resistance.....	124
Figure 34a. Core genome SNP tree displaying the distribution of AMR genes across the <i>Klebsiella</i> population. Isolates are highlighted according to their source of infection. Clades are highlighted according to species in clockwise order: brown clade: <i>K. oxytoca</i> ; green clade: <i>K. pasteurii</i> ; dark blue clade: <i>K. grimontii</i> ; red clade: <i>K. michiganensis</i> ; black node: <i>K. aerogenes</i> ; light blue clade: <i>K. variicola</i> ; pink clade: <i>K. quasipneumoniae</i> ; purple clade: <i>K. pneumoniae</i> b. Core genome SNP tree on <i>K. pneumoniae</i> only, highlight MDR for ST15 and ST307.....	126
Figure 35. A visualisation through Bandage of the structure of the genomic regions containing different AMR genes (<i>bla</i> _{CTX-M-15} in red, <i>bla</i> _{TEM-1D} in orange, <i>aac(3)IIa</i> in green, <i>aac(6)-Ib-cr</i> in blue and <i>bla</i> _{OXA-1} in pink) for all ST15 and the only one ST147 (34419) containing NDM (black).....	129
Figure 36. Characterisation and comparison of the genomic regions containing <i>bla</i> _{NDM-1} in MDR ST15. Group numbers represent a set of genes that match >90% and vertical lines show genes that are the same.....	130
Figure 37. Characterisation and comparison of the genomic regions containing <i>bla</i> _{CTX-M} and <i>bla</i> _{TEM} in MDR ST15. Group numbers represent a set of genes that match >90% and vertical lines show genes that are the same.....	131
Figure 38. Characterisation and comparison of the genomic regions containing <i>bla</i> _{OXA} and <i>aac(6)-Ib-cr</i> in MDR ST15. Group numbers represent a set of genes that match >90% and vertical lines show genes that are the same.....	132
Figure 39. Characterisation and comparison of the genomic regions containing <i>bla</i> _{SHV} in MDR ST15. Group numbers represent a set of genes that match >90% and vertical lines show genes that are the same.....	133
Figure 40. Graph displaying the number of isolates harbouring the most common virulence factor genes previously associated with BSIs.....	146

Figure 41. Graph displaying the distribution of virulence gene content of <i>E. coli</i> BSIs.....	147
Figure 42. A core genome SNP tree consisting of 667 <i>E. coli</i> (n=11 isolates with bad quality assemblies that are not present in the tree) displaying the distribution of phylogroups and its associated AMR profiles. Reprinted from Chapter 1.....	148
Figure 43. A core genome SNP tree consisting of 667 <i>E. coli</i> (n=11 isolates with bad quality assemblies that are not present in the tree) displaying the distribution of phylogroups and its associated virulence profiles.....	150
Figure 44. A core genome SNP tree consisting of 667 <i>E. coli</i> (n=11 isolates with bad quality assemblies that are not present in the tree) displaying the distribution of phylogroups and its associated plasmid replicon profiles.....	155
Figure 45. Graph showing the number of plasmid replicons, AMR and key virulence genes in MDR <i>E. coli</i> BSI isolates.....	156
Figure 46. Pairwise alignment of the assembly of isolate 39868 and a IncFIA reference (Accession: AP019526.1).....	157
Figure 47. Core genome SNP tree displaying the distribution of plasmids, AMR and virulence genes across the <i>Klebsiella</i> spp. population. The highlighted pink clade represents <i>K. pneumoniae</i>	161
Figure 48. A visualisation through Bandage of the structure of the genomic regions containing different AMR genes (<i>bla</i> _{CTX-M-15} in red, <i>bla</i> _{TEM-1D} in orange, <i>aac(3)-IIa</i> in green, <i>aac(6)-Ib-cr</i> in blue and <i>bla</i> _{OXA-1} in pink) for all NDM-carrying ST15 and the only one ST147 (34419) containing NDM (black). Reprinted from Chapter 2.....	163
Figure 49. A visualisation through Bandage of the structure of the chromosome and plasmids including the genomic regions containing AMR and virulence genes for isolate 39583.....	166
Figure 50. A visualisation through Bandage of the structure of the chromosome and plasmids including the genomic regions containing AMR and virulence genes for isolate 39924.....	167
Figure 51. A visualisation through Bandage of the structure and the size of the chromosome and plasmids including the genomic regions containing AMR and virulence genes for isolate 39915.....	168
Figure 52. Characterisation and comparison of the genomic regions containing <i>bla</i> _{CTX-M} , <i>bla</i> _{TEM} , <i>bla</i> _{OXA} and <i>aac(6')-Ib-cr</i> in MDR ST15 (256662E, 256660E, 256663E). Group numbers represent a set of genes that match >90% and vertical lines show genes that are the same.....	170
Figure 53. BLAST comparison of the IncR plasmids identified in 256662E and 256663E, with 256662E acting as the reference.....	173
Figure 54. BLAST comparison of IncFIB plasmids identified in 256662E and 256663E, with 256662E acting as the reference.....	174
Figure 55. BLAST comparison of col440 plasmids identified in 256662E and 256663E, with 256662E acting as the reference. Putative genes located on this plasmid could not be identified by Prokka and BLASTn.....	175
Figure 56. Annotation of genes on the IncR plasmid present in 256660E.....	176
Figure 57. Detection of the Col440 plasmid present in 256660E. Putative genes located on this plasmid were unable to be identified by Prokka and BLASTn.....	177
Figure 58. A chart displaying concordance (%) between phenotypic resistance data for 12 antimicrobials used clinically to treat BSI and WGS data for BSI <i>E. coli</i> received in 2020. Co-amoxiclav is amoxicillin/clavulanate; pip.taz is piperacillin/tazobactam.....	188
Figure 59. Graph displaying the percentage of <i>E. coli</i> samples producing true positives (TP), true negatives (TN), false positives (FP) (non-critical errors) and false negatives (FN) (critical errors) for ABRicate, ARIBA and ResFinder.....	190

Figure 60. Graph displaying the percentage of all *Klebsiella* spp. isolates producing true positives (TP), true negatives (TN), false positives (TP) (non-critical errors) and false negatives (FN) (critical errors) for ABRicate, ARIBA, ResFinder with PointFinder and Kleborate.....193

Figure 61. Graph displaying the percentage of all *K. pneumoniae* (n=125) samples producing true positives (TP), true negatives (TN), false positives (TP) (non-critical errors) and false negatives (FN) (critical errors) for ABRicate, ARIBA, ResFinder with PointFinder and Kleborate.....197

Figure 62. Graph displaying the percentage of all *K. oxytoca* (n=21) samples producing true positives (TP), true negatives (TN), false positives (TP) (non-critical errors) and false negatives (FN) (critical errors) for ABRicate, ARIBA, ResFinder with PointFinder and Kleborate.....199

Figure 63. Graph displaying the percentage of all *K. variicola* (n=17) samples producing true positives (TP), true negatives (TN), false positives (TP) (non-critical errors) and false negatives (FN) (critical errors) for ABRicate, ARIBA, ResFinder with PointFinder and Kleborate.....200

Figure 64. Flowchart displaying a summary of the number of isolates tested for concordance and the numbers of isolates retested phenotypically with disc susceptibility and PCR. Created using Biorender.....202

Figure 65. A gel from CTX-M multiplex PCR displaying the presence and absence of CTX-M gene.....205

List of Tables

Table 1. A table listing the various kinds of uncomplicated UTIs. Adapted from (Medina & Castillo-Pino, 2019).....	19
Table 2. The antimicrobial treatment provided for patients with asymptomatic, cystitis, pyelonephritis and complicated UTIs caused by <i>E. coli</i>	21
Table 3. Summary of the function of virulence genes in their respective groups found in various ExPEC types. Taken from (Sora et al, 2021).....	26
Table 4. displaying the different kinds of infections caused by <i>Klebsiella</i> spp. and the ranking in comparison with other pathogens (Podschun & Ullmann, 1998).....	32
Table 5. Table displaying the 7 phylogroups of <i>K. pneumoniae</i>	33
Table 6. Overview of the different generations of cephalosporins and activity against pathogens (Das et al, 2019).....	44
Table 7. Overview of the quinolone classification system, adapted from Andriole, 2005.....	50
Table 8. Plasmid reference sequences.....	66
Table 9. Volumes of reagents used for mastermix.....	68
Table 10. Table detailing the CTX-M group primers and product size.....	69
Table 11. χ^2 analysis revealed there was a statistically significant bias towards <i>E. coli</i> infections being in the summer compared with other quarters, when compared to the infections caused by <i>K. pneumoniae</i> , <i>Proteus</i> spp., <i>Pseudomonas</i> spp., <i>Enterobacter</i> spp., and <i>Citrobacter</i> spp. combined in the summer versus not in the summer.....	80
Table 12. χ^2 analysis on isolates with a known source revealed there was no significant association between <i>E. coli</i> infections from different sources in the summer compared to the other seasons. Sources of infection not considered in this table had a sample size too low for statistical analysis.....	82
Table 13. χ^2 analysis revealed there was no association between ST131 causing an increase in infections in the summer compared to the other seasons.....	85
Table 14. Significance of associations between phylogroups and any particular source of infection.....	88
Table 15. Significance of associations between resistance genes and between urinary and GI tract source of infection.....	89
Table 16. The percentage of <i>E. coli</i> isolates associated with each phylogroup. The colours for each phylogroup are shown and can be compared with the core genome SNP tree in Figure 19.....	90
Table 17. Isolates sharing similar AMR and plasmid profiles.....	99
Table 18. Other genes surrounding gene of interest.....	99
Table 19. χ^2 analysis showing the significance in the change of AMR mechanisms among 3GC-R BSI isolates between 2018 and 2020.....	103
Table 20. Significance in the change of AMR mechanisms associated with 3GCs, aminoglycosides and FQs in 3CR-R UTI <i>E. coli</i> between 2018 and 2020.....	105
Table 21. χ^2 analysis revealed there was no significant association between <i>Klebsiella</i> spp. infections of different sources with different seasons. χ^2 analysis conducted on sources with the highest numbers. Other sources of infection with <i>K. aerogenes</i> and <i>K. varriicola</i> had a sample size too low for statistical analysis.....	120
Table 22. Significance of associations between <i>K. pneumoniae</i> and <i>K. oxytoca</i> and any particular source of infection. The sample sizes for <i>K. aerogenes</i> and <i>K. varriicola</i> were too low for statistical analysis.....	121
Table 23. χ^2 analysis on <i>E. coli</i> and <i>Klebsiella</i> spp. collected throughout the year revealed there was a stronger association with urinary and GI source of infection in <i>E. coli</i> . compared to <i>Klebsiella</i> spp. Other sources of infection in both species had a sample size too low for statistical analysis.....	121

Table 24. Other STs of <i>K. pneumoniae</i> other than ST307 and ST15 harbouring multiple AMR genes and the frequency of which these STs occur.....	125
Table 25. Ward data associated with ST307 and ST15.....	127
Table 26. Virulence genes, their associated encoded functions, functional group and presence in different <i>E. coli</i> pathotypes. Adapted from Sora et al, 2021.....	141
Table 27. Table detailing the main virulence factors in ExPEC causing BSIs.....	151
Table 28. χ^2 analysis revealed strong associations between carriage of one or more specific virulence genes (defined in Table XX) and <i>E. coli</i> BSI with urinary source, versus all other sources combined.....	152
Table 29. χ^2 analysis revealed strong associations between carriage of genes encoding aerobactin, yersiniabactin, salmochelin, p-fimbriae, serum resistance and capsule among <i>E. coli</i> BSI with urinary source, versus all other sources combined.....	152
Table 30. χ^2 analysis revealed strong associations between virulence factors associated with aerobactin and capsules and ST131 from urinary source.....	154
Table 31. Table displaying the plasmid reference-based aligned contigs from selected MDR <i>E. coli</i> isolates from urinary source which also details detectable AMR and virulence genes.....	159
Table 32. Table displaying the plasmid reference-based associated contigs from MDR NDM-positive <i>K. pneumoniae</i> isolates which also details detectable AMR and virulence genes. Virulence genes <i>ybt</i> encodes for yersiniabactins, <i>iuc</i> encodes for aerobactin, <i>iro</i> encodes for aerobactin and <i>clb</i> encodes for colibactin and <i>rmp</i> encodes for invasins.....	164
Table 33. Table detailing the number of contigs and their identification in each sample after <i>de novo</i> assembly.....	171
Table 34. Table showing the statistical comparison of precision, recall and F1 score for the detection of AMR determinants using several bioinformatics tools for <i>E. coli</i>	191
Table 35. Table showing the statistical comparison of precision, recall and F1 score for the detection of AMR determinants using several bioinformatics tools for <i>Klebsiella</i> spp.....	194
Table 36. Table showing the statistical comparison of precision, recall and F1 score for the detection of AMR determinants using several bioinformatics tools for <i>K. pneumoniae</i> . (Precision measures the accuracy of positive predictions of a test. Recall measures how well a test is at getting the correct result. F1 takes precision and recall into account, giving a value between 0 and 1).....	198
Table 37. Table showing discordance of <i>E. coli</i> isolates resistant to cefotaxime with the associated disc testing results after re-testing phenotypically.....	204

List of Abbreviations

BSI/BSIs – bloodstream infection/bloodstream infections
UTI/UTIs – urinary tract infection/urinary tract infections
NHS – National Health Service
IPC – infection prevention control
ExPEC – extraintestinal pathogenic *E. coli*
IPEC – intestinal pathogenic *E. coli*
DAEC – diarrheagenic *E. coli*
STEC – shiga-toxin producing *E. coli*
EPEC – Enteropathogenic *E. coli*
EIEC – enteroinvasive *E. coli*
ETEC – enterotoxigenic *E. coli*
EAEC – enteroaggregative *E. coli*
UPEC – uropathogenic *E. coli*
MNEC – meningitis associated *E. coli*
SEPEC – human associated sepsis *E. coli*
KpsC – *K. pneumoniae* species complex
KPC – *K. pneumoniae* carbapenemase
PBP – penicillin binding proteins
GI – gastrointestinal tract
AMR – antimicrobial resistance
MDR – multi-drug resistant
3GC – 3rd generation cephalosporins
3GC-R – 3rd generation cephalosporin resistant
FQ – fluoroquinolones
BL/BLI - β -lactam/ β -lactamase inhibitor
ESBL – extended spectrum β -lactamases
PMQR – plasmid mediated quinolone resistance
ST – sequence type
SNP – single nucleotide polymorphism
IS – insertion sequences
WGS – whole genome sequencing
PCR – polymerase chain reaction
MALDI-TOF - Matrix Assisted laser Desorption Ionisation Time of Flight
TBX – Tryptone Bile X-Glucuronide
MGEs – mobile genetic elements
TP – true positive
TN – true negative
FP – false positive
FN – false negative
RND – resistance-nodulation-division
ATP – adenosine triphosphate

1.0 Introduction

1.1 General Overview

Bacteria are immensely diverse and encounter antimicrobials from various sources including those produced from natural sources, those synthesised and released into the environment by pharmaceutical factories, or through the wastewater system. Thus, AMR is ubiquitous. The mobility of AMR genes enables their exchange between bacteria carried by humans, animals and those found in the environment. Increased use of antimicrobial agents in humans, animals and agriculture, in combination with the rise in human and livestock populations promote the dissemination of AMR. Furthermore, the paucity of novel antimicrobials exacerbates global concerns about AMR. Therefore, there is an urgent need for prudent antimicrobial use; for protecting the antimicrobials currently utilised by targeting their use to the right infection in the right patient and for the right length of time. BSIs and UTIs, predominantly caused by *E. coli*, are an increasing clinical challenge. Rapid empiric antimicrobial therapy is especially vital for the management of BSIs in order to prevent or reduce the severity of sepsis. This is due to the multi-day delay inherent to the use of traditional microbiological antimicrobial susceptibility testing methods. Moreover, treatment of UTI in the community is also empiric, with UK guidelines suggesting that for most infections, samples are not cultured prior to initial treatment. Even when samples are submitted, the results can take several days to be returned. Treatment failure for UTI due to AMR increases the risk of pyelonephritis (bacteria ascending to the kidneys) and the likelihood of BSI and urosepsis, therefore, understanding the genotypic basis of AMR can contribute to improving appropriate antimicrobial choice in two ways: first, at the population (subgrouped by geographical region, age, sex, co-morbidities and other risk factors) level, genomic surveillance of UTI or BSI pathogens can demonstrate linkage

between resistance (and pre-resistance, where resistance is only one mutation away, for example) to first and second line empiric antimicrobial choices, allowing clinicians to tailor empiric choices to the circulating resistance patterns in each specific patient group. Secondly, there is a move to use rapid WGS directly on clinical samples, to predict AMR phenotype, without the same delay as is inherent to traditional culture-based phenotypic tests, removing the need for prescribing to be empiric in the first place.

1.2 UTIs

UTIs can involve any site within the urinary system such as the bladder, urethra or kidneys. Gupta et al. (2001) estimated that there were approximately 150 million global cases of UTI per annum, with incidence increasing by 16.1% between 1990 and 2013 worldwide (GBD, 2013). UTIs are the most common bacterial infection diagnosed in outpatients and primary care in the UK (Reid, Al-Bayati & Samarasinghe, 2018), particularly in the elderly (Ruben et al, 1995; Wojsze & Toczńska-Silkiewicz, 2018; Cortes-Penfield et al, 2017). UTIs also account for 19.9% of healthcare associated infections (Smyth et al, 2008) and Smith et al. (2019) reported that between 43% and 56% of UTIs were associated with catheter use. UTIs in England are one of the most common cause of emergency hospital admissions among ambulatory care sensitive conditions with a 55% rise in admissions from 2001/2002 to 2012/2013 (Blunt, 2013). UTIs can be categorised into complicated or uncomplicated. To understand the epidemiology and pathophysiology of UTIs, knowledge of the classifications of UTIs is important. Uncomplicated UTIs can be symptomatic and occur in patients with genitourinary tracts without history of instrumentation (Johnson 2017). Uncomplicated UTIs can be further categorised into multiple classifications (Table 1) (Medina & Castillo-Pino, 2019).

Table 1. A table listing the various kinds of uncomplicated UTIs. Adapted from (Medina & Castillo-Pino, 2019).

Uncomplicated UTI Type	Description
Asymptomatic bacteriuria	Patient displaying no urinary symptoms however, the presence of bacteria is detected in urine culture
Uncomplicated cystitis	Refers to patients developing symptoms in the lower urinary tract such as pollakiuria, dysuria and urgency
Uncomplicated pyelonephritis	A UTI with symptoms such as flank pain and fever, only in the upper urinary tract
Recurrent uncomplicated UTIs	Involves multiple reoccurrence of UTIs within the timeframe of 6 months and 12 months

Cystitis and pyelonephritis are also associated with complicated UTIs, which involve functional or structural abnormalities within the genitourinary tract, or after instrumentation and are often asymptomatic (Nicole, 2005). Having indwelling urinary catheters is a major factor contributing to the progression of cystitis from asymptomatic bacteriuria (25%) and it increases the incidence of complicated UTIs (Sabih & Leslie, 2023). Gender disparity is most commonly observed in UTIs with an increased likelihood (20-40 times) for women to have a UTI compared to men of the same age (Deltourbe et al, 2022). This is due to the difference in anatomy as females have a shorter urethra, resulting in faecal commensal bacteria travelling into the urethral opening due to closer proximity (Deltourbe et al, 2022).

There can be difficulties with accurate assessment of the incidence of UTIs as diagnosis is dependent upon symptomatic patients attending a clinic and a positive urine culture being produced (Foxman, 2002). As a consequence, diagnostic errors can be made in patients with uncomplicated UTIs in primary care settings as the initial diagnosis is usually made in absence of a urine culture (Foxman, 2002). In England,

culture is only used if the patient returns to primary care following initial empiric antimicrobial treatment when symptoms have not resolved.

UTIs can be caused by a range of micro-organisms, including certain species of fungi (Flores- Mireles et al, 2015). *E. coli* is the most common organism responsible for both complicated (65%) and uncomplicated UTIs (75%), followed by other *Enterobacterales* such as *Klebsiella pneumoniae* (Flores-Mireles et al, 2015). In uncomplicated UTIs globally, other than *E. coli*, *K. pneumoniae*, *Staphylococcus saprophyticus*, *Enterococcus faecalis*, group B Streptococcus (GBS), *Proteus mirabilis*, *Pseudomonas aeruginosa*, and *Staphylococcus aureus* are found in order of prevalence (Flores- Mireles et al, 2015). In comparison, *Enterococcus* spp. are the most prevalent organism other than *E. coli* in complicated UTIs, followed by *K. pneumoniae* and the yeast *Candida* spp. (Flores-Mireles et al, 2015).

As discussed, the majority of uncomplicated UTIs are treated empirically, in the absence of a urine culture. Consequently, recognition of AMR patterns circulating within the community is crucial in order for clinicians to make the best judgement about the choice of antimicrobial for treatment. In the UK, current first line therapy for uncomplicated UTIs is nitrofurantoin (NICE, 2018). Trimethoprim (sometimes potentiated with sulfamethoxazole) or first generation (oral) cephalosporins such as cefalexin may also be used as empiric antibiotic choices; oral ciprofloxacin and amoxicillin/clavulanate are also sometimes administered (Ahmed et al, 2019). However, trimethoprim (/sulfamethoxazole) should only be administered if prevalence of resistance in *E. coli* is less than 20% in Europe (Bader et al, 2019; Bartoletti et al, 2016; Bonkat et al, 2017). Whilst treatment is usually with the same types of oral agents, in some countries, complicated UTIs and pyelonephritis are treated with IV carbapenems, especially for *E. coli* producing Extended-Spectrum β -Lactamases

(ESBLs) (Bader et al, 2019) in order to reduce the risk of urosepsis. Furthermore, third generation cephalosporins (3GCs) may be used for these presentations if patients show no clinical risk factors for AMR (Bischoff et al, 2018). Table 2 below details the international clinical guideline for antimicrobial treatment administered for the aforementioned types of UTI caused by *E. coli* (Gupta et al, 2011).

Table 2. The antimicrobial treatment provided for patients with asymptomatic, cystitis, pyelonephritis and complicated UTIs caused by *E. coli*.

UTI	Antimicrobial treatment
Asymptomatic bacteriuria	No antibiotic required
Uncomplicated cystitis	Nitrofurantoin, trimethoprim/sulfamethoxazole, Fosfomycin, pivmecillinam
Uncomplicated pyelonephritis	Trimethoprim/sulfamethoxazole and oral FQs such as ciprofloxacin
Complicated UTIs	Ciprofloxacin

1.3 BSIs

Within infectious diseases, the leading causes of morbidity and mortality in patients globally across all ages is BSI (Laupland & Church, 2014; UKHSA 2021). Minino *et al.* (2011) reported BSIs are the 11th most common cause of death in the United States. Another study reported an estimated 157,000 deaths from BSIs annually across Europe, with 1,110 and 12,000-19,000 deaths in Finland and England respectively (Goto & Al-Hasan, 2013). BSIs can lead to sepsis and UTI is the most common cause of BSI that leads to sepsis: referred to as urosepsis (Kalra & Raizada, 2009). It is estimated that there are 30 million cases of sepsis per year, with 2.8-9.8 million of these cases being urosepsis, causing 1.6 million deaths (Levy *et al.*, 2012). Urosepsis has a high mortality rate ranging between 20% and 40% (Grabe *et al.*, 2015; Wagenlehner *et al.*, 2013) and a study revealed that 40% of community acquired BSIs originated from catheter associated UTIs (Lark *et al.*, 2001). Furthermore, the source for 20% of BSIs from acute healthcare facilities and >50% of BSIs from long term care facilities are catheter associated UTIs (Nicolle, 2014). Sepsis, including urosepsis are medical emergencies, thus they are deemed a priority in hospitals and are of serious concern to the World Health Organisation (NICE, 2016).

Pathogens invade the lymphatic vessels or through intravenous devices such as catheters and enter the blood to cause BSIs. Additionally, the breakdown of capillaries in the kidney during pyelonephritis and perforation (including micro-perforations caused by some chemotherapy drugs, some autoimmune diseases, as a result of chronic enteritis, and in old age) of the gastrointestinal (GI) tract cause BSIs. Similar to UTIs, *E. coli* is one of the leading organisms responsible for BSIs and sepsis in adults (Mora- Rillo *et al.*, 2015). However, the most frequently isolated pathogen in BSIs can alter between geographical regions. For example, *Salmonella* Paratyphi and

Salmonella Typhi are predominantly isolated from patients with BSIs in Africa and Asia respectively (Deen et al, 2012).

E. coli that survive in the bloodstream and urinary tract are known as extraintestinal pathogenic *E. coli* (ExPEC) and can possess a wide range of virulence factors such as that encoded by *irp2* located on pathogenicity islands (Lefort et al, 2011) and plasmids (Daga et al, 2019). Accurate associations have not been made between the severity and outcome of infection and the presence of virulence factors alone; other host factors, source of infection (“portal of entry”, e.g. UTI, leaky GI tract) and underlying causes for infection that affect outcome (Daga et al, 2019).

A correlation between pathogen infection source and BSI severity and outcome has been reported. Infection source can be established from both clinical information and microbiological analysis. For example, a UTI pre-dating a BSI, where the pathogen cultured in both is the same species and has the same phenotypic AMR profile. However, the blood culture is often negative due to the administration of an IV antimicrobial prior to the blood sample being taken, resulting in the killing of any bacteria present. Therefore, there is no opportunity for microbiological comparison and an assignment of a presumed infection source is made only with the aid of clinical information. Infection source can be reported as undetermined or unknown when clinical data is inconclusive, and in fact very few hospitals routinely report infection source for BSI at all. Nonetheless, a study has shown significant association between pulmonary tract source and development of BSI into sepsis, and death (Denamur et al, 2022). In comparison, there was a negative correlation between UTI source and death (Denamur et al, 2022). Furthermore, GI tract source was positively associated with admission into intensive care (Denamur et al, 2022).

It is critical for patients with BSIs, especially those with sepsis to be prescribed the most appropriate antimicrobial therapy within an hour of diagnosis (Lee et al, 2017). Oral therapy is used in some countries for treatment of BSIs caused by Gram-negative bacteria (Nisly et al, 2020). Fluoroquinolones (FQs) have demonstrated reliable efficacy in treatment, however, increases in FQ resistance have heightened the concern for use (Mercuro, Stogsdill & Wungwattana, 2018). Oral cephalosporinase e.g. cefalexin and trimethoprim/sulfamethoxazole have been discussed as alternative therapeutic options, however data remains scarce (Kutob et al, 2016). In many UK hospital settings, IV antimicrobials are prescribed for sepsis straight away, with first-line options being the β -lactam/ β -lactamase inhibitor (BL/BLI) combination piperacillin/tazobactam and the aminoglycosides gentamicin or amikacin, and in some cases a 3GC, though this has been less common since measures were introduced to restrict *Clostridium difficile* infection rates. Upon improvement of symptoms, an oral switch is made to the BL/BLI combination amoxicillin/clavulanate or the FQ ciprofloxacin.

1.4 *E. coli*

1.4.1 Characteristics of pathogenic *E. coli*

Theodor Escherich first described *Bacterium coli commune*, later renamed *E. coli* in his honour, from faeces of infants in 1885 (Méric et al, 2016). The rise of modern microbiology and bacterial genomics can be attributed to a few select microorganisms and among them, *E. coli* has been studied for 130 years. *E. coli* is a notifiable organism to UKHSA, in particular *E. coli* causing BSIs and during the ten-year period since 2009, the incidence rate of *E. coli* BSIs have increased, with the highest rate reported between 2017 and 2019 (PHE, 2019). Moreover, it is the most commonly isolated organism in UTIs and BSIs in the UK, as discussed previously. Pathogenic *E. coli* can be classified into two types, ExPEC and intestinal pathogenic *E. coli* (IPEC), also known as diarrheagenic *E. coli* (Kaper et al, 2004). These two major pathotypes can be categorised into further pathotypes (Figure 1).

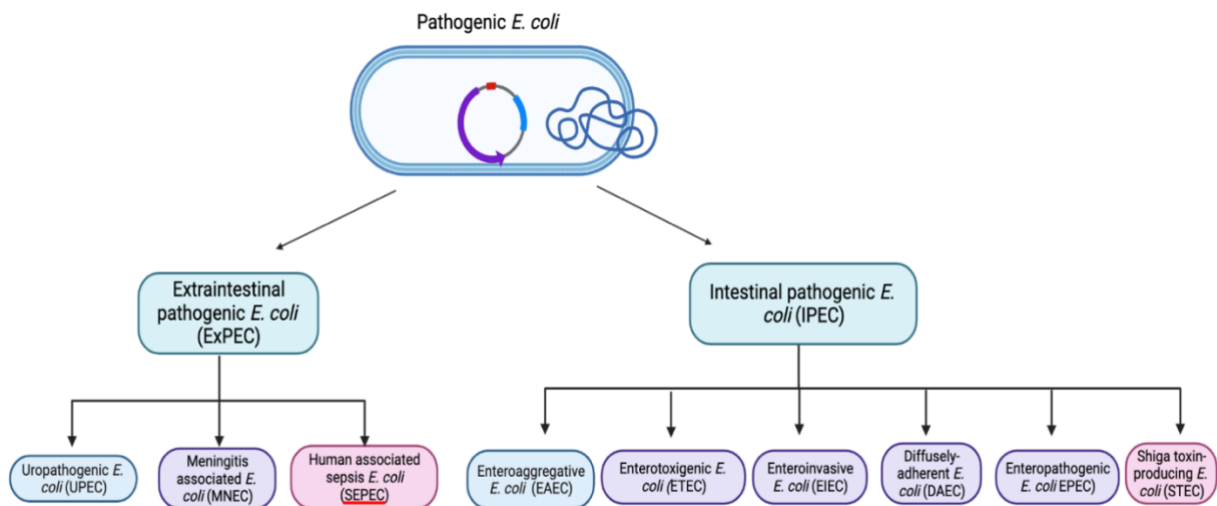


Figure 1. Summary of the different pathotypes of pathogenic *E. coli* created using biorender.com.

ExPEC can be characterised by their ability to cause infection outside of the GI tract. As mentioned previously, ExPEC can cause UTIs and BSIs in a process involving colonisation and biofilm formation and through the use of virulence factors, which can be classified further into toxins, adhesins, invasins, siderophores and protectines. (Table 3) (Sora et al, 2021).

Table 3. Summary of the function of virulence genes in their respective groups found in various ExPEC types. Taken from Sora *et al.* (2021).

Description	Virulence Genes	Function	ExPEC Pathotype
Adhesins			
Type 1 fimbriae	<i>fim</i>	Factor of colonization in extraintestinal infections, biofilm formation	UPEC, NMEC, SEPEC, APEC
Afimbrial adhesin	<i>afa</i>	The non-fibrous adhesin binds to the DAF receptor on the cell surface epithelium as well as type IV collagen and members of the CEACAM family, hemagglutination capacity	UPEC
Dr fimbriae	<i>dra</i>	Binding to the DAF receptor on the surface epithelial cells as well as type IV collagen and members of the CEACAM family, mediation of internalization bacteria to the host cells	UPEC
P fimbriae	<i>pap</i>	Stimulate the production of cytokines by T lymphocytes, colonization factor in extraintestinal infections	UPEC, SEPEC, APEC
S fimbriae	<i>sfa</i>	Adhesion to intestinal epithelial cells, kidney, lower urinary tract cells; facilitate the penetration of bacteria into the tissues	UPEC, NMEC
FIC fimbriae	<i>foc</i>	Adhesion to renal epithelial cells and endothelial cells of the bladder and kidneys	UPEC
Iha	<i>iha</i>	Iron-regulated-gene-homolog adhesion	UPEC
Mat	<i>mat</i>	Meningitis associated and temperature regulated fimbriae	NMEC
Curli fiber gene	<i>crl, csg</i>	Enable biofilm formation and promote pathogenicity	UPEC, SEPEC, APEC
Antigen43	<i>agn43(flu)</i>	Protein of autotransporter family, adhesion and biofilm development	UPEC
Invasins			
Ibe ABC	<i>ibeA,B,C</i>	Cell invasion into the host tissues	NMEC, SEPEC, APEC

Untreated *E. coli* UTIs can progress into BSIs caused by bacteria travelling across the tubular epithelial barrier in the kidneys (Flores-Mireles et al, 2015). Adherence and colonisation play an integral role in the colonisation of the urethra and migration upwards through the urinary tract. Adhesins that are frequently identified amongst patients with UTIs include *sfa*, *iha*, *papC* and *foc* (Hagan et al, 2007). Pathogens such as uropathogenic *E. coli* (UPEC) utilise a range of adhesins and pili encoded by *fimH* for adherence to help facilitate adherence, colonisation and invasion (Flores-Mireles et al, 2015). UPEC have s-fimbrial and p-fimbrial adhesins which bind to the S and P

fimbrial receptors on epithelial cells in the urinary tract. The presence of particular virulence factors has been attributed to certain symptoms and clinical outcomes of infection. For example, immune evasion via human endothelial cell invasion has been associated to presence of the *ibeA* gene (Bonacorsi & Bingen, 2005), which is involved in the pathogenesis of MNEC (Huang et al, 1995). Furthermore, siderophores including aerobactin and yersiniabactin are secreted for obtaining iron and toxins such as *hlyA* and *cnf1* are released to aid with overcoming host immunity (Nielubowicz & Mobley, 2010).

As well as ExPEC with known virulence factors, it is possible for *E. coli* to cause BSI with a limited repertoire of virulence genes by entering the bloodstream through a perforation of the GI tract, or through an IV catheter, for example. Hence these are entirely “opportunistic” infections.

Diarrhoea causing IPEC are characterised as *E. coli* that cause infection within the GI tract in humans due to its associated virulence factors identified in IPEC, with the same virulence factors found to also cause infection in animals, though often they are animal commensals, leading to cases of “food poisoning” where animal faeces contaminates food, which is then not cooked or washed properly prior to consumption (Kaper et al, 2004). Enteraggregative *E. coli* (EAEC) are characterised by the ability to create “stacked brick” formations by binding to each other. Aggregative adherence fimbriae (AAFs) are structures that aid with the aggregation of EAEC (Kaper et al, 2004) and *aggR* regulates the genes encoding AAFs (Morin et al, 2013). Thus, to identify EAEC, *aggR* is used as a gene marker using molecular methods (Nataro et al, 1994). Enterotoxigenic *E. coli* (ETEC) are characterised by heat-labile enterotoxins and heat-stable enterotoxins (Kaper et al, 2004). These enterotoxins disrupt the fluid homeostasis of the intestine and cause hypersecretion of fluid and electrolytes

(Hughes et al, 1978; Moon, 1978). Heat labile enterotoxins are also produced by *Vibrio cholerae*, with 80% of amino acids shared with ETEC. Thus, they both cause watery diarrhoea (Kaper et al, 2004). Enteroinvasive *E. coli* (EIEC) are characterised by their invasive ability due to their possession of the plasmid-borne type III secretion system encoded by genes *mxi* and *spa* (Kaper et al, 2004). *Shigella* spp. are pathogenically and genetically related to *E. coli* and both possess this secretion system (Pupo et al, 2000). Secretion of four main proteins, IpaA, IpaB, IpaC and IpgD cause a cascade of events which optimise invasive ability (Kaper et al, 2004). Similar to ETEC, EIEC can also cause watery diarrhoea (Kaper et al, 2004). Diffusely-adherent *E. coli* (DAEC) are characterised by the mechanism utilised for colonisation to induce a diffuse pattern of adherence from bowel enterocytes subsequent to the binding of adhesion F1845 to the receptor (Kaper et al, 2004). Acute and persistent diarrhoea are often caused by DAEC (Lozer et al, 2013). The characteristics of Enteropathogenic *E. coli* (EPEC) involve attachment to intestinal epithelial cells and the production of lesions, known as 'attaching and effacing' (Kaper et al, 2004). EPEC causes diarrhoea with concerns of infant diarrhoea commonly occurring in developing countries (Podewils et al, 2004; Ugboko et al, 2020). Lastly, characteristics of Shiga toxin-producing *E. coli* (STEC) involve the production of shiga toxins encoded by *stx1* and *stx2*, causing haemorrhagic colitis which can lead to the development of haemolytic uremic syndrome (Joseph et al, 2020).

1.4.2 *E. coli* population structure

Classification of the clonal population of *E. coli* includes the assignment of 8 phylogroups (A, B1, B2, C, D, E, F and G) (Beghain et al, 2018). ExPEC comprises of many lineages involving a variety of STs defined by using multi-locus sequence typing (MLST), which is a strain subtyping method based on the sequencing and comparison of 7 housekeeping genes. The alleles of each of the housekeeping genes are assigned an allele number and the allele numbers of all 7 housekeeping genes equate to a unique ST (Maiden et al, 1998; Maiden, 2006; Maiden et al, 2013). STs of ExPEC are constrained to their geographical location. Despite the fact this, ST131, S69, ST95, ST73 and ST127 are predominant lineages (Riley, 2014; Kallonen et al, 2017; Yamaji et al, 2018). A study was conducted to identify the most prominent lineages globally between 1995 to 2018 and analysis revealed variation was observed with ST95 over this time period whilst ST10 remained constant (Manges et al, 2019). Furthermore, ST131 has been the prominent ExPEC ST since 2000 (Manges et al, 2019). ST131 belongs in phylogroup B2 and phylogenetics show ST131 comprises of 3 clades, A, B, C, with C subdividing into C1 and C2 (Figure 2). The majority of ST131 have O25:H4 serotypes, which are defined by their combination of O (somatic), H (flagella) and K (capsular) antigens. The dissemination of serotypes such as O16:H5 have been observed in Europe and Asia (Dahbi et al, 2013; Matsumura et al, 2012; Olesen et al, 2013).

Core single-nucleotide variants, also known as single nucleotide polymorphisms (SNPs) aid with understanding evolutionary rates (the rate at which new mutations arise within species or lineages) during the divergence of each ST131 clade. An evolutionary rate of ST131 was estimated at approximately 2.46×10^{-7} mutations per site annually, equating to 1 mutation arising in a single genome per year by Stoesser

et al. (2016). High prevalence of ST131 has been reported across UK and Europe and often display the highest resistance to β -lactams and FQs of all STs causing human infections (Rooney *et al.*, 2009; Dhanji *et al.*, 2011; Findlay *et al.*, 2020; Flament-Simon *et al.*, 2020).

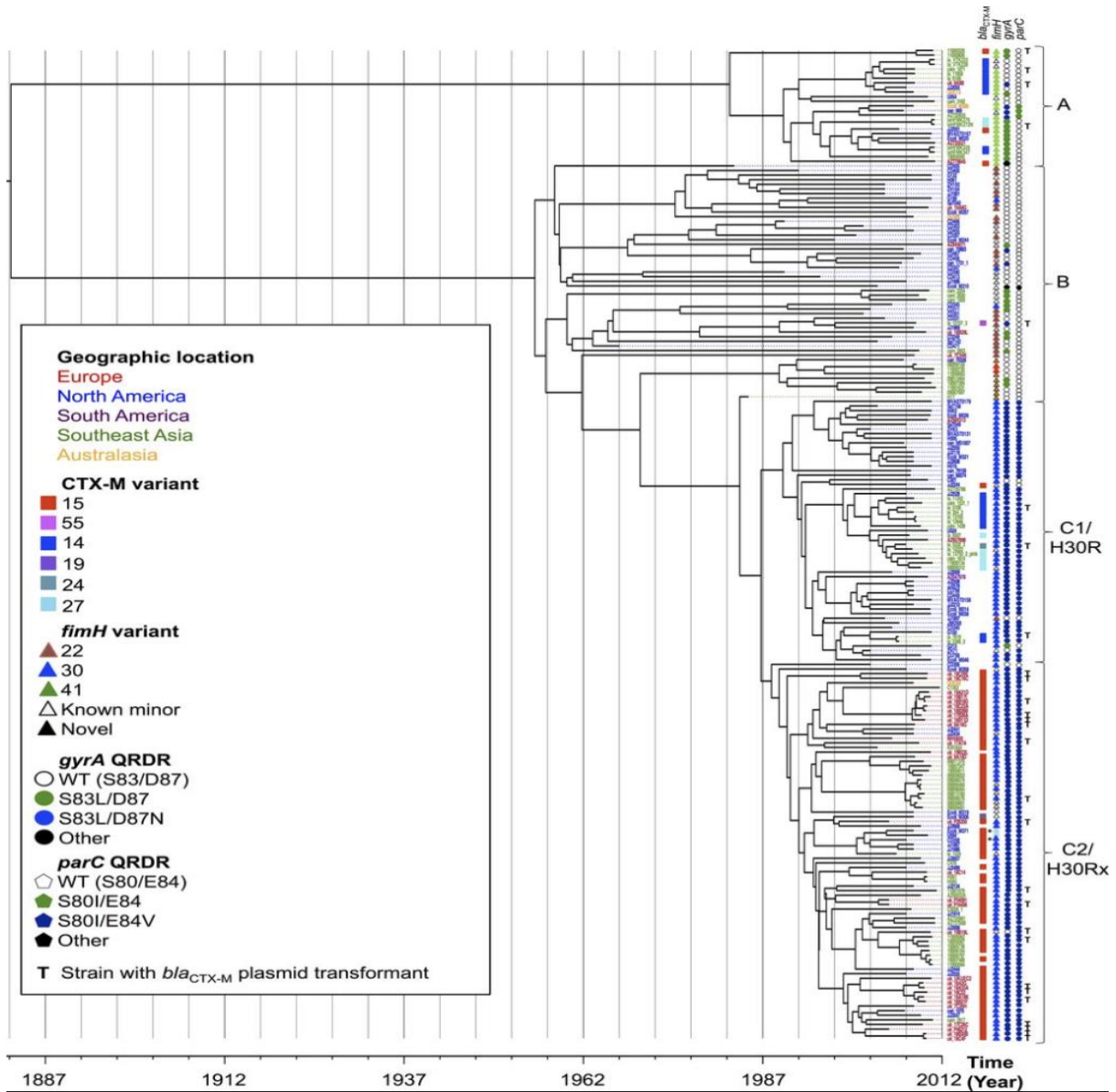


Figure 2. A timed-scale phylogeny displaying all clades of ST131 with the associated *fimH* variants, associated AMR profiles including mutations in quinolone resistance determining regions and CTX-M variants, global transmission from geographical information. Taken from Stoesser *et al.* (2016).

ST69, also referred to as clonal group A, belongs to phylogroup D and is commonly associated with UTIs and BSIs (Skjøt-Rasmussen et al, 2012; Adams-Sapper et al, 2013). Serotypes O11, O15, O17, O44, O73, O77, O86 and O125ab form the majority of serotypes identified in ST69. The prevalence of ST69 varies with studies revealing up to 15% in Europe and South America (Blanco et al, 2011; Souza da-Silva et al, 2020).

ST95 is associated mainly with BSIs, specifically neonatal meningitis in addition to UTIs. This ST belongs to phylogroup B2 (Riley, 2014) and is classified into serogroups O1:K1:H7, O2:K1:H7 and O18:K1:H7 (Riley, 2014). Within the ST95 lineage, the ColV⁺⁺ clade were sourced from both humans and avians (Cummins et al, 2022). Avian pathogenic *E. coli* (APEC) can be identified in ST95 causing colibacillosis in birds (Riley, 2014). In contrast to other widespread ExPEC lineages, ST95 display low frequency of AMR, in particular, resistance to antimicrobials used as treatments for UTIs and BSIs (Allegretti et al, 2022).

ST73 belongs to phylogroup B2 and is often associated with serotypes O6, O2 and O18, however the most dominant serotype is O6:H1 (Saidenberg et al, 2022; Riley, 2014). This serotype can cause BSIs and UTIs, however a study revealed zoonotic potential between APEC and ST73 due to the large percentage of virulence genes shared between the two types (Cunha et al, 2017). The prevalence of ST73 of BSIs is relatively high in the UK (up to 15%) and associated with high levels of resistance to a range of antimicrobial classes (Jauneikaite et al, 2022; Alhashash et al, 2016).

ST127 belongs to phylogroup B2 and is associated with UTIs. The main serotype observed in ST127 is serotype O6:31 also carry high zoonotic potential and has been observed in canine infections (Johnson et al, 2008). A phylogenetic study revealed clusters of ST127 containing origin isolates from household pets such as dogs and

cats together with human origin isolates (Elankumaran et al, 2022). Low levels of AMR and prevalence (up to 6%) have been reported for ST127 lineages (Gibreel et al, 2012)

1.5 *Klebsiella* spp.

1.5.1 Characteristics of pathogenic *Klebsiella* spp.

Carl Friedlander first described *K. pneumoniae* after isolation from lungs of patients with pneumoniae (Ashurst & Dawson, 2023). *Klebsiella* spp. frequently cause healthcare-associated infections (Table 4) (Podschun & Ullmann, 1998).

Table 4. Table displaying the different kinds of infections caused by *Klebsiella* spp. and the ranking in comparison with other pathogens. Taken from Podschun & Ullmann, 1998.

Infection	% of infections caused by <i>Klebsiella</i>	Rank ^a
UTI	6–17	5–7
Pneumonia	7–14	2–4
Septicemia	4–15	3–8
Wound infections	2–4	6–11
Nosocomial infections in intensive care unit patients	4–17	4–9
Neonatal septicemia	3–20	2–8

K. pneumoniae is highly prevalent in clinical settings and categorised as an ESKAPE organism (*E. faecium*, *S. aureus*, *K. pneumoniae*, *Acetobacter baumannii*, *P. aeruginosa* and *Enterobacter* spp.), notable for high levels of AMR and possessing a multitude of virulence factors (Navon-Venezia et al, 2017).

K. pneumoniae can be characterised by its ability to cause community and healthcare-associated infections, especially BSIs and UTIs. With similar mechanisms to UPEC described previously, *K. pneumoniae* strains utilise type 1 pili containing *fimH* to aid with colonisation, however protein modelling and mouse infection models reveal weaker binding specificity than the *fimH* located at the end of pili in UPEC (Rosen et al, 2008). In spite of this, *K. pneumoniae* possess numerous pili, such as chaperone-usher pathway (CUP) and type 3 pili that promote biofilm formation and the persistence of UTIs (Murphy et al, 2013).

1.5.2 *Klebsiella* spp. population structure

A large diversity of species are classified under *Klebsiella* spp., with a distinguished *K. pneumoniae* complex, referred to as *K. pneumoniae* species complex (KpsC) separate to other *Klebsiella* spp., despite sharing a 90% average nucleotide identity. (Figure 3) (Wyres et al, 2020). KpsC can be classified into 7 phylogroups (Dong et al, 2022) (Table 5), which can be further divided into respective STs in their clonal group/complexes using a clustering algorithm, eBURST (Feil et al, 2004).

Table 5. Table displaying the 7 phylogroups of *K. pneumoniae*.

Phylogroup	Name
Kp1	<i>K. pneumoniae</i>
Kp2	<i>Klebsiella quasipneumoniae</i> subspecies <i>quasipneumoniae</i>
Kp3	<i>Klebsiella variicola</i> subspecies <i>varicola</i>
Kp4	<i>Klebsiella quasipneumoniae</i> subspecies <i>similipneumoniae</i>
Kp5	<i>Klebsiella variicola</i> subspecies <i>tropica</i>
Kp6	<i>Klebsiella quasivarricola</i>
Kp7	<i>Klebsiella africana</i>

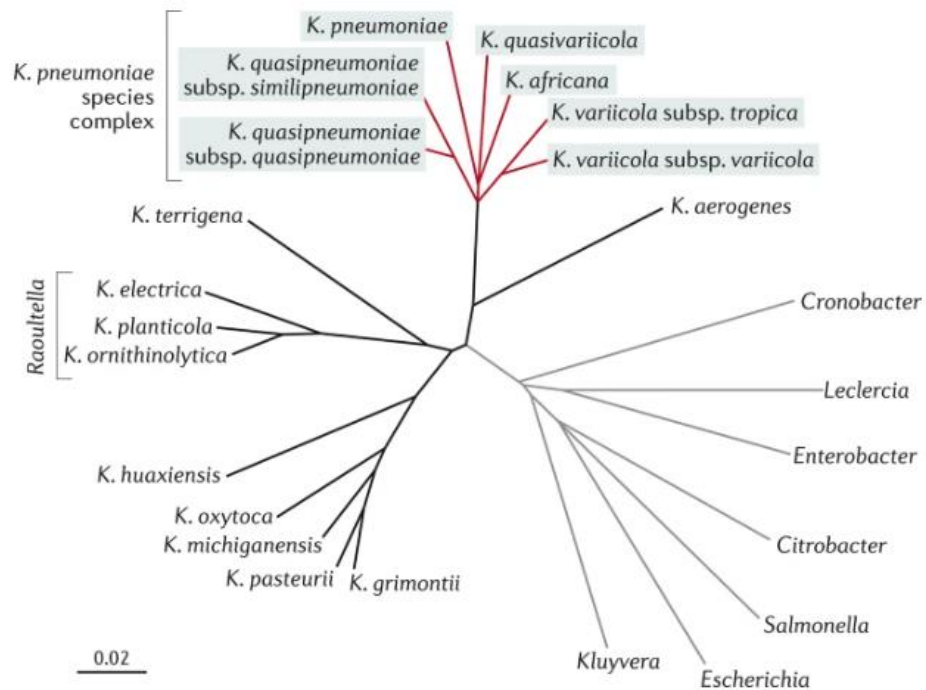


Figure 3. Phylogeny showing the relationships between KpSC, (red branches) and the other *Klebsiella* spp., *E. coli* and *Salmonella* spp. Taken from Wyres *et al.* (2020).

The size of *K. pneumoniae* genomes range between 5-6Mbp with the core genome containing ~1,700 genes compared to the >100,000 genes in the total pangenome (Wyres et al, 2020). Phylogenies based on the core genome display definitive clonal groups, defined by cgMLST (Bialek-Davenet et al, 2014) (Figure 4), which show different rates of resistance to β -lactams, aminoglycosides and quinolones (Wyres & Holt, 2016).

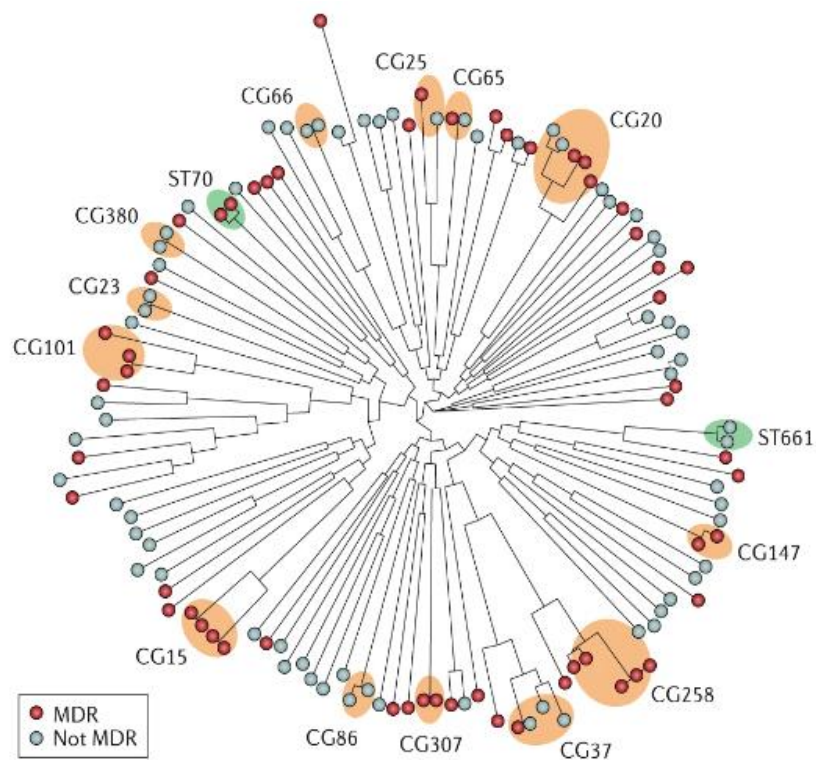


Figure 4. Phylogenetic lineages of *K. pneumoniae* establishing different clonal groups and the association with AMR. Taken from Wyres *et al.* (2020).

The majority of the CG258 clone, including ST512, ST258, ST11, ST340 and ST437 belongs to *Klebsiella* carbapenemase (KPC)-producing *K. pneumoniae*, a globally multidrug resistant (MDR) and hypervirulent clone (Dong et al, 2018). Hypervirulent *K. pneumoniae* strains are normally acquired from the community and affect immunocompromised patients in comparison to classical strains, which is associated with nosocomial infections amongst immunocompromised patients. Hypervirulent *K. pneumoniae* can be identified with their possession of extensive virulence genes in comparison to classical *K. pneumoniae* strains, including *peg334*, *iroB*, *iucA*, *prmpA* and *prmpA2* (Russo et al, 2018). Hypervirulent clones were first reported from the Asian Pacific Rim and are now distributed globally. CG23 is predominantly the most hypervirulent clone, possessing a high pathogenicity cassette harbouring a multitude of virulence factors (Dong et al, 2022). MDR and virulent *K. pneumoniae* established two separate lineages, nevertheless, genetic diversity and recombination have resulted in lineages displaying multidrug resistance and hypervirulence in the same lineage simultaneously (Dong et al, 2022), posing a public health concern. To date, many studies have reported MDR and hypervirulent strains worldwide (Tang et al, 2020). Dong *et al.* 2022 collated information regarding MDR and hypervirulent STs of *K. pneumoniae* previously described in literature, providing an overview of the MDR and hypervirulent STs worldwide (Figure 5).

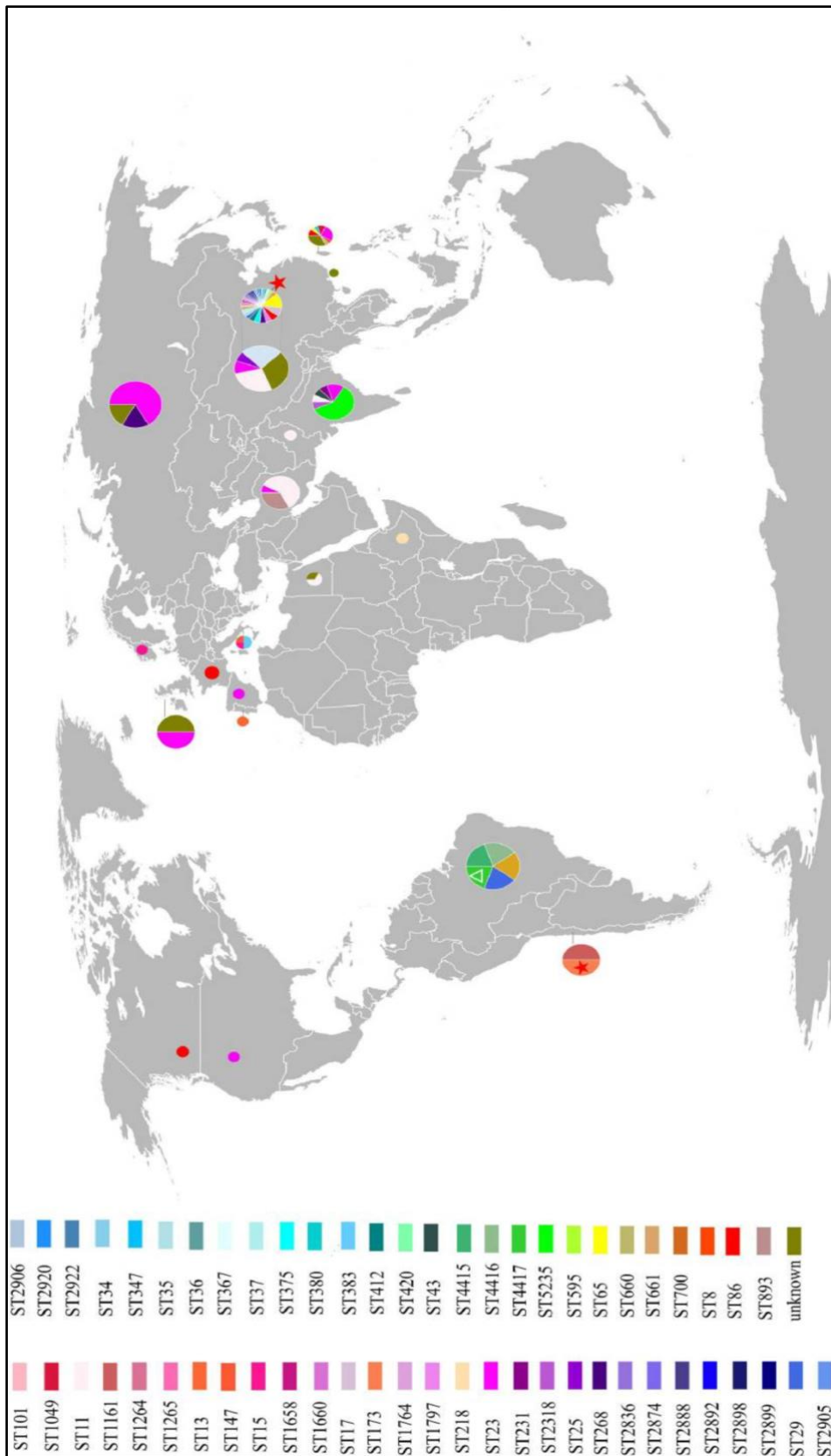


Figure 5. Global distribution detailing most resistant and hypervirulent STs of *K. pneumoniae* revealing regional differences. Taken from Dong *et al.* (2022).

1.6 Typing and WGS of *E. coli* and *Klebsiella* spp.

Traditional microbiological and biochemical approaches have historically been utilised for distinguishing *E. coli* and *Klebsiella* spp. For example, spot indole tests were utilised for distinguishing between members of *Enterobacteriales* family (Vracko & Sherris, 1963). Rapid identification of *E. coli* involved a combination of indole, oxidase tests and observing morphology on sheep blood agar plates. *E. coli* display as Gram-negative rods under microscopy and are lactose positive, indole positive and oxidase negative (York et al, 2000). Similarly, *Klebsiella* spp. display as Gram-negative rods, and are oxidase positive, lactose positive but indole negative (Hansen et al, 2004). Currently, Matrix Assisted laser Desorption Ionisation Time of Flight (MALDI-TOF) mass spectrometry is commonly used to identify species for positive blood cultures. For surveillance purposes, molecular methods using sequencing technologies and bioinformatics are increasingly used. Examinations of the population structures of *E. coli* and *Klebsiella* spp. are performed by MLST, as described above. However, MLST alone is not able to provide sufficient information to distinguish variants of a single clone such as different lineages of ST11 in *Neisseria meningitidis* (Jolley et al 2012). WGS enables the curation of databases where systems are required to organise the wealth of data now available. These data allow the identification of pathogens by species and ST, detection of the presence of AMR genes, virulence factors which can infer drug susceptibility and pathogenicity. These can be used to study phylogenies, potential transmission, mobile genetic elements, and horizontal gene transfer. This information is crucial to tracking outbreaks, facilitating outbreak management and informing policy.

1.7 AMR in BSI and UTI pathogens:

1.7.1 Burden of AMR

AMR is a public health concern and the O'Neill report estimated that by 2050, 10 million people per year will die from infections caused by AMR pathogens globally (O'Neill, 2016). AMR bacteria are currently costing the EU \$1.5 billion per annum to combat in direct healthcare costs. Increasing AMR in combination with increased incidence of BSI and UTI, will consequently have a great impact on financial costs in healthcare settings. Investment for new classes of antibiotics, better co-ordination of animal and human AMR surveillance systems and improvement of empiric antibiotic choices for treatment are a few of the current strategies outlined by UK's 5 year AMR Strategies led by Public Health England (now UKHSA) (O'Neill, 2016). As discussed earlier, antimicrobials such as 3GCs, are initiated empirically for BSIs and complicated UTIs. They are generally prescribed in the absence of a microbiological culture and the associated antimicrobial susceptibility testing results. (Najar, Saldanha & Banday, 2009; Lee et al, 2017). AMR is inextricably associated with antibiotic prescribing. The inappropriate use of antimicrobials has exacerbated the global issue of AMR, resulting in reduced choices for empiric antimicrobial treatment. A study conducted by Kadri *et al.* (2021) revealed 1 in 5 BSI patients in US hospitals received inappropriate antimicrobial therapy, even reducing survival amongst patients not initially presenting with sepsis. Curtailing the selection and dissemination of AMR is a possibility and laudable progress has been made to mitigate the impact. AMR local indicators are publicly available data (Public Health England, 2020) enabling comparisons between AMR patterns observed locally and nationally. Nevertheless, there is still insufficient knowledge of the relationship between circulating local AMR genotypes, how they manifest as phenotypic AMR and how this data could optimise and inform empiric

antimicrobial prescribing. Data produced from surveillance of local AMR patterns from clinical samples can be correlated with clinical data and demographics from patients, which enable investigation into the underlying epidemiology. AMR surveillance data can therefore drive better decisions on empiric antibiotic choice in a way stratified by patient group (AMR rates in children is different from that in elderly patients in residential care, for example) and can facilitate formulation of infection prevention and control (IPC) policies. It is possible that in the near future as WGS technologies inevitably improve, that WGS of bacteria directly from clinical samples may become routine. Therefore, WGS data in combination with computational methodologies enable the ability to identify transmission networks and potential to predict phenotypic AMR, virulence and other clinically important traits, will become central to IPC and antimicrobial stewardship policies set at regional level.

1.8 Phenotypic and genotypic AMR detection

AMR detection can be performed by traditional phenotypic, molecular based methods, and in more experimental cases, mass spectrometry (Figure 6). (Gajic et al, 2022).

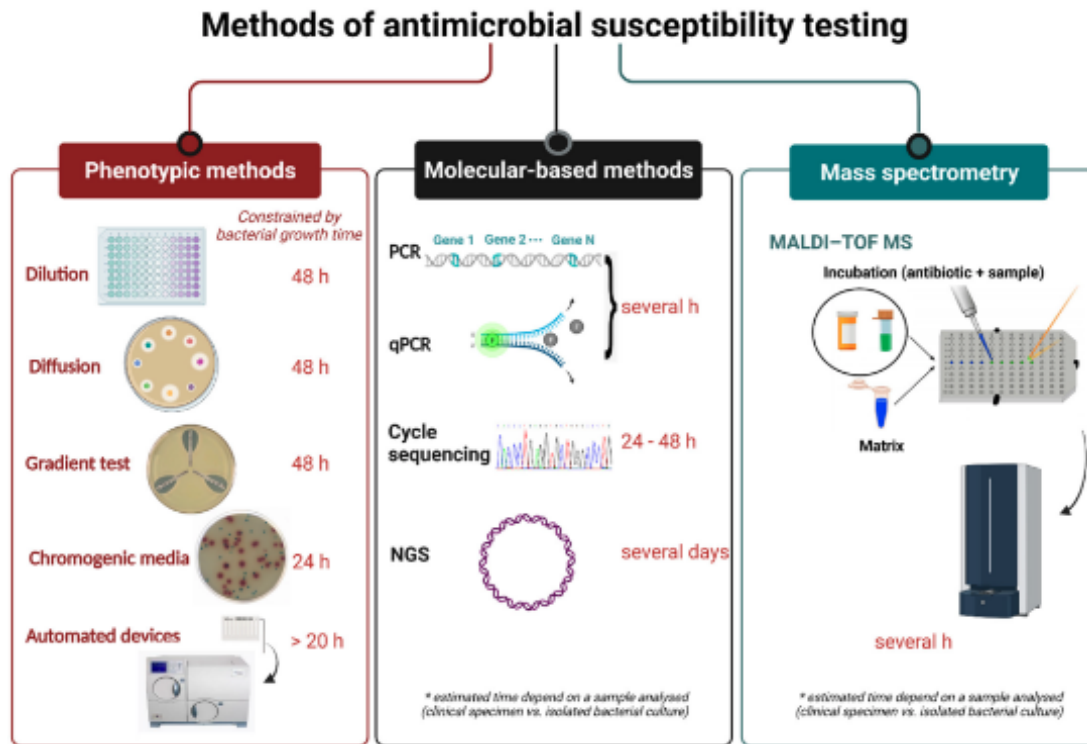


Figure 6. Summary of the different methods utilised for antimicrobial susceptibility testing and the associated turnover time. Taken from Gajic *et al.* (2022).

Broth and agar based dilution methods define the minimum inhibitory concentrations (MICs) of antimicrobials, where the MIC value defines drug susceptibility or resistance to the antimicrobial tested based on a clinically-defined “breakpoint” (Gajic et al, 2022). The gradient test involves an antimicrobial strip placed on inoculated agar. An MIC value can be detected from the zone of inhibition using the concentration measurements on the strip. E-tests is a type of gradient test used for the determination

of MICs, and for phenotypic ESBL and AmpC β -lactamase detection in *Enterobacterales* by using strips with a BL/BLI combination since, for example, ESBLs are susceptible to the BLI clavulanic acid but AmpC enzymes are not (Gajic et al, 2022). Disc diffusion is used widely in clinical settings and involves the measurement of zone of inhibition from outward antibiotic diffusion from the disc placed on inoculated agar, where the zone of inhibition is proportional to MIC (Gajic et al, 2022). Double disc synergy is another approach where inhibitors and inducers are used to manipulate the MIC (and so zone diameter) around a disc containing the test antibiotic, providing indicators at the mechanism.

All phenotypic antimicrobial susceptibility methods used clinically are standardised by the European Committee on Antimicrobial Susceptibility Testing (EUCAST) and or the American Committee for Laboratory Standards Institute (CLSI), which also publish MIC and disc zone of inhibition breakpoints set to define resistance and susceptibility, where different breakpoints can be defined for different species (EUCAST, 2023; CLSI, 2018). Automated devices such as VITEK, COMPACT and Alfred 60AST systems measure bacterial growth from growth curves and provide a pseudo MIC, which is calibrated against standardised methods. They are separately validated from EUCAST or CLSI and widely used because of their ability to be automated (Kaprou et al, 2021). Unconventional methods such as MALDI-TOF can potentially be used in AMR diagnostics (Kaprou et al, 2021). The sample is combined with a matrix and crystallises when dried. This is placed in the MALDI-TOF where separation of the ionised sample is based on mass to charge ratio takes place, producing a mass spectrum (Kaprou et al, 2021). The peaks provide information on the identification of the pathogen and has the ability to detect carbapenem resistance because pre-incubation of a carbapenemase-producing bacterium with a carbapenem leads to the carbapenem

being broken down, resulting in a signature peak on the mass spectrum (Hoyos-Mallecot et al, 2014).

Contrary to phenotypic methods, WGS including both long and short read sequencing always defines the molecular mechanisms of AMR (provided that the mechanism is one that has been reported previously). For this, bioinformatics tools are used to detect known AMR genes or mutations in chromosomal genes. Numerous studies have performed WGS analysis to determine the occurrence and presence of AMR genes in bacterial populations (Vélez et al, 2017; Brouwer et al, 2023). Due to the rapid dissemination of AMR genes worldwide, long read sequencing with Nanopore enables the determination of islands on chromosomes and plasmids harbouring multiple AMR genes, providing crucial information for infection control and monitoring. This is because such islands usually include repetitive sequences that cannot be resolved as contiguous in the assembly of short read sequencing data. Hence these elements are generally fragmented into multiple short contigs; the AMR genes are found but their relative position in the genome is not necessarily defined.

1.9 Cephalosporins and the associated mechanisms of resistance

β -lactam antimicrobials are composed of four groups, penicillins, cephalosporins, monobactam and carbapenems (Nordman et al, 2012). The mode of action involves targeting penicillin binding proteins (PBPs) to prevent peptidoglycan synthesis (Nordmann et al, 2012). Cephalosporins comprises of a β -lactam- Δ^3 -dihydrothiazine double-ring system (El-Shaboury et al, 2007). Cephalosporins are further classified into five generations by their antimicrobial properties and discovery (Table 6) (Das et al, 2019).

Table 6. Overview of the different generations of cephalosporins and activity against pathogens. Taken from Das *et al.* (2019).

Generation	Derivatives (brand names)	Description	Treatment
First	Cefazolin (ancef, kefzol), cefadroxil (duricef), cephalexin (keflex)	Gram-positive: has activity against penicillinase-producing, methicillin-susceptible, staphylococci and streptococci. Gram-negative: has moderate activity against <i>Proteus mirabilis</i> , <i>Escherichia coli</i> , and <i>Klebsiella pneumoniae</i>	Upper and lower respiratory tract infections, uncomplicated urinary tract infections
Second	Cefaclor (keflor), cefuroxime (zinacef), ceftiofur (mefoxin)	Gram-positive: has less activity than first-generation. Gram-negative: has greater activity than first-generation	Upper respiratory tract infections, skin and soft tissue infections, urinary tract infections
Third	Cefoperazone (cefobid), cefotaxime (claforan), cefdinir (omnicef)	Gram-positive: has decreased activity against Gram-positive organisms. Gram-negative: have a broad spectrum of activity and more increased activity than previous generations	Gram-negative mediated meningitis, complicated urinary tract infections and osteomyelitis
Fourth	Cefepime (maxipime), ceftazidime (ceftaz), ceftiofur (mefoxin)	Gram-positive: have extended-spectrum activity as first-generation cephalosporins. Gram-negative: exist as zwitter ions that can penetrate the outer membrane of Gram-negative bacteria. They also have a greater resistance to β -lactamases than the third-generation cephalosporins	Used in treating meningitis
Fifth	Ceftazidime, ceftazidime (ceftaz), ceftiofur (mefoxin)	Gram-negative: strongly active against <i>Pseudomonas</i> sp. and appears to be less susceptible to resistance development	Complicated abdominal and urinary tract infections

Bacteria possess a variety of mechanisms of cephalosporin resistance which can be summarised into four main types: enzymatic activity for hydrolysis of cephalosporins, mutation in PBPs altering binding affinity, reduced permeability through porin mutations or efflux pump over-production and acquisition of a non-susceptible target, which is specific to Methicillin Resistant *S. aureus* (Figure 7) (Nordmann et al, 2012).

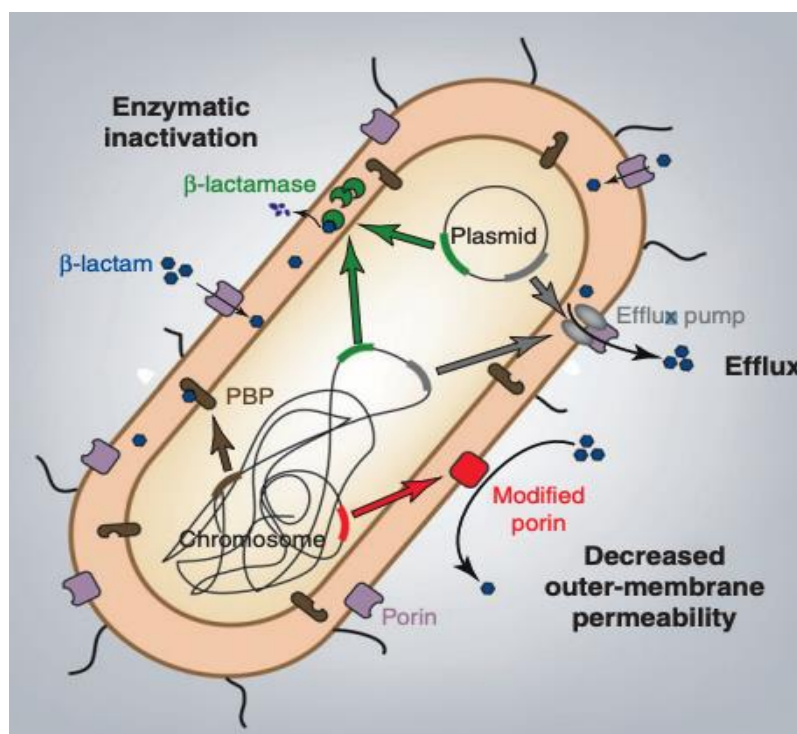


Figure 7. Primary mechanisms involved in resistance to cephalosporins.

β -lactamase production is the predominant cephalosporin resistance mechanism in clinical Gram-negative bacteria. β -lactamases are categorised into 4 classes, A, B C and D based on ancestral amino acid sequence, however another classification scheme is used based on functional properties of the enzymes, comprising group 1 cephalosporinases belonging to molecular class C, group 2 serine β -lactamases belonging to classes A and D and group 3 metallo- β -lactamases belonging to class B (Bush & Jacoby, 2009). ESBLs (extended spectrum β -lactamases) are serine β -lactamases that hydrolyse 3GCs and fourth generation cephalosporins, rendering them ineffective. Avibactam, a BLI has been used in combination with the 3GC ceftazidime to combat ESBLs, particularly KPC (*K. pneumoniae* carbapenemase), which is an ESBL with additional carbapenemase activity (Radha et al, 2023). Nevertheless, AmpC β -lactamases are cephalosporinases often encoded on the chromosome of *Enterobacterales*, mediating resistance to cephalosporins, and when expressed at high levels, this includes 3GCs and BL/BLI combinations (Jacoby, 2009). AmpC hyper-production, necessary for 3GC resistance (3GC-R) can be caused by mutations in *ampD* in *Enterobacterales* such as *Enterobacter* spp. but not in *E. coli* or *K. pneumoniae* (Jacoby et al, 2009). In *E. coli*, instead, plasmid mediated AmpC enzymes such as CMY and mutations in the normally weakly expressed, non-inducible chromosomal *ampC* gene's promoter region contributing to AmpC over-production are necessary for 3GC-R (Peter-Getzlaff et al, 2011). *Klebsiella* spp. isolates do not have chromosomal *ampC* genes, and plasmid-mediated AmpCs are therefore the only relevant molecular class C enzymes in this genus.

PBPs are enzymes involved in peptidoglycan synthesis and are the targets for β -lactams. DD-transpeptidase PBPs are involved in the last stage of peptidoglycan synthesis, catalysing the cross-linking of peptidoglycan chains to form rigid structures.

These transpeptidases harbour three structural motifs: SXXK, (S/Y)XN and (K/H)(S/T)G, defining an active site similar to those also found in class A and C β -lactamases that share the same three specific motifs and evolved from PBPs (Zapuri et al, 2008). During the acetylation stage, the active site serine of PBPs forms a covalent acyl-enzyme complex with the β -lactam, which entirely blocks future catalysis by the PBP. The β -lactamases have evolved to de-acylate this β -lactam acyl-enzyme complex, releasing hydrolysed, inactive β -lactams (Zapun et al, 2008). Mutations in PBPs can lower the binding affinity between the active site and the β -lactam, bypassing inhibition of peptidoglycan synthesis. For example, mutations in PBPs in *Salmonella* confer increased MICs of penicillin G (Sun et al, 2014) and mutations in PBP2 cause lower binding affinity for ceftriaxone in *Neisseria gonorrhoea* (Singh et al, 2020). Furthermore, insertions within PBP3 associated with aztreonam resistance in *E. coli* is another example (Zhang et al, 2017).

In order to reach the PBP targets in the periplasms of Gram-negative bacteria, β -lactams must first cross the outer membrane via porin channels. In addition to regulating the diffusion of chemicals, porins play a role in envelope integrity. β -lactams can only enter through certain porins. In Gram-negative bacteria such as *E. coli* and *Klebsiella* spp. this provides a “point of failure” by which resistance can occur. For example, mutations in *ompR* cause downregulation of OmpF and OmpC porin production in *E. coli* and *rseA* mutations activates DegP production, resulting in degradation of these porins; in both cases leading to cefalexin resistance (Alzayn et al, 2021). In *K. pneumoniae*, OmpK35 and OmpK36 are the two major porins used by cephalosporins and the loss of these porins, particularly in ESBL-and plasmid AmpC-producing *K. pneumoniae* contributes to carbapenem resistance (Khalifa et al, 2021; Din et al, 2016; Ejaz, 2022).

Efflux pumps are also found in both Gram-negative and Gram-positive bacteria, and are involved in the extrusion of antibiotics. Efflux pumps can be categorised into 5 groups: major facilitator superfamily, multidrug and toxic efflux, resistance-nodulation-division (RND), small multidrug resistance and ATP binding cassette (Sharma et al, 2019) families. Structure of the RND superfamily comprises of three components: a protein pump in the inner membrane, membrane fusion protein and an outer membrane channel protein (Figure 8). Increased production of efflux pumps contribute to AMR. For example, overexpression of *acrAB-toIC* encoding an efflux pump from the RND family leads to carbapenem resistance in *Klebsiella* producing ESBLs (Chetri et al, 2019). Furthermore, Källman *et al.* (2008; 2009) demonstrated *acrAB-toIC* gives rise to cefuroxime resistance in both *K. pneumoniae* and *E. coli*. Given its importance in *E. coli*, AcrAB-ToIC, has been well studied. Crystallography has enabled elucidation of the structure of AcrAB-ToIC, revealing the location of binding sites for antimicrobials such as ciprofloxacin within the central cavity of the periplasmic domain in AcrB (Nikaido & Takatsuka, 2009). Studies have reported significant increases in resistance to β -lactams in isolates by simultaneous overexpression of efflux pumps and β -lactamase activity (Maurya et al, 2019; Xavier et al, 2010).

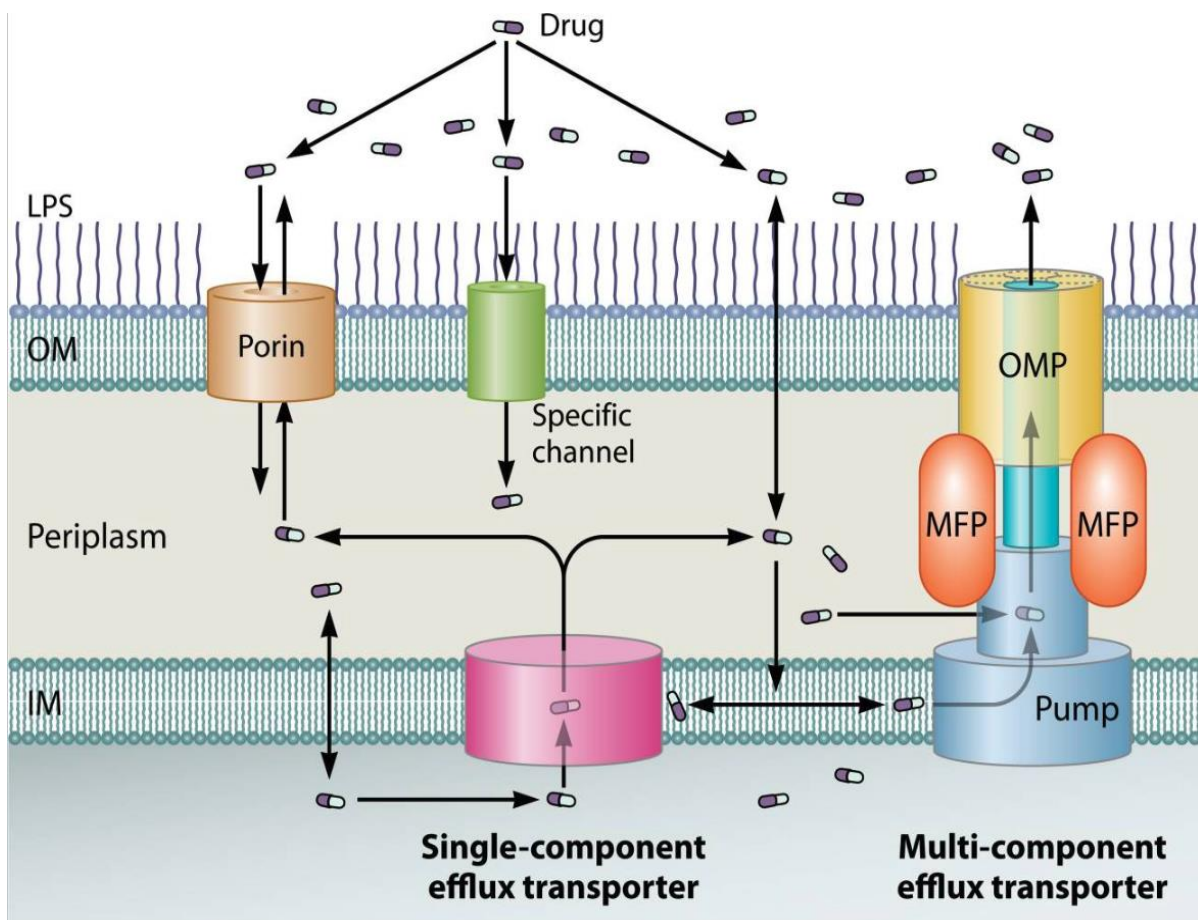


Figure 8. An illustration of the components of efflux pumps and the process by which drugs or antimicrobials are transported out of the cell in Gram-negative bacteria. IM and OM stands for inner and outer membrane respectively. Taken from Li, Plésiat & Nikaido, 2015.

1.10 Quinolones, FQs and associated mechanisms of resistance

Quinolones, in particular the FQs, are synthetic antimicrobial agents, with the first quinolone, nalidixic acid, discovered in 1962 as an impurity during the manufacture of chloroquine (Leshner et al, 1962). This discovery led to synthesis of a library of compounds which can be categorised in a classification system derived from their chemical structures, from first generation to fourth generation quinolones (Table 7).

Table 7. Overview of the quinolone classification system, adapted from Andriole, 2005.

First generation quinolone	Second generation quinolone	Third generation quinolone	Fourth generation quinolone
Nalidixic acid Cinoxacin	Norfloxacin Ciprofloxacin Lomefloxacin Ofloxacin Levofloxacin	Sparfloxacin Gatifloxacin Grepafloxacin	Trovafloxacin Moxifloxacin Gemifloxacin

In 1980, norfloxacin containing additional chemical groups fluorine and cyclic diamine piperazine, was the first FQ synthesised, a second generation quinolone, with the FQ name derived from the addition of fluorine at the C-6 position (Brighty et al, 2000). Quinolones exhibit a broad spectrum of antimicrobial activity against both Gram-negatives such as *Enterobacterales* and Gram-positive bacteria, in addition to anaerobes, with FQs exhibiting greater spectra of intrinsic activity.

Bacteria employ a myriad of strategies to overcome quinolone antimicrobial activity. Usually more than one mutation or mobile gene acquisition event is required to give resistance. One of these strategies involve chromosomal mutations in genes encoding the primary enzyme targets of resistance to FQs. In Gram-negative bacteria these are DNA gyrase and topoisomerase IV, both of which play an integral role in DNA synthesis

(Hooper, 2001). Both are tetrameric enzymes comprising of 2 subunits, GyrA and GyrB, and ParC and ParE respectively (Horowitz & Wang, 1987). Efflux is also important for FQs in Gram-negative and Gram-positive bacteria (Hooper & Jacoby, 2015). In *E. coli*, AcrAB-TolC is the most important for this (Hooper & Jacoby, 2015). FQs also enter through the OmpF porin in *E. coli* and mutations in OmpF that reduce pore size, can therefore increase MICs of FQs. Mutations in *marR* and *soxR*, part of related global regulatory systems in *E. coli* and *Klebsiella* spp., cause decreased production of OmpG as well as increased production of AcrB (Hooper & Jacoby, 2015).

There are a variety of efflux transporters that differ in their subcellular organisation, however within Gram-negative bacteria, the RND superfamily, located in the cytoplasmic membrane, are most important, conferring high levels of resistance to quinolones (Li, Plésiat & Nikaido, 2015).

Upon entry of quinolones into the periplasmic space of *E. coli*, located between the inner and outer membranes, quinolones are captured in the periplasm and extruded out of the cell by efflux pump AcrAB-TolC (Hooper & Jacoby, 2015). FQs can enter through porin diffusion channels, OmpF in *E. coli* and mutations in OmpF can confer resistance to FQs. Furthermore, reduced intake of FQs through the outer membrane and simultaneously increasing efflux is another mechanism of resistance to FQs, caused by mutations in regulators *marR* and *soxR* which contributes towards decreased expressions in *ompF* and higher levels of expression in AcrB (Hooper & Jacoby, 2015).

Plasmid mediated quinolone resistance (PMQR) has been extensively reported. The mechanisms involved include *qnr* genes which are categorised into 6 families (*qnrA*, *qnrB*, *qnrC*, *qnrD*, *qnrVS* and *qnrS*), *aac-(6')-Ib-cr* and efflux pumps encoded by *qepA* and *oxqAB* (Rodríguez-Martínez et al, 2016). Qnr prevents inhibition of FQ activity

through binding the DNA gyrase and topoisomerase IV targets and protecting them (Rodríguez-Martínez et al, 2016). The *qnr* genes have been identified on integrons located near a gene named *orf513*, which encodes a recombinase responsible for acquisition of AMR genes (Jacoby, 2005). A study reported 59.88% of ESBL-producing *E. coli* strains isolated from hospitalised patients with UTIs carried a range of *qnr* genes (Farajzadeh-Sheikh et al, 2019). Another study reported 69% of ESBL-producing *E. coli* and *Klebsiella* spp. harboured at least one *qnr* gene in addition to genes encoding the CTX-M, TEM and SHV β -lactamases (Salah et al, 2019). These studies emphasise the high frequency of plasmid mediated *qnr* genes distributed amongst ESBL-producing *E. coli* and *Klebsiella* spp., indicating the importance for infection control measures for this particular mechanism. Other PMQR genes include the aminoglycoside transferase *aac-Ib-cr*, a variant of *aac-Ib* harbouring two amino acid alterations, Trp102Arg and Asp179Tyr, is associated with resistance to kanamycin, amikacin and tobramycin (Robicsek et al, 2006). The variant *aac-Ib-cr* is responsible for the additional acetylation of the nitrogen located on the piperazine C7 ring in ciprofloxacin, norfloxacin and some other FQs (Robicsek et al, 2006). Enzymatic models indicated the point mutation Asp179Tyr is involved with interactions with the piperazine ring, whilst the point mutation Trp102Arg played a role in the strengthening of quinolone binding through position of Tyr for optimal binding (Rodríguez-Martínez et al, 2016). The prevalence of *aac-Ib-cr* is increasing globally in *E. coli* causing UTI and often associated with mobile genetic elements (MGEs) (Kim et al, 2022; Mohapatra et al, 2023; Soundararajan et al, 2016). PMQR also involve QepA and OqxAB efflux pump mechanisms. In *K. pneumoniae*, *oqxAB* is a chromosomal operon, found in all members of the species (Perez et al, 2013), where higher expression levels of *rarA* in *oqxR* mutants cause upregulation of *oqxAB* transcription, contributing

towards FQ resistance (Rodríguez-Martínez et al, 2016). The QepA efflux pump, encoded by the plasmid mediated *qepA1*, belongs to the major facilitator superfamily, responsible for reduced susceptibility to FQs and increase in the MIC (Rodríguez-Martínez et al, 2016). One study observing only 3.6% of ESBL-producing *Enterobacterales* isolates harbouring *qepA* (Shinu et al, 2020). A recent study revealed the detection of *qepA* in 12.3% of isolates, however the detection of *qnr* genes doubled (Adekanmbi et al, 2022). Similar observations have been reported in previous literature, with one study from Japan identifying 0.3% of urinary isolates harbouring *qepA* (Yamane et al, 2008) and another study revealing no isolates from a range of UTIs and BSIs harbouring *qepA* (Peirano et al, 2012). Overall, the prevalence of PMQR genes are high, with a study conducted during the pandemic revealing the detection of PMQR genes in 73.5% of *K. pneumoniae* isolates, with the detection of *aac-Ib-cr* (47.1%), *qnr* (<32.4%) and *qepA* (11.8%) in order of predominance (Abdulkareem et al, 2023). The distribution of a variety of PMQR genes in both *E. coli* and *Klebsiella* spp., including *oqxAB* have been identified in over 80% of ciprofloxacin-resistant isolates from children in Kenya (Kariuki et al, 2023). Dissemination and transmission of PMQR genes between different bacterial species is a concern due to plasmid mobility, resulting in increased difficulty for treatment.

1.11 Transmission of AMR bacteria and genes

The global threat of AMR has been attributed to a multitude of factors, one of which involves the inappropriate use of antimicrobials in both humans and animals (Figure 9). Increasingly, AMR has been observed in humans and animals without prior exposure to antibiotics, emphasising the complexity in transmission of AMR between humans and animals. To highlight that antimicrobial use contributes towards AMR in bacteria isolated from humans, an ecological study reported strong correlations of AMR patterns across multiple classes of antimicrobials in *E. coli* between humans and food-producing animals in 11 countries across Europe (Vieira et al, 2011).

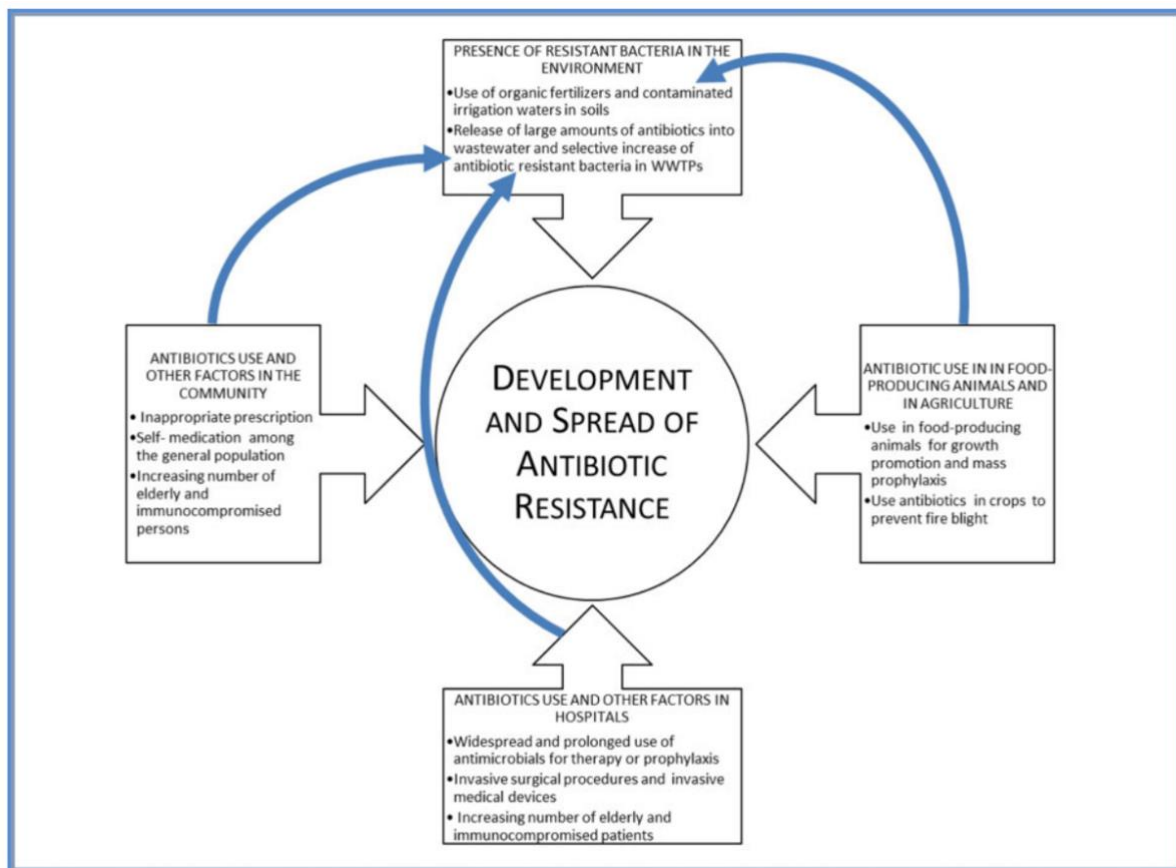


Figure 9. A schematic displaying an overview of the main factors contributing towards the spread of resistance. Taken from Prestinaci *et al.* (2015).

AMR genes are commonly associated with MGEs, which are regions of DNA that have the ability to move between different bacterial cells, and between different parts of the genome of a single cell, contributing towards the dissemination of AMR throughout a bacterial community (Patridge et al, 2018). MGEs range in size with insertion sequences (ISs) being the smallest. ISs are mobile due to a transposase enzyme, encoded by a gene which is part of the IS and usually flanked by an inverted repeat, which forms the sites of recombination essential for IS transposition (movement). ISs have an ability to alter gene expression and can mobilise other genes by forming composite transposons (Harmer et al, 2020). Elements from the IS26 family in particular, which belong within the IS6 family, can form pseudo-composite/pseudo-compound transposons (Harmer et al, 2020) and are often associated with AMR genes found in a range of Gram-negative and Gram-positive bacteria (Harmer & Hall, 2019). The IS6 family members including IS26, are homogenous and form 8bp direct repeats on insertion (Figure 10) (Varani et al, 2021). IS26 is increasingly associated with clinically important conjugative plasmids, where AMR genes are sequestered. Tseng *et al.* (2023) traced the evolution of IS26 in IncFII plasmids in carbapenem-resistant *K. pneumoniae* and revealed the structural organisation responsible for carbapenem resistance was IS26-*bla*_{KPC-2}-*bla*_{CTX-M}.

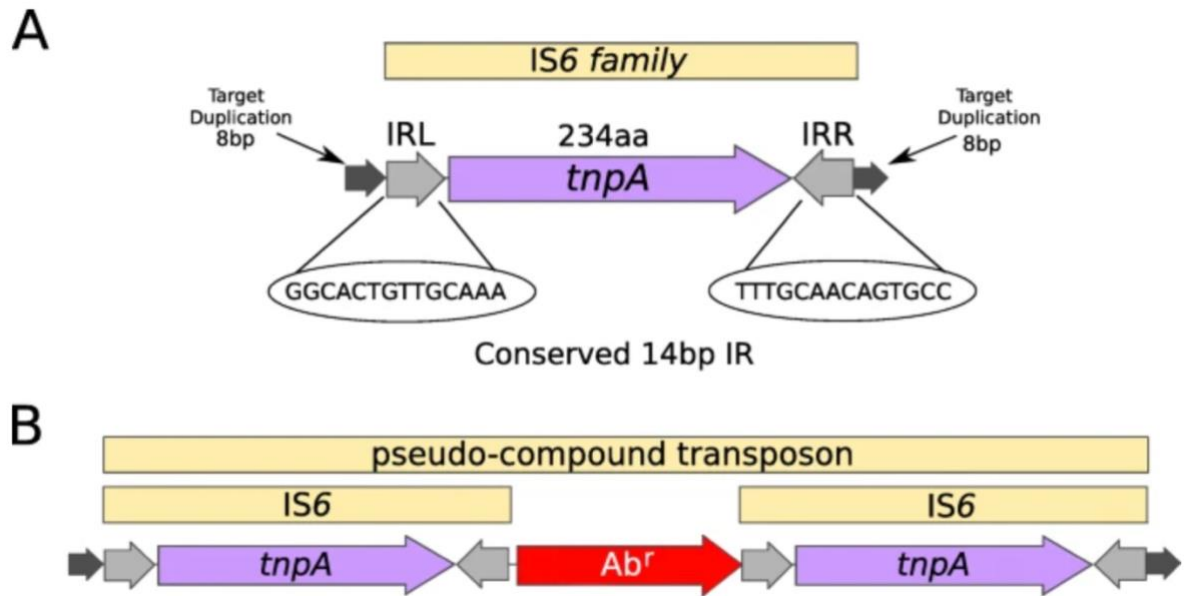


Figure 10. Overview of the characteristics of the *IS6* family including *IS26* taken from Varani *et al.* (2021). A) Displays the structure of *IS26* and the 8bp repeats are represented with black arrows. B) Displays the structure of a pseudo-compound transposon. Ab^r represents any AMR gene.

1.12 Impact of WGS, bioinformatics and surveillance on improving antimicrobial therapy and better targeted infection control

WGS has revolutionised pathogen genomics as sequencing technologies are able to provide comprehensive insight into microbial genomes, generating a plethora of biological data, producing hypotheses that need to be tested by experiments that produce and explain biological data. The power of bioinformatics has made mining WGS data more accessible. For example, the development of bioinformatics tool MobileElementFinder enables detection of MGEs and their association with AMR genes, virulence and plasmids in *Salmonella enterica* (Johansson et al, 2021).

Moreover, WGS has proven to be invaluable in infection control, identification outbreaks and studying transmission dynamics. Evidence of this was observed during the epidemic of Ebola in West Africa, where results from positive Ebola samples were generated under 24 hours due to a short sequencing process (Quick et al, 2016). These results contributed towards the surveillance system devised using Nanopore technologies, which supported the epidemic response (Quick et al, 2016). Further evidence of this was observed during local surges of SARS-COV2 cases in Netherlands from the spread of SARS-COV2 in Southern and Western Europe. With the power of WGS and bioinformatics, a time-resolved phylogeny was produced, indicating the timepoint at which SARS-COV2 emerged and circulated in Netherlands, resulting in the facilitation of early public health decision making for control of transmission (Munnink *et al*, 2020). Furthermore, the advantages of WGS have been observed for *E. coli* STEC O157:H7 foodborne outbreaks in national reference laboratories in lower and middle income countries. Comparisons between previously known STEC O157:H7 foodborne outbreaks in 2012 and 2013 in Belgium with conventional methods and WGS unveiled higher resolution of STEC O157:H7 data, enabling identification of definitive clusters and additional O157:H7 circulating in the

region, which had remained undetermined previously (Nouws et al, 2020). Despite WGS reshaping surveillance of infectious disease and outbreak tracking, challenges are still encountered. This was observed with the Zika virus outbreak in South America, where there was a delay in the detection of the transmission of the virus. As a consequence of significant reduction in viral load upon onset of symptoms, this resulted in the scarcity of viral load present in clinical samples, which affected the success of WGS (Grubaugh et al, 2018). A similar problem has been reported in the detection of West Nile Virus in birds to monitor spread in the Netherlands using Nanopore technologies (Sikkema et al, 2020).

Establishing AMR profiles by conducting antimicrobial susceptibility forms an integral part of clinical bacteriology and public health microbiological surveillance. As described above, conventional susceptibility testing involves slow, and potential inaccurate measurements of MIC or zone diameter, which is difficult to automate and subject to sample processing and batch to batch variation. For example, Bortolaia *et al.* (2020) reported 95% phenotype to genotype concordance across Gram-negative and Gram-positive species when testing WGS based antimicrobial susceptibility prediction with defined phenotypic susceptibility. However, interpretation to phenotypic tests mainly explained the 5% discordance, not the bioinformatics tool itself (Bortolaia et al, 2020). Hence, WGS may potentially become an invaluable tool for epidemiology and surveillance of AMR bacteria and in diseases such as UTIs and BSIs, where treatment is usually initiated in absence of a microbiological culture. The combination of WGS and bioinformatics tools for analysis of bacterial genomes generated directly from clinical samples (when this becomes more routinely possible) will provide real-time detection of AMR determinants and rapid prediction of susceptibility that can inform prescribing. Additionally, assessment of the genomic context of AMR

determinants plays an integral role in the prediction of emerging AMR profiles, which will enable clinicians to make better empiric choices. Whilst short read sequencing technologies such as Illumina typically produce fragmented assemblies of bacterial genomes, due to homologous sequences within the genome, generating a complete genome can be achieved by the use of long-read technologies such as Oxford Nanopore Technologies and Pacific Biosciences. Despite the ability to generate complete, closed-assemblies, long-read derived assemblies have to undergo numerous quality control and polish/error-correction steps (Loman, Quick & Simpson, 2015). The benefit to generating complete, closed-assemblies is identification of the locus of genes of interest, for example whether they are present on plasmids or the chromosome (Jain et al, 2018). This can lead to further analysis to track transmission of AMR within the community, both human and bacterial.

The implementation of WGS has already proved highly beneficial for tracking transmission of resistant infection in hospitals, leading to better infection control. A prospective epidemiological study in Melbourne Australia using WGS, reported 30.8% of patients acquired multi-drug resistance from multiple institutions and hospitals, with *vanA* vancomycin resistant *Enterococcus faecium* spreading within and between hospital sites, especially in Victoria (Sherry et al, 2022). Another study conducted in small wards in the intensive care unit in hospitals involved combining WGS and clinical data to inform transmission of outbreaks (Chi et al, 2022). It was reported that 7 carbapenem-resistant *K. pneumoniae* healthcare-associated infection outbreaks with ST11 causing 2 clonal outbreaks, A1 and A2 (Chi et al, 2022).

As described previously, multiple factors play a pivotal role in maintaining and causing high AMR rates, one of which is inappropriate antimicrobial treatment. Inadequate empirical therapy can often be made in absence of a positive microbiological culture, potentially contributing to AMR. With the power of WGS and bioinformatics software, manipulation of genomic datasets generated from sequencing can help identify AMR patterns in real-time within the community and better understand the genomic environment the AMR determinants in. These approaches will improve accuracy in administration of empirical antimicrobial choices.

1.13 PhD aims

Due to the increasing clinical challenge associated with accurate empiric therapy for patients with BSIs and UTIs, the use of WGS alongside phenotypic and clinical data may optimise antimicrobial therapy, both empirically (by the integration of regional surveillance data) and not (by speeding up susceptibility testing). Therefore, this project primarily aims to use a combination of *in silico* based AMR detection, surveillance and clinical data to understand change over time and the convergence of AMR genes in a specific region. This project also aims to consider the linkage between resistance to different antimicrobials and source of infection and whether existing tools are able to determine AMR profiles accurately. In order to achieve this, the following aims were set:

Aim 1: To understand how the prevalence of BSI caused by Gram-negative bacteria, in particular *E. coli* in Bristol and surrounding regions and its associated source of infection is affected by seasonality. Furthermore, utilising WGS and comparative genomics to monitor and compare the population structures of 3GC-R *E. coli* from community UTIs and BSIs collected in Bristol and surrounding regions between 2020

(pandemic year) and 2018 (non-pandemic year data provided prior to commencement of this project). This was conducted to assess the change in clonality.

Aim 2: To define the population structure and prevalence of *Klebsiella* spp. from BSIs in Bristol and the surrounding regions during 2020 and gain insight into the distribution of AMR genes as a function of infection source.

Aim 3: To understand the relationships between virulence genes, plasmids and AMR genes amongst *E. coli* and *Klebsiella* spp. as examples in our study region.

Aim 4: To gain an understanding of discrepancies between AMR phenotype and that predicted from genotype in the *E. coli* and *Klebsiella* BSI isolates from 2020 using Illumina sequencing data. Furthermore, to make comparisons between bioinformatics tools for the prediction of AMR to determine whether genotypic AMR prediction alone is sufficient for AMR diagnostics.

2.0 Methods

2.1 Study area

Gram-negative bacterial isolates were obtained from routine bloodstream microbiology testing at NHS diagnostic laboratory Severn Pathology, North Bristol NHS Trust, between January 2020 and December 2020 based on patients with suspected BSI admitted to, or acquiring their infection in hospitals in Bristol, Bath and Weston-Super-Mare, serving a population of 1.5 million. Isolates from UTIs were also obtained from Severn Pathology from the same population. Information regarding the study area for the *E. coli* collected in 2018 are detailed in Findlay *et al.* 2020.

2.2 Provision of clinical data

Limited, non-identifiable patient demographic data and antimicrobial susceptibility profiles for all Gram-negative isolates collected were provided by Severn Pathology.

2.3 Bacterial isolates from BSI in 2020, identification and demographics

2.3.1 *E. coli* bacterial isolates from BSI

Confirmation of purity and bacterial identification for *E. coli* was carried out upon receipt from Severn Pathology using Tryptone Bile X-glucuronide (TBX) agar (Sigma-Aldrich, Dorset, UK), where *E. coli* grew as blue colonies after incubation at 37°C for approximately 18 h. For cultures containing mixed growth of *E. coli* and other Gram-negative bacteria, these were inoculated onto MacConkey agar (Sigma-Aldrich, Dorset, UK) for differentiation in the ability for lactose fermentation. The presence of *E. coli* was identified by growth of pink to dark pink, small roundly shaped colonies surrounded by pink precipitation on MacConkey agar, which aided purification.

2.3.2 *Klebsiella* spp. isolates from BSIs

Confirmation of bacterial identification for *Klebsiella* spp. was performed by inoculation on Luria-Bertani agar (made in-house) to check for fresh confluent growth and purity after incubation at 37°C for approximately 18 h. For cultures containing mixed growth of *Klebsiella* spp. and other Gram-negative pathogens, these were inoculated onto MacConkey agar (Sigma-Aldrich, Dorset, UK) for differentiation in the ability for lactose fermentation. The presence of *Klebsiella* spp. was identified by growth of large, pink mucoid colonies on MacConkey agar, which aided purification.

2.4 Bacterial isolates from UTI in 2020, identification and demographics

2.4.1 *E. coli* bacterial isolates from UTIs

E. coli isolates from patients presenting to primary care with UTIs were collected from Severn Pathology between September 2020 and October 2020. All *E. coli* isolates were inoculated on TBX as above. For cultures containing mixed growth of *E. coli* and other species, mixtures were inoculated onto brilliance UTI clarity agar (Thermo-fisher, UK) for differentiation, detecting β -galactosidase and β -glucosidase enzyme activity, which grow as pink colonies for *E. coli*., which aided purification.

2.5 3GC-R *E. coli* BSI and UTI in 2020

3GCR *E. coli* from BSIs were defined by resistance to cefotaxime. From antimicrobial susceptibility data provided by Severn Pathology, for 3GCR- *E. coli* from BSIs, cefotaxime-resistant *E. coli* were inoculated on Tryptone Bile X-glucuronide (TBX) agar containing 2 mg/mL of cefotaxime to confirm 3GC-R status.

3GC-R *E. coli* isolates from UTIs where patients had presented to a GP practice (community UTI) within the same geographical region were also obtained from Severn Pathology based on a diagnostic flag showing resistance to cefpodxime (a 3GC). All

isolates were plated onto TBX agar (Sigma-Aldrich, Dorset, UK) containing cefotaxime (2 mg/L) to confirm 3GC-R status, and to allow comparison with 2018 isolates select this way (see section 2.4).

2.6 3GC-R *E. coli* BSI and UTI in 2018, identification, molecular screening and antimicrobial susceptibility

Information regarding 3GC-R community UTI *E. coli* collected in 2018, their identification and antimicrobial susceptibility is detailed in Findlay *et al* (2020). In summary, *E. coli* were obtained from Severn Pathology following direct culture of urine samples submitted by 147 GP practices in Bristol and surrounding regions. Cephalexin (first generation cephalosporin)-resistant *E. coli* were inoculated on TBX agar (Sigma-Aldrich, Dorset, UK) containing 2 mg/mL of cefotaxime to select 3GC-R isolates. 225 representative 3GC-R isolates were selected for WGS based on a combination of patient metadata and resistance gene complement as identified by PCR (Findlay *et al*, 2020).

3GC-R bloodstream *E. coli* isolates (n=80) were also obtained from Severn Pathology as frozen stocks based on a diagnostic flag for cefotaxime resistance. Growth on TBX agar (Sigma-Aldrich, Dorset, UK) plus cefotaxime (2 mg/L) was used to confirm resistance prior to sequencing all isolates without using any PCRs to select isolates.

2.7 WGS with Illumina and long read sequencing

2.7.1 Illumina sequencing and data processing for all isolates from 2018 and 2020

WGS was performed on BSI isolates in 2020 (irrespective of resistance) and all 3GC-R *E. coli* isolated from UTI in 2020 (collected between September and October). 3GC-R *E. coli* urinary and BSI isolates from 2018 were prepared for sequencing by Dr Jackie Findlay. All sequencing was performed by Microbes NG on the Illumina HiSeq 2500 (Illumina, San Diego, CA, USA) producing paired-ended 2x250bp reads.

Sequencing data from 2018 UTI isolates is published (Findlay et al, 2020). Data for 2018 BSI isolates were provided by Dr Jacqueline Findlay. The FASTQ reads were processed using Trimmomatic v0.39 (Bolger et al, 2014) and quality of the reads were assessed by Microbes NG's in-house scripts in combination with Samtools v1.11 (Li et al, 2009), BedTools v2.29.2 and BWA v0.5.9 (Li et al, 2009). Reads were assembled using SPAdes v3.13.0 (Bankevich et al, 2012).

2.8 Long read sequencing and data processing for selected NDM-positive *K. pneumoniae* isolates from BSIs

Long read sequencing was performed on all NDM-positive ST15 *K. pneumoniae* isolates causing BSIs with Oxford Nanopore Technologies by Microbes NG. Detailed description on the Oxford Nanopore Sequencing Platform and the bioinformatics pipeline is not publicly available from Microbes NG. Using raw reads provided by Microbes NG, isolates with lower quality assemblies were reassembled using Flye (Kolmogorov et al, 2019).

2.9 Genotyping and detection of plasmid, AMR and virulence genes

ST of *E. coli* was determined from WGS data using MOST v1.0 (Tewolde et al, 2016) (<https://github.com/phe-bioinformatics/MOST>). Abriicate v.1.0.1 (<https://github.com/tseemann/abriicate>) was used with default parameters to identify AMR genes and detect the presence of known replicon types of plasmids using the Resfinder v2.0 and PlasmidFinder v2.0 database respectively (Zankari et al, 2012; Carattoli, et al, 2014). Clermontyping v20.03 was used to identify the phylogroups within the *E. coli* population (Beghain et al, 2018). VirulenceFinder software v2.0 was used for detection of virulence genes in *E. coli*. Phenotypic AMR data for all BSI and UTI isolates were provided by Severn Pathology. ST, AMR and virulence factor genes

were determined for *Klebsiella* spp. from WGS data using Kleborate (Lam et al, 2021). Kelborate-Viz was used to visualise output from Kleborate (Lam et al, 2021).

2.10 Genome visualisation, annotation and pairwise alignment comparisons for MDR *E. coli* ST15 of *K. pneumoniae*

2.10.1 Characterisation of regions encoding AMR genes

The assembled genomes were visualised with Bandage v.0.6.2 (Wick, 2015). BLASTn (blast.ncbi.nlm.nih.gov/Blast.cgi) analysis was used to detect the presence of AMR genes and their location in the assembly graph (FASTG). Prokka v1.14.5 (Seeman, 2014) was used to annotate genome sequences and Artemis v5.1 (Rutherford et al, 2000) was used to visualize the resistance region. The orientation and position of AMR gene cassettes were visualised using Easyfig v2.2.2 (Sullivan et al, 2011) and Clinker v0.0.27 (Gilchrist & Chooi, 2021).

2.10.2 Detection of virulence and AMR genes on plasmid associated contigs from short-read assemblies for *E. coli* and *K. pneumoniae*, as well as long read assemblies for *K. pneumoniae*

Alignments were produced from Illumina assemblies of MDR *E. coli* and *K. pneumoniae* BSI isolates with plasmid references (Table 8) using progressive Mauve (Darlin et al, 2004) with default parameters to detect the presence of virulence and AMR genes.

Table 8. Plasmid reference sequences.

Plasmid type	Accession Number
IncFIA	AP019526.1
IncFIB	AP018458.1
IncFIC	NZ_CP053724.1
Incl	KP347127
Col156	NC_009781
Col440	CP023920.1
IncR	DQ449578.1

Plasmid contigs were annotated using prokka v1.14.6 before importation and comparison using Brig v0.95 (Alikhan et al, 2011).

2.11 Phylogenetic analysis

Phylogenetic trees of the same STs of *E. coli* were constructed using each sample's FASTQ file to show population variation and assess transmission and clonality. AMR data was visualised with the phylogenetic trees using iTOL v5 (Letunic & Bork, 2021). Snippy v4.3.2 (<https://github.com/tseemann/snippy>) was utilised for a core genome alignment by aligning the reads of the bacterial isolates to the reference genome. Gubbins v2.4.1 (Croucher et al, 2015) was used to account for recombination. Snp-Dists v0.7.0(<https://github.com/tseemann/snp-dists>) was used for core variant calling. RAxML v8.0.0 (Stamatakis, 2014) was used to form a maximum likelihood tree (phylogeny) of the non-recombinant SNPs.

Core genome SNP trees for were constructed for all *Klebsiella* spp. and *E. coli* isolates of different STs and using ParSNP v1.5.3 with default parameters (Treangen, et al 2014). AMR data were visualised with the phylogenies using iTOL v5 (Letunic et al, 2021).

2.12 Antimicrobial susceptibility

Fresh confluent growth was maintained through subculturing onto Mueller-Hinton agar (made in-house). A single colony was suspended in PBS and the optical density was adjusted to 0.5 McFarland (0.8-1.2OD at 600nm). Phenotypic antimicrobial susceptibility data was generated using VITEK and provided to us by Severn Pathology for all BSI sequenced. Disc susceptibility testing was performed on *E. coli* and *Klebsiella* spp. isolates and interpreted according to CLSI guidelines (CLSI, 2018; CLSI, 2021) for *E. coli* and *Klebsiella* spp. displaying discordance to the predicted

resistance profile based on genotypic data derived from WGS. Antibiotic discs used were cefuroxime (CXM 30 µg), ceftazidime (CAZ 10 µg), cefotaxime (CTX 30 µg) and cefepime (FEP 30 µg) were utilised. In addition, amoxicillin/clavulanate (AMC) and CAZ disks were placed close together (double disc synergy test) to test for ESBL production.

2.13 Polymerase Chain Reaction

2.13.1 Sample preparation for polymerase chain reactions

A single colony of each isolate tested was suspended in 100 µl of elgastat water and bacteria lysed at 95°C for 10 min. 1 µl of this lysate was added to each PCR reaction as a source of template DNA and mastermix was made containing primers (0.5 pmol/µl) (Table 9), water and 1x MyTaq polymerase (Meridian Bioscience) (Table 9). PCR tubes containing lysates were centrifuged at 3500 rpm for 5 min prior to multiplex PCR. A list of PCR primers used for this analysis is provided in Table 10.

Table 9. Volumes of reagents used for mastermix.

Reagent	Volume (µl)
Forward primer (Eurofins)	0.5/1 µl
Reverse primer (Eurofins)	0.5/1 µl
MyTaq (Meridian Bioscience)	10 µl
Elgastat water (in-house)	8 µl

Table 10. Table detailing the CTX-M group primers and product size.

Primer	Sequence (5'-3')	Product size (bp)
Group1_F	AAAAATCACTGCGCCAGTTC	415
Group1_R	AGCTTATTCATCGCCACGTT	
Group2_F	CGACGCTACCCCTGCTATT	552
Group2_R	CCAGCGTCAGATTTTTCAGG	
Group9_F	CAAAGAGAGTGCAACGGATG	205
Group9_R	ATTGGAAAGCGTTCATCACC	

2.13.2 Screening for β -lactamase genes with polymerase chain reactions

Multiplex PCRs were performed for the detection of β -lactamases genes from the five known bla_{CTX-M} groups. The PCR thermocycler conditions running for 35 cycles were followed as detailed below:

- Initial denaturation step: 95°C for 5 min
 - 35 cycles of:
- Denaturation step: 95°C for 30 s
- Annealing step: 62°C for 30 s
- Extension step: 72°C for 30 s
 - Then
- Final extension step: 72°C for 5 min

2.13.3 Gel electrophoresis

PCR amplicons from *E. coli* and *Klebsiella* spp. samples were separated on agarose gel for confirmation of product size. 1.5 g of agarose (Sigma-Aldrich, UK) was dissolved in 100 ml of 1X Tris Acetate-EDTA (TAE) buffer prior to pipetting 6 μ l of ethidium bromide (6%). 10 μ l of PCR reaction was loaded in the wells in the gel 5 μ l of 100 bp ladder (Bioline) was used. Gel electrophoresis was run in 1X TAE buffer for 50 min at 100 V using the PowerPac 200 (Bio-Rad, UK).

2.14 Comparison of variation in AMR detection with R to analyse true positive (TP), true negative (TN), false positive (FP) and false negative (FN) rates

Using R, a script was written to produce a bar chart displaying the proportions of TP, TN, FP and FN for *E. coli* and *K. pneumoniae*, *K. oxytoca*, *K. variicola*. The general script for analysis of *E. coli* and *Klebsiella* spp. are as below. Also detailed below is the script adjusted from analysis with *E. coli* to analyse specific species of *Klebsiella*.

R code for *E. coli*:

```
library(ggplot2)
df <- read.delim("~/scp/winnie/R_V4/counts_esc.txt", header = TRUE, sep = "\t", dec = ".")
p <- ggplot(df, aes(fill= class, x = method, y = count/585)) + geom_bar(position="stack",
stat="identity") + theme(axis.text.x = element_text(angle = 45, vjust = 1, hjust = 1, size = 8),
axis.text.y = element_text(size = 8), axis.title.x = element_text(size = 8), strip.text.x =
element_text(size = 7), axis.title.y = element_text(size = 8), strip.placement = "outside",
strip.background = element_rect(fill = "white")) + facet_grid(~AB, switch = "x",) +
scale_fill_manual(values = c("Red", "Orange", "Blue", "Green")) + scale_y_continuous(labels
= scales::percent)
p <- p + labs(fill = "Predicted values")
p <- p + labs(y = "Precent of samples", x = "Antibiotics and algorithms")
ggsave("~/scp/winnie/R_V4/esc_winnie.pdf")
```

R code for *Klebsiella* spp.:

K. PNEUMONIAE:

```
library(ggplot2)
df <- read.delim("~/scp/winnie/R_V4/counts_klebpneu.txt", header = TRUE, sep = "\t", dec
= ".")
p <- ggplot(df, aes(fill= class, x = method, y = count/125)) + geom_bar(position="stack",
stat="identity") + theme(axis.text.x = element_text(angle = 45, vjust = 1, hjust = 1, size = 8),
axis.text.y = element_text(size = 8), axis.title.x = element_text(size = 8), strip.text.x =
element_text(size = 7), axis.title.y = element_text(size = 8), strip.placement = "outside",
strip.background = element_rect(fill = "white")) + facet_grid(~AB, switch = "x",) +
scale_fill_manual(values = c("Red", "Orange", "Blue", "Green")) + scale_y_continuous(labels
= scales::percent)
p <- p + labs(fill = "Predicted values")
p <- p + labs(y = "Precent of samples", x = "Antibiotics and algorithms")
ggsave("~/scp/winnie/R_V4/lebpneu_winnie.pdf")
```

K. OXYTOCA:

```
library(ggplot2)
df <- read.delim("~/scp/winnie/R_V4/counts_kleboxy.txt", header = TRUE, sep = "\t", dec =
".")
p <- ggplot(df, aes(fill= class, x = method, y = count/21)) + geom_bar(position="stack",
stat="identity") + theme(axis.text.x = element_text(angle = 45, vjust = 1, hjust = 1, size = 8),
axis.text.y = element_text(size = 8), axis.title.x = element_text(size = 8), strip.text.x =
element_text(size = 7), axis.title.y = element_text(size = 8), strip.placement = "outside",
strip.background = element_rect(fill = "white")) + facet_grid(~AB, switch = "x",) +
scale_fill_manual(values = c("Red", "Orange", "Blue", "Green")) + scale_y_continuous(labels
= scales::percent)
p <- p + labs(fill = "Predicted values")
```

```
p <- p + labs(y = "Precent of samples", x = "Antibiotics and algorithms")
ggsave("~/scp/winnie/R_V4/kleboxy_winnie.pdf")
```

K. *VARIICOLA*:

```
library(ggplot2)
```

```
df <- read.delim("~/scp/winnie/R_V4/counts_klebvari.txt", header = TRUE, sep = "\t", dec = ".")
```

```
p <- ggplot(df, aes(fill= class, x = method, y = count/17)) + geom_bar(position="stack",
stat="identity") + theme(axis.text.x = element_text(angle = 45, vjust = 1, hjust = 1, size = 8),
axis.text.y = element_text(size = 8), axis.title.x = element_text(size = 8), strip.text.x =
element_text(size = 7), axis.title.y = element_text(size = 8), strip.placement = "outside",
strip.background = element_rect(fill = "white")) + facet_grid(~AB, switch = "x",) +
scale_fill_manual(values = c("Red", "Orange", "Blue", "Green")) + scale_y_continuous(labels
= scales::percent)
```

```
p <- p + labs(fill = "Predicted values")
```

```
p <- p + labs(y = "Precent of samples", x = "Antibiotics and algorithms")
```

```
ggsave("~/scp/winnie/R_V4/klebvari_winnie.pdf")
```

2.15 Statistical analysis

2.15.1 Associations between source, phylogroups, AMR and virulence

Chi-squared analysis was conducted to determine the significance of associations between phylogroups, ST, source of infection and pathogenicity.

2.15.2 Statistical comparison of precision and recall for the prediction of phenotypic AMR using several bioinformatics tools

The false positive (FP), false negative (FN), true positive (TP) and true negative (TN) rates were determined for each antibiotic class for both *E. coli* and *Klebsiella* for ABRicate, ResFinder, ARIBA and Kleborate by comparison with the “true” resistance phenotype provided by Severn Pathology. For example, if the phenotype is resistant for a particular test antimicrobial, and the isolate has an associated AMR gene located in its genome based on analysis of WGS data, AMR is correctly predicted from genotype and this is a TP. If the phenotype is resistant but the associated resistance gene or mutation is not detected, and so resistance is not predicted, this is a FN. If the

phenotype is susceptible and there is no prediction of resistance based on WGS, this is a TN. If the phenotype is susceptible, however the resistance gene is present, this is a FP. The F1 score involving precision and recall that represents the accuracy of these tools was calculated with the formulae below:

$$Precision = \frac{TP}{TP + FP} \quad Recall = \frac{TP}{TP + FN}$$

$$F1 \text{ score} = 2 * \left(\frac{(precision * recall)}{(precision + recall)} \right)$$

3.0 Results Chapter 1

Seasonality and AMR trends observed in *E. coli* from BSIs and UTIs in 2020 and 2018

3.1 Introduction

As stated in the introduction (section 1.2), there can be difficulties with accurate assessment of the incidence of UTIs in the community as diagnosis is dependent upon symptomatic patients providing positive urine cultures (Foxman, 2002). This is problematic because *E. coli* causing UTIs can lead to ascending infection through the kidneys and into the bloodstream, causing urosepsis, which is a particular public health challenge. Furthermore, as mentioned in Section 1.2 in the introduction, antimicrobials such as 3GCs, are initiated empirically for complicated UTIs to prevent sepsis. 3GCs are also administered as treatment for sepsis. 3GC-R can arise via various mechanisms including overproduction of chromosomally encoded AmpC β -lactamase enzymes and plasmid mediated AmpCs such as CMY, however it is predominantly due to dissemination of plasmid-mediated ESBLs, for example CTX-M (Findlay et al, 2020; Bevan et al, 2017). CTX-M variants are the largest group of ESBLs found within clinical isolates and their distribution varies globally, however it is evident that *bla*_{CTX-M-15} is dominant in most countries and *bla*_{CTX-M-14} is significant across Asia (Figure 11) (Bevan et al, 2017). Determination of 3GC-R mechanisms circulating in the population plays a critical role in optimising management as this information can help clinicians better understand the optimal stage to administer 3GCs during the infection in particular patients.

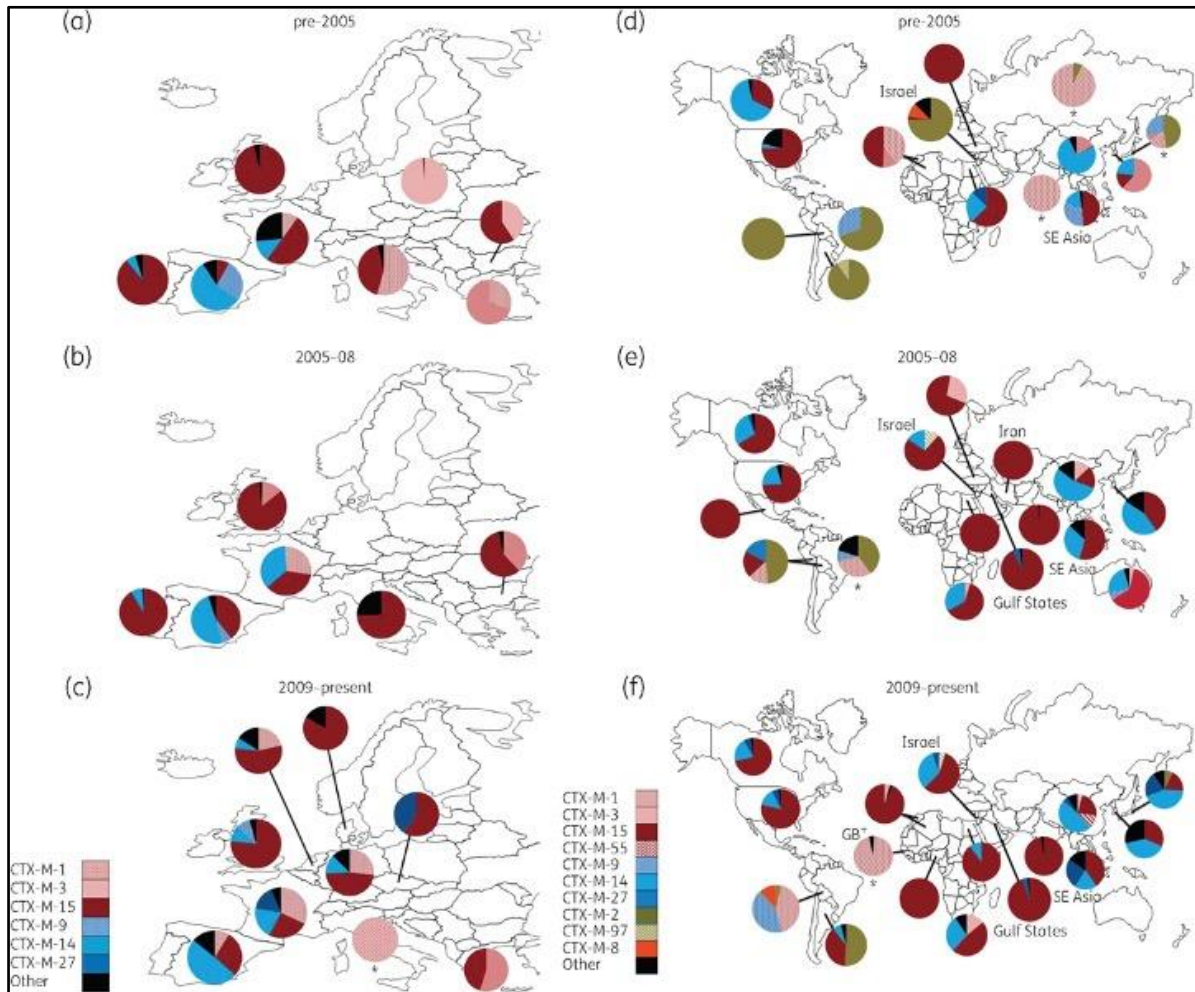


Figure 11. Overview of CTX-M variants in different time periods within Europe (a,b,c) and the rest of the continents in the world (d,e,f). Coloured pie charts represent different CTX-M variations identified in the different continents. Taken from Bevan *et al.* (2017).

The population of *E. coli* consists of 8 phylogroups (A, B1, B2, C, D, E, F and G), involving a rapid easy phylogenetic grouping technique that is based on a triplex PCR to detect *chuA*, *yjA*, *TspE4* and *arpA* (Beghain et al, 2018). As stated in the introduction, each phylogroup comprises of a variety of STs. Epidemiological surveillance of BSIs from across the United Kingdom, United States, Europe and Asia found that strains causing BSIs belong to a few clonal lineages including ST131, ST73, ST95, ST69 and

ST1193. These 5 STs were found to represent 48-66% of the isolates (Denamur et al, 2021; Kallonen et al, 2017; Day et al, 2016; Yoon et al 2018). The most prevalent ExPEC clone is ST131, which comprises of 3 clades based on *fimH* types: A, B and C and is commonly known for its resistance to multiple antimicrobial classes (Denamur et al, 2021). Within clade C, FQ-resistant sublineages C1/H30R and C2/H30Rx frequently harbour CTX-M-ESBLs, most commonly CTX-M-14 and CTX-M-15 respectively, making them resistant to 3GCs commonly used in UK hospitals, for example, cefotaxime and ceftazidime (Denamur et al, 2021). A study by Findlay *et al.* (2020) revealed clade C2 was dominant from analysis of 3GC-R urine isolates from patients in Bristol and the surrounding regions. Additionally, these 3GC-R urine isolates were resistant to ciprofloxacin (Findlay et al, 2020), displaying the same characteristics as described in the literature.

Effective treatment for suspected BSIs must involve timely intervention, including early initiation of antibiotic therapy and identification of the source of infection so that “source control” can be obtained and re-infection therefore prevented. BSIs can originate from multiple sources such as the urinary tract, as described above skin wounds, the GI tract, cardiovascular system, central nervous system, via a central line catheter and from the respiratory tract. The most common source of infection associated with sepsis overall is the respiratory tract (64%), subsequently GI tract (20%), bloodstream (15%) and urinary tract (14%) (Vincet et al, 2009; Vincet et al, 2006; Karlsson et al, 2007). Pathogen phylogroup can be associated with different sources of sepsis, as reported by Denamur *et al.* 2022, in which a strong association between phylogroup B2 *E. coli* and the urinary source of infection was shown, whilst phylogroup A and B1 displayed strong associations with the GI tract. Furthermore, there is a possibility that variation

in pathogenicity contributes to the variation of the source of infection associated with sepsis (Denamur et al, 2022).

AIM: The aim of the work reported here was to use WGS to describe the population structure of *E. coli* from BSIs and UTIs to identify changes in resistance patterns between 2018 and 2020 for both types of infection, with particular focus on 3GC-R *E. coli* processed by the NHS diagnostic laboratory Severn Pathology between January 2020 and December 2020 in Bristol and surrounding regions, serving a population of 1.5 million people.

3.2 Results

3.2.1 Temporal trend in Gram-negative BSI isolates cultured by Severn Pathology in 2020 with a focus on *E. coli*

Positive blood cultures (n=2,169) were reported by Severn Pathology between January 2020 and December 2020 where the species grown was Gram-negative, based on a Gram stain performed directly on culture-positive blood. Due to the exclusion of samples representing polymicrobial infections, 1873 bacteria were isolated in total. Bacterial species was identified using MALDI-TOF by Severn Pathology and AMR profile determined using the phenotypic, culture based VITEK system. Following removal of duplicates (n=296) (same patient, same species isolated with the same phenotypic AMR profile in more than one blood sample collected within 7 days), 1577 isolates were included in this analysis. The most common bacterial species received across the year were *E. coli* (55%), *K. pneumoniae* (10%), *P. mirabilis* (4%), *P. aeruginosa* (6%) and *Enterobacter cloacae* (5%). All isolates exhibited different seasonal variations during 2020, with *E. coli*, *K. pneumoniae* and *E. cloacae* displaying an increase in BSI frequency in the summer months between June and August, whilst *P. mirabilis* displayed a decrease in BSI frequency in this period (Figure 12). From the Gram-negative bacterial isolates obtained, there were significantly more *E. coli* infections in the summer compared to *E. coli* infections in other seasons (Table 11).

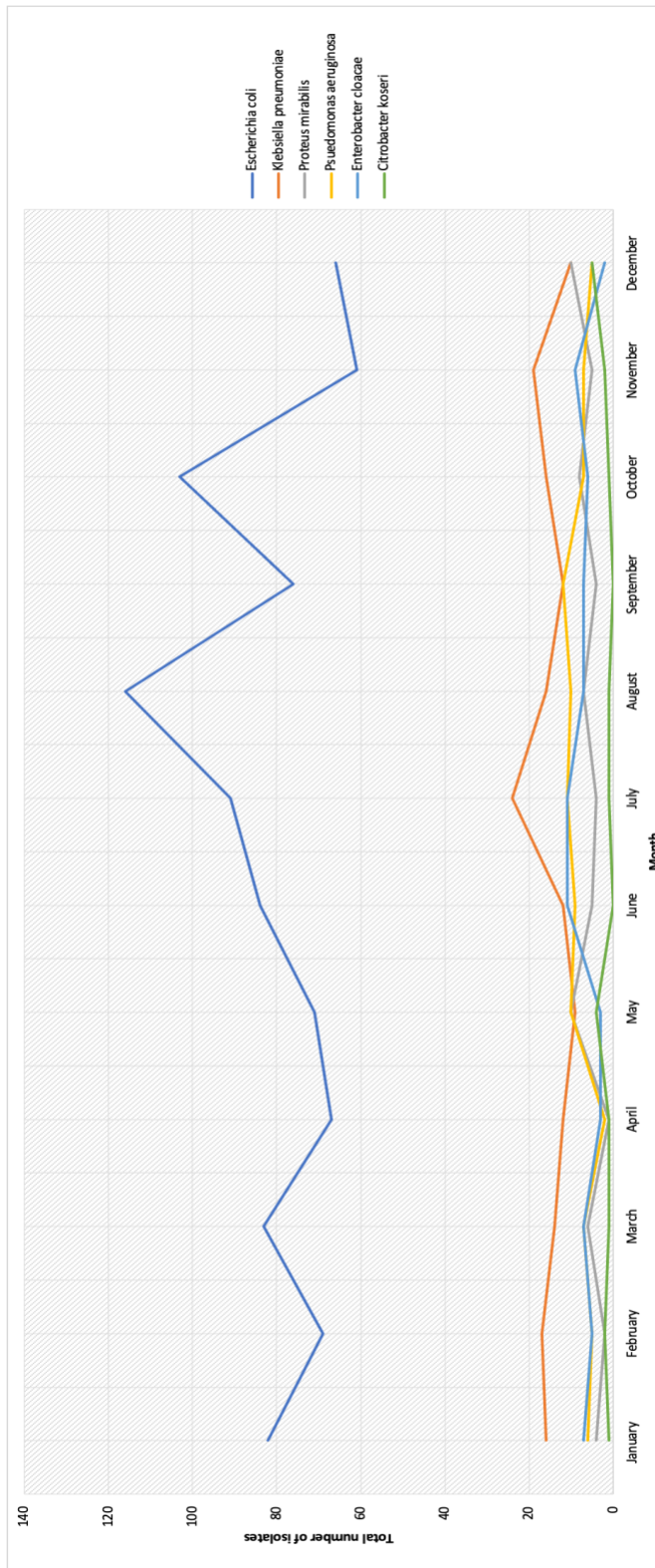


Figure 12. Total number of bacterial isolates most commonly found from different bacterial species in 2020. Details regarding species identification and study area can be found in the methods section (sections 2.1 & 2.3)

Table 11. Chi (χ^2) analysis revealed there was a statistically significant bias towards *E. coli* infections being in the summer compared with other quarters, when compared to the infections caused by *K. pneumoniae*, *Proteus* spp., *Pseudomonas* spp., *Enterobacter* spp., and *Citrobacter* spp. combined in the summer versus not in the summer.

	Winter (Dec- Feb)	Spring (Mar- May)	Summer (Jun- Aug)	Autumn (Sept- Nov)	P value	Significance
<i>E. coli</i>	217	221	291	240	0.033	Significant. at p <0.05
<i>K. pneumoniae</i>	43	35	52	47	0.896	Not significant at p <0.05
<i>Proteus</i> spp.	16	17	16	17	0.320	Not significant at p <0.05
<i>Pseudomonas</i> spp.	16	19	30	26	0.494	Not significant at p <0.05
<i>Enterobacter</i> spp.	14	13	25	22	0.441	Not significant at p <0.05
<i>Citrobacter</i> spp.	8	6	2	3	0.064	Not significant at p <0.05

3.2.2 Urinary source *E. coli* BSI was not associated with the observed increase of *E. coli* BSI in the summer months

To understand the reason behind the significant increase of *E.coli* as a cause of BSI in the summer months observed in 2020, further analysis was conducted considering the source of BSI. It was hypothesised that *E. coli* UTI may increase in the summer due to hydration or hygiene issues, therefore this may fuel a rise in urinary source BSI. Predicted BSI source data (where known) were made available for all 1577 BSI isolates provided by Severn Pathology. Analysis of the *E. coli* isolate data specifically, revealed that the most common infection sources were GI tract and urinary tract (Figure 13), with a greater proportion of *E. coli* BSI from these sources seen in July (68% of all infections represented by these two sources combined) and August (52%) respectively. However, statistical analysis revealed no association between urinary source *E. coli* specifically – i.e. compared with *E. coli* from other sources – and a rise in incidence of *E. coli* BSI in the summer months (June to August, $p > 0.05$) (Table 12). Hence, this in 2020, there appears to be a general rise in *E. coli* BSI incidence.

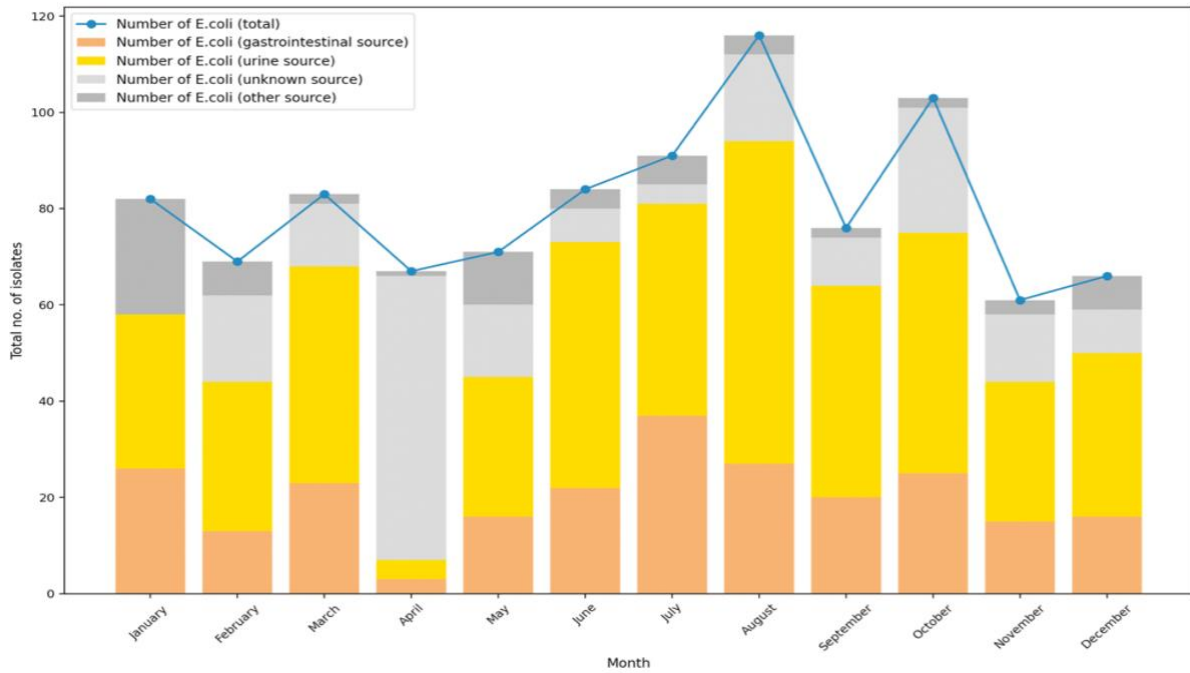


Figure 13. Number of *E. coli* collected per month in 2020 broken up by source of infection, including gastrointestinal source, urinary source, other and unknown source.

Table 12. χ^2 analysis on isolates with a known source revealed there was no significant association between *E. coli* infections from different sources in the summer compared to the other seasons. Sources of infection not considered in this table had a sample size too low for statistical analysis.

	Winter (Dec-Feb)	Spring (Mar-May)	Summer (Jun-Aug)	Autumn (Sept-Nov)	P value	Significance
<i>E. coli</i> from urinary	97	78	162	123	0.735	Not significant p <0.05
<i>E. coli</i> from gastro	55	48	86	60	0.926	Not significant p <0.05
<i>E. coli</i> from respiratory	5	4	3	1	0.372	Not significant p <0.05

3.2.3 ST131 was not responsible for the increase of *E. coli* BSI in the summer of 2020

In order to identify the STs of *E. coli* responsible for each BSI, ST analysis was conducted with genomic data from Illumina sequencing. Not all *E. coli* isolates were sequenced due to lack of growth, loss between the diagnostic and research lab, or lack of purity on arrival at research lab, therefore the total number of *E. coli* sequenced was 678. To indicate there was no seasonal selection bias for the sequenced *E. coli*, which may affect analysis of seasonality trends, Figure 14 was constructed, which showed that sequenced BSI *E. coli* numbers mirrored total BSI *E. coli* isolate numbers, as shown in Figure 13. Statistical analysis also revealed a summer bias for sequenced *E. coli* with the summer months between June and August ($p=0.05$).

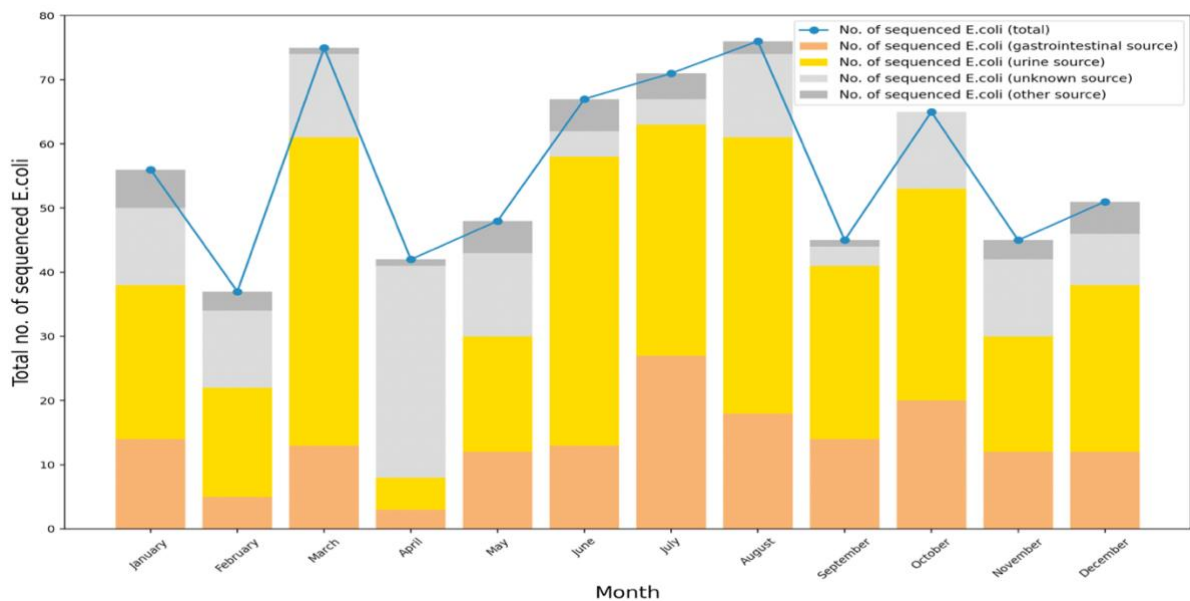


Figure 14. Number of *E. coli* sequenced per month displaying broken down by predicted source of infection.

ST analysis revealed ST131 (n=132, 19.0% of all sequenced *E. coli*), ST69 (n=92, 13.3%), ST73 (n=107, 15.4%) and ST95 (n=64, 9.2%) were the four most common STs identified, with both ST69 and ST95 peaking in numbers during August and September 2020, respectively whilst the numbers of ST131 peaked in the summer months between June to August 2020 (Figure 15). However, statistical analysis revealed no significant rise of ST131 relative to all other STs during the summer months in 2020 ($p>0.05$) (Table 13), therefore indicating there is a seasonal increase in *E. coli* BSI overall in the 2020 data.

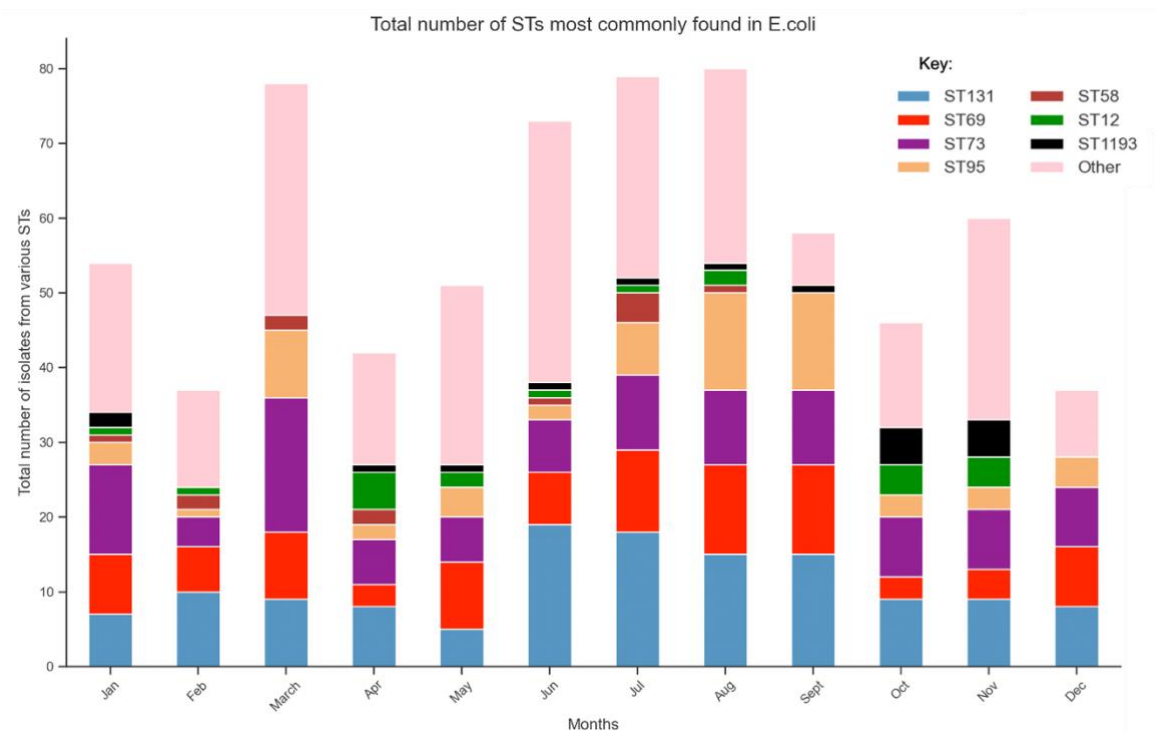


Figure 15. A stacked bar chart containing the most common STs found per month, amongst 696 *E. coli* isolated from BSIs between January 2020 and December 2020.

Table 13. Chi (χ^2) analysis revealed there was no association between ST131 causing an increase in infections in the summer compared to the other seasons.

	Winter (Dec- Feb)	Spring (Mar- May)	Summer (Jun- Aug)	Autumn (Sept- Nov)	P value	Significance
ST131	25	22	52	33	0.104	Not significant p <0.05
ST69	22	21	30	19	0.866	Not significant p <0.05
ST73	24	30	27	26	0.052	Not significant p <0.05
ST95	8	15	22	19	0.860	Not significant p <0.05
ST58	3	4	6	0	0.324	Not significant p <0.05
ST12	2	7	4	8	0.157	Not significant p <0.05
ST1193	2	2	3	11	0.128	Not significant p <0.05

To understand whether changes in NHS infrastructure, including change in health services and heavy focus to COVID as a result of the pandemic mitigations could be associated with the seasonality trends observed in 2020, incidence data from 2021 and 2022 for *E. coli* BSI infections were analysed to investigate whether the same seasonal trend in overall *E. coli* BSI was observed in these later years. In 2021, a higher number of *E. coli* infections was observed between winter and spring with an increase in *E. coli* infections between January and February (Figure 16). In comparison, a higher number of *E. coli* infections were observed for the autumn months in 2022, with an increase in *E. coli* infections between August and September (Figure 17). A Mann-Whitney statistical test revealed that this is significant p<0.05 (pvalue =0.013). In comparison, an increase in infections were observed between July and August, with a decrease between August and September in 2021.

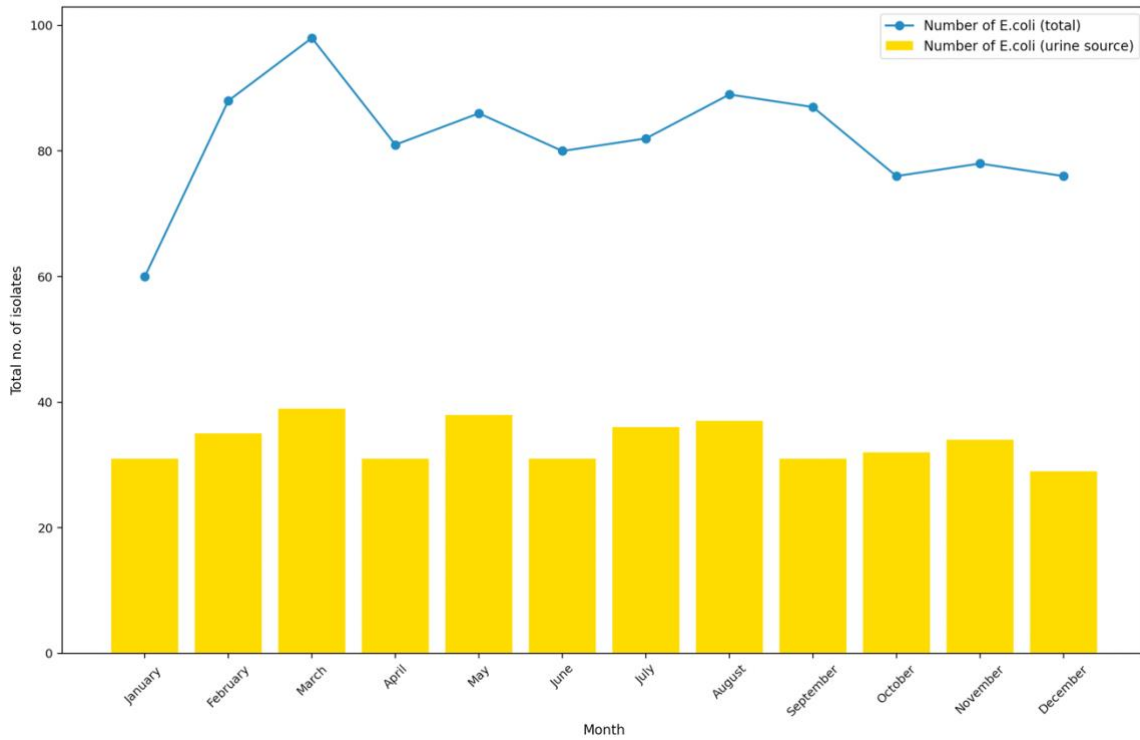


Figure 16. Monthly number of *E. coli* BSI per month from Severn Pathology displaying the number of urine source of infection in 2021.

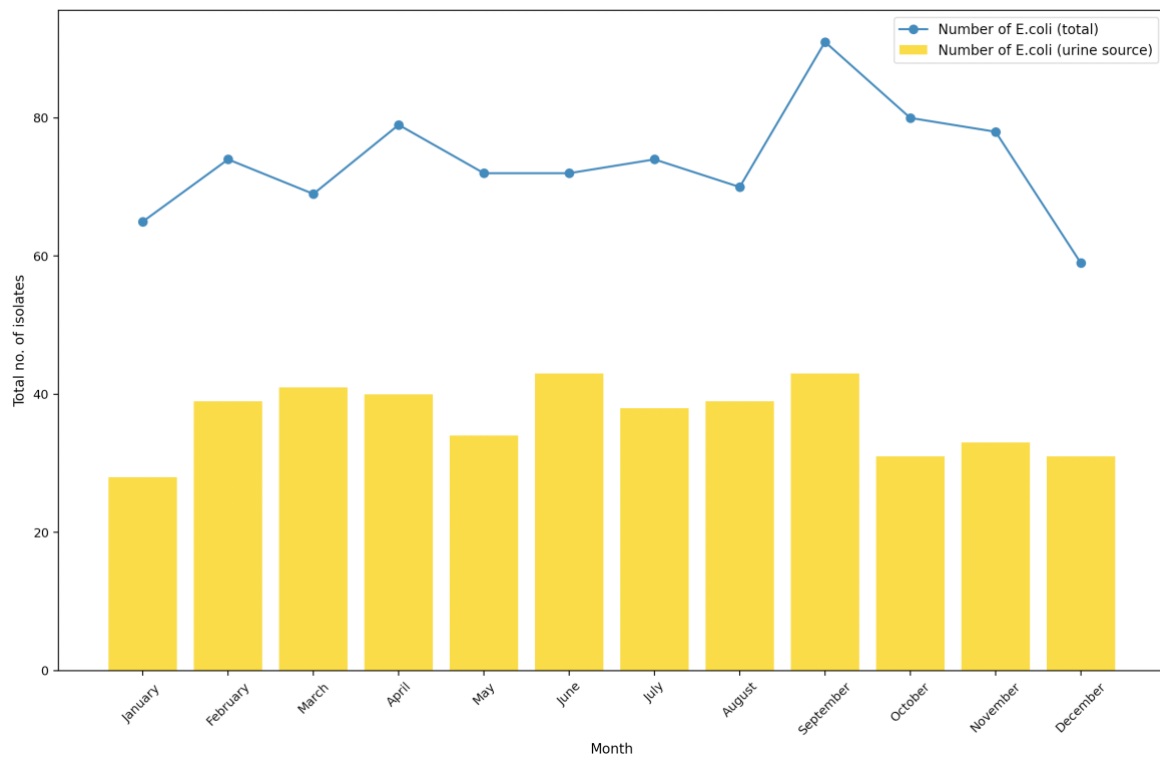


Figure 17. Monthly number of total *E. coli* BSIs per month from Severn Pathology also displaying the number of urine source of infection in 2022.

As this study has revealed significant increases in *E. coli* infections only in the summer for 2020 and the autumn for 2022, average temperatures were analysed across this year in the Southwest, UK, showing a peak between July and August in all years (Figure 18). There was therefore no association between increase in infections and average temperature, potentially relating to dehydration, in the three years being studied.

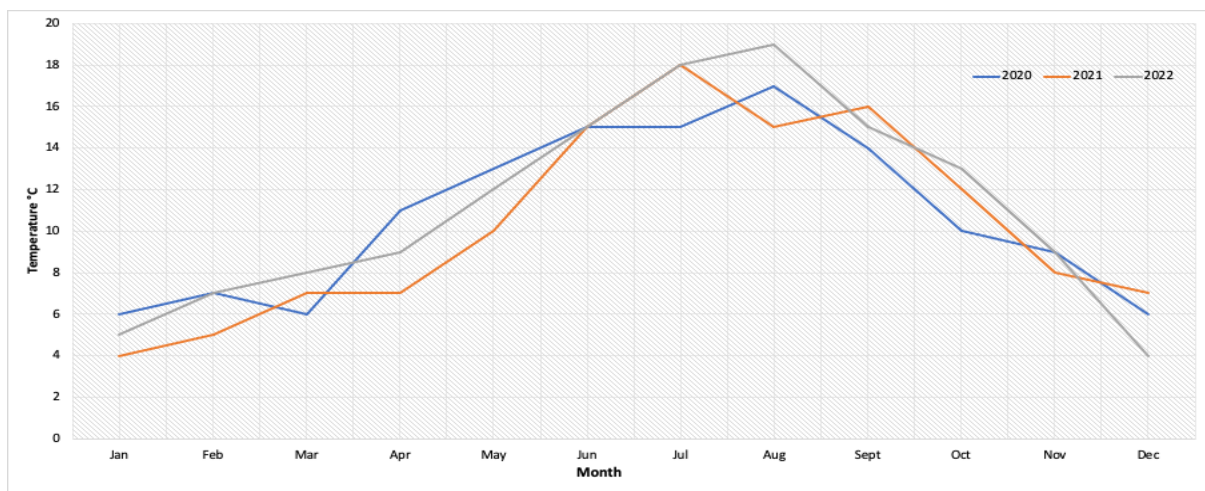


Figure 18. Average monthly temperature in Bristol, Southwest UK in 2020, 2021 and 2022.

3.2.4 Association between phylogroups, AMR and source of infection

To determine whether specific *E. coli* phylogroups are associated with particular sources of BSI, χ^2 analysis was conducted. Table 14 showed there was a stronger association between phylogroup A and B1 *E. coli* with GI source than any other source. There were no significant associations with any other particular sources of infection and phylogroup B2, however, analysis comparing ST131 versus other STs within phylogroup B2 revealed associations between ST131 as the causative ST and urinary source of infection.

Table 14. Significance of associations between phylogroups and any particular source of infection. Unsignificant associations between phylogroups and other sources of infection were excluded from this table.

Phylogroup	Source	Significance
A+B1	Association with GI source	Significant at $p < 0.05$ (p value 0.0003)
B2	No association with urinary source	Not significant at $p > 0.05$ (p value 0.536)
ST131 within B2	Association with urinary source	Significant at $p < 0.05$ (p value 0.00007)

To investigate whether particular resistance genes were associated with certain sources of infection, statistical analyses were conducted. The genes *bla_{TEM}*, *bla_{OXA}*, *bla_{CTX-M}* and *aac(3)-IIa/d* are the most common mechanisms of resistance to amoxicillin-clavulanate (*bla_{TEM}*, *bla_{OXA}*), 3GCs (*bla_{CTX-M}*) and gentamicin (*aac(3)-IIa/d*) in, which are currently used as treatment for presumed BSIs in Bristol. Hence, these genes were the focus for this analysis. Overall, results reveal that no significant associations with harbouring 3GC-R genes and a particular infection source. For TEM-1B carriage, there was no association with GI tract source but there was a significant association with urinary tract source (Table 15). Gene *aac-1b-cr* was less likely to be

associated with GI tract source (Table 15) but not more likely to be associated with urinary source.

Table 15. Significance of associations between resistance genes and between urinary and GI tract source of infection.

Resistance	Source	Significance
TEM	No significant association with GI source	Not significant at $p > 0.05$ (p value 0.813)
	Association with urinary source	Significant at $p < 0.05$ (p value 0.048)
<i>aac-1b-cr</i>	Less likely to be associated with GI source	Significant at $p < 0.05$ (p value 0.024)
	Not more likely to be associated with urinary source	Not significant at $p > 0.05$ (all p values > 0.694)
CTX-M, OXA	No associations with harbouring 3GC resistance with urinary or GI source	Not significant at $p > 0.05$ (all p values > 0.774)

3.2.5 Phylogenetic relationships showed AMR mechanisms found in 2020 BSI isolates are dispersed and intermixed with isolates from different phylogroups

A core genome SNP tree for *E. coli* BSI was constructed to analyse the distribution of phylogroups and assess whether resistance was acquired independently or due to a spread of clonal isolates (Figure 19). Table 16 below shows the distribution (%) of *E. coli* and their phylogroups. Most *E. coli* isolates are phylogroup B2, with the lowest percentage of *E. coli* for Phylogroup E and G.

Table 16. The percentage of *E. coli* isolates associated with each phylogroup. The colours for each phylogroup are shown and can be compared with the core genome SNP tree in Figure 19.

Phylogroup	Percentage
A (light green)	4.9
B1 (yellow)	5.9
B2 (red)	66.2
C (light blue)	2.5
D (purple)	15.9
E (lilac)	0.3
F (pink)	2.8
G (khaki/dull green)	1.2

Phylogenetic relationships showed AMR mechanisms are dispersed and intermixed with isolates from different phylogroups, with the highlighted subclade (purple) containing ST131 harbouring CTX-M, OXA genes and chromosomal mutations associated with ciprofloxacin resistance (Figure 19).

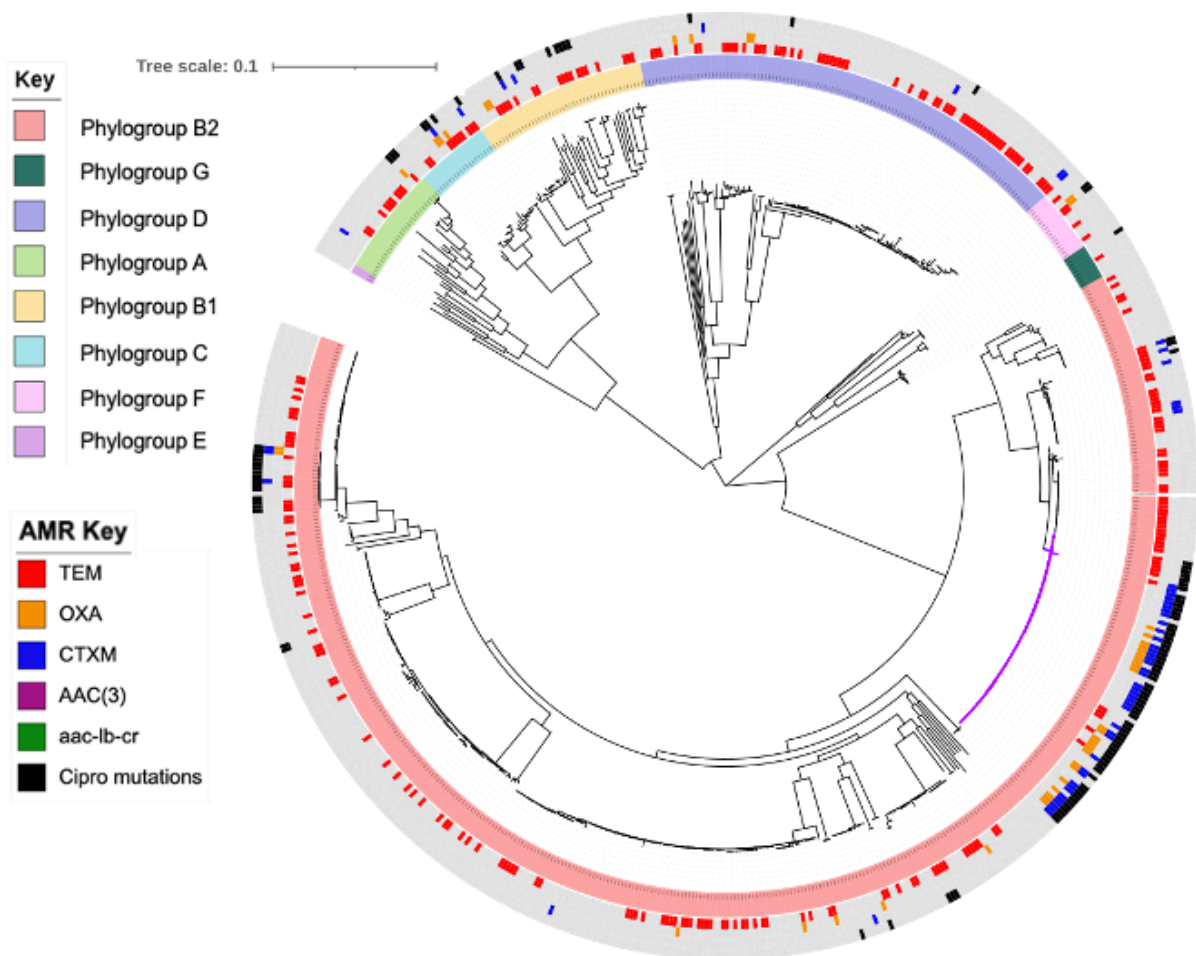


Figure 19. A core genome SNP tree consisting of 667 *E. coli* (n=11 isolates with bad quality assemblies that are not present in the tree) displaying the distribution of phylogroups and its associated AMR mechanisms.

3.2.6 Phylogenetic analysis reveals ST131 and ST1193 clades within the UTI population in 2020 conferring MDR including and resistance to ciprofloxacin

After analysing BSI *E. coli* population structures, including 3GC-R *E. coli*, we next set out to understand the population structure of 3GC-R *E. coli* causing urinary infections in the community in October to December 2020 in the same geographical region as the hospitals from which the BSI isolates were collected. For this analysis resistance genes associated with antibiotics used for treatment for BSIs were used. In particular, antimicrobial classes of BL/BLIs, 3GCs, aminoglycosides and FQs formed the focus of this study. The antibiotic selected from each class were amoxicillin/clavulanic acid from BL/BLIs, cefotaxime from 3GCs, gentamicin from aminoglycosides and ciprofloxacin from FQs. Following WGS of 199 3GC-R (no more than one per patient) UTI *E. coli*, AMR gene data were mapped with phylogenetic data. As seen for the BSI isolates, AMR mechanisms were dispersed amongst the *E. coli* UTI population, however with no aminoglycoside resistance genes associated with aminoglycosides used in human medicine found in phylogroups D, E, C and B1. However, phylogroup B2 isolates displayed the most diversity of resistance, with ST131 (clade highlighted in blue) harbouring the most AMR mechanisms (Figure 20). All ST1193 isolates within phylogroup B2 harboured mutations associated with resistance to ciprofloxacin (Figure 20).

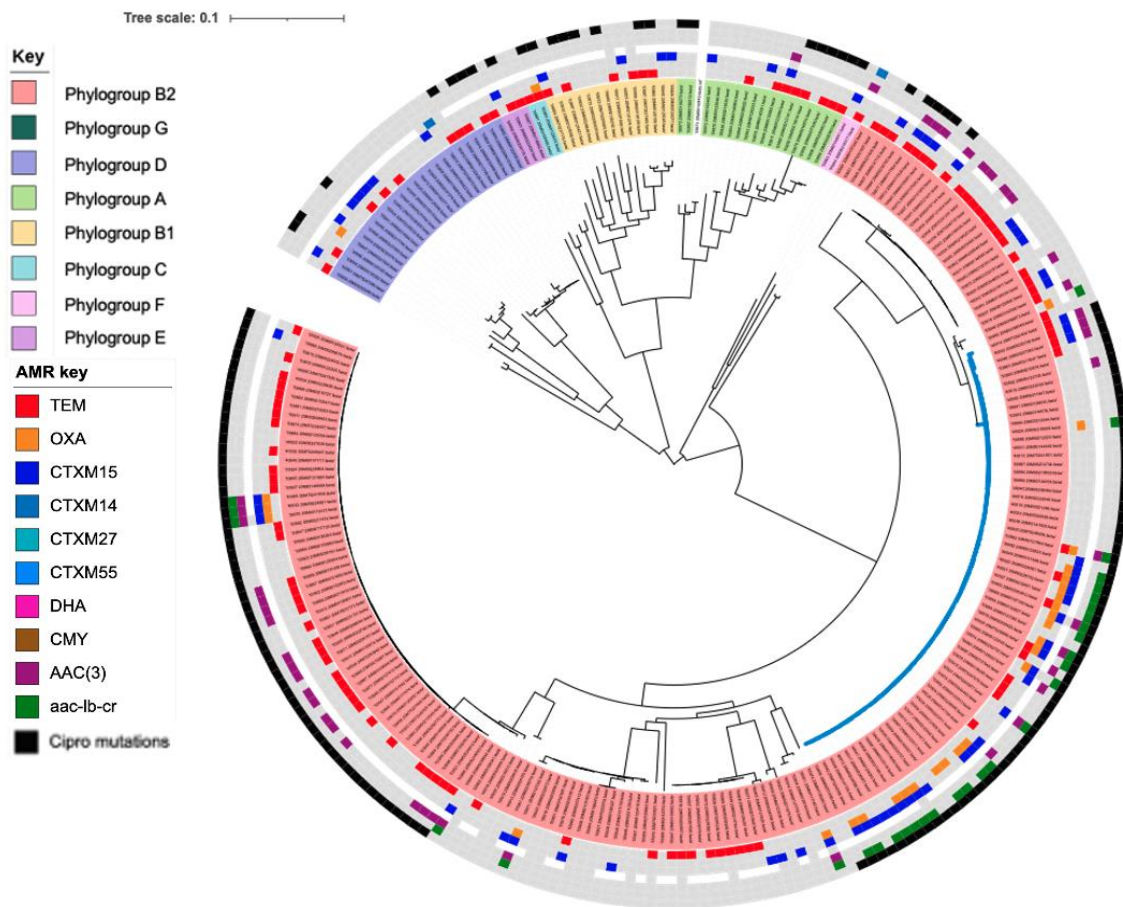


Figure 20. A core genome SNP tree consisting of 3GC-R *E. coli* (n=199) from UTI from 2020 displaying the distribution of phylogroups and its associated resistance profiles.

3.2.7 Sequenced genomes of 2018 3GC-R *E. coli* from BSI and UTI showed a clonal spread in the community

Whilst BSI isolates were collected throughout 2020, UTI isolates were only collected between September and October because of pandemic related issues. In order to generate a fair assessment of spread in the community for both types of infections, only BSI isolates collected between September and October 2020 were taken forwards for analysis. However, data from 2020 from both type of infections collected in the same timeframe lacks the power to determine and understand clonal spread in the community as clonal spread can occur in a longer timeframe, and the fact that UTIs were deduplicated, means that it may be that for some patients, a period of repeated UTI might drag on into 2021 before urinary source BSI emerged. Therefore, to gain a better insight of the spread of 3GC-R *E. coli* in the community, and the role of this spread in UTI and BSI, and in the former possibly driving the latter, isolates from 2018 for both type of infections were compared, as both were collected across the whole year. STs from 3GC-R *E. coli* isolates obtained from BSIs (n=80) were compared with the published dataset comprising of 225 3GC-R *E. coli* isolates obtained from patients with UTI, and found that ST131 (n=101, 44.8%) was the most common ST of *E. coli* that was identified. In addition to ST131 the most common STs from urine were ST73 (n=14, 0.6%), ST38 (n=13, 0.6%) and ST1193 (n=12, 0.5%). Similarly, ST131 (n=44, 55%), ST73 (n=6, 0.8%) and ST38 (n=3, 0.4%) were amongst the most common ST found in BSIs. These STs were also the most commonly found 3GC-R BSI and UTI *E. coli* seen in 2020 (Figure 15), and therefore formed the focus of this part of the study.

Genomes of 145 3GC-R ST131 BSI and UTI *E. coli* isolates collected in 2018 were screened for known AMR genes. Resistance profiles to only aminoglycosides and β -lactams have been displayed as these classes of antimicrobials are those most

commonly used to treat BSIs. The main resistance gene profiles observed in 96 isolates (66.2%) and 49 isolates (33.8%) gave resistance to aminoglycosides (*aac-Ib-cr*) and 3GCs (*bla_{CTX-M-27}*, *bla_{CTX-M-15}*, *bla_{CMY-60}*, *bla_{CTX-M-14}*, *bla_{CTX-M-1}*) and those with the potential to give resistance to amoxicillin/clavulanate and piperacillin/tazobactam (*bla_{TEM-1B}*, *bla_{OXA-1}*). Phylogenetic analysis indicated that the *E. coli* population fell into 2 main clades with isolates harbouring *bla_{CTX-M-27}* and *bla_{TEM-1B}* present in the first clade (Figure 21).

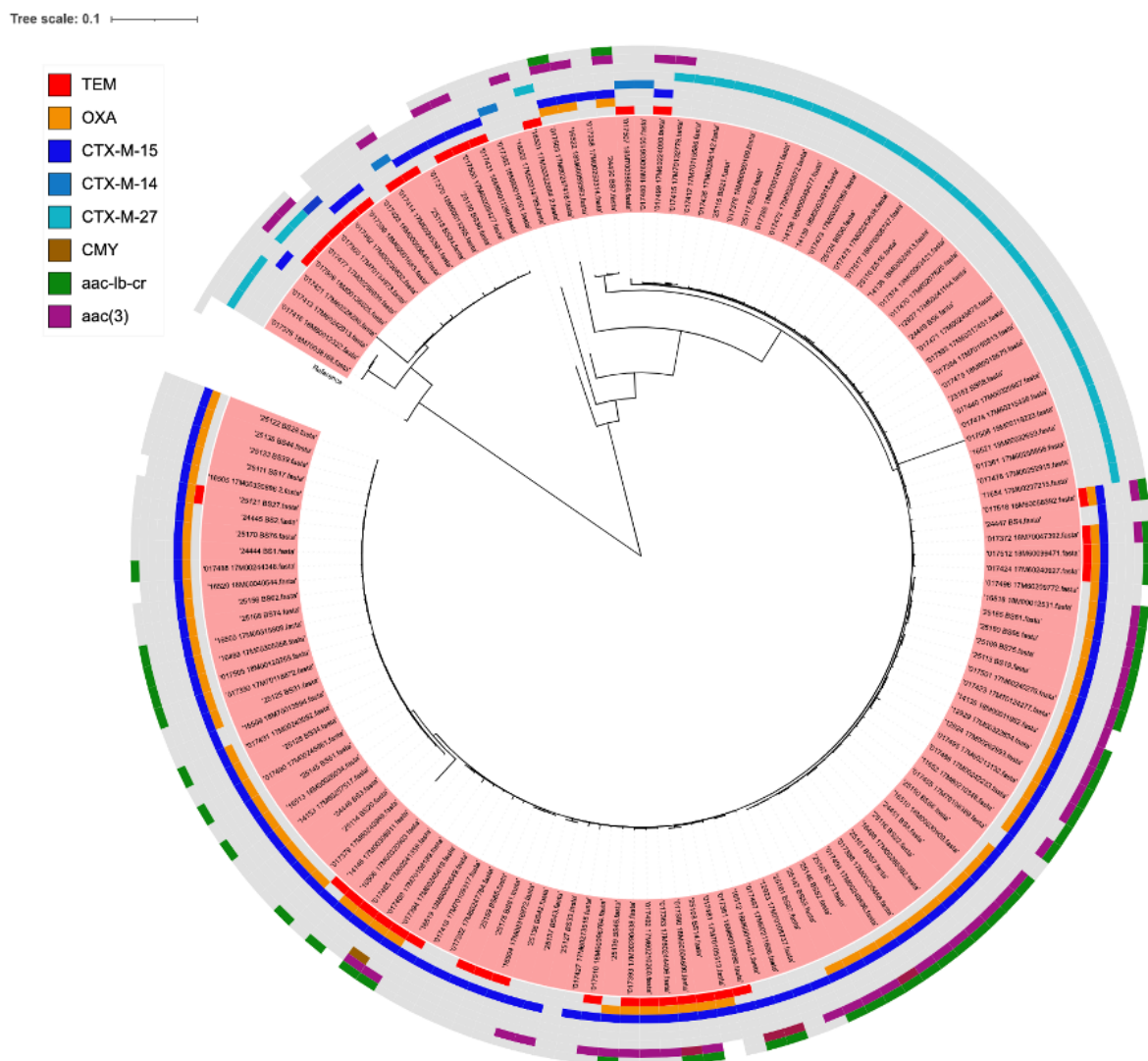


Figure 21. Maximum likelihood tree containing 145 3GC-R ST131 *E. coli* core Illumina genomes from BSIs and UTIs in 2018 displaying the presence of AMR resistant genes present within this *E. coli* population.

To investigate whether the same AMR patterns were observed in the 20 3GC-R ST73, AMR genes were identified and overlaid onto the phylogenetic tree (Figure 22). In comparison to ST131, fewer variants of *bla*_{CTX-M} were found and *bla*_{TEM-1} was less widespread across the population. The highlighted pink and blue clades have short branches and appear to be similar, however SNP analysis showed the average SNP difference across the blue and pink clades are 394 SNPs and 294 SNPs respectively. This indicates that ST73 is phylogenetically diverse. However, SNP analysis amongst the isolates on the highlighted green clade, showed ≤ 30 SNP differences. Urine isolate 18M6002979 and 18M60058542 were obtained from 46 and 58 year old females respectively. These isolates harboured the same plasmid replicon types and AMR genes, and were 17 SNPs different to BS9, which was obtained from a baby <1 year old and also contained the same AMR genes and plasmids replicon types.

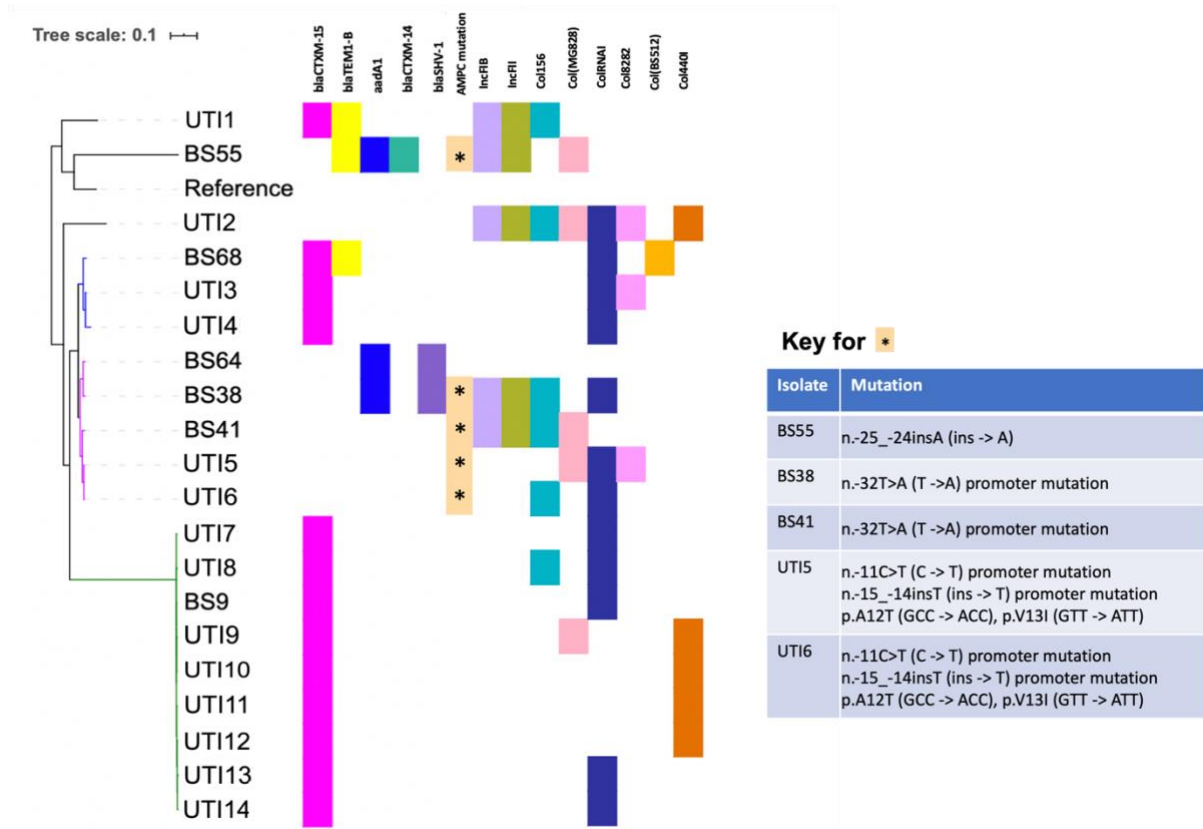


Figure 22. A maximum likelihood tree of consisting of 20 ST73 *E. coli* and their associated AMR, plasmid type and point mutations profiles. The coloured branches represent clusters of isolates which are most likely genetically similar.

The presence of AMR genes and plasmid replicon types were also determined for 16 ST38 isolates. Variant calling on the core genome alignments for these isolates showed no more than 23 SNP differences between all the isolates. However, *in silico* AMR typing showed that there is more variation of AMR genes and associated plasmid replicon types between isolate compared with other STs. The indicated pink, blue and yellow clades from the phylogenetic tree (Figure 23) consist of ST38 isolates that are most genetically similar, with only a minimum of 3 SNP differences between UTI16 and UTI17. As shown in Table 17, BS32 and UTI19 in addition to BS5 and UTI20 have a variety of plasmids and AMR genes. Core variant calling showed there was only 4

SNP differences between BS32 and UTI19, despite only having one plasmid type in common. Similarly, there are 8 SNP differences between BS5 and UTI20 (Table 17).

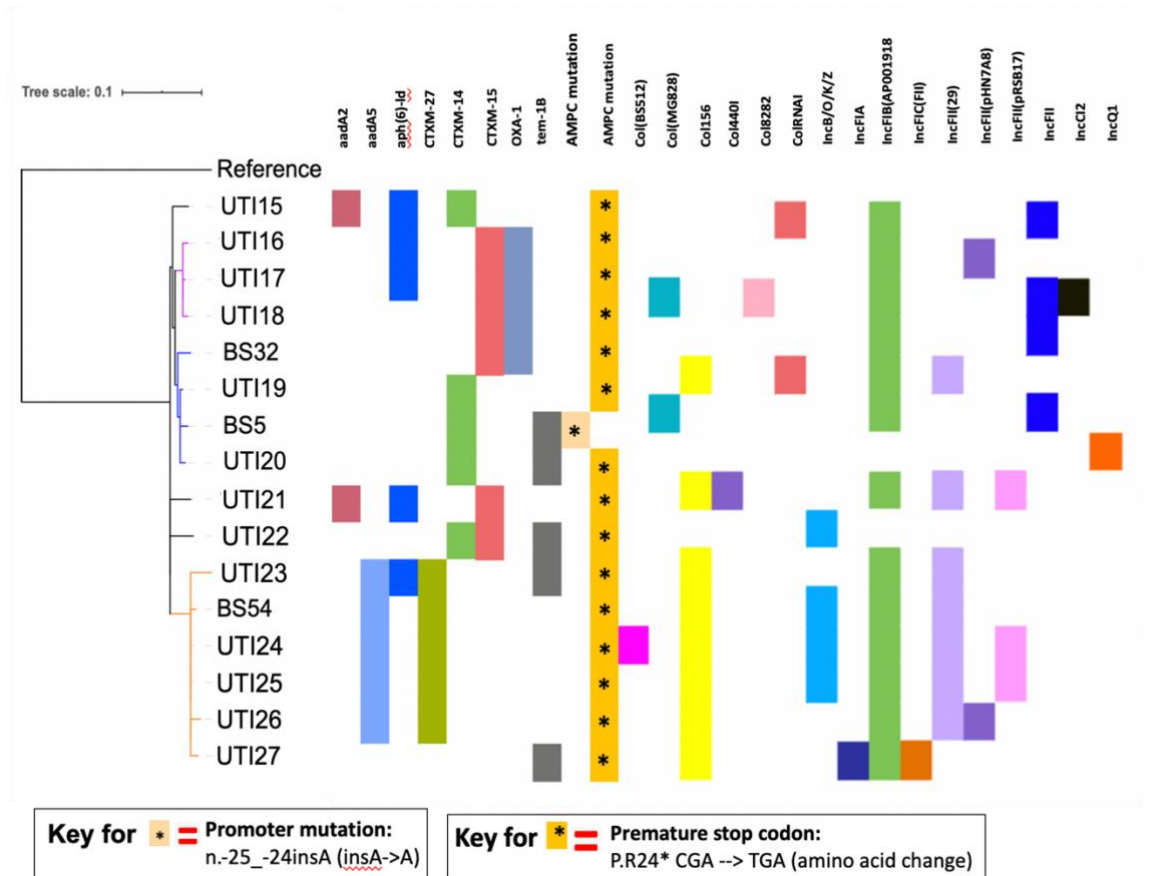


Figure 23. A maximum likelihood tree of consisting of 16 *E. coli* of ST38 and its associated resistance, plasmid and point mutations profiles. The coloured branches represent clusters of isolates which are most genetically similar.

Table 17. Isolates sharing similar AMR and plasmid profiles.

	Blood 1	Urine 1	Blood 2	Urine 2
Code	BS32	UTI19	BS5	UTI20
AMR genes:	<i>bla_{CTX-M-15}</i> , <i>bla_{OXA-1}</i>	<i>bla_{CTX-M-14}</i>	<i>bla_{CTX-M-14}</i>	<i>bla_{CTX-M-14}</i>
Plasmids:	IncFIB (AP001918), IncFII (pRSB107), IncFIB (AP001918)	IncFII, IncFIB (AP001918), Col156, ColRNAI	IncFIB (AP001918), IncFII (pRSB107), Col(MG828)	IncQ1

Characterisation of the regions containing *bla_{CTX-M-14}* and *bla_{CTX-M-15}* indicates the presence of various MGEs (Table 18). Isolates UTI19, BS5 and UTI20 contain chromosomal genes close to the AMR genes, which could indicate the MGEs carrying these AMR genes are integrated into the chromosome (Table 18).

Table 18. Other genes surrounding gene of interest.

Isolate	Genes surrounding CTX-M-14/CTX-M-15
UTI16	IS1380, CTX-M-15, hypothetical protein
UTI17	TN3, hypothetical protein, CTX-M-15, hypothetical protein, IS13180, hypothetical protein, dnaT, hypothetical protein
UTI18	tetR, Tn3, IS26, cat, CTX-M-15, aacA4, IS26, Tn2, hypothetical protein
BS32	Hypothetical protein, CTX-M-15, hypothetical protein, IS1380
UTI19	fhuC, yhiD, IS1380, CTX-M-14, hdeB, hdeA, hdeD, gadE, hypothetical protein
BS5	Hypothetical protein, CTX-M-14, hdeB, hdeA, hdeD, gadE
UTI20	yhiD, ISEcp1, hypothetical protein, CTX-M-14, hdeB, hdeA, hdeD, gadE, hypothetical protein
UTI23	ISE, CTX-M-14, IS5
BS54	ISE, CTX-M-14, ISE, IS5
UTI24	IS6, CTX-M-14, ISE, IS5
UTI25	ISE, CTX-M-14, IS5
UTI26	Tn3 family transposase, <i>fiu₂</i> , IS5, CTX-M, 14
UTI27(Has no CTX-M but has DHA)	<i>yncD</i> , IS5, DHA-1, hypothetical protein, ISEcp1

3.2.8 Diversity of AMR genes among 3GC-R *E. coli* has stayed consistent, with an increase of resistance to aminoglycosides observed between 2018 and 2020 within BSIs

To understand the change in population dynamics of 3GC-R *E. coli* causing BSIs between 2018 and 2020, a comparison of AMR gene carriage data from these two years were conducted along with phylogenetic data. The population structure of 3GC-R *E. coli* was dominated by ST131, ST69, ST73 and ST95, with ST131 being the most widespread clone in both 2018 and 2020. The subclade (highlighted in purple) consisting of ST131 harboured a variety of determinants that confer resistance to both 3GCs and aminoglycosides (Figure 24). DHA was mainly observed in phylogroups A and D in 2018 BSI isolates, however only observed once in phylogroup B2 in 2018.

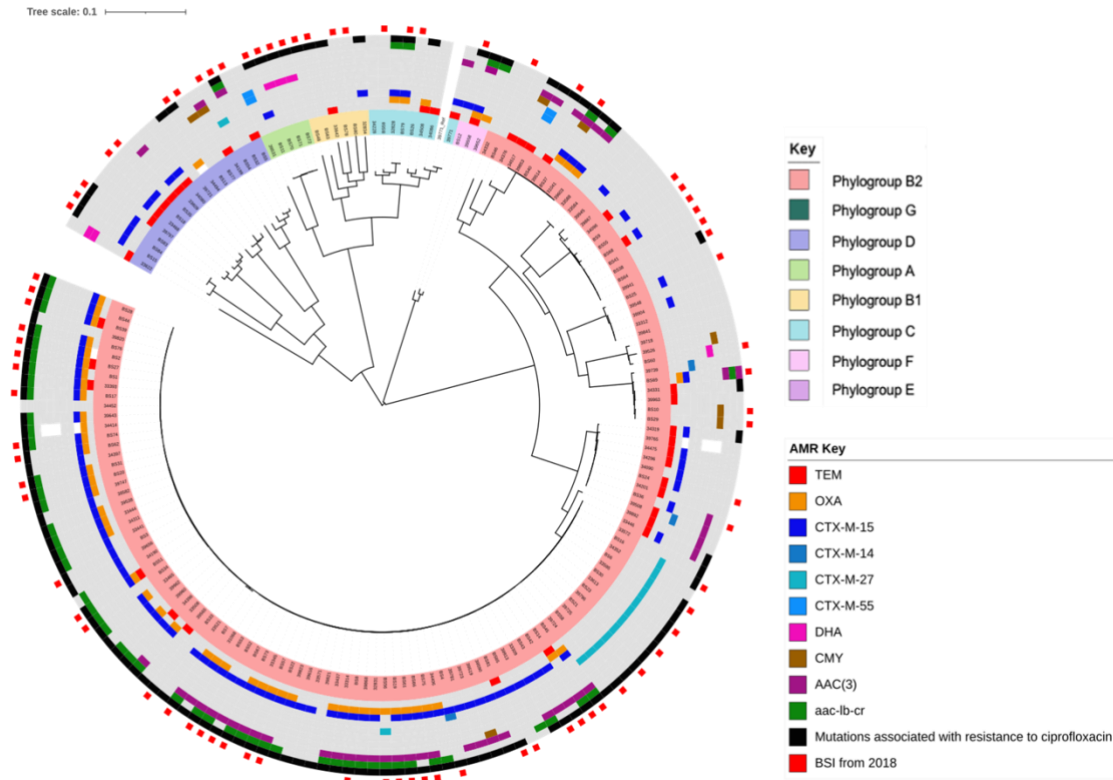


Figure 24. A core genome SNP tree consisting of 3GCR *E. coli* from BSI from 2018 and 2020 displaying the distribution of phylogroups and its associated AMR mechanism profiles. Isolates from 2018 are labelled by the red squares on the most outer ring of the tree.

Decreases in AMR gene carriage associated to most key antimicrobial classes between 2018 and 2020 were observed, with an increase in the presence of TEM in 2020 (62%) (Figure 25). The biggest decrease in resistance was seen with OXA (47%), which was statistically significant ($p=0.012$) (Table 19).

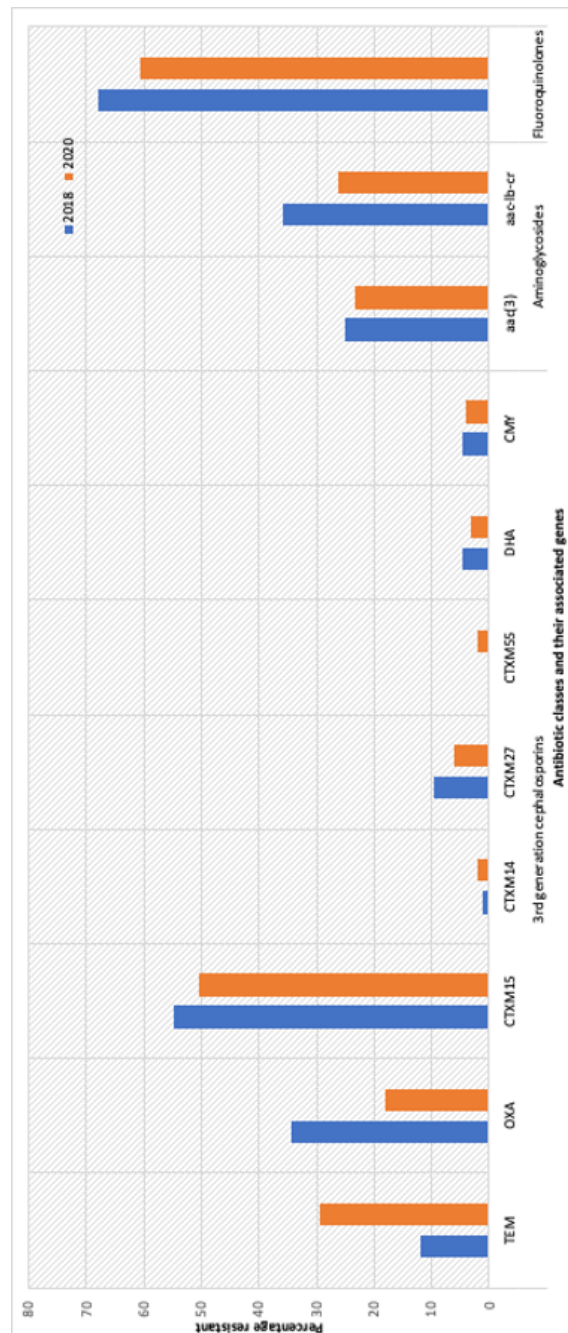


Figure 25. Trends in AMR mechanisms carried in 3GC-R isolates conferring resistance to 3GCs, aminoglycosides and FQs in BSI *E. coli* in 2018 and 2020.

Table 19. Chi (χ^2) analysis showing the significance in the change of AMR mechanisms among 3GC-R BSI isolates between 2018 and 2020.

Resistance genes associated with 3GC, aminoglycosides and fluoroquinolones	Significance
TEM	Significant p <0.05 (p value 0.004)
OXA	Significant p <0.05 (p value 0.012)
CTX-M-15	Not significant at p < 0.05 (p value 0.566)
CTX-M-27	Not significant at p < 0.05 (p value 0.380)
<i>aac(3)</i>	Not significant at p < 0.05 (p value 0.780)
<i>aac-lb-cr</i>	Not significant at p < 0.05 (p value 0.167)
<i>gyrA</i> , <i>parC</i> mutations	Not significant at p < 0.05 (p value 0.309)

3.2.9 ST131 within the 3GC-R UTI populations in 2018 and 2020 were divided into two clusters, with one cluster harbouring CTX-M-14 and mutations associated with resistance to FQs

To observe whether similar AMR trends and population dynamics were seen across the 3GC-R UTI *E. coli* populations in 2018 and 2020, phylogenetic analysis was conducted. 3GC-R UTI isolates were collected in September and October 2020, therefore 3GC-R UTI isolates within these months in 2018 were taken forwards for comparison. The population structure of 3GC-R *E.coli* in UTIs were dominated by ST131 (highlighted clade in blue), where all isolates harboured mutations associated with FQ resistance (Figure 26). The ST131 clade revealed further division into two clusters, with one cluster mainly containing CTX-M-14 and another containing multiple AMR genes associated with resistance to 3GCs and aminoglycosides. All isolates within the ST1193 clade (in purple) revealed resistance to FQs and a diversity of AMR genes associated with 3GC-R.

Changes in AMR genes between 2018 and 2020 were observed for 3GC-R UTI *E. coli*, with decreases in the presence of TEM, *aac(3)* and CTX-M-15 seen in 2020 (Figure 27). CTX-M-15 and CTX-M-27 production, and mutation within *gyrA* and *parC* (FQ resistance) displayed the biggest percentage change between 2018 and 2020,

therefore statistical analysis was conducted to investigate the significance (Table 20). The biggest decrease in resistance was observed with CTX-M-15 (18%), which was not statistically significant at ($p=0.07$). The biggest increases in resistance was observed with CTX-M-27, which was not statistically significant but the increase seen of *gyrA* and *parC* mutation (FQ resistance) between 2018 and 2020, was statistically significant ($p=0.0002$).

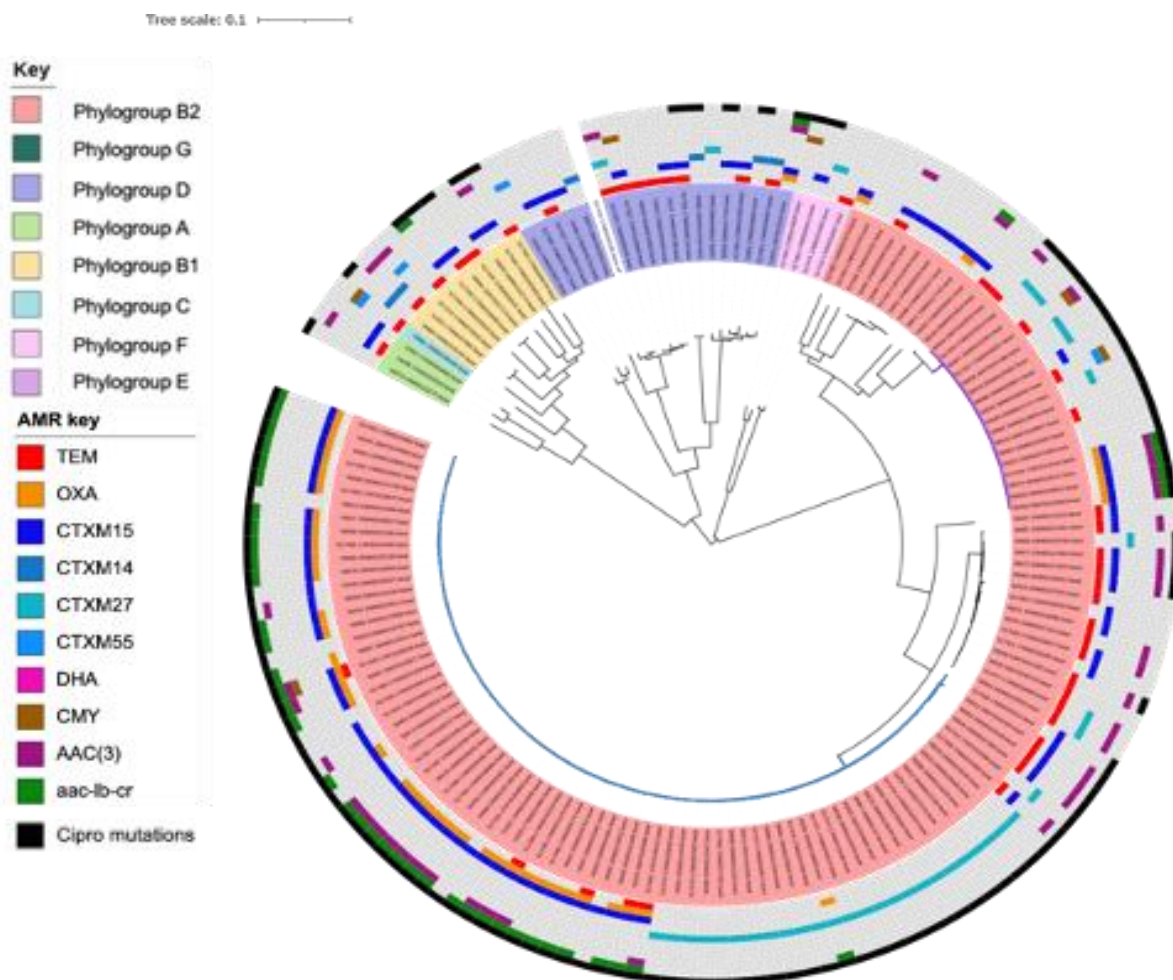


Figure 26. A core genome SNP tree consisting of 3GC-R *E. coli* from UTI from September and October in both 2018 and 2020 displaying the distribution of phylogroups and its associated AMR profiles.

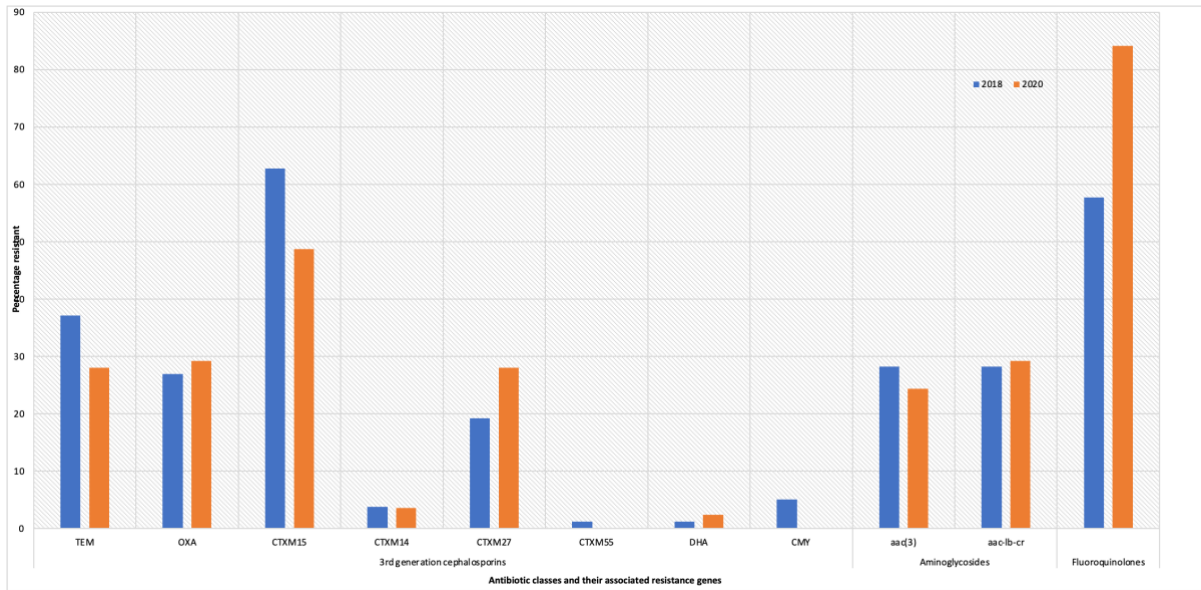


Figure 27. Trends in AMR determinants among 3GC-R *E. coli* associated with 3GCs, aminoglycosides and FQs in UTI *E. coli* in September and October of 2018 and 2020.

Table 20. Significance in the change of AMR mechanisms associated with 3GCs, aminoglycosides and FQs in 3CR-R UTI *E. coli* between 2018 and 2020.

Resistance genes associated with 3GC, aminoglycosides and fluoroquinolones	Test	Significance
CTXM15	chi	Not significant at $p < 0.05$ (p value 0.073982)
CTXM27	chi	Not significant at $p < 0.05$ (p value 0.190153)
gyrA, parC mutations	chi	Significant at $p < 0.05$ (p value 0.000219)

3.3 Discussion and Conclusion

E. coli and *K. pneumoniae* are members of the *Enterobacterales* family that is becoming increasingly 3GC-R (Livermore et al, 2013; Lin et al, 2019). Previous population-based BSI surveillance is consistent with this study's findings regarding the prominence of *E. coli* and *K. pneumoniae* as BSI pathogens. A cohort study by Magret *et al.* (2011) showed that *E. coli* and *K. pneumoniae* were the most common pathogens reported as the cause of BSI. However, a review of population-based studies across various world regions by Laupland 2013 showed *E. coli* and *S. aureus* as the most common BSI pathogen, with *Streptococcus pneumoniae* and *K. pneumoniae* as third and fourth most frequent pathogens isolated from BSIs. As the present study only considered Gram-negative bacteria, this also fits with this study's findings (Figure 12). This study also showed *Citrobacter spp.* as one of the less common Gram-negative pathogens associated with BSIs, however, it is reported to be associated more with neonatal patients (Pammi et al, 2014).

BSIs can occur from various infection sources, with urinary tract and GI tract being the main sources. Little research has been conducted that focus on the associations between infection and source of infection. Daga *et al.* (2019) revealed 50% and 12.5% of their BSI isolates originate from the urinary tract and GI tract respectively. In keeping with this, this study's data show that urinary tract and GI tract were the two most common infection sources, with a peak in the summer months (Figures 13 & 14). The literature reports that the incidence of UTIs increases during the summer months, with one of the contributing factors being dehydration, particularly among residents in caring homes (Lean et al, 2019). Figures 13 and 14 show that urinary source BSI increases in the summer months between June and August, but this was not found to be statistically significant. As a consequence of the UK government introducing

lockdown restrictions in April 2020 for the COVID pandemic, this could be a contributing factor for the observed decrease of *E. coli* from urinary and GI source as shown in Figure 13 from March to April. Lockdown restrictions impacted the availability of clinicians and hospital facilities for the treatment of non-COVID patients. As the main concern for hospitals was the treatment of COVID, lack of time for clinicians for assigning sources to BSI *E. coli* infections may explain the dramatic decrease in urinary and GI source *E. coli* during that time as there was a major increase in “unknown” or “other” source infections (Figure 13).

Studies have shown increases in the incidence of *E. coli* in BSIs in the warmer seasons with higher temperatures due to increased virulence and growth of *E. coli* in food and the environment (Gradel et al, 2016; Blot et al, 2022, Deeny et al, 2015). This study revealed an increase in *E. coli* BSI between June to August 2020 where the temperatures in the Southwest, UK were at their highest (Figure 18). Feldman *et al.* (2022) reported increases in total community onset *E. coli* BSI with higher temperatures but not with hospital onset *E. coli* BSI. To investigate whether the seasonality trends for *E. coli* BSIs in 2020 were due to changes in NHS infrastructure from the pandemic, seasonality trends for *E. coli* BSIs in 2021 and 2022 were analysed. Both years showed more consistency in infections throughout the year. In 2021 increases between July and August as well as January to February were seen (Figure 16). In 2022 an increase in the autumn months between September and October was seen (Figure 17). Average temperatures in the Southwest were also compared in 2021 and 2022 and peaks in infections did not coincide with the highest temperatures (Figure 18).

Numerous surveillance studies have identified ST69, 73, 95 and 131 to be the most prevalent STs found amongst *E. coli* causing BSIs (Adams-Sapper et al, 2013;

Jayreguy et al, 2008). Studies in the United Kingdom showed that these STs were isolated from 58% of BSIs in Northern England between 2010 and 2012 (Gibreel et al, 2012). An epidemiological study conducted in the UK revealed ST131, ST73, ST69 and ST95 account for over half the population (Jauneikaite et al, 2022). These studies fit with our findings from Figure 15. ST69, ST73 and ST95 have been reported widely geographically, however they rarely harbour resistance determinants which are associated with 3GC-R (Doumith et al, 2015). In contrast, reports have shown ST131 to harbour resistance to multiple antimicrobial classes, including 3GCs, FQs and aminoglycosides, with a global increase of CTX-M-15-producing *E. coli* from the ST131 O25:H4 clone (Peirano & Pitout, 2010). Furthermore, studies have shown strong association between ST131 and *bla*_{CTX-M} and *bla*_{OXA} genes (Dhanji et al, 2011). In keeping with this, we show in our dataset that the subclade of ST131 harboured most AMR genes to various antimicrobial classes, including a range of *bla*_{CTXM} genes and *bla*_{OXA-1} gene, compared to other STs belonging to other phylogroups (Figure 19& 21). Acquisition of resistance can also co-occur with an increase virulence within ST131 and analysis on this amongst ST131 will be discussed in the results chapter 3. Within the literature, phylogroup B2 *E. coli* from BSIs have been reported as the most frequent phylogroup identified in *E. coli* globally (Mickenková et al, 2017; Koga et al, 2014; Rodríguez et al, 2021) and that was also seen in this study (66.2% of isolates). In contrast, a study from Lithuania showed that phylogroup A was most common (79.3%) and only 15.6% were phylogroup B2 within the *E. coli* population (Kirtikliene et al, 2022). Usein *et al.* (2016) observed similar patterns for phylogenetic group classification of their *E. coli* isolates. Furthermore, Biggel *et al.* (2020) revealed repeated horizontal acquisition of *papGII* in clonal complexes within phylogroup B2, D and F, underlying the emergence of lineages associated with UPEC. In this study, χ^2

analysis revealed associations between ST131 from phylogroup B2 isolates with urinary tract source of infection, however a positive association between TEM and urinary source of infection was observed (Table 15).

There was a high detection rate of ST73, especially in the urinary isolates. ST73 has been described as a virulent clone, encoding mostly plasmid-encoded CTX-M genes (Alhashash et al, 2016). Multiple isolates sequenced here harboured plasmids and multiple CTX-M genes (Figure 22), however the absence of long read sequencing to confirm plasmid-encoded CTX-M was a limitation of this study.

ST38 is a clone predominantly causing UTIs (Chattaway et al, 2014) and a similar finding was reported, where levels of ST38 were high, however there is little understanding as to why this clone has emerged and it has therefore been suggested that continuous surveillance of this clone is necessary (Algoribi et al, 2015). Furthermore, ST38 has been found to harbour numerous AMR genes to 9 classes of antibiotics and contain multiple plasmids, however, the majority of these resistance determinants were found in the chromosome (Grieg et al, 2018). Whilst this study has shown that BSI ST38 from Bristol harbour a wide variety of AMR genes and plasmids (Figure 23), the full genomic environment in which the AMR genes are located cannot be explored unless long-read sequencing is carried out.

The molecular epidemiology of *E. coli* has altered dramatically globally, with the emergence of currently the most prevalent clones conferring MDR (Denamur et al, 2021). In this study, a comparison between resistance populations between 3GC-R *E. coli* BSIs from 2018 and 2020 were conducted. As *E. coli* in 2018 had a selection bias for 3GC-R, isolates from 2020 that displayed 3GC-R were taken forwards for analysis. The proportion of the most common STs remained relatively unchanged between 2018 and 2020, however resistance to aminoglycosides increased in 2020. Figure 24 shows

frequent association between *aac(3)-Ib-cr* and CTX-M-15, which is a consistent observation with a surveillance study conducted in Switzerland, where there were frequent co-occurrences between *acc(3)-Ib-cr* and CTX-M-15/OXA (Bodendoerfer et al, 2020).

The composition of STs, mainly ST131, ST1193 causing UTIs in this study is reflective of dominant groups causing UTIs in reports globally (Matsui et al, 2020; Ali et al, 2019). Population based epidemiology since 2016 revealed a rise in the emergent clone, ST1193 in UTIs globally (Birgy et al, 2017; Valenza et al, 2019; Nguyen et al, 2021; Menino et al, 2022), becoming the fifth most common ST and second most resistant clone, in particular FQ-resistant, after ST131 (Pitout et al, 2022). In keeping with this, results from this study revealed 100% of ST1193 harbouring *gyrA* and *parC* mutations causing FQ resistance (Figure 20 & 26). In contrast, Chin et al. (2015) showed lower prevalence of ciprofloxacin resistance in 2015 in the Southwest UK, demonstrating how ST1193 has become an emergent clone in this region, emphasising the importance in continuous monitoring of this clone. The majority of ST1193 also harboured resistance to aminoglycosides (Figure 20), in contrast with Nguyen et al. (2021) where several clusters of ST1193 harboured CTX-M variants, mostly CTX-M-27, CTX-M-55 and CTX-M-15. With phylogroup B2 ST1193 and ST131 harbouring multiple AMR determinants, this is can cause a significant health burden. Population variation of STs in UTI *E. coli* remained relatively unchanged between 2018 and 2020, however FQ resistance significantly increased in 2020 (Figure 27, Table 20). Similar observations have been reported within Europe with substantial increases from 25% to 40% between 2008 and 2014 in Asia (Stapleton et al, 2020). The underlying mechanism by which lineage ST1193 has risen globally remains unclear. Huang *et al.* (2020) revealed similar pathogenicity and survivability characteristics in lineage

ST1193 to ST131, such as possessing the ability for adhesion to T cells and formation of biofilms. The prevalence of resistance to ciprofloxacin, attributed to clonality of ST131 and ST1193, rises concern regarding the efficacy of ciprofloxacin as prophylaxis especially for catheter-associated UTIs (Langford et al, 2021).

There were several limitations to this study. Firstly, although all Gram-negative BSI in 2020 were collected from Severn Pathology, funding limitations resulted in sequencing the most common bacterial species responsible for BSIs. For the comparison in population dynamics and resistance between 2018 and 2020 for BSIs, only 3GC-R isolates in 2020 were taken forwards for analysis. This was due to the fact that prior to starting this study in 2020, isolates in 2018 were selected based on 3GC-R. The comparisons in population dynamics and resistance between 2018 and 2020 UTI could only be carried out between September and October as collection for UTI in 2020 occurred between this time period. Another limitation involved not undertaking in-depth analysis into the impact of host genetic factors, which may influence the severity of BSI. Furthermore, whilst infection source could be determined for the majority of BSI isolates, this could not always be determined by the clinician. Thus, the actual number of *E. coli* with a source is likely to be more than the stated amount presented in this study.

In conclusion, there are currently insufficient surveillance systems in place which take into account source of infection in addition to AMR patterns when it comes to monitoring AMR. Thus, future work includes continuous surveillance on AMR trends and associations with source of infection for *E. coli* in this region for identification of MDR clones in Bristol and surrounding regions. Ongoing global and local efforts are integral to help curtail AMR. Clonal diagnosis, antimicrobial susceptibility testing, mining genomic and surveillance data for AMR genes will improve monitoring the progression of UTIs to urosepsis. For characterisation of BSIs, factors such as antimicrobial susceptibility and host determinants play an integral role in the facilitation and improvement of empiric treatment for *E. coli* BSIs and UTIs.

4.0 Results Chapter 2

Characterisation of MDR *Klebsiella* spp. from BSIs

4.1 Introduction

The genus *Klebsiella* contains some very challenging human pathogens including *K. pneumoniae* (including subspecies *pneumoniae andozonae*), *K. oxytoca* and *K. variicola*. *Klebsiella* species are known to cause a range of diseases, some of which can be linked to specific species for example, *K. pneumoniae* is a primary cause of pneumonia, UTI, sepsis and soft tissue infection (Ashurst & Dawson, 2023). Additionally, *K. pneumoniae*, is second only to *E. coli* as a cause of BSI's in hospital and community settings (Meatherall et al, 2009). With a high mortality ranging from 20-40% of cases (Meatherall et al, 2009), *K. pneumoniae* BSI is one of the most fatal infections and among ICU patients mortality can rise to 67.6% of cases (Rose et al, 2015).

Surveillance of AMR data in Europe in 2019 revealed 36.6% of *K. pneumoniae* strains displaying resistance to a minimum of one antimicrobial class important for treatment of BSI, mainly 3GCs, carbapenems, FQs or aminoglycosides. Furthermore, concomitant resistance to FQs, aminoglycosides and cephalosporins, in particular 3GCs was exhibited in 4.9% of isolates (ECDC, 2019; Boucher et al, 2009; Davido et al, 2020). The acquisition of AMR determinants such as ESBLs and carbapenemases and their enhanced mobility through plasmids and transposons has resulted in the dearth of antimicrobial therapeutic options. Carbapenem-resistant *K. pneumoniae* is considered an urgent global public health concern by the World Health Organisation and Centres for Disease and Control and Prevention (CDC) (WHO 2019, CDC, 2019). *K. pneumoniae* produces a multitude of carbapenemases such as KPC (Ambler class A carbapenemases) the most prevalent carbapenemase which first

emerged from the United States in 1990s (Kitchel et al, 2009) , NDM, VIM, IMP (Ambler class B metallo- β -lactamases) and OXA-48 or OXA-like enzymes such as OXA-181 (Ambler class D carbapenemases) (Effah et al, 2020; Poirel et al, 2012; Queenan & Bush, 2007). The distribution of these enzymes differ geographically (Figure 28).

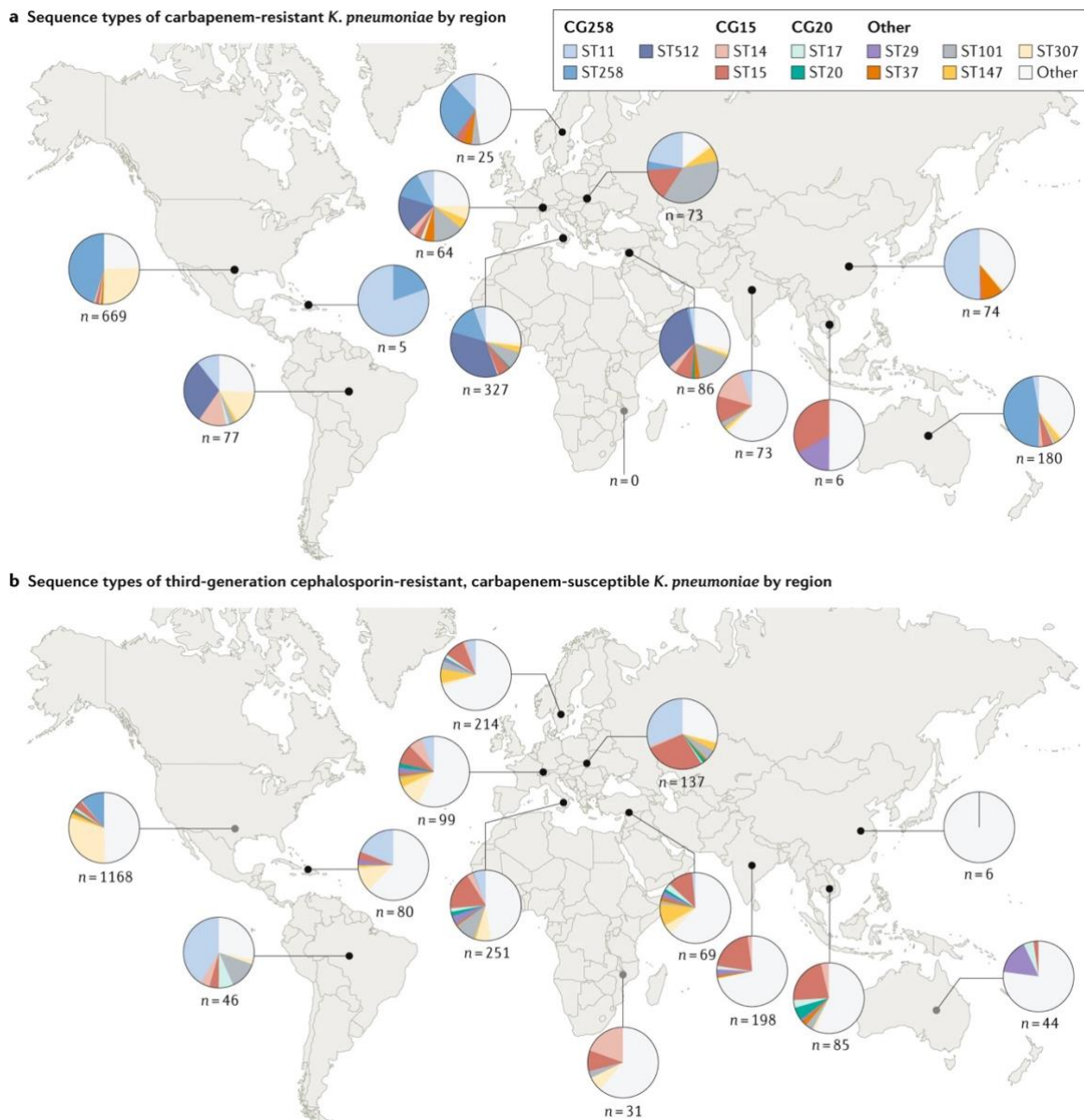


Figure 28. Global distribution detailing the resistance associated with a range of STs of *K. pneumoniae* to carbapenems and 3GCs. Taken from Wyres et al (2020).

K. pneumoniae is reported as globally disseminating very successfully and a prime example of this is the epidemic *K. pneumoniae* ST258 strain, which disseminated *bla_{KPC}* globally since its emergence in the mid-1990s (Bowers et al, 2015). ST14 and ST15 *K. pneumoniae* make up approximately 2.1% and 5.2% of publicly available genomes, respectively (Rodrigues et al, 2023). Both STs are commonly known to harbour ESBL or carbapenemases and are linked to hospital outbreaks worldwide (Rodrigues et al, 2023). ST14 and ST15 are single locus variants of each other, with one point mutation in *infB* (Diancourt et al, 2005; Breurec et al, 2013).

The New Dehli metallo- β -lactamase (NDM) confers resistance all β -lactams, excluding monobactams, with 59 variants of NDM reported to date and disseminated worldwide (NCBI, 2023). The most predominant variant is NDM-1, followed by NDM-5, first identified in a MDR ST648 *E. coli* isolate from the United Kingdom (Hornsey, Phee & Wareham, 2011). Both NDM-1 and NDM-5 are often encoded on IncX3 plasmids and mostly identified in *Enterobacterales*, with NDM-5 most prevalent in *E. coli* (Dong et al, 2022). NDM is often associated with Inc plasmid types such as IncA/C and IncX plasmids and various MGEs such as ISCR1, ISAb_a125 and Tn125 (Poirel et al, 2012). A study in China reported 2 plasmids identified in a novel NDM-producing ST4523 *K. pneumoniae* strain isolated from a BSI, harbouring 11 AMR genes associated with 5 antimicrobial classes located on 3 genomic regions with various transposons and integrons (Jia et al, 2022). Resistance rates of over 50% for 17/20 tested antimicrobials were observed for pathogens harbouring NDM-1 and characterisation of plasmids identified in *K. pneumoniae* revealed *tnpA* and *ble* located upstream of NDM (Xiang et al, 2020). Transposons and integrons can enhance mobility for transmission of NDM-producing pathogens, in particular NDM-producing *Klebsiella*, compromising the efficacy of β -lactams, including carbapenems in healthcare.

Though NDM is prevalent worldwide, OXA-48-like carbapenemases have gained prominence, spreading across multiple species of *Enterobacterales* with outbreaks reported across multiple continents (Findlay et al, 2017; Mairi et al, 2018; Alboushi et al, 2018). OXA-48 like enzymes are associated with resistance to penicillins, narrow spectrum cephalosporins and imipenem. Unlike the carbapenemase KPC, BLIs do not inhibit OXA-48 like carbapenemase activity well, and so they have been seen to be associated with resistance to new carbapenem/BLI inhibitor combinations such as meropenem/vaborbactam (Fröhlich et al, 2019; Dulyayangkul et al, 2020). To date, 49 variants of OXA-48 have been identified (NCBI, 2023), with OXA-181 and OXA-232 constituting the 2nd and 3rd most prevalent variants following OXA-48 (Pitout et al, 2019). OXA-181 and OXA-232 can be differentiated from OXA-48 by four amino acid substitutions (T104A, N110D, E168Q, S171A) and one amino acid substitution at R214S (Pitout et al, 2019). Increased hydrolysis activity has been reported for blaOXA-181 compared to OXA48 (Potron et al, 2011). Furthermore, ST14 and ST410 from *K. pneumoniae* and *E. coli*, respectively, have been reported as predominant high-risk clones responsible for global dissemination of bla_{OXA-181} (Pitout et al, 2019). Increasing reports have emerged detailing the co-existence NDM and OXA, in carbapenemase-producing *Enterobacterales* (CPE), for example, NDM-5 and OXA-181 in *E. coli*, NDM-1 and OXA-232 in *K. pneumoniae* and NDM4 and OXA-181 in *K. pneumoniae* (Kim et al, 2021; Mahamat et al, 2019; Espinal et al, 2019; Kim et al, 2020; Zhang et al, 2023). This highlights the necessity for surveillance and control of CPE.

Whilst high prevalence of NDM in MDR *Klebsiella* spp. have been reported as detailed previously, further understanding of co-existing carbapenemases and distribution of these in Bristol and surrounding regions is required. Herein, this chapter reports the genetic environment, distribution of AMR mechanisms and clonal spread of NDM-

producing *K. pneumoniae* from BSI. Additionally, this chapter describes the population structure of *Klebsiella* spp. and its association with source of infection.

AIMS: To define the population structure and prevalence of *Klebsiella* spp. from BSIs in Bristol and surrounding regions during a pandemic year, 2020, and to gain insight into the distribution of AMR genes within the *Klebsiella* spp. population and characterise the genetic environment of AMR genes, especially *bla*_{NDM} in MDR *K. pneumoniae*

4.2 Results

4.2.1 Temporal trend in *Klebsiella* spp. in BSIs received by Severn Pathology in 2020

To determine the burden of *Klebsiella* spp. causing BSIs between January 2020 and December 2020, seasonal incidence was analysed. The second most common Gram-negative bacterial species received across the year (after *E. coli*) was *K. pneumoniae*. Out of a total of 261 *Klebsiella* spp., *K. pneumoniae* (67.8%) was most common, followed by *K. oxytoca* (21.8%), *K. varriicola* (5.7%) and *Klebsiella. aerogenes* (4.6%). *K. pneumoniae* displayed an increase in BSI frequency in the summer months between June and August (Figure 29).

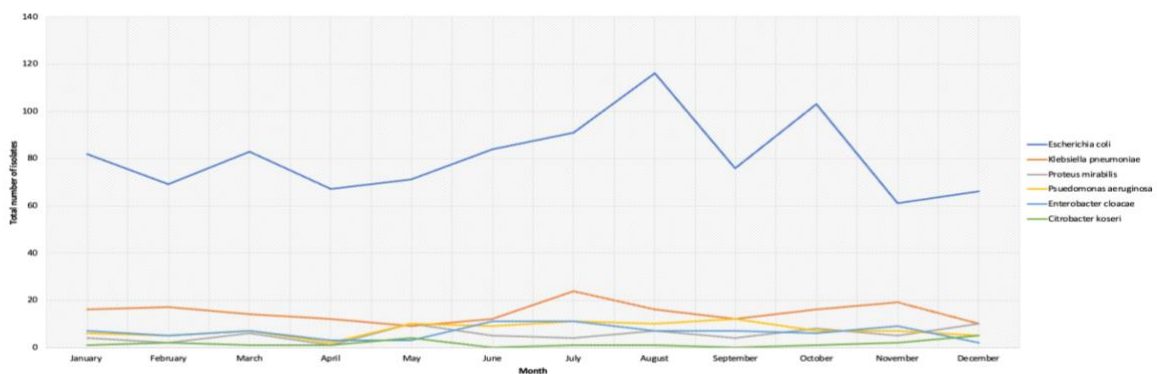


Figure 29. Total number of BSI isolates of the species most commonly found in 2020 . Reprinted from Chapter 1 (See Figure 12).

4.2.2 Source of infection for *Klebsiella* spp. collected in 2020 is not associated with seasonality

To understand whether there was an association with source of BSI and seasonality, the distribution of source of infection across 2020 was analysed. As mentioned in the previous chapter, BSIs can originate from various parts of the body such as the respiratory tract, urinary tract, GI tract, surgical site, skin and soft tissue. In some instances, source of infection can be unknown due to limited information on the history of the patient. The most common sources of infection for *Klebsiella* spp. were the urinary tract, GI tract and central line (Figure 30) and statistical analysis revealed no association between infections arising from these sources and the infection occurring in any particular season (Table 21).

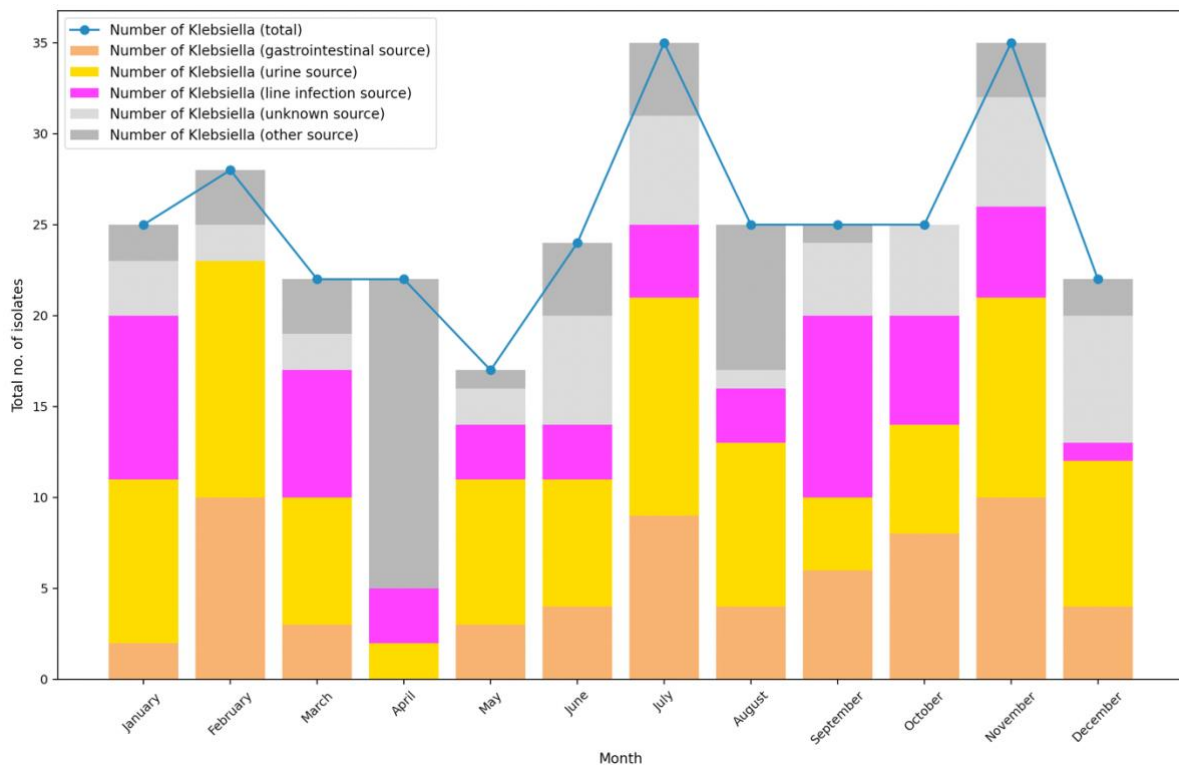


Figure 30. Monthly number of *Klebsiella* spp. collected divided by source of infection.

Table 21. Chi (χ^2) analysis revealed there was no significant association between *Klebsiella* spp. infections of different sources with different seasons. χ^2 analysis conducted on sources with the highest numbers. Other sources of infection with *K. aerogenes* and *K. varriicola* had a sample size too low for statistical analysis.

	Winter (Dec-Feb)	Spring (Mar-May)	Summer (Jun-Aug)	Autumn (Sept-Nov)	P value	Significance	Result
<i>Klebsiella</i> spp. from gastro	16	6	17	24	0.196	Not significant p <0.05	No association between <i>Klebsiella</i> spp. Infections and GI source in autumn
<i>Klebsiella</i> spp. from urinary	30	17	28	21	0.183	Not significant p <0.05	No association between <i>Klebsiella</i> spp. Infections and urinary source in winter
<i>Klebsiella</i> spp. from line infection	10	13	10	21	0.199	Not significant p <0.05	No association between <i>Klebsiella</i> spp. And line infections

In order to determine whether different *Klebsiella* spp. were significantly associated with either urinary, GI or central line source (the power for other sources of infection being too low to test), statistical analysis was conducted. Table 22 below revealed that the only statistically significant associations between source of infection and a particular species was that *K. pneumoniae* was less likely than chance to be associated with a central line source.

Table 22. Significance of associations between *K. pneumoniae* and *K. oxytoca* and any particular source of infection. The sample sizes for *K. aerogenes* and *K. varriicola* were too low for statistical analysis.

<i>Klebsiella</i> spp.	Source	Significance
<i>K. pneumoniae</i>	Not associated with urinary source	Not significant p >0.05 (p=0.206)
	Not associated with gastrointestinal source	Not significant p >0.05 (p=0.600)
	Association with non-line source	Significant p <0.05 (p=0.016)
<i>K. oxytoca</i>	Not associated with urinary source	Not significant p >0.05 (p=0.513)
	Not associated with gastrointestinal source	Not significant p >0.05 (p=0.176)
	Not associated with line source	Not significant p <0.05 (p=0.086)

To investigate there were different biases towards urinary and GI sources of infection compared to all other sources for *Klebsiella* spp. versus *E. coli*, urinary and GI source data for *E. coli* was compared with all *Klebsiella* spp. during 2020. Results reveal significant associations with GI and urinary source for *E. coli* compared to *Klebsiella* (Table 23).

Table 23. χ^2 analysis on *E. coli* and *Klebsiella* spp. collected throughout the year revealed there was a stronger association with urinary and GI source of infection in *E. coli*. compared to *Klebsiella* spp. Other sources of infection in both species had a sample size too low for statistical analysis.

	<i>E. coli</i>	<i>Klebsiella</i> spp.	Test	P value	Significance
GI source	144	24	chi	0.007	p <0.05
Urinary source	460	96	chi	0.00001	p <0.05

4.2.3 *K. pneumoniae* displayed higher resistance and virulence score in comparison to *K. quasipneumoniae*

From the sequenced BSI *Klebsiella* spp. isolated from BSIs, the 3 most common species identified were *K. pneumoniae*, *K. quasipneumoniae* and *K. varriicola*. *K. quasipneumoniae* was not identified through MALDI by Severn Pathology previously. *K. quasipneumoniae* were identified as *K. pneumoniae* by MALDI-TOF.

The resistance and virulence scores were analysed with Kleborate (Lam et al, 2021) for all isolates of these three species (Figure 31). Resistance is scored between 0 and 3, with 0 being least resistance (no ESBLs or carbapenemases) and 3 being the most resistant (presence of carbapenemases with colistin resistance). Virulence is scored between 0 and 5. Results reveal *K. pneumoniae* contained no ESBL or carbapenemase resistance and a range of virulence factors whilst all *K. variicola* species contained no ESBL or carbapenemase. *K. quasipneumoniae* contained no ESBL, carbapenemase or yersiniabactin.

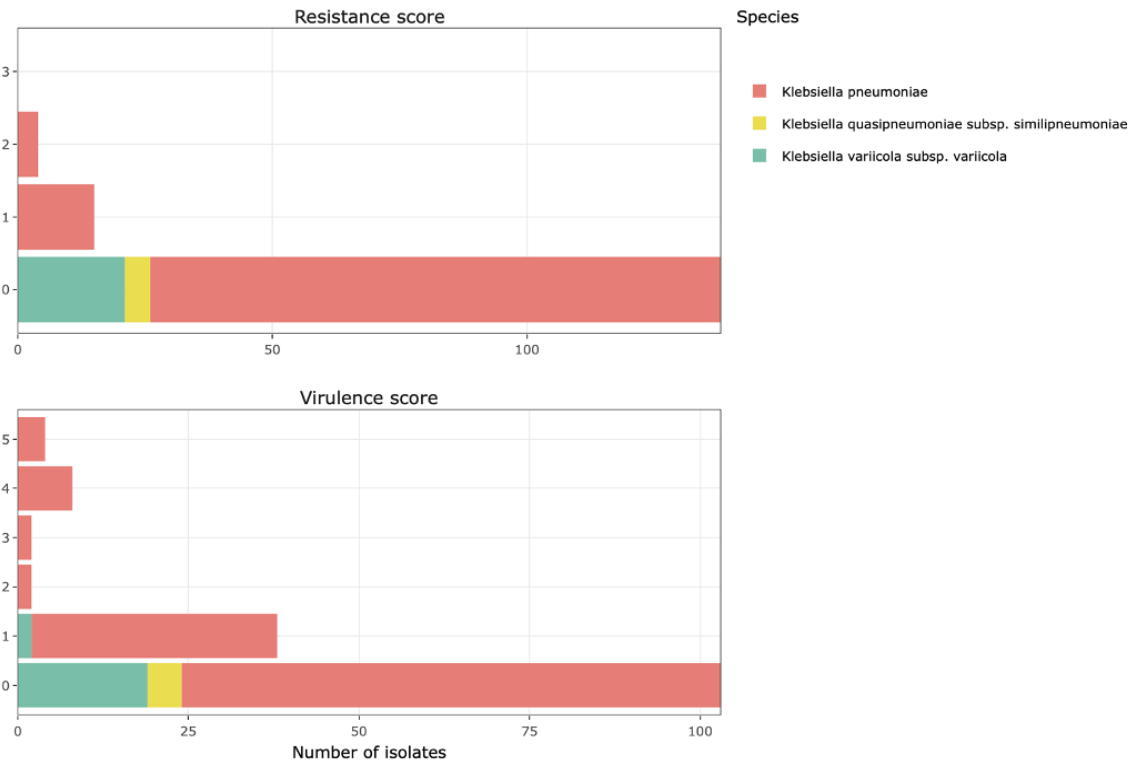


Figure 31. Resistance and virulence scores for *Klebsiella* spp.

Out of 108 STs identified in BSI *Klebsiella* spp., ST307 was most commonly identified (Figure 32).

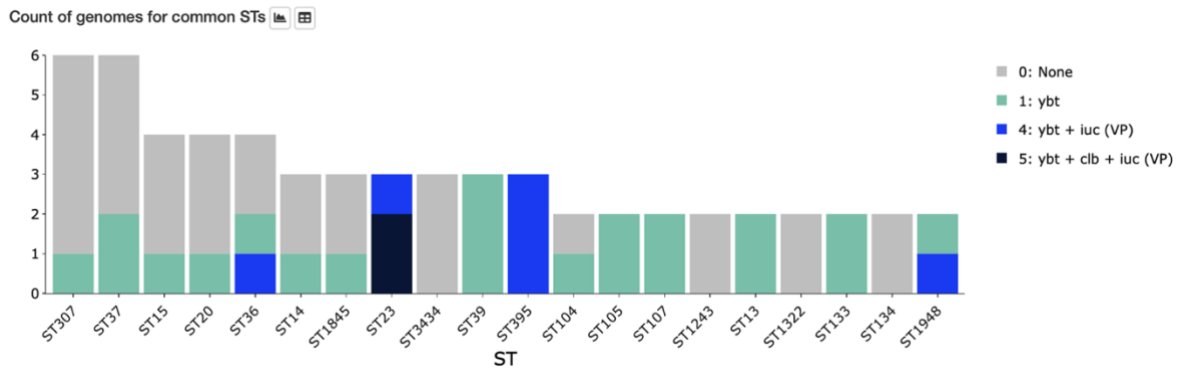


Figure 32. Graph showing most common STs detected in BSI *Klebsiella* spp.

A heatmap of resistance and virulence produced from Kleborate-Viz (Lam et al, 2021) revealed that this ST harboured AMR genes associated with aminoglycosides (AGly), FQs (fluoroquinolones), phe (phenicols), sul (sulphonamides), tet (tetracyclines), tmt (trimethoprim) and resistance to β -lactams (bla_ESBL)(red columns), with individual genomes displayed in rows (Figure 33). The heatmap also shows one individual genome of ST307 containing one virulence factor, yersiniabactin and 6 individual genomes harbouring different AMR mechanisms (Figure 33).

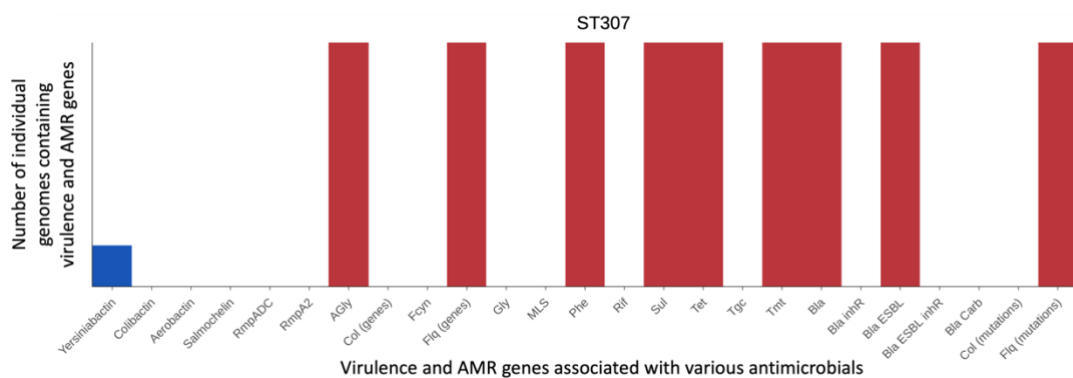


Figure 33. A bar graph displaying the presence different virulence factors and AMR mechanisms within the ST307 population. The red bars show the presence of resistance to specific antimicrobials and the blue bar shows the presence of specific virulence factors. No bars represent the absence of virulence factors and resistance.

4.2.4 Phylogenetic relationships reveal the majority of AMR mechanisms identified in *K. pneumoniae*, with MDR are detected in both ST307 and ST15

A core genome SNP tree for BSI *Klebsiella* spp. isolates was constructed to understand the population structure of *Klebsiella* spp. and assess whether AMR has been acquired independently or due to a spread of clonal isolates. Phylogenetic relationships with AMR overlaid showed no resistance determinants associated with any antimicrobial class important for treatment of BSI found in isolates from *K. oxytoca*, *K. pasteurii*, *K. grimontii*, *K. variicola* and *K. quasipneumoniae* (Figure 34a). Additionally, only two *K. michiganensis* isolates harboured CTX-M-15 (Figure 34a). Nevertheless, *K. pneumoniae* harboured the majority of AMR mechanisms, with clonal ST307 and NDM- carrying ST15 displaying resistance to 6 antimicrobial classes (Figure 34a, Figure 34b). Other STs of *K. pneumoniae* harboured AMR genes to at least 2 classes of antimicrobials (Table 24).

Table 24. Other STs of *K. pneumoniae* other than ST307 and ST15 harbouring multiple AMR genes and the frequency of which these STs occur.

ST of <i>K. pneumoniae</i>	Quantity	AMR genes
ST405	1	TEM-1D, OXA-1, CTXM-15, aac(3)-IIa, qnrB1
ST35	1	TEM-1D, OXA-1, CTXM-15, aac(3)-IIa, qnrB1
ST323	1	CTXM-15, aac(3)-IIa, qnrB1
ST395	2	TEM-1D, OXA-1, aac(6')-Ib-cr
ST1564	2	TEM-1D, CTXM-15, qnrB1

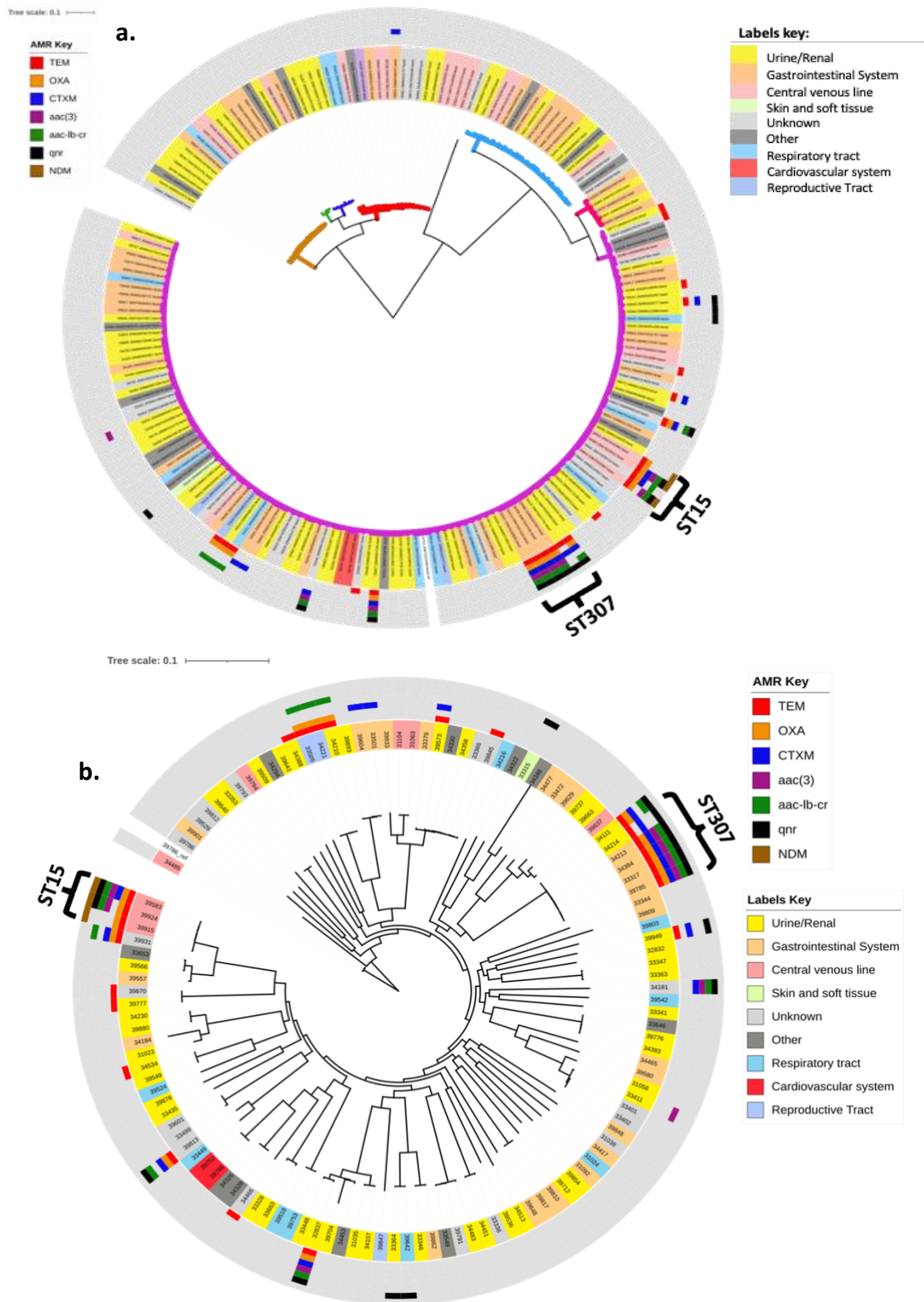


Figure 34a. Core genome SNP tree displaying the distribution of AMR genes across the *Klebsiella* population. Isolates are highlighted according to their source of infection. Clades are highlighted according to species in clockwise order: brown clade: *K. oxytoca*; green clade: *K. pasteurii*; dark blue clade: *K. grimontii*; red clade: *K. michiganensis*; black node: *K. aerogenes*; light blue clade: *K. variicola*; pink clade: *K. quasipneumoniae*; purple clade: *K. pneumoniae*. **b.** Core genome SNP tree on *K. pneumoniae* only, highlighting MDR for ST15 and ST307.

Hospital ward data was used to investigate whether the clonal ST307 and ST15 BSI isolates were isolated from patients in the same ward. Table 25 showed all ST15 isolates all came from patients situated in the same ward and 50% of ST307 isolates came from patients situated in A&E Bristol and A&E Bath, suggesting a community origin. These source of infection for these A&E isolates were considered most likely to be urinary and gut.

Table 25. Ward data associated with ST307 and ST15.

Sequence type	Quantity	Ward data
ST307	3	Ward 1
ST307	1	Ward 2
ST307	1	Ward 3
ST307	1	Ward 4
ST15	4	Ward 5

4.2.5 Characterisation of the genetic environments of 1 MDR ST147 and 3 MDR ST15 harbouring NDM-1 reveal the same resistance genes present in 5 separate genomic regions, with all ST15 identified from the same hospital ward

Due to reports of plasmid-mediated, MDR, NDM-carrying *K. pneumoniae*, investigation into the location of the AMR genes for all NDM-positive ST15 *K. pneumoniae* (isolates 39924, 39915 and 39583) and the only other NDM-carrying isolate in the collection, an ST147 *K. pneumoniae* (isolate 34419) were carried out. Using the in-built BLASTN within Bandage, all isolates matched in the assembly for *bla*_{CTX-M-15}, *bla*_{TEM-1D}, *aac(3)IIa*, *aac(6)-Ib-cr*, *bla*_{OXA-1} and *bla*_{SHV-12}, with *bla*_{NDM-1} alone present on a single contig. Genes *bla*_{CTX-M-15}, *bla*_{TEM-1D}, *aac(6)-Ib-cr* and *bla*_{OXA-1} were present on a single contig. Genes *bla*_{CTX-M-15}, *bla*_{TEM-1D} in addition to *aac(6)-Ib-cr* and *bla*_{OXA-1} were identified on the same contig for 3 out of 4 isolates (Figure 35).

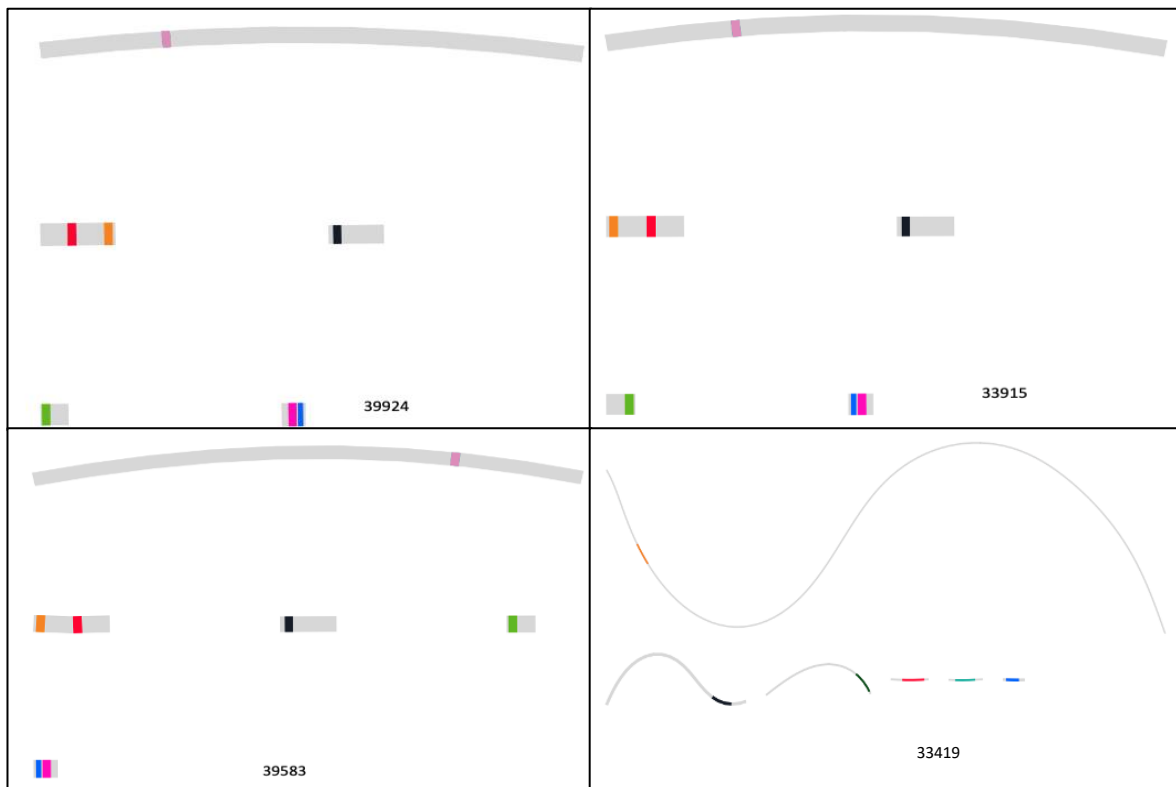


Figure 35. A visualisation through Bandage of the structure of the genomic regions containing different AMR genes (*bla*_{CTX-M-15} in red, *bla*_{TEM-1D} in orange, *aac*(3)-IIa in green, *aac*(6)-Ib-cr in blue and *bla*_{OXA-1} in pink) for all ST15 and the only one ST147 (33419) containing NDM (black).

Further characterisation and comparative genomics of contigs in all isolates containing *bla*_{NDM-1}, revealed the same genomic region and environment in all ST15 isolates, with ST147 harbouring a different genetic arrangement (Figure 36). The structure of the *bla*_{NDM-1} resistance region showed that genes adjacent to *bla*_{NDM-1} were on the same MGE.

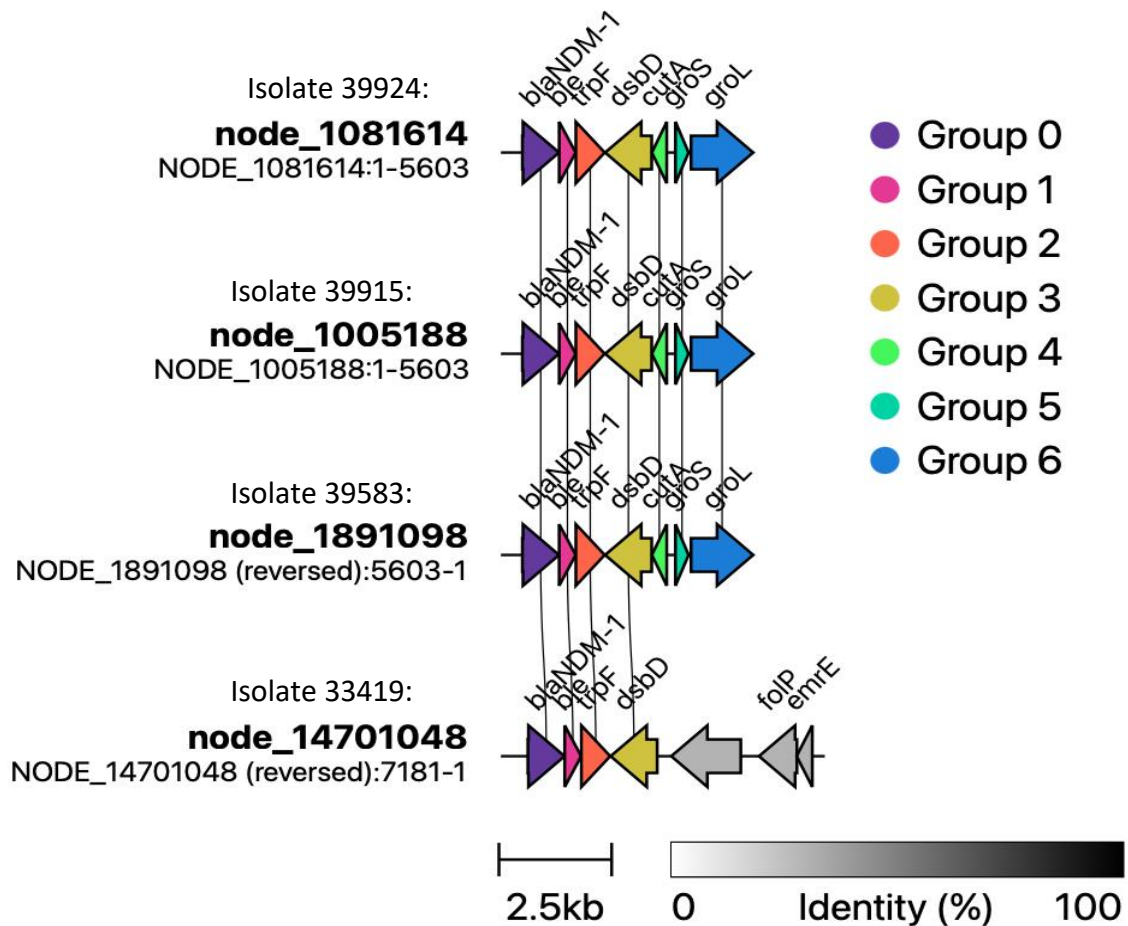


Figure 36. Characterisation and comparison of the genomic regions containing *bla*_{NDM-1} in MDR ST15. Group numbers represent a set of genes that match >90% and vertical lines show genes that are the same. The node numbers represent the name of the contig the genes are located on.

*bla*_{TEM-1D} and *bla*_{CTX-M-15}, were both found on the same contig, surrounded by the same genes in all ST15 isolates, with the NDM-1-producing ST147 harbouring different genetic arrangements (Figure 37). Clinker annotates gene families, therefore *bla*_{CTX-M-15} labelled by prokka was annotated as *bla*_{CTX-M-1}. The structure of the TEM and CTX-M encoding region showed that this region was identified on the same MGE.

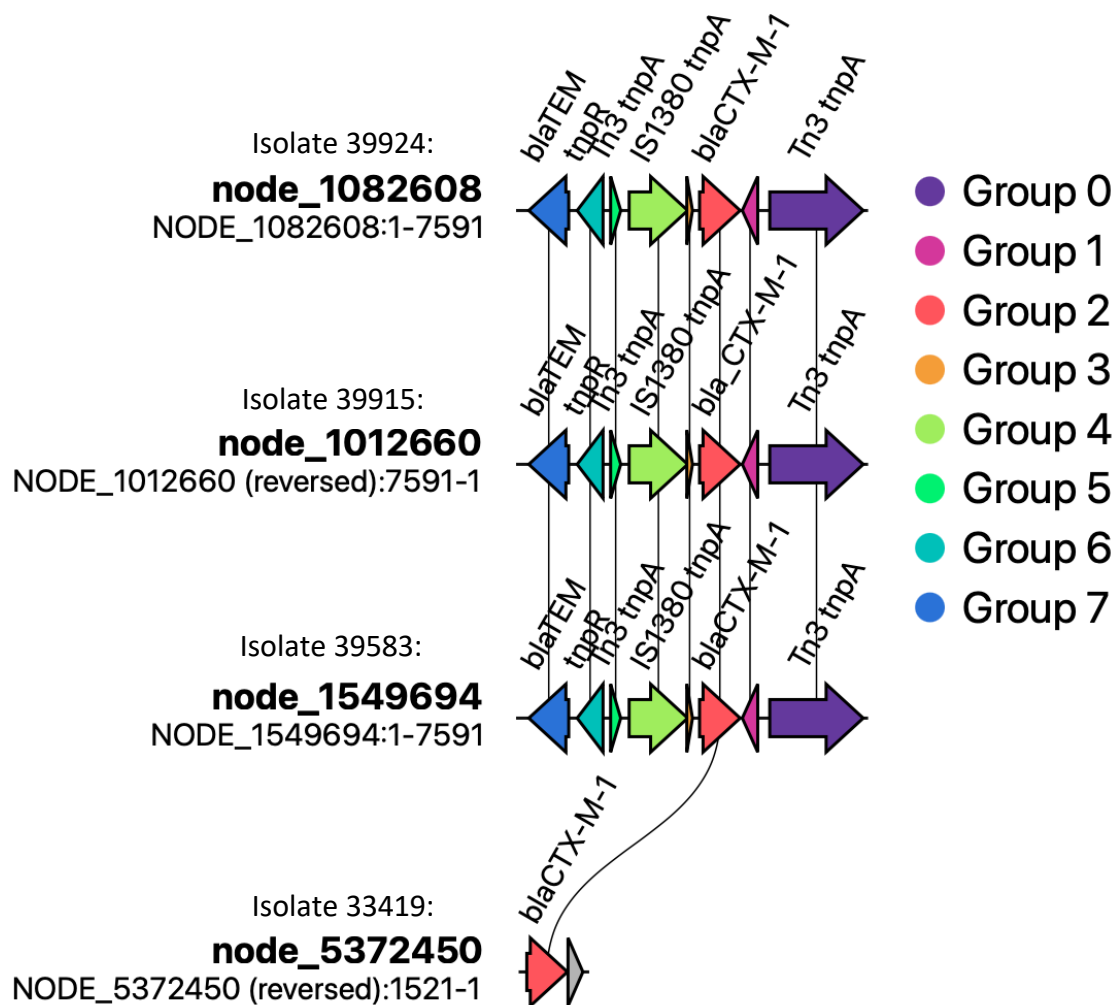


Figure 37. Characterisation and comparison of the genomic regions containing *bla*_{CTX-M} and *bla*_{TEM} in MDR ST15. Group numbers represent a set of genes that match >90% and vertical lines show genes that are the same. The node numbers represent the name of the contig the genes are located on.

Further characterisation of the contigs containing *aac(6)-lb-cr* and *bla_{OXA-1}*, revealed both genes paired on the same contig with *cat* in all ST15 isolates, with the NDM-1-producing ST147 again harbouring a different genetic arrangement (Figure 38) as also seen for the other genes.

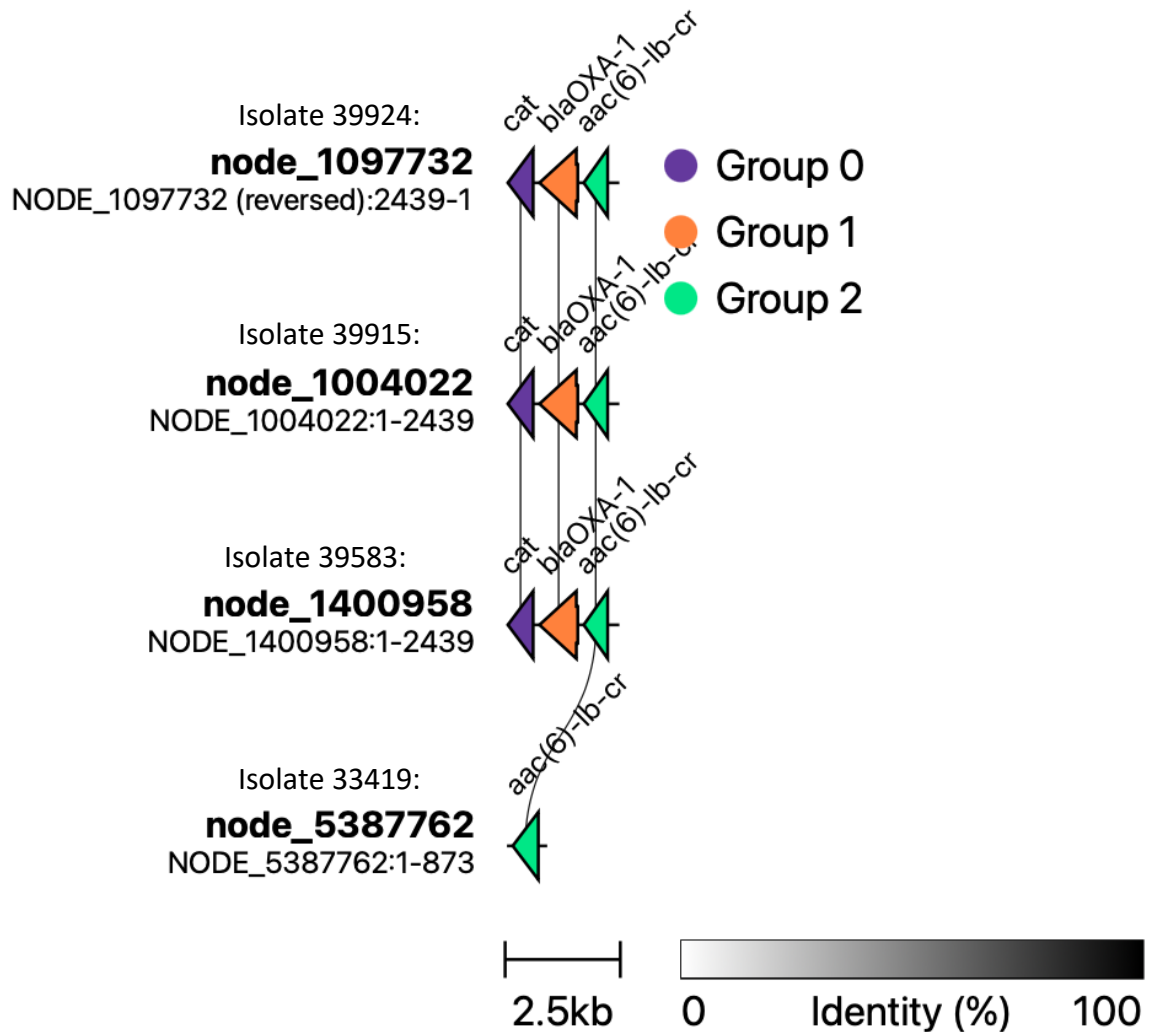


Figure 38. Characterisation and comparison of the genomic regions containing *bla_{OXA}* and *aac(6)-lb-cr* in MDR ST15. Group numbers represent a set of genes that match >90% and vertical lines show genes that are the same. The node numbers represent the name of the contig the genes are located on.

Further characterisation of the contigs containing *bla*_{SHV}, revealed it located near genes such as *lacZ* and *lacY*, as expected given that this is a chromosomal gene in *K. pneumoniae* (Figure 39).

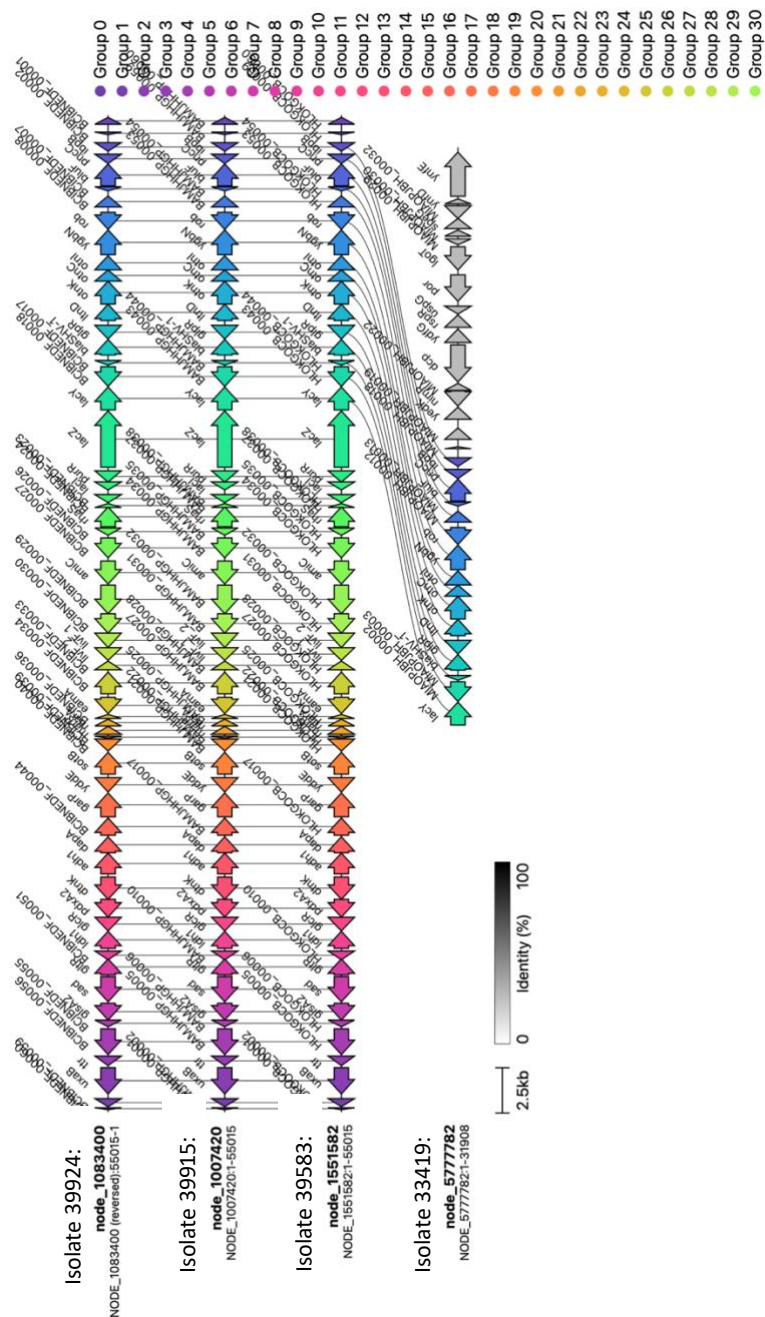


Figure 39. Characterisation and comparison of the genomic regions containing *bla*_{SHV} in MDR ST15. Group numbers represent a set of genes that match >90% and vertical lines show genes that are the same. The node numbers represent the name of the contig the genes are located on.

4.3 Discussion and Conclusion

K. pneumoniae was the most frequent *Klebsiella* spp. cause of BSIs in Bristol and surrounding regions in 2020 (Figure 29), with *K. varriicola*, *K. michiganensis*, *K. oxytoca*, *K. pasteurii*, *K. grimontii* and *K. aerogenes* in order of prevalence. Population-based BSI surveillance is consistent with this study's findings regarding the prominence of *K. pneumoniae* as a Gram-negative BSI pathogen, second to *E. coli* (Figure 29).

Comprehensive reviews have detailed the taxonomy of *Klebsiella* spp., revealing *K. variicola* and *K. quasipneumoniae* as new species, in contrast to previous classification as *K. pneumoniae* phylogroups KpII and KpIII (Rosenbleuth et al, 2004; Brisse et al, 2014). However, the misidentification of *K. variicola* as *K. pneumoniae* with automated systems and laboratory tests has been observed (Rodríguez-Medina et al, 2019), with one study reporting incorrect diagnosis for fatal sepsis caused by *K. variicola* (Seki et al, 2013). Furthermore, misidentification of *K. quasipneumoniae* as *K. pneumoniae* by MALDI-TOF has also been reported (Long et al, 2017). In keeping with this, the identification provided by Severn Pathology for *Klebsiella* spp. isolated from BSIs revealed no isolates identified as *K. quasipneumoniae*. Nevertheless, WGS showed *K. quasipneumoniae* had been erroneously identified as *K. pneumoniae* by MALDI-TOF, though these isolates harboured no resistance genes associated with any antimicrobial class important for the treatment of BSI.

This study showed a two-fold increase in *K. pneumoniae* causing BSIs between June and July in the summer, confirming the results of previous analyses. For example, Anderson *et al.* (2008) reported an incidence rate of 1.5 times higher across 4 continents during the 4 warmest months between 2001 and 2006 for *K. pneumoniae* causing BSIs. In contrast with this, Al-Hasan *et al.* (2010) conducted a population-

based study on *Klebsiella* spp. showing no significant difference in the incidence during the warmer months. Little research has been conducted that focus on the associations between infection caused by *Klebsiella* spp., source of infection and seasonality. Li & Huang. 2017 reported intra-abdominal site of infection lead to significantly higher mortality rates for *Klebsiella* causing BSIs. Al-Hasan *et al.* (2010) revealed urinary tract source of infection was most common source of *Klebsiella* causing BSIs. Furthermore, Kito *et al.* (2022) showed a positive correlation between higher average monthly temperatures and frequency of isolation of *K. pneumoniae* from the urinary tract. This suggests a possible reason for an increase in urinary source *K. pneumoniae* BSIs during the summer months. However, Figure 30 in this study also showed an increase in *K. pneumoniae* BSIs during the winter.

Table 22 in this study no association was observed with central line source of infection and *K. oxytoca*, which does not support findings from a previous study reporting an outbreak of catheter associated *K. oxytoca* BSIs (Watson *et al.*, 2005). Additionally, Advani *et al.* (2011) reported increased risk of Gram-negative pathogens causing BSIs, including *K. oxytoca* associated with central venous catheters in hospitalised children in intensive care. These findings emphasize the need for understanding associations between source of infection and common pathogens, particularly related species causing BSIs due to variation across species. This enables facilitation of infection control and subsequently, empiric antimicrobial therapy.

There is a public health concern for AMR *K. pneumoniae* clones and increasing numbers of reports have discussed a rise in ST307, due to its carriage of ESBLs and/or carbapenemases. Whilst the majority of *Klebsiella* isolates in this BSI survey contained no ESBL or carbapenemase, ST307 was the most common ST identified, all harbouring CTX-M-15 and OXA-1 encoding genes (Figure 34a, Figure 34b). ST307

was also isolated from patients being admitted to A&E, suggesting this ST is circulating in the community, and driving infection there. A *K. pneumoniae* ST307 clone harbouring *bla*_{CTX-M-15} and *bla*_{OXA-48} has increased worldwide, with this clone reported across Spain, Russia, Brazil and Japan (Ruiz-garbajosa et al, 2016; Lazareva et al, 2016; Dropa et al, 2016; Harada et al, 2016). Heiden *et al.* (2020) demonstrated that an outbreak an ST307 lineage in the community and genomic analysis suggested inter patient transmission of ST307, with resistance genes shared between ST307 and other STs.

No *K. pneumoniae* virulence plasmid that encodes salmonchelin, aerobactin siderophores and RmpA/RmpA2 was detected, however Figure 33 showed some isolates harboured yersiniabactin and Wyres *et al.* (2016; 2020) reported similar findings. The molecular mechanism causing enhanced fitness and virulence of ST307 worldwide is still unknown, however, Villa *et al.* (2017) discussed a large plasmid, pKPN-307, type A, harbouring 5 main virulence factors and a MDR region encoding *bla*_{CTX-M-15}, *bla*_{TEM-1}, *bla*_{OXA-1}, *qnrB1*, *sul2*, *dfra14* and heavy metal resistance, which may contribute towards enhanced pathogenicity, persistence and virulence, though this would need to be experimentally determined. In addition to MDR clones such as ST258 and ST11, many studies have reported outbreaks of KPC-2- and NDM-producing ST37, mainly from Europe and Asia (Yang et al, 2013; Illiaquer et al, 2012). Whilst 85% of ST37 isolates within the dataset were not MDR and did not produce NDM or KPC, this ST was the second most common identified in this dataset (Figure 32). ST37 harbouring IncR plasmids including an MDR region with *bla*_{DHA-1} and *qnrB4* genes have been reported, with identical IncR backbones suggesting dissemination of IncR in ST37 (Guo et al, 2016). However, this was not observed in our study of isolates from Bristol and surrounding regions. Out of all STs, ST23 showed the highest

virulence score, followed by ST395 (Figure 32). ST395 is identified as an emerging international hypervirulent and MDR clone (Arca-Suárez et al, 2022; Shaidullina et al, 2023). In depth genomic analysis of ST395 isolates from the surveillance study presented here identified four clades further subdivided by 8 smaller clade and the majority of ST395 harboured ESBL, carbapenems, other AMR genes associated with multiple antimicrobial classes together with hypervirulence markers and multiple plasmid types (Shaidullina et al, 2023). The phylogeny and evolution of ST395 in this study could not be carried out due to small sample size, however, all ST395 contained at least 5 virulence markers and AMR genes relevant to at least 5 antimicrobial classes, matching with previous findings. In contrast, this study revealed all ST23 containing at least 6 virulence markers, however only harbouring 1 resistance gene, *bla*_{SHV-12}. In the literature previously, hypervirulent ST23 *K. pneumoniae* demonstrated susceptibility to all antimicrobials tested (Shankar et al, 2018), however in recent years, this particular ST is no longer pan-susceptible. A study reported MDR and hypervirulent ST23, attributed by the detection of up to 7 MDR plasmids and a virulence plasmid carrying *catA1* (Shankar et al, 2020). In keeping with this, a report conducted on the ST23 *K. pneumoniae* clone in Spain demonstrated isolates harbouring a hybrid virulence and MDR IncFIB plasmid co-producing CTX-M-15 and extensive virulence factors such as those encoded by *rmpA*, *rmpA2* *iucABCD-iutA* and *iroBCDN* (Hernández et al, 2021). Furthermore *bla*_{OXA-48} and *armA* were located on the same genomic region amongst transposons and MGEs (Hernández et al, 2021). These studies indicate the need for monitoring ST23 in our region, despite the lack of AMR observed currently, as previous recent studies have demonstrated potential for the co-existence of MDR and hypervirulence. This emphasizes the importance of surveillance to monitor emergence of both hypervirulent and MDR *K. pneumoniae*.

A large diversity of species are classified under *Klebsiella* spp. with a distinguished *K. pneumoniae* complex, referred to as KpsC separate to other *Klebsiella* spp., despite sharing a 90% average nucleotide identity (Wyres et al, 2020). In this study, *K. pneumoniae* formed the majority of the population, harbouring the most AMR genes compared to other species (Figure 34). *K. oxytoca*, *K. quasipneumoniae*, *K. grimontii*, *K. pasteurii* and *K. variicola* harboured no AMR genes, with only resistant determinant CTX-M detected in *K. michiganensis*. In contrast to this, Prah et al. reported the emergence and spread of KPC-producing *K. michiganensis* clones. Furthermore, studies have reported high prevalence of MDR in *K. oxytoca* and *K. variicola* (Al-Sheboul et al, 2023; Moradigaravand et al, 2017; Amabile de Campos et al, 2021). Resistance has also been identified recently in *K. quasipneumoniae*. A study in China identified plasmid-encoded efflux pumps in MDR *K. quasipneumoniae* and high transmissibility between MDR plasmids in *K. pneumoniae* (He et al, 2021). Data on AMR patterns and clonality is scarce for *K. grimontii*. However, Campos-Madueno et al. (2021) revealed *bla_{VIM-1}* and *mcr-9* located on the plasmid IncH2/HI2A found in *K. grimontii* and phylogenetics showed <15 nucleotide variants to Swedish and Swiss *K. grimontii* strains. Whilst prevalence of AMR was low in non-*K. pneumoniae* spp. in this study, others have highlighted the necessity for strengthening surveillance in these species as high transmissibility of AMR genes and conjugation between plasmids show the potential for bacterial species to become AMR in future.

This study identified associations between source of infection and pathogens from BSIs irrespective of resistance in addition to in-depth characterisations for MDR isolates from specific wards have not been conducted previously in our region. Nevertheless, there are several limitations to this study. One of this study's limitations involves conducting this study during the pandemic year. Due to changes in NHS

infrastructure and increased attention to COVID-19 patient cases, source of infection and portal of entry for some *Klebsiella* causing BSIs were undetermined. Thus, the actual number of *Klebsiella* spp. with a source is likely to be more than the stated amount presented in this study and therefore the dataset used has some limitations of power for analysis. Furthermore, due to collection of isolates during the pandemic year, distribution of AMR mechanisms across the population may not reflect the trends observed previously in the literature in other geographical regions. Therefore, future work would involve collecting *Klebsiella* causing BSIs for a longer duration for comparison. Further work could also involve predictions of emerging AMR profiles from analysing the interplay between AMR mechanisms and data linkage involving clinical background information for patients, including underlying disease and previous antibiotic therapy administered.

5.0 Results Chapter 3

Understanding the interplay between plasmids replicons, AMR and virulence gene complement among *E. coli* and *K. pneumoniae* from BSIs

5.1 Introduction

As detailed in the main introduction, pathogens such as *Klebsiella* spp. and *E. coli*, in particular ExPEC have the ability to access and colonise in the bloodstream, causing BSIs, where a multitude of virulence factors have been associated with this process. ExPEC and *Klebsiella* spp. strains are of great importance as they can harbour a variety of AMR genes which can be located on plasmids, accelerating transmission to other pathogenic or opportunistic bacteria. The challenge of providing antimicrobials initiated empirically for BSIs is exacerbated by the presence of virulence factors which can increase the severity of infection. Virulence factors identified in ExPEC strains can be categorised into 5 groups as detailed below (Table 26).

Table 26. Virulence genes, their associated encoded functions, functional group and presence in different *E. coli* pathotypes. Adapted from Sora *et al.* (2021).

Virulence gene	Description	Function	Group	Presence in different ExPECs
<i>fim</i>	Type 1 fimbriae	Colonisation and biofilm formation	Adhesins	UPEC, MNEC, SEPEC
<i>afa</i>	Afimbral adhesion	Cell surface adhesion	Adhesins	UPEC
<i>pap</i>	P fimbriae	Adherence to host cells	Adhesins	UPEC, ExPEC
<i>sfa</i>	S fimbriae	Adhesion to cells in urinary tract	Adhesins	UPEC
<i>foc</i>	FIC fimbriae	Adhesion to bladder and kidneys	Adhesins	UPEC
<i>ibeA</i>	IbeABC	Invasion in tissues	Invasion	SEPEC, MNEC
<i>iuc</i>	Aerobactin	Siderophore	Iron uptake	UPEC
<i>iroN</i>	Salmochelins	Siderophore receptor	Iron uptake	UPEC, MNEC, SEPEC
<i>traT</i>	Transfer protein	Inhibits complement pathway	Serum resistance/protectines	MNEC, SEPEC
<i>KpsMII</i>	Capsular antigens	Protection factor against phagocytosis	Serum resistance/protectines	MNEC, SEPEC
<i>ompT</i>	Outer membrane protein	Evasion against host defense	Serum resistance/protectines	UPEC, MNEC
<i>iss</i>	Serum survival	Protection against phagocytosis	Serum resistance/protectines	MNEC, SEPEC
<i>cvaC</i>	CvaC	Aids colonisation	Serum resistance/protectines	MNEC, SEPEC
<i>hlyA</i>	Haemolysin A	Creation of host membrane pores	Toxins	UPEC
<i>cnf</i>	Cytotoxic necrotising factor	Cell necrosis	Toxins	UPEC, SEPEC
<i>vat</i>	Vacuolating autotransporter toxin	Host cell vacuolisation	Toxins	UPEC

Virulence factors can assist with survival in and colonisation of the host and this is often linked with worsened clinical outcomes. A study conducted by D'Onofrio *et al.* (2023) to investigate the associations between virulence profiles and severity of outcome from clinical *E. coli* revealed increased frequency of *mch* and *pap* genes in patients with sepsis and urosepsis respectively. Furthermore, *kpsMIII_K23* was identified in patients who died whilst the identification of *cvaC* was associated with patients admitted to ICU. However, another study reported a positive correlation between virulence gene *iroN*, the isolate being of ST405 and increased 30-day mortality (Hung et al, 2019). Studies on AMR and virulence and their impact on mortality have also been conducted on *Klebsiella* spp. One study revealed an increase in mortality for *K. pneumoniae* isolates with the carriage of *pks* gene cluster, which plays a role in colibactin synthesis (Kim et al, 2019). Moreover, a mortality rate of 47.2% was associated with ST11-K64 co-harboring a KPC plasmid along with *iutA*, in comparison with a mortality rate of 30.4% associated with *K. pneumoniae* BSI alone (Wu et al, 2021). This highlights the necessity of surveillance of virulence profiles to facilitate better management of patients with BSIs caused by hypervirulent strains through the development and improvement of anti-virulence drugs .

The presence of genes encoding CTX-M variants on plasmids has accelerated the global spread of this ESBL. Various studies have revealed that members of the IncF plasmid family, for example IncFIB and IncFII replicons are predominantly associated with *bla*_{CTX-M-15} (Gonullu et al, 2008; Diestra et al, 2009). An IncF plasmid was identified in a pandemic of MDR ST131 *E. coli* harbouring *bla*_{CTX-M-15} (Woodford, 2008). IS elements and the composite transposons they generate are responsible for the dissemination of *bla*_{CTX-M-15}, with *ISEcp1* most commonly associated with CTX-M variants, enabling mobilisation on to plasmids (Zhao & Hu, 2013). Epidemic IncF

plasmids have contributed towards the success of ExPEC, with IncF::CTX-M-15/ST131-C2 being one of the most successful plasmid/host strain combinations to date since its first emergence in the early 2000s (Pitout & Chen, 2023). Furthermore, a ST410-B3 subclade harbouring *bla*_{CTX-M-15} has been found that has integrated *bla*_{NDM-5} into its IncF plasmid, expanding resistance to carbapenems (Pitout & Chen, 2023). An increase in the prevalence of convergence between AMR and virulence (i.e. where both traits are encoded in the same bacterium) has also been reported. One study demonstrated increased co-occurrence of *papGII* and *bla*_{CTX-M-15} located on the chromosome and the acquisition and loss of IncFII:AI:B plasmids observed within ST131 subclade C2 in ST131 (Biggel et al, 2022).

In *Klebsiella* spp., the ability to transfer KPC plasmids (encoding carbapenem resistance) into K2-ST65 hypervirulent *K. pneumoniae* without the loss of virulence has been observed (Yu et al, 2008). Convergence of AMR and virulence in the same plasmid has become more common and has been identified in a hypervirulent ST25 *K. pneumoniae* plasmid pCY814036 harbouring a virulence *iuc* operon encoding for aerobactin and AMR genes, which has also been observed to coexist with a KPC plasmid. Phenotypic work and mouse infection models demonstrated transfer of these AMR and virulence genes to a recipient bacterium (Xia et al, 2022). This highlights the importance of genomics analysis to characterise plasmids and monitor the convergence of virulence and AMR which can lead to difficulty in treatment.

Knowledge about circulating local AMR determinants, virulence genes and plasmids in addition to understanding associations between these factors, especially with consideration of data on source of infection, may help determine genotypic profiles and the impact on severity of BSI. This could help optimise patient management and inform empiric antimicrobial prescribing. This chapter describes the distribution of

virulence, plasmid replicon and AMR profiles in *E. coli* and *Klebsiella* spp. isolates from BSIs in addition to investigating whether virulence and AMR genes are converged on plasmid-associated contigs. Whilst associations between phylogroup and source of infection for *E. coli* BSIs have been conducted in Chapter 1, little is known on the associations between specific virulence factors and *E. coli* causing BSIs originating from the urinary tract, or other specific sources. Therefore, this chapter also describes the relationship between virulence factors and *E. coli* BSIs, focusing on urinary source versus other sources.

AIMS: To understand the relationships between virulence genes, plasmid replicon types and resistance genes among BSI Gram-negative bacteria in this study region using *E. coli* and *Klebsiella* spp. as examples. Furthermore, this chapter aims to investigate whether particular virulence factors are associated with *E. coli* that cause BSIs from a urinary or other source of infection.

5.2 Results

5.2.1 Dominance of a small number of virulence factors including yersiniabactin, aerobactin, salmochelin and serum resistance were found among *E. coli* causing BSIs

Across the sequenced *E. coli* BSI population (n=667), with isolates collected in 2020 and not selected for resistance to any particular antibiotic, or because of any particular source of infection, as described in Chapter 1, at least one virulence gene (based on the Virulence finder database) was detected in 491 (73.6%) isolates. A total count of the number of *E. coli* BSI isolates containing commonly detected virulence factors that have previously been associated with BSIs in the literature (Bongyoung et al, 2022) was next conducted. Figure 40 shows *fyuA* encoding a yersiniabactin uptake receptor, *ompT* encoding outer membrane proteins, *iss* and *traT* associated with serum resistance, and *iucC* and *iutA* encoding aerobactin receptors were most commonly identified. Whilst 237 isolates harboured *papC*, zero isolates harboured *papG* associated with fimbrial adhesion in UPEC. Figure 41 also shows the range of the total number of virulence genes present in BSI *E. coli* isolates, with one isolate harbouring 3 virulence genes and one isolate harbouring 49 virulence genes. The median number of genes per isolate was 25 and the mode (the highest number of virulence genes that most isolates harboured) was 23.

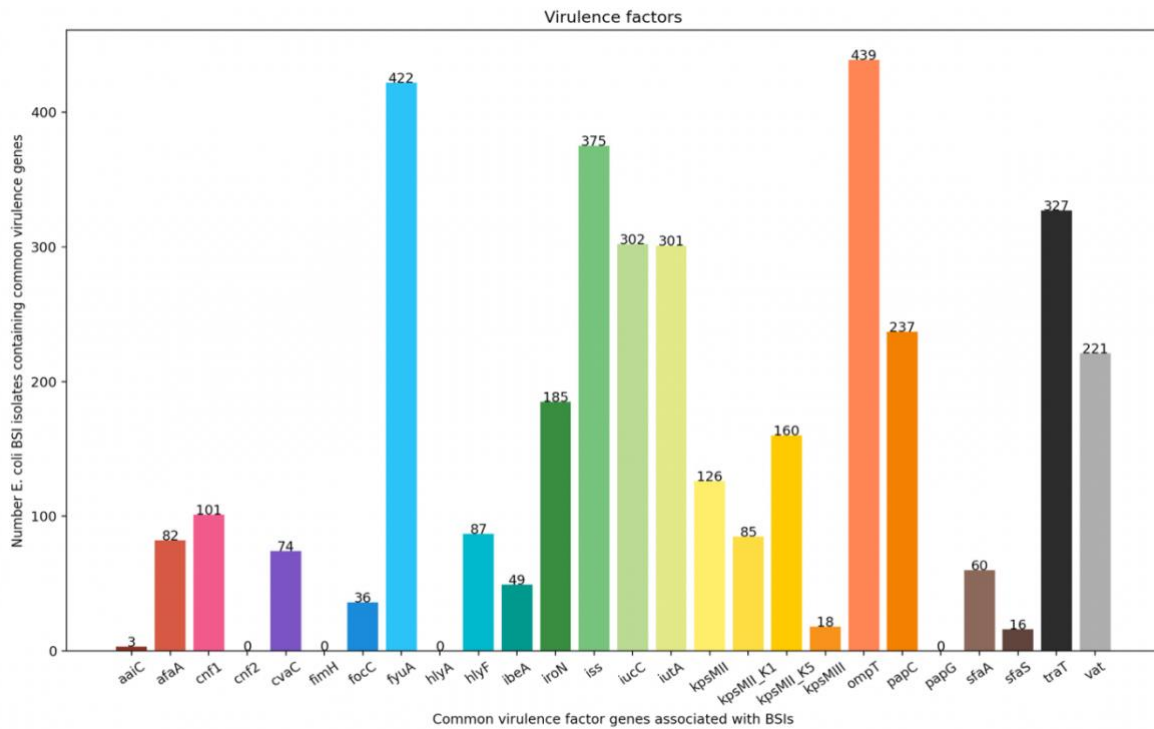


Figure 40. Graph displaying the number of isolates (n=491, total) harbouring the most common virulence factor genes previously associated with BSIs.

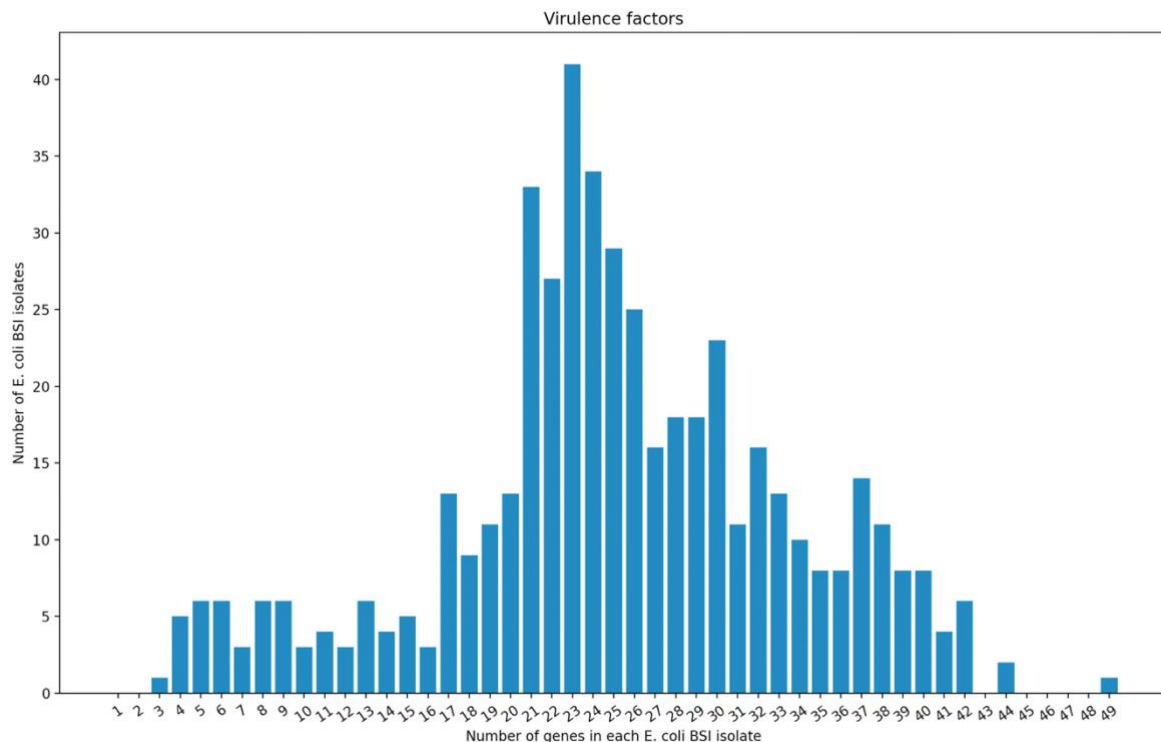


Figure 41. Graph displaying the distribution of virulence gene content of *E. coli* BSIs.

5.2.2 Understanding the distribution of AMR, virulence and plasmid replicons in the BSI *E. coli* population

Associations between AMR and source of infection were investigated in chapter 1. Therefore, this chapter focuses on identifying the associations between virulence gene presence and infection source data in addition to investigating the associations between AMR and virulence genes on plasmid-associated contigs in the most MDR *E. coli* isolates (section 5.2.3).

As mentioned in Chapter 1, AMR mechanisms are intermixed with isolates from different phylogroups, with the purple subclade (Figure 42) containing ST131 harbouring CTX-M, OXA and chromosomal mutations associated with resistance to ciprofloxacin (Figure 42).

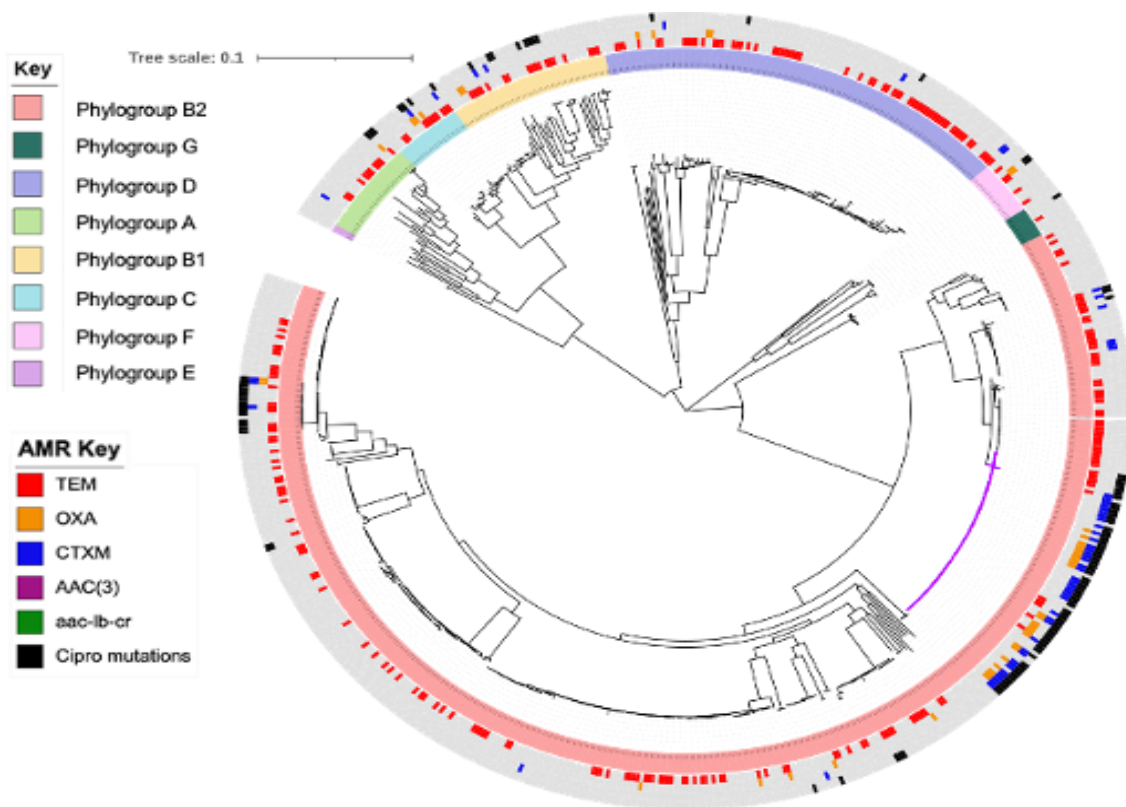


Figure 42. A core genome SNP tree consisting of 667 *E. coli* (n=11 isolates with bad quality assemblies that are not present in the tree) displaying the distribution of phylogroups and its associated AMR profiles. Reprinted from Chapter 1.

To understand the virulence patterns in *E. coli* causing BSIs in 2020, virulence gene data was mapped with phylogenetic data, with virulence genes being aggregated into their class, where at least one gene from that class is required to label the isolate as positive. Virulence factor classes were dispersed amongst the population, with fewer classes being produced by phylogroup A and B1 isolates (Figure 43). No virulence factor classes were identified by phylogroup E isolates, however at least two virulence factor classes were detected in all other phylogroups, with phylogroup B2 displaying the most diversity among virulence factor classes (Figure 43).

From Figure 43 (red dots represent urinary source BSIs), it is apparent that more virulence classes were identified among BSI *E. coli* from a urinary source. In the literature it is established that a wide variety of virulence factors in *E. coli* aid in colonisation, ascension through the urinary tract and penetration of endothelial cells into the bloodstream, resulting in BSI (Kaper et al, 2004). There is little knowledge concerning which virulence factors are specifically associated with urinary source BSI, therefore, to investigate this further, statistical analysis was conducted. Isolates with no determined source of infection were excluded from this analysis (n=120). The genes selected for this analysis were those mainly detected in ExPEC causing BSIs (Table 27) (Johnson & Stell, 2000; Koga et al, 2014, Daga et al, 2019).

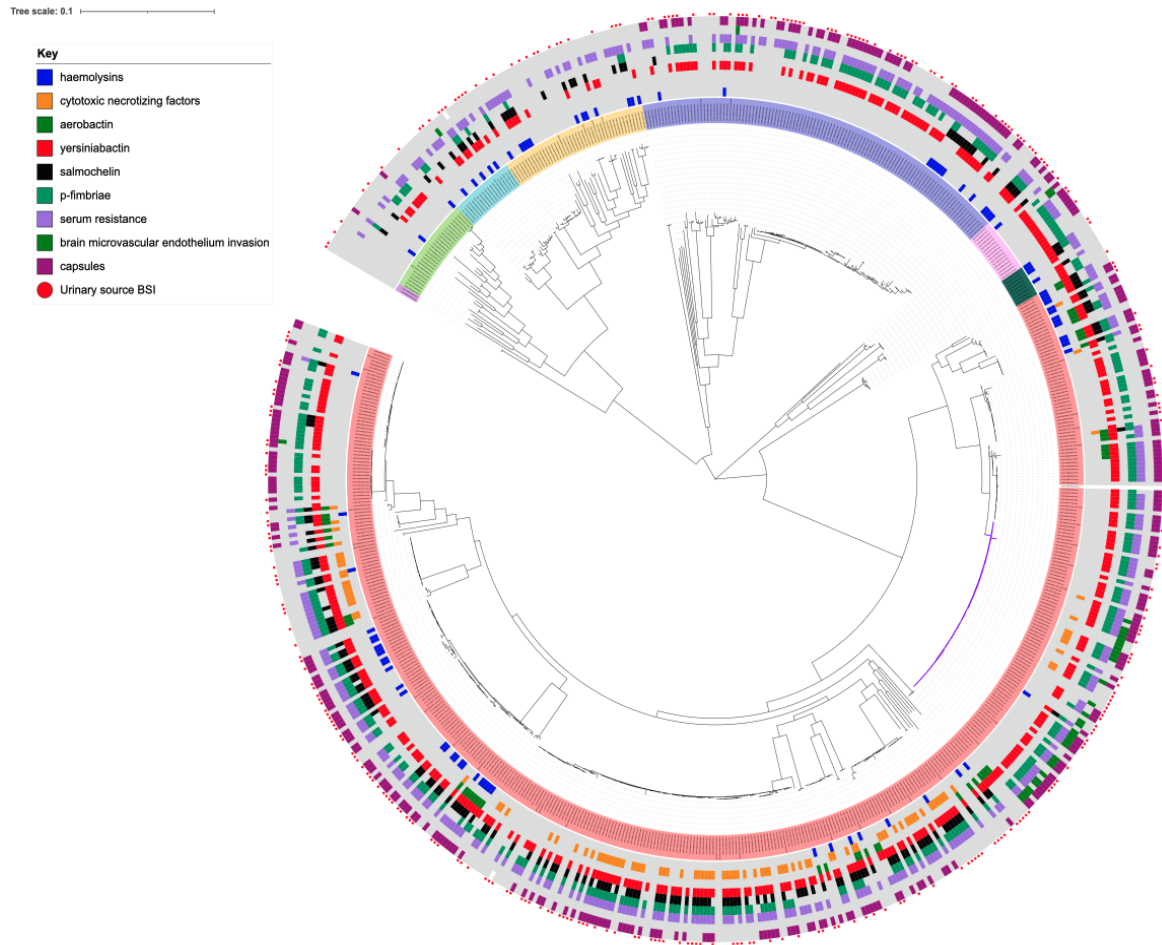


Figure 43. A core genome SNP tree consisting of 667 *E. coli* (n=11 isolates with bad quality assemblies that are not present in the tree) displaying the distribution of phylogroups and its associated virulence profiles.

Table 27. Table detailing the main virulence factors in ExPEC causing BSIs.

Virulence	Virulence genes
Haemolysins	<i>hlyA, hlyF</i>
Cytotoxic necrotizing factors	<i>cnf1, cnf2</i>
Aerobactin	<i>iutA</i>
Yersiniabactin	<i>fyuA</i>
Salmochelin	<i>iron</i>
P-fimbriae	<i>papC, papG</i>
Serum resistance	<i>iss, traT</i>
Brain microvascular endothelium invasion	<i>ibeA</i>
Capsules	<i>kpsMTK1, kpsMTK5, kpsMTII, kpsMTIII</i>

Overall, results reveal a strong statistical association between the main virulence factors combined (isolates containing one or more of the genes listed in Table 27) with urinary source of infection at $p < 0.05$ ($p < 0.00001$) (Table 28). Analysis on the genes separately revealed a strong significance for the association between carriage of aerobactin, yersiniabactin, salmochelin, p-fimbriae, serum resistance and a capsule-associated gene and urinary source BSI ($p < 0.00001$) (Table 29). Borderline significant association was detected for haemolysins ($p = 0.049$) and cytotoxic necrotising factors ($p = 0.045$) with urinary source *E. coli* BSI infections (Table 29). No statistical significance was detected at $p < 0.05$ for brain microvascular endothelium invasion factor ($p = 0.925$).

Table 28. χ^2 analysis revealed strong associations between carriage of one or more specific virulence genes (defined in Table 27) and *E. coli* BSI with urinary source, versus all other sources combined.

Source of BSI	Number of isolates containing any of the main virulence factors associated with <i>E. coli</i> causing BSIs (haemolysins, cytotoxic necrotizing factors, aerobactin, yersiniabactin, salmonchelin, p-fimbriae, serum resistance, brain microvascular endothelium invasion, capsules)	Significance
Urinary source	236	Significant p <0.05 (p value <0.00001)
Non-urinary source	176	

Table 29. χ^2 analysis revealed strong associations between carriage of genes encoding aerobactin, yersiniabactin, salmochelin, p-fimbriae, serum resistance and capsule among *E. coli* BSI with urinary source, versus all other sources combined.

Virulence factors associated with <i>E. coli</i> causing BSIs	Significance
haemolysins	Significant at p <0.05 (p value 0.0486)
cytotoxic necrotizing factors	Significant at p <0.05 (p value 0.0453)
aerobactin	Significant at p <0.05 (p value <0.00001)
yersiniabactin	Significant at p <0.05 (p value <0.00001)
salmochelin	Significant at p <0.05 (p value 0.003)
p-fimbriae	Significant at p <0.05 (p value <0.00001)
serum resistance	Significant at p <0.05 (p value <0.00001)
brain microvascular endothelium invasion	Not significant p >0.05 (p value 0.925)
capsules	Significant at p <0.05 (p value <0.00001)

Numerous reports have described hypervirulence associated with ST131, and it was shown in results Chapter 1 that ST131 was significantly associated with urinary source infections, therefore in order to confirm that urinary source of BSI is associated with carriage of more specific virulence factors, even among an ST that is known to be biased towards urinary source, and dominant among the population being studied here, χ^2 analysis was conducted as above specifically for ST131 isolates that harboured virulence genes (Table 30) (n=38). This analysis confirmed that ST131 isolates also had a bias towards carriage of certain virulence genes, if they came from a urinary source. χ^2 analysis revealed strong associations between virulence and ST131 *E. coli* infections with urinary source ($p = 0.16027$). Statistical analysis could not be performed on urinary source ST131 harbouring yersiniabactin, as the presence of genes associated with yersiniabactin were observed in all ST131. Additionally, statistical analysis could not be performed with urinary source ST131 with salmochelin as no urinary source ST131 harboured salmochelin.

Table 30. χ^2 analysis revealed strong associations between virulence factors associated with aerobactin and capsules and ST131 from urinary source.

Virulence genes	test	Significance
Cytotoxic necrotizing factors	chi	Not significant at $p < 0.05$ (p value 0.560)
Aerobactin	chi	Significant at $p < 0.05$ (p value <0.0039)
P-fimbriae	chi	Not significant at $p < 0.05$ (p value <0.204)
Serum resistance	chi	Not significant at $p < 0.05$ (p value <0.598)
Brain microvascular endothelium invasion	chi	Not significant $p > 0.05$ (p value 0.275)
Capsules	chi	Significant at $p < 0.05$ (p value <0.0001)

To analyse the distribution of plasmid replicons across the BSI *E. coli* population, a core genome SNP tree was constructed with plasmid data mapped onto phylogenetic data. More plasmid replicon types were observed in phylogroups A, B1 and D, with the least number of plasmids observed in phylogroup G. Within phylogroup B2, Col and IncFII replicons were mostly detected, with IncFII, IncFIA and Col replicons most commonly detected in ST131 (purple clade) (Figure 44).

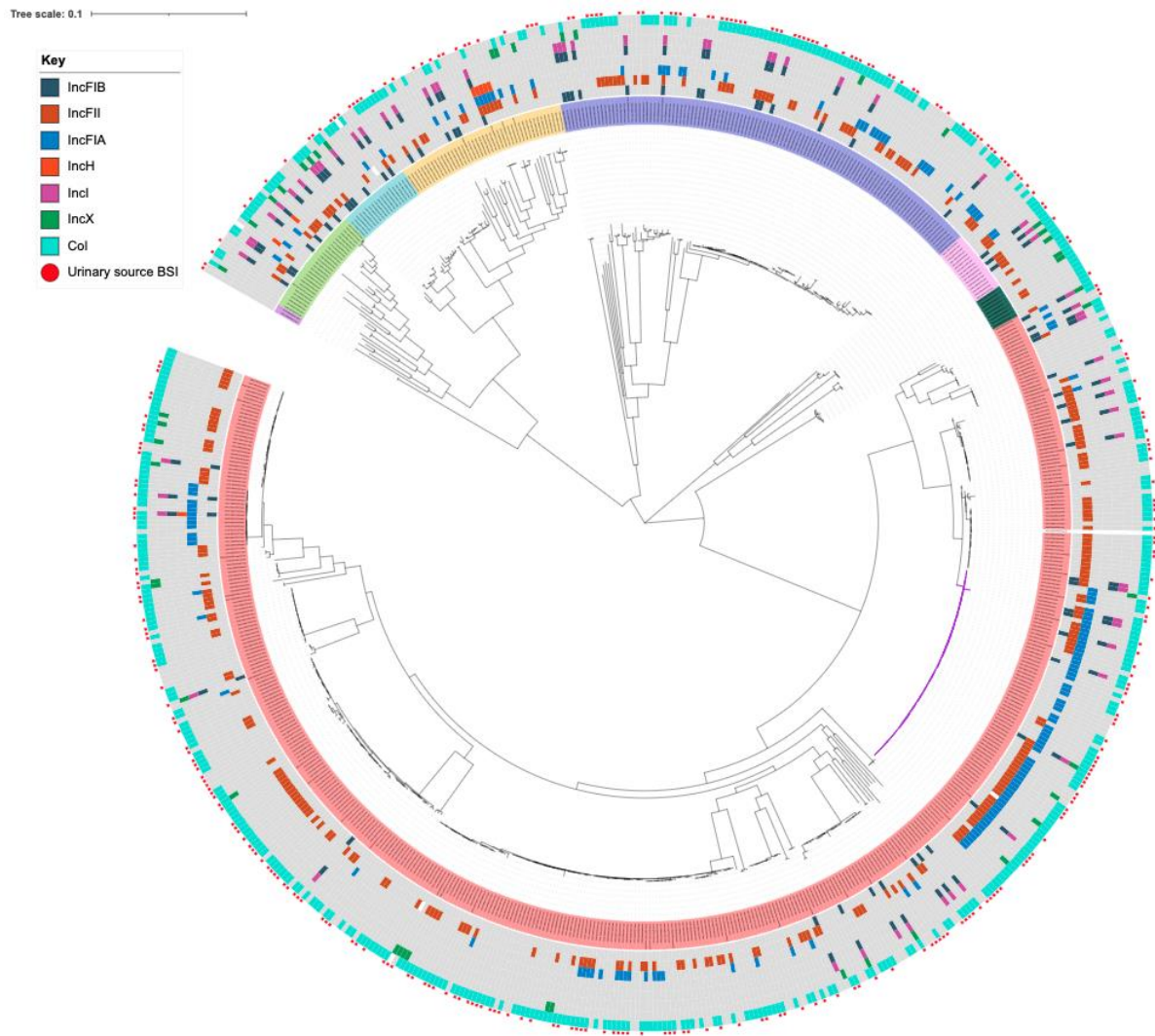


Figure 44. A core genome SNP tree consisting of 667 *E. coli* (n=11 isolates with bad quality assemblies that are not present in the tree) displaying the distribution of phylogroups and its associated plasmid replicon profiles.

5.2.3 In MDR *E. coli* isolates, most virulence and AMR genes were not detected on plasmid associated contigs

In order to investigate whether particularly MDR isolates also harboured a wide range of virulence genes and plasmids, a graph detailing the count of the total number of virulence genes (only the specific virulence genes referred to in section 5.2.2), plasmid replicons and AMR genes (conferring resistance to cephalosporins, aminoglycosides, FQs and BL/BLIs) was produced. Isolates were chosen based on presence of genes and mutations associated with all of these antibiotic classes listed above. Figure 45 revealed isolate 39868 and 31068 contained the greatest number of virulence, plasmid replicons and AMR genes. Despite isolates 39833, 39823, 39853 and 34311 harbouring multiple AMR genes, no virulence genes were detected.

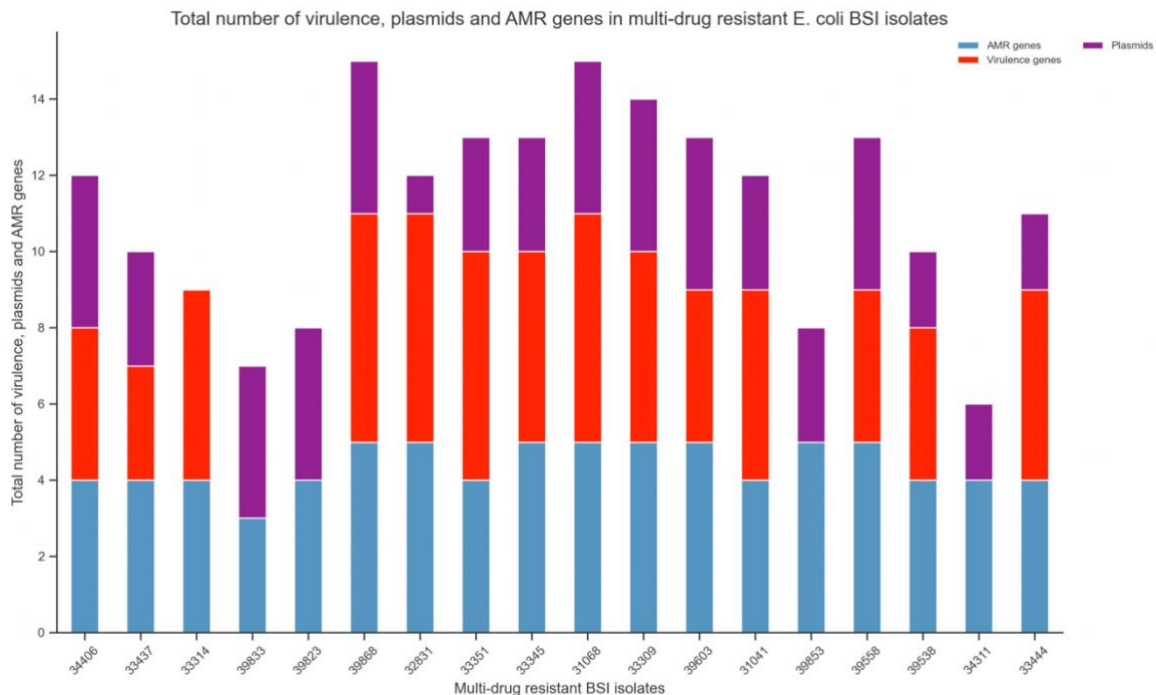


Figure 45. Graph showing the number of plasmid replicons, AMR and key virulence genes in MDR *E. coli* BSI isolates.

To attempt to localise and link AMR and virulence genes with plasmids from short read sequencing data, firstly the presence of plasmid replicons were searched for in each sample's raw reads (reference plasmid replicons can be found in Table 8, section 2.10.2). Secondly, a pairwise alignment with a reference plasmid of the same ST and replicon type was conducted. Upon identification of plasmid replicons in these isolates, an attempt to identify AMR and virulence present using short reads was made. From the MDR isolates in Figure 45, isolates with a urinary source formed the focus of the following analysis as these isolates from urinary source contained the highest number of AMR and virulence genes. Figure 46 shows an example for an assembly of isolate 39868 aligned with IncFIA plasmid reference (Accession: AP019526.1). The grey bar represents isolate contigs matching sequences with the IncFIA reference, with the bar below displaying the sequence of the IncFIA reference. The presence of plasmid replicons on contigs are referred to as plasmid-associated contigs. These plasmid-associated contigs have specific node numbers derived from the assembler during *de novo* assembly of the isolate.

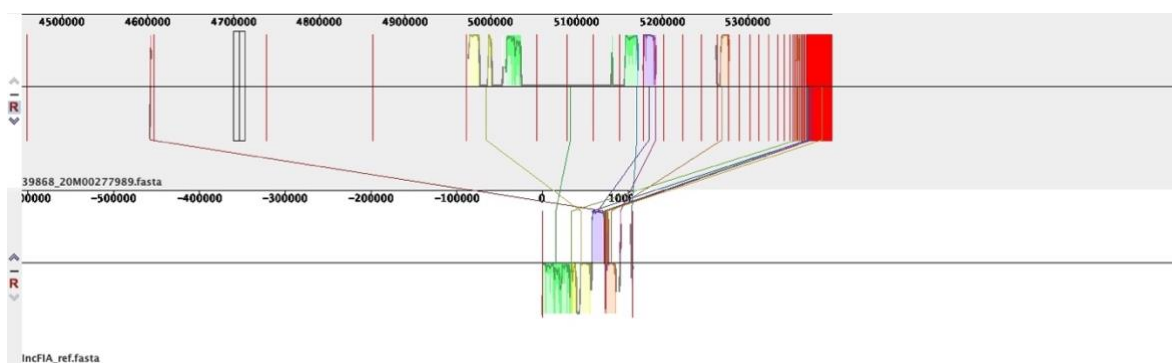


Figure 46. A figure visualising matching sequences i.e. a pairwise alignment of the assembly of isolate 39868 (top row) and a IncFIA reference (Accession: AP019526.1)(bottom row). Lines in the figure demonstrate sequence similarity greater than >80%

Analysis using BLASTn (threshold for percentage identity and percentage coverage were set to 90% minimum) revealed the presence or absence of the main virulence genes and AMR genes associated with resistance to cefotaxime, gentamicin, amoxicillin/clavulanate and ciprofloxacin, which are currently used as treatment options for BSIs on plasmid-associated contigs. AMR genes were mainly detected on IncFIC and IncFII-associated contigs for isolates 39868 and 39558 respectively (Table 31). Virulence gene *fyuA* encoding yersiniabactin was identified on an IncFIA-associated contig in isolate 32831, however this was not present on an IncFIA-associated contig in other isolates (Table 31). Isolates mainly contained the same plasmid replicons but in each assembly on different contigs, as might be expected, however isolate 39968 matched to two plasmid references on the same nodes: 20, 24, 25, 29, one with an IncFIA and one with an IncFIB replicon (Table 31).

Table 31. Table displaying the plasmid reference-based aligned contigs from selected MDR *E. coli* isolates from urinary source which also details detectable AMR and virulence genes.

Multi-drug resistant BSI isolate (<i>E. coli</i>)	Presence of plasmid	Plasmid presence detected on nodes	Presence of resistance genes on nodes containing plasmids				Presence of virulence genes on nodes containing plasmids								
			R genes associated with cefotaxime	R genes associated with gentamicin	R genes associated with amoxicillin- clavulanate	R genes associated with ciprofloxacin	iatA	fyuA	pap genes	iss	kpsMII	crf			
39868	IncFIA	20, 24, 25, 29	no	no	no	no	yes	no	no	no	no	no	no	no	no
	IncFIB	20, 24, 25, 29	no	no	no	no	yes	no	no	no	no	no	no	no	no
	IncFIC	17, 20, 24, 29, 33, 36	no	yes	yes	no	yes	no	no	no	no	no	no	no	no
32831	Col156	31, 32, 35, 36, 39, 45	no	no	no	no	no	no	no	no	no	no	no	no	no
	IncFIA	17, 31, 32, 35, 36, 38, 45,37	no	no	no	no	no	no	yes	no	no	no	no	no	no
	IncFIB	31, 32, 35, 36, 39, 45	no	no	no	no	no	no	no	no	no	no	no	no	no
33345	IncFIC	31, 35, 36, 39, 45	no	no	no	no	no	no	no	no	no	no	no	no	no
	IncI	37, 45	no	no	no	no	no	no	no	no	no	no	no	no	no
	IncFIA	30, 31, 35, 37	no	no	no	no	no	no	yes	no	no	no	no	no	no
39558	IncFIB	26, 30, 31, 37	no	no	no	no	no	no	yes	no	no	no	no	no	no
	IncFIC	30, 31, 37, 38, 41, 45	no	no	no	no	no	no	yes	no	no	no	no	no	no
	IncFIA	34, 35, 36, 43, 48, 51, 54	no	no	no	no	no	no	no	no	no	no	no	no	no
IncFIB	16, 21, 30, 34, 35, 36, 43	no	no	no	no	no	no	no	no	no	no	no	no	no	no
	IncFII	7, 34, 35, 36	yes	yes	yes	no	no	no	no	no	no	no	no	no	no

5.2.4 Phylogenetic analysis shows the presence of only yersiniabactin and invasins in MDR ST307 and NDM producing ST15 *K. pneumoniae*

To understand the distribution of virulence, AMR and plasmid replicons in the MDR isolates from the BSI *Klebsiella* spp. population, these data were mapped onto phylogenetic data. Figure 47 revealed IncFIB and IncFII replicons were widely distributed across the *Klebsiella* population, with carbapenem resistant NDM-producing ST15 harbouring only virulence factors associated with invasins and an IncFIB replicon. Only one isolate from the MDR ST307 clade (n=6 isolates in the clade) carried yersiniabactin. MDR ST307 was defined as any ST307 isolate harbouring AMR genes conferring resistance to at least 4 class of antimicrobials. *K. oxytoca* harboured no AMR genes (of those relevant to important BSI therapies, as previously defined) but contained an IncFIB replicon and virulence associated with yersiniabactin.

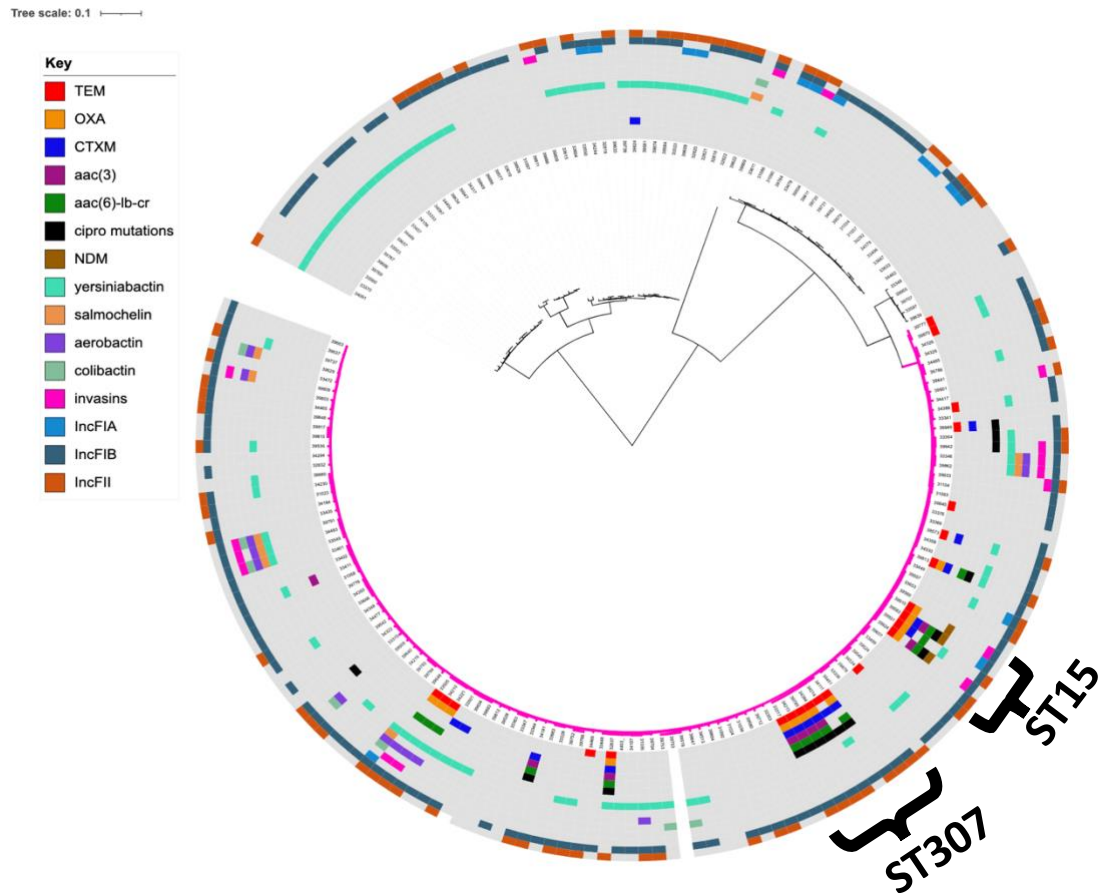


Figure 47. Core genome SNP tree displaying the distribution of plasmids, AMR and virulence genes across the *Klebsiella* spp. population. The highlighted pink clade represents *K. pneumoniae*.

5.2.5 No virulence genes were detected on plasmid associated contigs in NDM-positive *K. pneumoniae*, however AMR genes were detected

As carried out in Chapter 2, analysis was performed on NDM-carrying *K. pneumoniae* due to increased reports of plasmid-mediated, MDR, NDM-carrying *K. pneumoniae* in the literature. Figure 48 reprised from Chapter 2 details the location of AMR genes using in-built BLASTn. It was found that NDM-carrying ST15 isolates were all isolated from the same hospital ward. Therefore, in order to investigate whether plasmids were present in all NDM-carrying *K. pneumoniae* and whether they potentially played a role in the dissemination of MDR NDM-carrying ST15 within this ward, pairwise alignments (as done for *E. coli* previously) with a plasmid reference were conducted for these specific isolates to measure their relationships.

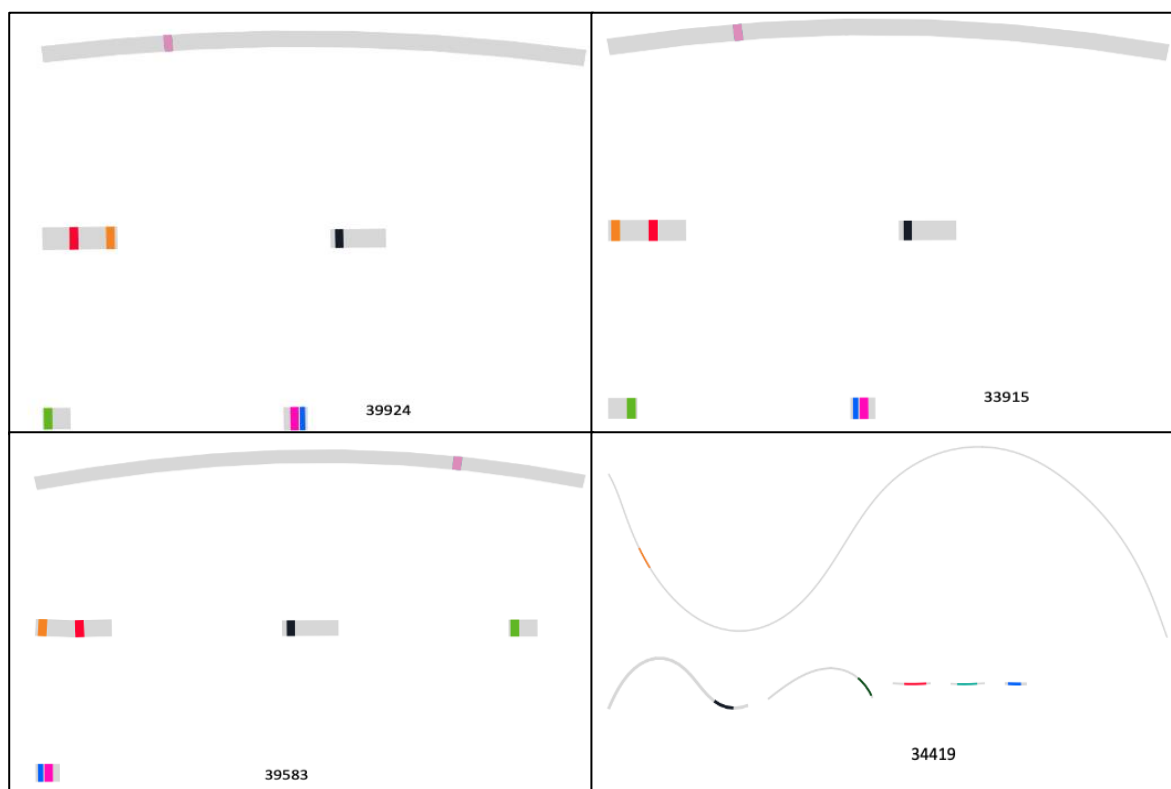


Figure 48. A visualisation through Bandage of the structure of the genomic regions containing different AMR genes (*bla*_{CTX-M-15} in red, *bla*_{TEM-1D} in orange, *aac*-(3)-IIa in green, *aac*(6)-Ib-cr in blue and *bla*_{OXA-1} in pink) for all NDM-carrying ST15 and the only one ST147 (33419) containing NDM (black). Reprinted from Chapter 2.

Analysis using BLASTn revealed the presence or absence of the main virulence genes and AMR genes associated with cefotaxime, gentamicin, amoxicillin/clavulanate and ciprofloxacin currently used as treatment options for BSIs on plasmid associated contigs. AMR genes associated with cefotaxime, gentamicin and amoxicillin-clavulanate were detected on all plasmids for isolates 39915, 39924 and 39583 (Table 32). Presence of AMR genes were not detected on plasmid-associated contigs for isolate 34419 (Table 32). No AMR genes associated with resistance to ciprofloxacin were detected on any plasmid-associated contigs for all isolates (Table 32). Mutations *gyrA* and *parC* were identified on contigs containing chromosomal genes. Similarly, no

virulence genes searched for were detected on any plasmid-associated contig in any isolate.

Table 32. Table displaying the plasmid reference-based associated contigs from MDR NDM-positive *K. pneumoniae* isolates which also details detectable AMR and virulence genes. Virulence genes *ybt* encodes for yersiniabactins, *iuc* encodes for aerobactin, *iro* encodes for aerobactin and *clb* encodes for colibactin and *rmp* encodes for invasins.

Multi-drug resistant NDM carrying BSI isolate (<i>K. pneumoniae</i>)	Presence of plasmid	Plasmid presence detected on nodes	Presence of resistance genes on nodes containing plasmids			Presence of virulence genes on nodes containing plasmids							
			R genes associated with cefotaxime	R genes associated with gentamicin	R genes associated with amoxicillin-clavulanate	R genes associated with ciprofloxacin	<i>ybt</i>	<i>iuc</i>	<i>iro</i>	<i>rmp</i>	<i>clb</i>		
33419	IncFII	27, 29, 44, 48, 58, 63, 70, 71, 87, 90	no	no	no	no	no	no	no	no	no	no	no
39515	IncFIA	1, 2, 24, 27, 29, 30, 35	yes	yes	yes	no	no	no	no	no	no	no	no
	IncFIB	2, 4, 11, 14, 24, 26, 27, 29, 30, 35	yes	yes	yes	no	no	no	no	no	no	no	no
	IncR	1, 8, 24, 26, 27, 33, 35, 38	yes	yes	yes	no	no	no	no	no	no	no	no
39524	IncFIA	23, 24, 27, 29, 35	yes	yes	yes	no	no	no	no	no	no	no	no
	IncFIB	1, 2, 3, 4, 5, 17, 24, 26, 27, 29, 30, 32	yes	yes	yes	no	no	no	no	no	no	no	no
	IncR	2, 10, 24, 28, 33, 35	yes	yes	yes	no	no	no	no	no	no	no	no
39583	IncFIA	23, 27, 28, 33	yes	yes	yes	no	no	no	no	no	no	no	no
	IncFIB	12, 14, 23, 24, 26, 27, 28, 29	yes	yes	yes	no	no	no	no	no	no	no	no
	IncR	1, 2, 23, 24, 31, 33	yes	yes	yes	no	no	no	no	no	no	no	no

5.2.6 Localisation and detection of AMR and virulence genes on plasmids from NDM-positive *K. pneumoniae* using Nanopore sequencing

As NDM carrying ST15 *K. pneumoniae* were isolated from the same ward (n=3) and one other ST147 isolate was NDM-positive, these isolates from Table 32 above formed the focus of the further analysis, and were therefore taken forwards for analysis with Nanopore sequencing to determine the structure of the complete plasmids and the locations of the regions containing virulence and AMR genes. Due to bad quality from long read sequencing for ST147, location of AMR genes, plasmid and chromosomal structures could not be determined. Thus, Nanopore-driven assemblies derived by Microbes NG for all ST15 *K. pneumoniae* (n=3) and the following results were determined for these NDM-positive isolates.

Using the in-built BLASTn function within Bandage, isolate 39583 matched for IncR, IncFIB and col440 (Figure 49). Virulence genes *iutA*, *gyrA* and *parC* were present on the 5,315,496 bp chromosome and AMR genes (*bla_{CTX-M}*, *bla_{TEM}*, *bla_{OXA}* and *aac(6')-Ib-cr*) were present on an IncR plasmid (99,422 bp)(Figure 49). Isolate 39924 matched for IncR and col440 (Figure 50). Again, virulence genes *iutA*, *gyrA* and *parC* were present on the 5,315,494 bp chromosome and AMR genes (*bla_{CTX-M}*, *bla_{TEM}*, *bla_{OXA}* and *aac(6')-Ib-cr*) were present on a IncR plasmid (270,292 bp) (Figure 50). Isolate 39915 matched for IncR, IncFIB and col440 (Figure 52). Virulence genes *iutA*, *gyrA*, *fyuA* and *parC* were present on the 5,434,736 bp chromosome and AMR genes (*bla_{CTX-M}*, *bla_{TEM}*, *bla_{OXA}* and *aac(6')-Ib-cr*) were present on IncR (99422 bp) (Figure 51).

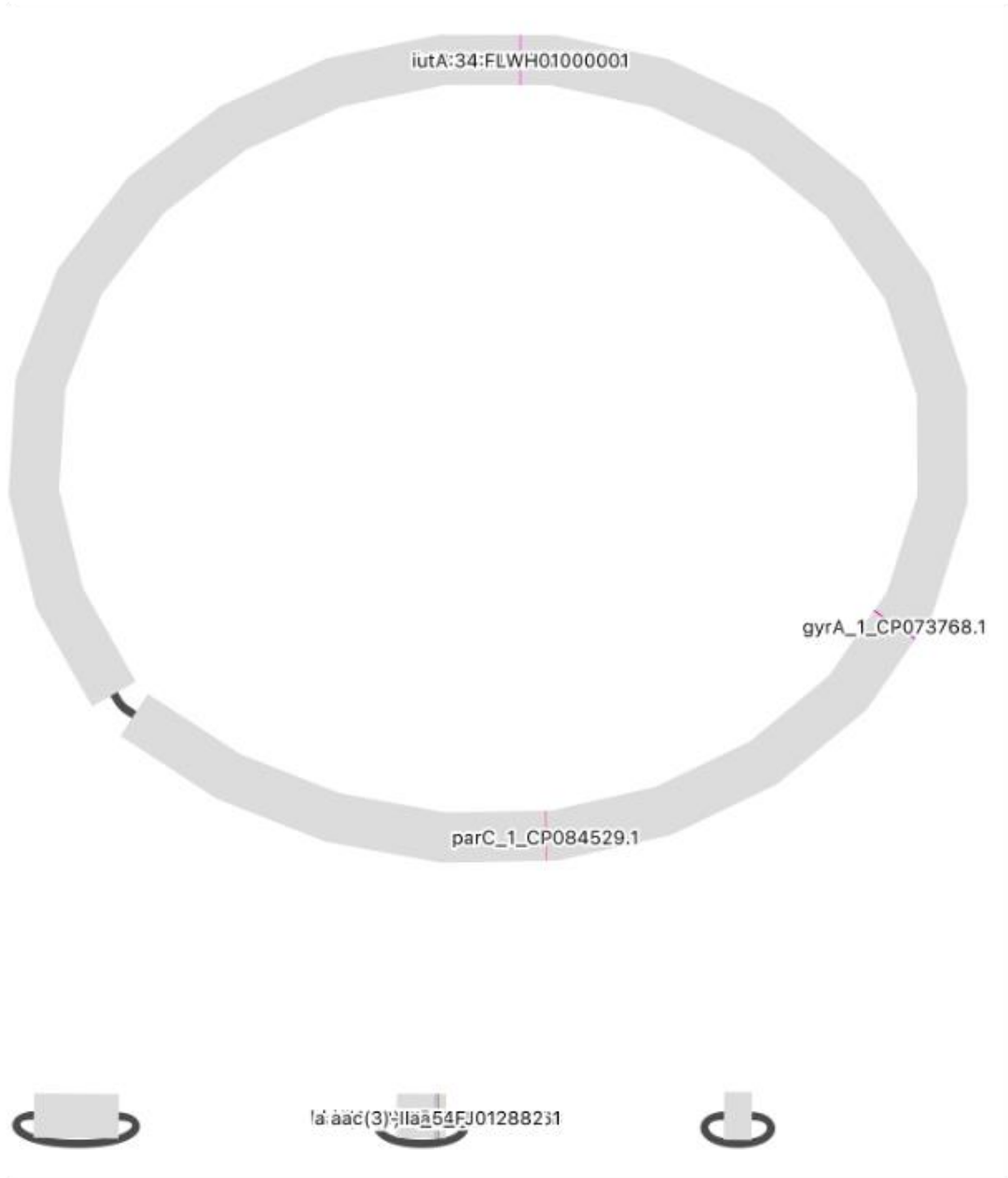


Figure 49. A visualisation through Bandage of the structure of the chromosome and plasmids including the genomic regions containing AMR and virulence genes for isolate 39583.

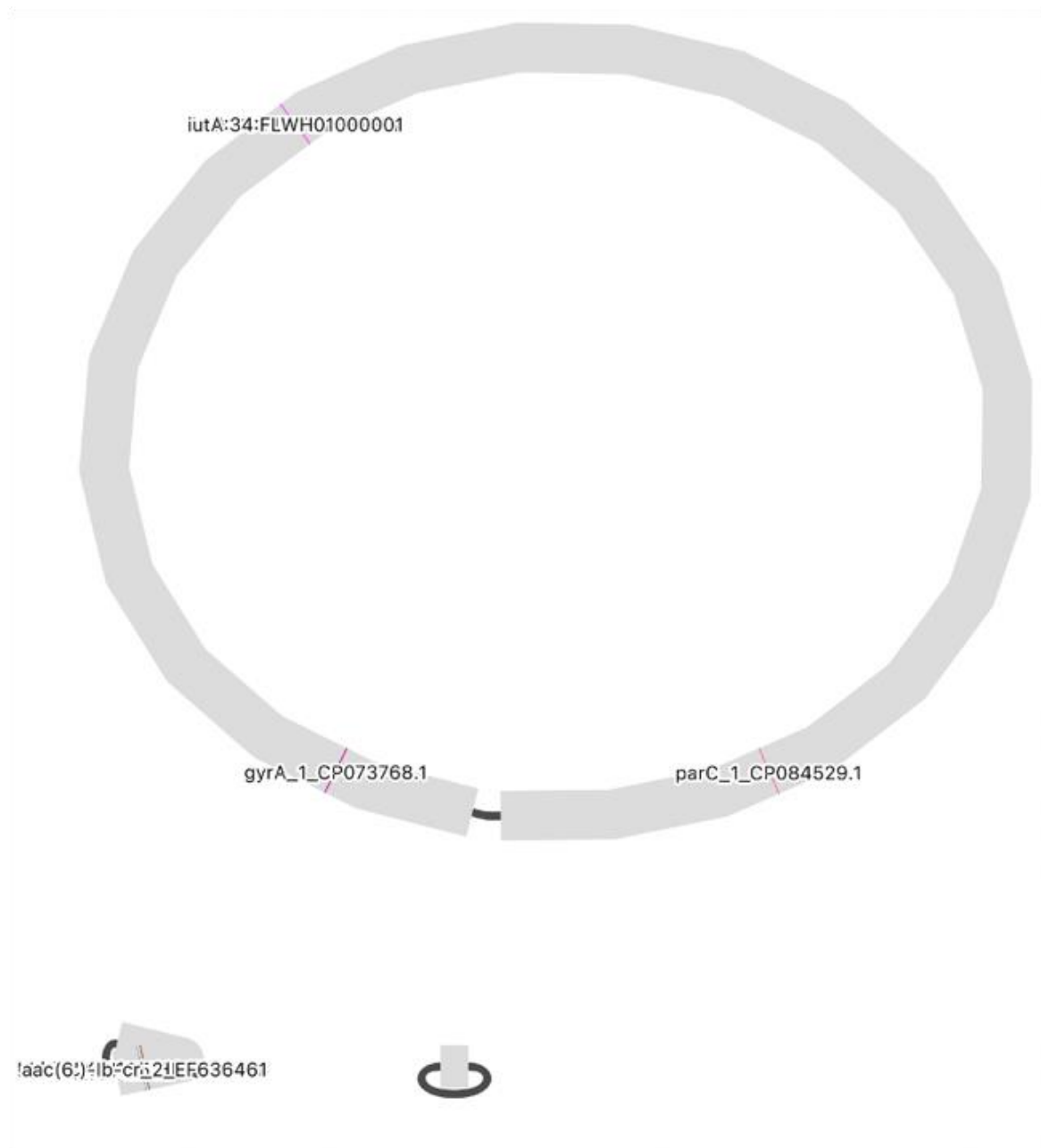


Figure 50. A visualisation through Bandage of the structure of the chromosome and plasmids including the genomic regions containing AMR and virulence genes for isolate 39924.



Figure 51. A visualisation through Bandage of the structure and the size of the chromosome and plasmids including the genomic regions containing AMR and virulence genes for isolate 39915.

Further characterisation and comparative genomics of contigs in all ST15 isolates containing NDM-1 from Chapter 2 and referred to above, revealed the same genomic region and environment in all ST15 isolates. In Chapter 2, the full AMR and NDM regions in these NDM positive isolates could not be determined, however the use of Nanopore sequencing has enabled the identification of these regions (Figure 52). Despite the difference in the structure of the plasmid, the integration region is in a similar region suggesting a hotspot for integration of MGEs.

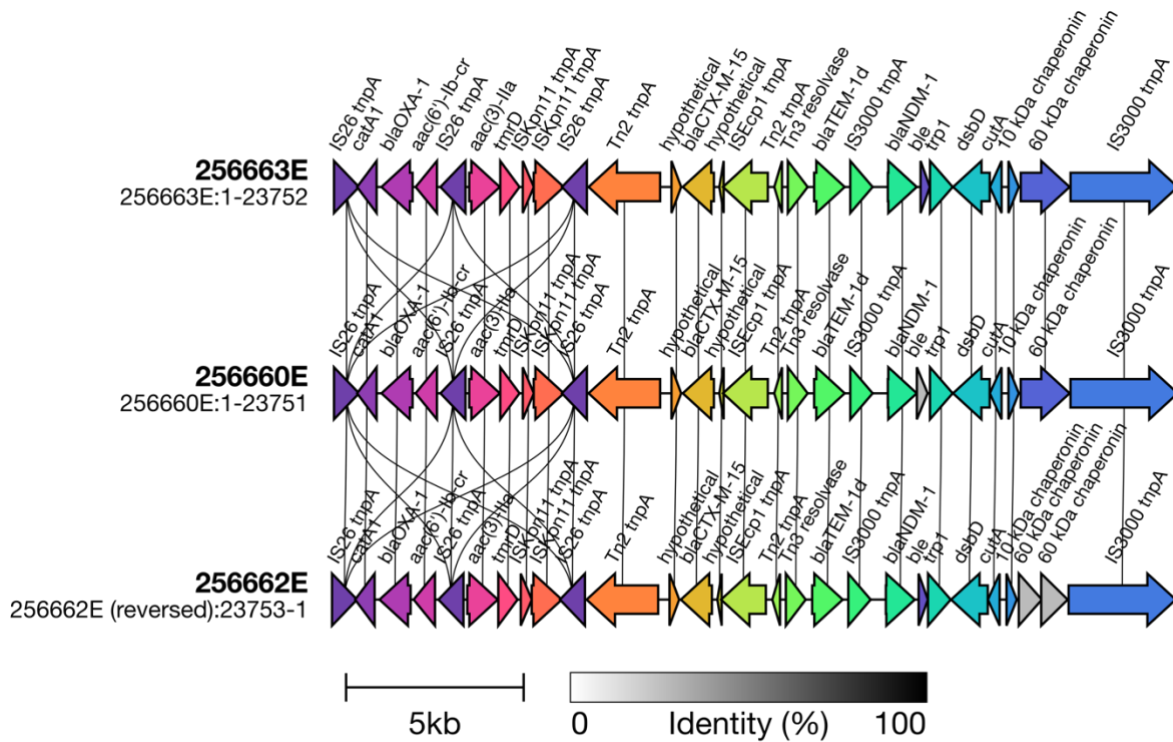


Figure 52. Characterisation and comparison of the genomic regions containing *bla*_{CTX-M}, *bla*_{TEM}, *bla*_{OXA} and *aac*(6')-Ib-cr in MDR ST15 (256662E, 256660E, 256663E). Group numbers represent a set of genes that match >90% and vertical lines show genes that are the same.

5.2.7 Plasmid annotations and comparisons all in MDR NDM carrying *K. pneumoniae*, show identical plasmids present in 2 different patients

NDM- carrying samples 256662E (referred to as sample number 39583 previously), 256663E (referred to as sample number 33915) and 256660E (referred to as sample 39924) were all ST15s and contained plasmids. To maximise the identification of AMR and virulence genes on complete plasmids, raw reads provided by Microbes NG were assembled (Table 33).

Table 33. Table detailing the number of contigs and their identification in each sample after *de novo* assembly.

WGS data	Contig, size and identification
256662E	Contig1 - 5315496bp - Chromosome Contig2 - 170882bp - Plasmid IncFIB Contig3 - 99407bp - Plasmid IncR Contig4 - 4161bp - Plasmid Col440
256663E	Contig1 - 5320711bp - Chromosome Contig2 - 170369bp - Plasmid IncFIB Contig3 - 99422bp - Plasmid IncR Contig4 - 4136bp - Plasmid Col440
256660E	Contig1 - 5315494bp - Chromosome Contig2 - 270292bp - Plasmid IncR Contig3 - 8660bp - Plasmid Col440

Samples 25663E and 256662E from different patients isolated from the same ward harboured an IncFIB, IncR and Col440 plasmid containing the same AMR regions. Plasmid comparisons were conducted and revealed these two patients had all 3 identical plasmids (Figure 53, Figure 54, Figure 55). Genes located on the col440 plasmid could not be identified by Prokka and BLASTN. Whilst 256660E formed part of the same ST15 clone, this sample harboured different IncR and col440 plasmids (Figure 56 & Figure 57). Again, genes located on the col440 plasmid in 256660E could not be identified by Prokka and BLASTN. Genes associated with heavy metal resistance and the NDM gene were identified on an IncR plasmid in all genomes. Overall, characterisation of these NDM-positive *K. pneumoniae* show these strains shared a common source.

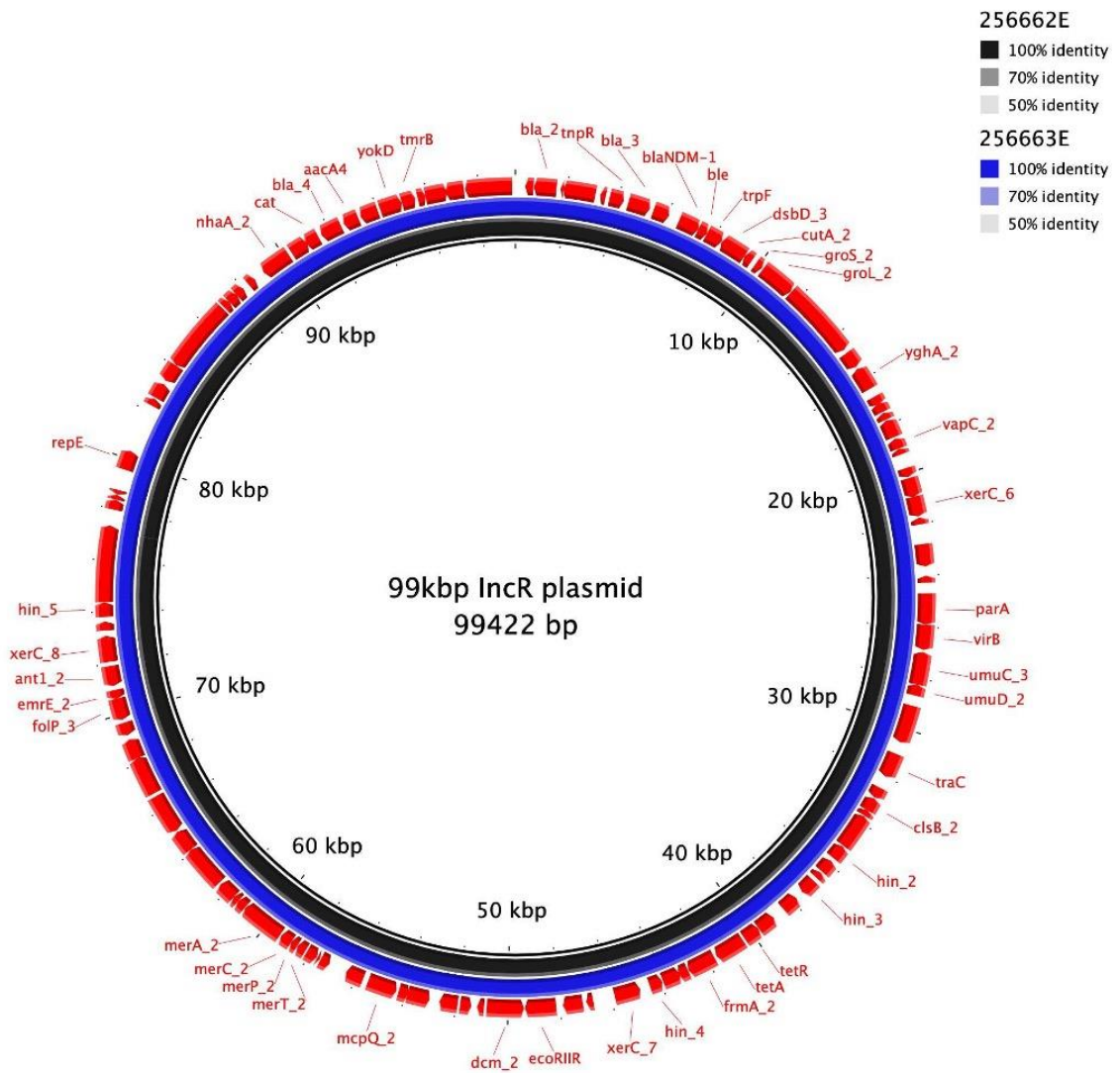


Figure 53. BLAST comparison of the IncR plasmids identified in 256662E and 256663E, with 256662E acting as the reference.

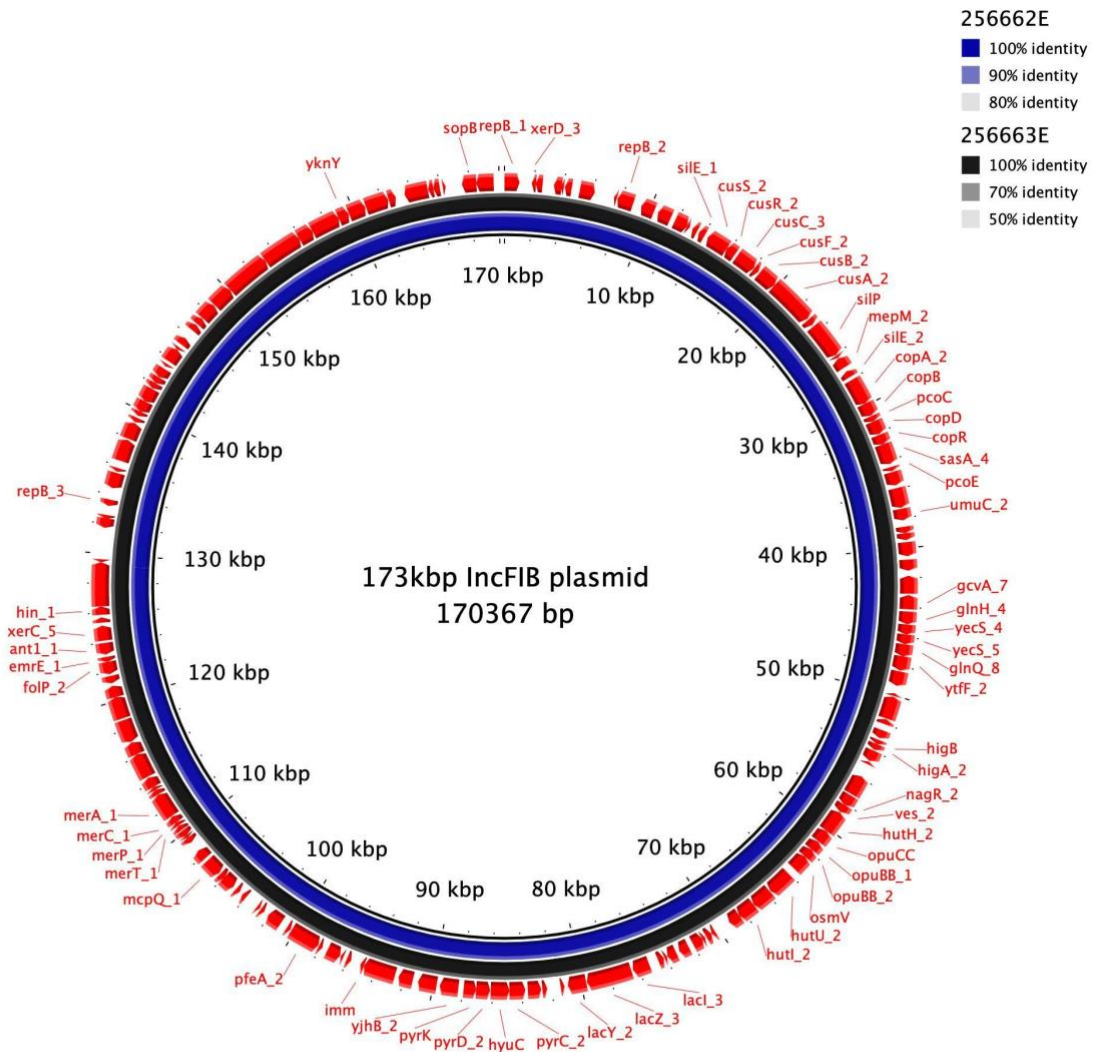


Figure 54. BLAST comparison of IncFIB plasmids identified in 256662E and 256663E, with 256662E acting as the reference.

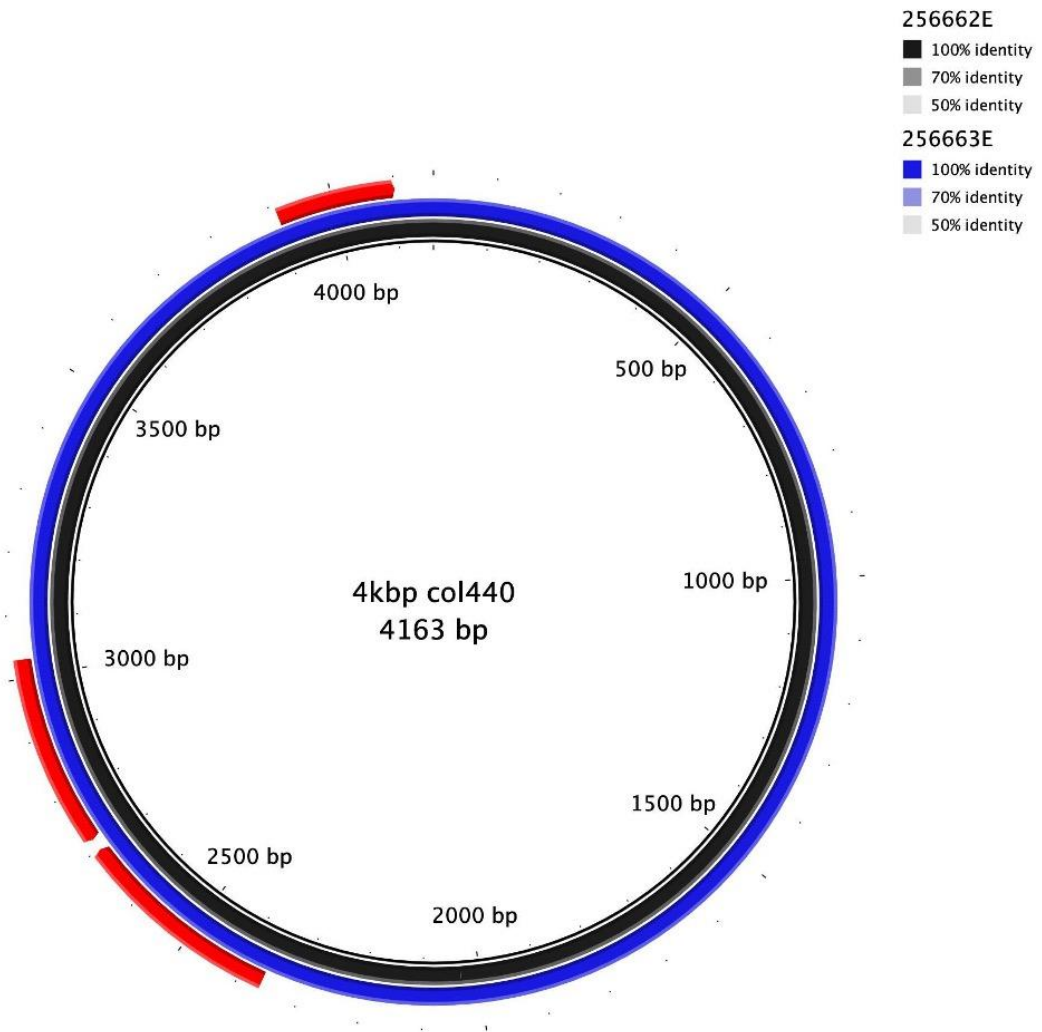


Figure 55. BLAST comparison of col440 plasmids identified in 256662E and 256663E, with 256662E acting as the reference. Putative genes located on this plasmid could not be identified by Prokka and BLASTn.

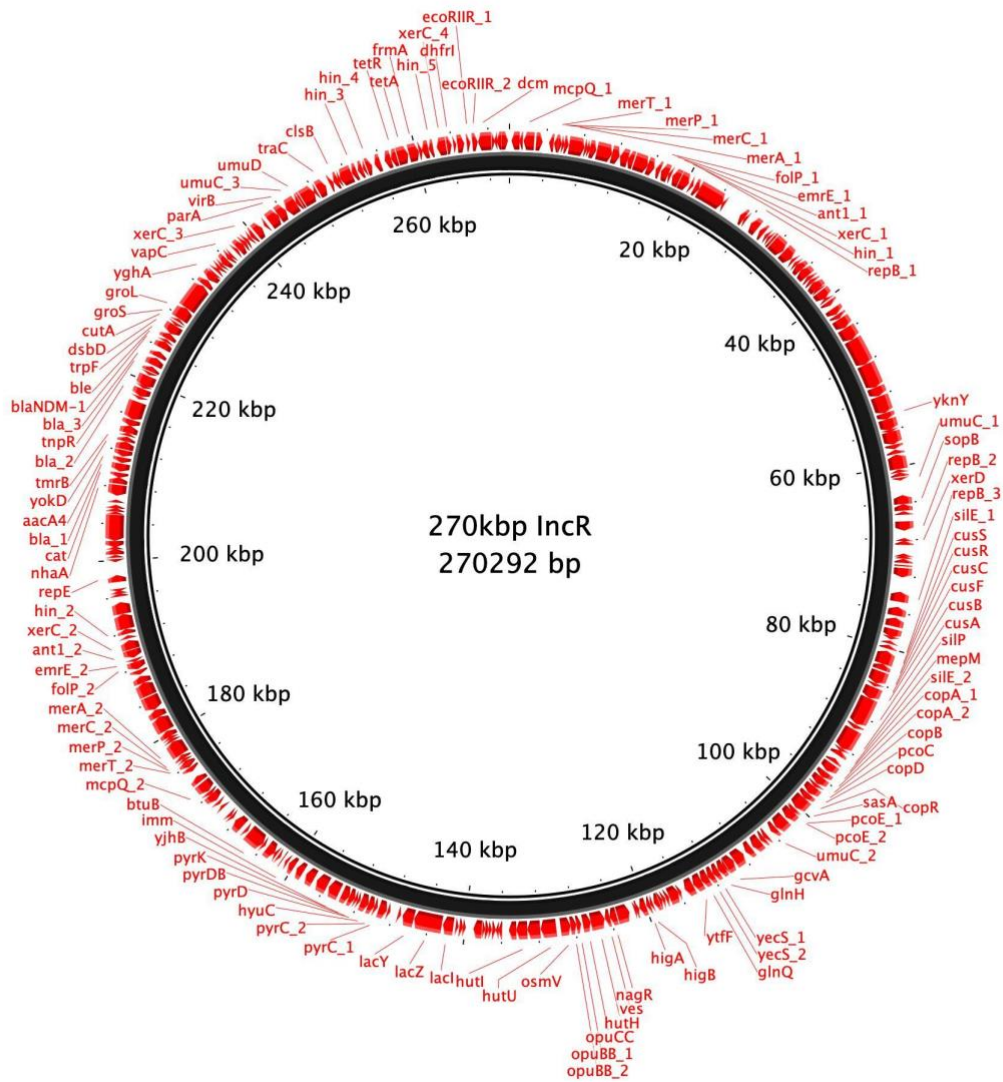


Figure 56. Annotation of genes on the IncR plasmid present in 256660E.

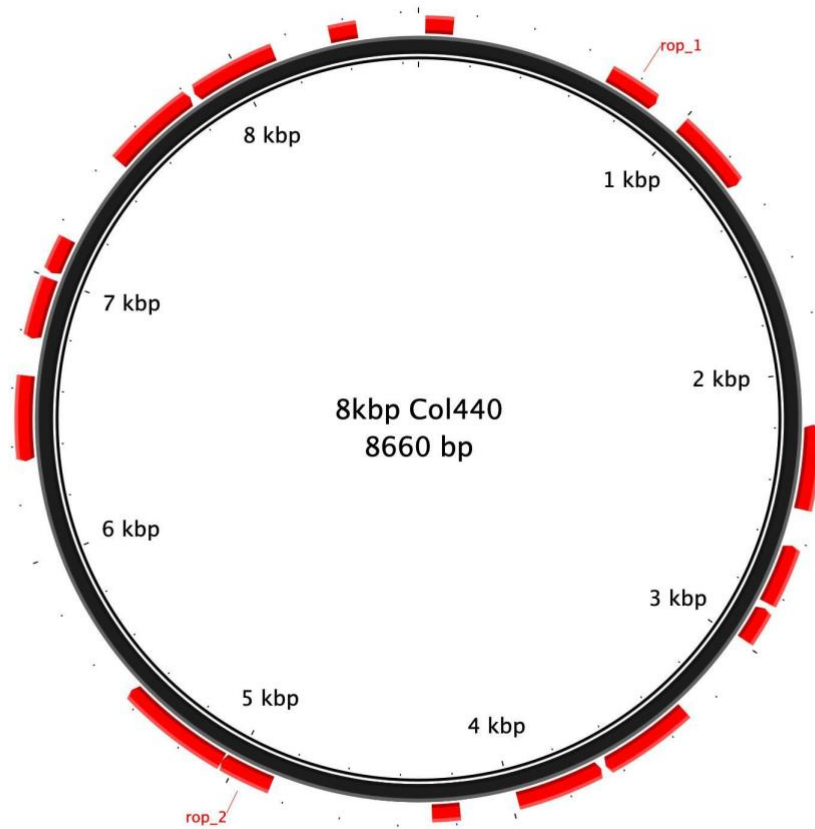


Figure 57. Detection of the Col440 plasmid present in 256660E. Putative genes located on this plasmid were unable to be identified by Prokka and BLASTn.

5.3 Discussion and Conclusion

As discussed in previous chapters, ExPEC is a common cause of BSIs and is often associated with high morbidity and mortality. Determinants such as AMR and virulence factors play a critical role in the survival and pathogenicity in the bloodstream, affecting the severity of outcome (Jauréguy et al, 2007; Lefort et al, 2011). Information regarding virulence and AMR profiles can help facilitate better infection control and the development of novel strategies to combat *E. coli* BSIs.

The number of virulence factors that can be present in *E. coli* is vast, however, *hly*, *cnf*, *iut*, *fyuA*, *ironN*, *pap*, *iss*, *traT*, *ibeA*, *kpsMT* genes are the main virulence factors that have been associated with ExPEC causing BSIs in other studies (Johnson & Stell, 2000; Koga et al, 2014; Daga et al, 2019). Serum resistance encoded by *iss* and *traT* contribute to the survival of *E. coli* in the bloodstream, with a study demonstrating 85.4% of BSI isolates harboured genes associated with serum resistance, in particular *traT* (Daga et al, 2019) with other studies reporting similar results (Miajlovic et al, 2016; Bozcal et al, 2018). In keeping with this, 76% of *E. coli* isolates in this study harboured genes encoding serum resistance (Figure 40). The expression of capsule antigens is also associated with invasive disease and resistance to host immune response. Expression of K1 antigen capsule (*kpsmT_K1*) has been associated with UTIs (Aldawood & Roberts, 2022) whereas K5 capsule confers pathogenicity in BSIs (Daga et al, 2019). Daga et al. (2019) reported 47.9% of *E. coli* isolates contained at least 1 capsule gene. In contrast, 17.3% and 32.5% BSI *E. coli* in this study harboured *kpsmT_K1* and *kpsmT_K5* respectively. Iron is essential to biochemical and biological processes. The high affinity for bacterial siderophores to iron results in bacteria outcompeting the host for iron uptake and are commonly observed in ExPEC causing BSIs (Koga et al, 2014; Bozcal et al, 2018). The most prevalent iron uptake system in

this study was yersiniabactin, encoded by *fyuA*, present in 85.9% of *E. coli* causing BSIs. In keeping with this, 70.8% of isolates harboured *fyuA* (Daga et al, 2019). Furthermore, Lefort *et al.* (2011) reported the increase of *fyuA* identified in survivors of BSIs. Additionally, in this study, genes encoding adhesins were analysed, including type 1 fimbriae, P fimbriae, binding adhesin and S fimbriae, all encoded by *fimH*, *papC* and *papG*, *afaA*, *sfaA* and/ *sfaS* respectively. In order of prevalence, this study revealed 48.2% of isolates harboured *papC*, 16.7% harbouring *afaA*, 12.2% of isolates harbouring *sfaA* and 3.2% of isolates harbouring *sfaS*. In contrast, Daga et al, 2019 reported the most prevalent genes encoding adhesins were *fimH*, followed by *papC*. *FimH* is a critically important virulence factor in UPEC by mediating adhesion to uroepithelial cells (Dale & Woodford, 2015). Despite this, *fimH* was not identified in any isolates in this study. A study by Watts *et al.* (2010) revealed *fimH* was most prevalent due to the detection in 98% of *E. coli* UTIs. Furthermore, Garofalo *et al.* (2007) revealed the presence of *fimH* in 100% of female UTIs. This suggests that the frequency of *fimH* being identified in UTIs are higher in comparison to BSIs, which were only used in this analysis. As *papC* are both involved in UTIs and subsequent BSIs (Lefort et al, 2011; Subashchandrabose & Mobley, 2015), this could explain the high prevalence of *papC* detected in this study and its high significance with urinary source BSIs. Only few studies have detailed the associations between specific virulence genes and portal of entry for BSIs. One study showed *ibeA* present in 27% of *E. coli* BSIs from GI tract (Mahjoub-Messai et al, 2011), which may be an explanation for the borderline significance observed for its association with urinary source BSIs from this study. The only virulence factor not significantly associated with urinary source BSIs were brain microvascular endothelium invasion, encoded by *ibeA*. In this study, a significant difference was found between ST131 *E. coli* BSI from urinary

source and carriage of certain virulence genes. One study reported virulence genes associated with iron acquisition, adhesion, and toxin production associated with ST131 and revealed no difference in mortality between ST131 and non-ST131 *E. coli* BSIs, however ST131 from a urinary tract source was associated with greater in-hospital mortality than non-ST131 *E. coli* BSIs (Brumwell et al, 2023).

From the *E. coli* BSI isolates harbouring genes conferring resistance to more than 4 classes of antibiotics relevant for the treatment of BSIs, the location of the AMR and virulence genes were analysed with Illumina data. In Table 31, hits to a plasmid with a particular replicon on different nodes were observed, however isolate 39868 contained hits to two plasmids, with IncFIA and IncFIB replicons, respective, on the same nodes: 20, 24, 25, 29. As only 1 replicon type per plasmid can be active, this suggests that one of those plasmid replicons was defunct. This can also be observed in the NDM-carrying *K. pneumoniae* plasmids analysed from long read sequencing data. As mentioned in results, this has been observed previously with STEC O157:H5 where non-active IncFII replicon types were detected within active, single IncFIB plasmids (Lim et al, 2010). Furthermore in Table 31, similarities with plasmid references of replicon types IncFIA and IncFIB were identified on nodes 30, 31 and 37, however node 35 was unique to IncFIA plasmid reference and node 26 was unique to the IncFIB for isolate 33345. This suggests plasmids share the same backbone, however they have a piece that is different in each. Due to short read assemblies, the location of the AMR and virulence genes analysed for *E. coli* BSIs can only be inferred. AMR genes were detected in 2 *E. coli* BSI isolates on plasmid associated contigs with only *iutA* and *fyuA* detected on plasmid-associated contigs. The limitations of this analysis are that virulence and AMR genes could be present on small plasmid-associated contigs, however small MGEs are not contiguous in assemblies, therefore they were not

detected in the process. Furthermore, contigs less than 1000 bp were filtered out. The additional caveat to this study is that no long read sequencing was conducted on these isolates, therefore the backbones of these plasmids are the focus of the analysis.

For *K. pneumoniae*, no virulence genes were detected on plasmid associated contigs, however long read sequencing revealed the presence of *iutA* and *fyuA* on the chromosome whilst the AMR resistance genes were present on smaller sized plasmids. Increasing reports have revealed the convergence of virulent and MDR plasmids. For example, a study reported two NDM-carrying *K. pneumoniae*, an IncFII plasmid was identified harbouring virulence genes *rmpA*, *iutA* and *iuc*, in addition to AMR genes *aadA2*, *armA*, *bla_{OXA-1}*, *mphE*, *sul1*, *dfrA14* and genes conferring resistance to heavy metals (Shanakar et al, 2022). It was also observed that IncR plasmids harbouring NDM and genes conferring resistance to heavy metals were present in 2 different patients in the same ward (Figure 53). Genes *tnp* and *ble* were also found surrounding NDM. In keeping with this, a study reported the presence of *ble* and *tnp* upstream and downstream of NDM, forming a 20-30kbp region on p11106 and p12 plasmids (Xiang et al, 2020). Furthermore, transmission of an IncR plasmid harbouring CTX-M genes and carbapenemase genes in addition to 9 other AMR genes has been reported across 6 patients (Hawkey et al, 2022). Whilst data in this study has shown virulence and AMR present on separate plasmids, there is potential for these to merge in future. As shown in Table 31, Table 32, Table 33), samples contain large >5 kbp plasmids of multiple replicon types, demonstrating during evolution plasmids have merged overtime. Therefore, this highlights the importance of genomic characterisation on isolates harbouring several AMR and virulence genes.

In summary, results from this study show that BSIs are mediated by Gram-negative bacteria producing a variety of virulence factors, with isolates harbouring their own

unique combination. The vast variety of virulence factors contribute towards genome plasticity, including plasmids and transposable elements. In order to improve the management and treatment of BSIs, understanding the associations between host characteristics, in particular source of infection, AMR and virulence profiles is important. This work highlights the importance of monitoring high risk MDR, hypervirulent clones in addition to the movement of plasmids containing MDR and virulent regions, which will aid empiric therapy.

6.0 Results Chapter 4

Comparison between *in silico* based and phenotypic detection of AMR

6.1 Introduction

WGS is becoming an invaluable tool for epidemiology and surveillance of AMR bacteria. Assembling bacterial genomes from short reads from Illumina sequencing protocols have low error rates, however there are limitations to the ability of these methods to allow full characterisation of bacterial genomes as assembly contiguity is constrained by repeat elements and homologous sequences (Moss et al, 2020). Short read sequencing alone is unreliable due to significant problems with the assembly of MGEs whereby obvious AMR genes can be missed. SMRT sequencing platforms such as those from Pacific Biosciences (PacBio) or nanopore sequencing by Oxford Nanopore Technologies (ONT) can produce closed *de novo* assemblies (Moss et al, 2020), allowing the integration of the accessory genome, where AMR determinants are typically located, to be maintained, but errors in the sequence can affect prediction of AMR, which often relies on the specific AMR gene variant present. Hence, hybrid assemblies involving combinations of long and short read sequence data, are used to improve characterising the locations of AMR genes on plasmids, whilst minimising error rate (Berbers et al, 2020). *In silico* AMR detection using bioinformatics tools is designed to enable the prediction of phenotypic AMR. Similar approaches can be used to predict virulence and other phenotypes where biological rules defining the link between phenotype and genotype have been established and can be encoded. Traditional phenotypic antimicrobial susceptibility cannot currently be applied in a high-throughput format, is generally too slow to inform empiric antimicrobial choice, and can potentially give erroneous results given inherent variability from test to test.

Considerable effort has been made to conduct large-scale studies involving characterisation of AMR mechanisms, resulting in the development of multiple highly curated databases such as CARD where many “biological rules of AMR” are contained (Alcock et al, 2020) and AMR associated bioinformatics tools such as ResFinder (Bortolaia et al, 2020), ABRicate (<https://github.com/tseemann/abricate>) and AMRFinder (Feldgarden et al, 2019), which are currently used in the field of bacterial genomics and epidemiology to apply these biological rules to predict AMR from genotype. However, studies have reported challenges regarding prediction of phenotype from genotype, even for *E. coli* which is the best studied organism (Stoesser et al, 2013; Mahfouz et al, 2020). For example, a validation study conducted on AMR bioinformatics tools, KOVER-AMR and ResFinder, for prediction on AMR phenotypes of clinical *E. coli* isolates, revealed major error rates, where known resistant isolates were predicted to be susceptible, of 5.1% and 5.8% for both these tools respectively, meaning they did not fulfil the FDA requirements for utilisation in Dutch diagnostics (Verschuuren et al, 2022). Furthermore, a second study highlighted poor concordance between phenotypic and genotypic predictions for resistance to BL/BLIs, in particular amoxicillin/clavulanate in *E. coli* (Davies et al, 2020). Validation of AMRFinder revealed 97% concordance across multiple antibiotic classes such as FQs, cephalosporins and aminoglycosides (Feldgarden et al, 2019). Comparisons between AMRFinder and ResFinder demonstrated 1,229 gene differences in the databases used between the two tools (Feldgarden et al, 2019). Comparisons also revealed 216 AMR genes that were identified by AMRFinder which were not detected by ResFinder (Feldgarden et al, 2019). These aforementioned studies emphasise the necessity for improvement and development of current AMR databases for optimal use in clinical settings.

AMR gene detection is also dependent upon accurate levels of annotation amongst AMR databases and can be categorised into two gene catalogues: AMR gene families, for example *bla_{CTX-M}* and alleles (or variants) of gene families such as *bla_{CTX-M-15}*. The percentage identity and coverage based on a DNA sequence alignment between the WGS and the database entry is responsible for the classification of presence or absence of each AMR gene (and its closest variant) in WGS data. Bioinformatics tools such as ABRicate and AMRFinder use an 80% and 90% nucleotide sequence identity respectively (<https://github.com/tseemann/abricate>). However, an output of the closest allele within a gene family is produced when an imperfect match is identified. For such AMR genes where a single mutation can affect function and so spectrum of activity, this can often lead to incorrect calling of alleles, and so phenotypes. This is particularly true for chromosomal AMR genes where there is a large degree of random genetic drift from isolate to isolate. In light of this, consistent improvements on the detection of novel AMR gene families, gene variants and phenotypic annotations must be conducted on AMR gene databases in order to optimise output accuracy. A recent study reported the creation and validation of a bioinformatics tool, *abritAMR*, utilised for AMR gene detection with clinical adaptations (Sherry et al, 2023), assisting the reporting of data to clinicians with limited understanding or knowledge on AMR. This tool implements components of AMRFinder where AMR genes are detected by BLASTx and classified into its respective functional AMR classes. Mutations are identified for validated specified species. An addition to this tool includes an inferred antibiogram from the AMR genes and mutations, though only for species that have been validated (Sherry et al, 2023).

Whilst WGS provides potential for the detection of AMR, utilising WGS exclusively as a tool for prediction of phenotype still require significant expansion of

evidence/knowledge base (Ellington et al, 2017). Several elements are necessary for comparisons and predictions of AMR phenotype and genotype. Firstly, a curated global reference database will need to be established, requiring regular updates for inclusion of new AMR genes and mutations associated with AMR. Moreover, robust references for AMR genes associating genetic sequences with their phenotype in addition to accurate levels of identification for AMR gene families and AMR genes are required. Lastly gene copy number and promotor mutations must be considered as these affect gene expression, and hence the resistance phenotype.

AIMS: To gain an understanding of discrepancies between resistance phenotype and that predicted from genotype using BSI *E. coli* and *Klebsiella* spp. Illumina sequencing data. Furthermore, to make comparisons between widely used bioinformatics tools for the detection of AMR genes and mutations (ABRicate, ARIBA, ResFinder with PointFinder and Kleborate) to determine whether genotypic AMR detection alone is comparable with “gold standard” clinical phenotypic susceptibility testing.

6.2 Results

6.2.1 Overall genotypic-phenotypic concordance ranged from 65% to 99% across the antimicrobial panel for *E. coli*

A pairwise comparison between *E. coli* isolates with resistance to a particular antimicrobial predicted from genotype (the presence or absence of a known AMR gene(s) and/or mutations) using ResFinder software with PointFinder software, with “true” resistance based on phenotypic antimicrobial susceptibility provide by Severn Pathology (n=585 *E. coli* BSI isolates) was made. Analysis of the concordance between phenotypic and genotypic resistance was based on 12 antimicrobials clinicians utilise for the treatment of BSI in the hospitals supplying samples for analysis by Severn Pathology. The 12 antimicrobials are listed in Figure 59. The overall genotypic-phenotypic concordance (match between phenotype and genotype) ranged from 65% to 99% across the antimicrobial panel. Amoxicillin/clavulanate (BL/BLI) displayed the lowest concordance of 65% whilst cefotaxime, ceftazidime, cefpodoxime (3GCs) and meropenem (carbapenem) displayed the best concordances of 98.0%, 95.6%, 95.6% and 99.7% respectively. The highest percentages of critical errors, 14.1% and 13.3% were observed with ciprofloxacin (FQ) and amoxicillin/clavulanate respectively (Figure 59). Critical errors represent isolates that are phenotypically resistant but predicted to be susceptible based on genotype. Here, if the WGS prediction informed therapy, a non-functional antimicrobial might be prescribed, with likely detrimental implications for patient outcome. The highest percentages of non-critical errors, 15.5%, 8.9% and 8.3% were observed with piperacillin/tazobactam (BL/BLI), gentamicin and amikacin (both aminoglycosides) respectively (Figure 58). Non-critical errors represent isolates that are phenotypically susceptible but predicted to be resistant based on genotype. Here there is no obvious impact on patient outcome,

but it means antimicrobials – potentially broader spectrum, last resort agents – might be used unnecessarily, which may drive resistance to these drugs.

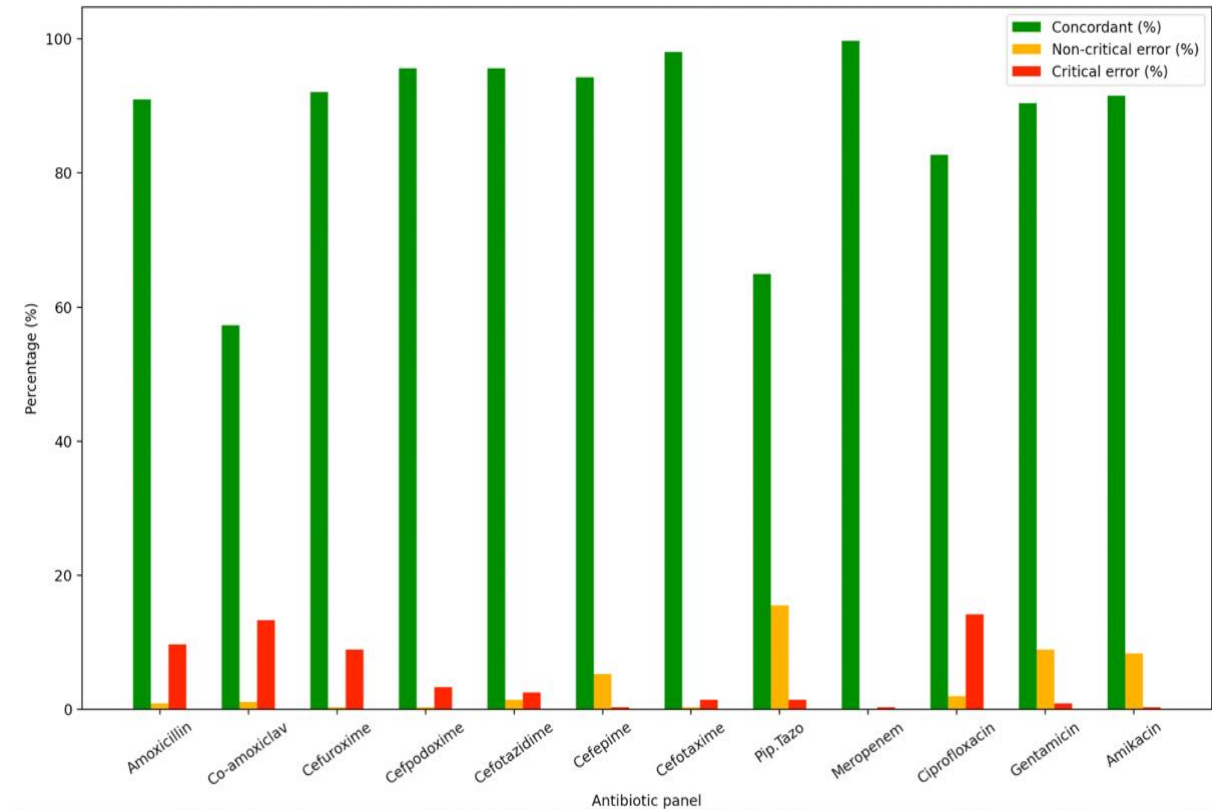


Figure 58. A chart displaying concordance (%) between phenotypic resistance data for 12 antimicrobials used clinically to treat BSI and WGS data for BSI *E. coli* received in 2020. Co-amoxiclav is amoxicillin/clavulanate; pip.tazo is piperacillin/tazobactam.

6.2.2 Concordance varied across bioinformatics tools, with ABRicate and ResFinder with PointFinder displaying the least accuracy for AMR detection of resistance in *E. coli* associated with amoxicillin/clavulanate acid. F1 score was greatest for detection of resistance in *E. coli* associated with cefotaxime

Comparisons of ABRicate, ResFinder (with PointFinder) and ARIBA for the prediction of resistance to various antimicrobials important for the treatment of BSI in *E. coli* were performed. The antimicrobials selected were amoxicillin/clavulanate (BL/BLI), cefotaxime (3GC), gentamicin (aminoglycoside) and ciprofloxacin (FQ). ResFinder was used in conjunction with PointFinder. Figure 59 demonstrates the lowest critical errors, represented by FN, were detected across all bioinformatics tools for cefotaxime. ARIBA had few critical errors for amoxicillin/clavulanate. In contrast ABRicate and ResFinder had very high critical error rates (FN) for amoxicillin/clavulanate. For ciprofloxacin, the least critical errors were detected by ARIBA with the most critical errors detected by ABRicate and ResFinder (with PointFinder). Precision and recall were determined for each bioinformatics tool across all antimicrobial classes. Precision measures the accuracy of positive predictions of a test. Recall measures how good a test is at getting the correct result. F1 takes precision and recall into account, giving a value between 0 and 1. The precision was lowest for gentamicin with the lowest precision at 0.521 associated with ABRicate and ResFinder (with PointFinder). The precision for amoxicillin/clavulanate, cefotaxime and ciprofloxacin were high, however low precision of 0.552 was associated with ARIBA for amoxicillin/clavulanate, because despite low critical errors (FN) there was a very high rate of non-critical errors (FP) (Table 34). Recall across all bioinformatics tools for all antimicrobial classes were generally high >0.6, nevertheless, lowest recall of 0.064 was associated with ARIBA for ciprofloxacin (Table 34). Overall, the F1 score for all

tools detecting gentamicin resistance was the lowest. The F1 score for all tools for detecting resistance associated cefotaxime was the highest (Table 34).

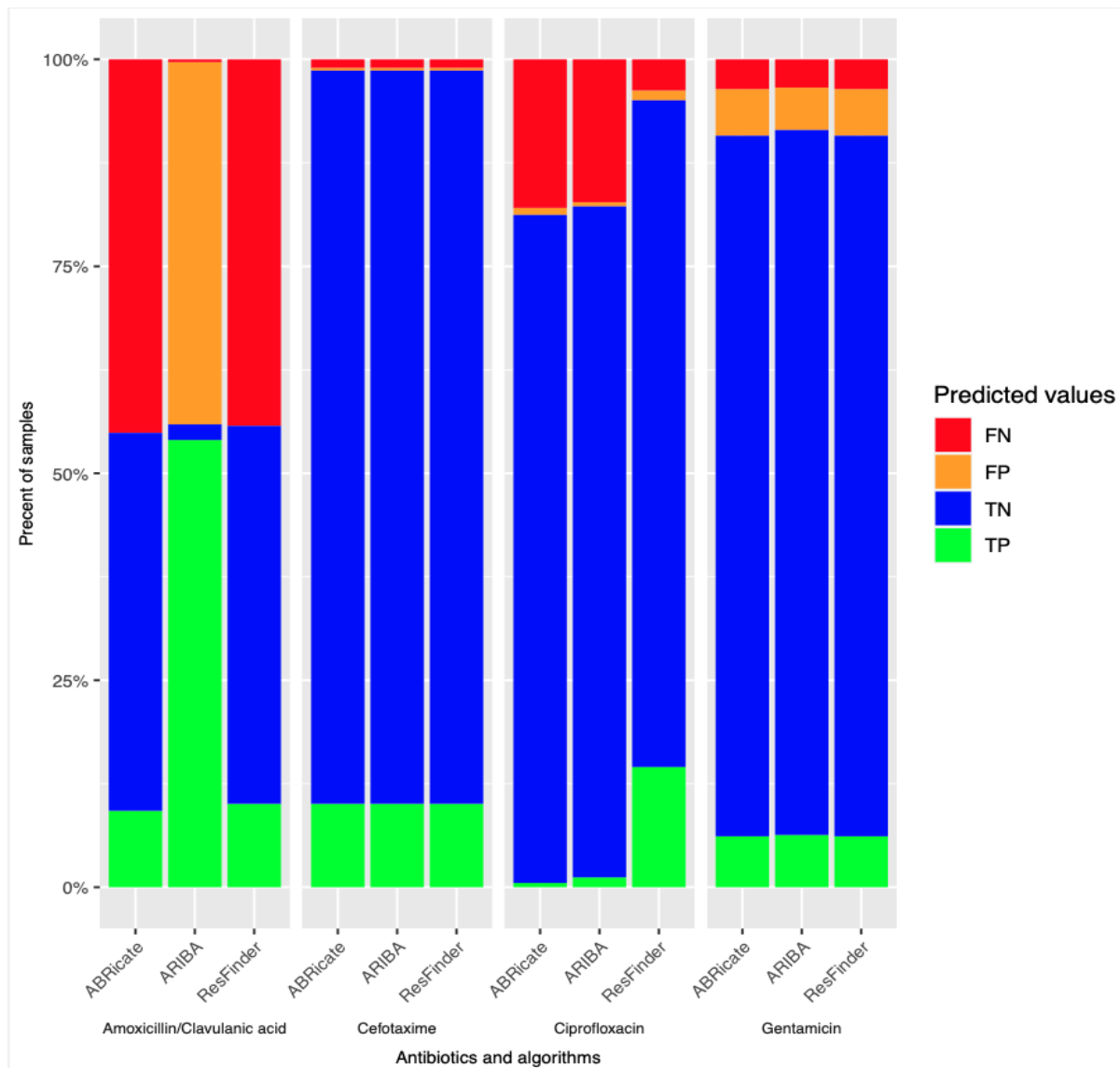


Figure 59. Graph displaying the percentage of *E. coli* samples producing true positives (TP), true negatives (TN), false positives (TP) (non-critical errors) and false negatives (FN) (critical errors) for ABRicate, ARIBA and ResFinder.

Table 34. Table showing the statistical comparison of precision, recall and F1 score for the detection of AMR determinants using several bioinformatics tools for *E. coli*.

Antibiotic		Precision	Recall	F1
Cefotaxime	Abricate	0.967	0.908	0.937
	ResFinder (with PointFinder)	0.967	0.908	0.937
	ARIBA	0.967	0.908	0.937
Gentamicin	Abricate	0.522	0.632	0.571
	ResFinder	0.522	0.632	0.571
	ARIBA	0.552	0.649	0.597
Amoxicillin/ Clavulanic acid	Abricate	1	0.170	0.290
	ResFinder (with PointFinder)	1	0.186	0.313
	ARIBA	0.552	0.994	0.710
Ciprofloxacin	Abricate	0.375	0.028	0.052
	ResFinder (with PointFinder)	0.924	0.794	0.854
	ARIBA	0.7	0.065	0.119

6.2.3 Concordance varied across bioinformatics tools (ABRicate, ResFinder with PointFinder, ARIBA and Kleborate) in all *Klebsiella* spp. F1 score was greatest for detection of resistance in *K. pneumoniae* associated with gentamicin

As *Klebsiella* spp. was the second most common genus amongst the 2020 BSI dataset, a comparison of accuracy for most commonly used tools for AMR detection of *Klebsiella* were evaluated. Lam *et al.* (2021) developed a tool, Kleborate designed for AMR gene detection for *Klebsiella* species. Therefore, comparison of ABRicate, ResFinder with PointFinder, ARIBA, as for *E. coli* and additionally here, Kleborate were conducted for amoxicillin/clavulanate, cefotaxime, gentamicin and ciprofloxacin. Figure 61 demonstrates the lowest critical errors across all bioinformatics tools for cefotaxime, as seen for *E. coli*. Figure 60 also demonstrates the highest critical errors for amoxicillin/clavulanate, in particular for ABRicate, ResFinder with PointFinder and

Kleborate, as also seen for *E. coli*. For ciprofloxacin, no critical errors were detected by ARIBA.

Precision and recall were determined for each bioinformatics tool across all antimicrobial classes. The precision was lowest for ciprofloxacin resistance with the lowest precision at 0.083 associated with ABRicate, ResFinder with PointFinder and ARIBA. The precision for amoxicillin/clavulanate was high, however low precision of 0.237 was seen with ARIBA for amoxicillin/clavulanate (Table 35). Recall across all bioinformatics tools for all antimicrobial classes were generally high >0.7, nevertheless, lowest recall of 0.2857429 was associated with both ABRicate and ResFinder with PointFinder for amoxicillin/clavulanate (Table 35) and highest recall of 1 was associated with ARIBA for FQs. Overall, the F1 score for tools detecting resistance associated with ciprofloxacin was the lowest, however Kleborate gave the highest F1 score of 0.864. The F1 score for all tools for detecting resistance associated with gentamicin, was the highest respectively (Table 35), with Kleborate generating the highest F1 scores for gentamicin, amoxicillin/clavulanate and ciprofloxacin.

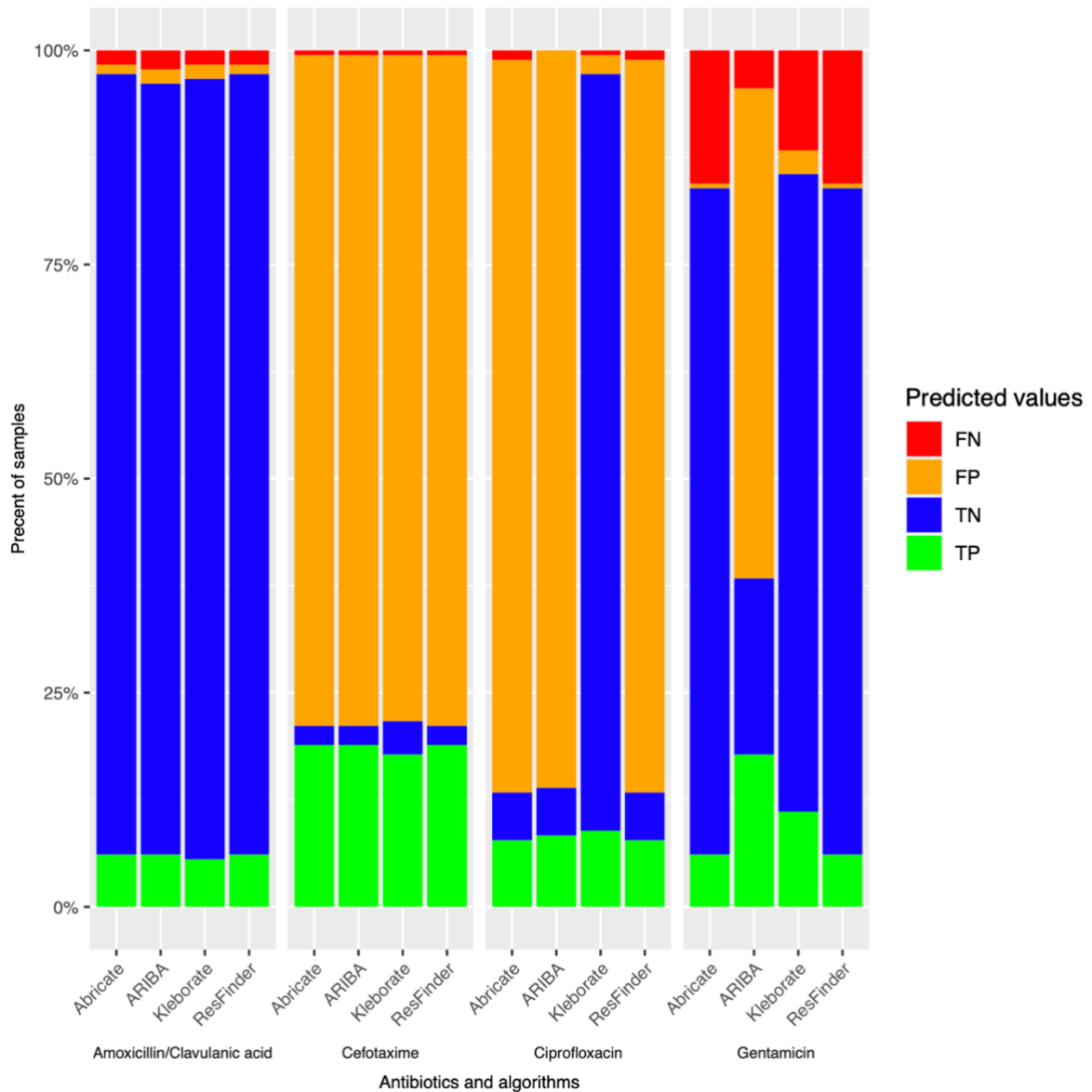


Figure 60. Graph displaying the percentage of all *Klebsiella* spp. isolates producing true positives (TP), true negatives (TN), false positives (FP) (non-critical errors) and false negatives (FN) (critical errors) for ABRicate, ARIBA, ResFinder with PointFinder and Kleborate.

Table 35. Table showing the statistical comparison of precision, recall and F1 score for the detection of AMR determinants using several bioinformatics tools for *Klebsiella* spp.

Antibiotic		Precision	Recall	F1
Cefotaxime	Abricate	0.194	0.971	0.324
	ResFinder (wth PointFinder)	0.194	0.971	0.324
	ARIBA	0.194	0.971	0.324
	Kleborate	0.186	0.970	0.312
Gentamicin	Abricate	0.846	0.786	0.815
	ResFinder (with PointFinder)	0.846	0.786	0.815
	ARIBA	0.786	0.733	0.759
	Kleborate	0.769	0.769	0.769
Amoxicillin/Clavulanic acid	Abricate	0.917	0.282	0.431
	ResFinder (with PointFinder)	0.917	0.282	0.431
	ARIBA	0.237	0.800	0.366
	Kleborate	0.800	0.488	0.606
Ciprofloxacin	Abricate	0.083	0.875	0.152
	ResFinder	0.083	0.875	0.152
	ARIBA	0.088	1	0.162
	Klebroate	0.800	0.941	0.865

6.2.4 Critical errors detected in all antimicrobial classes for *K. pneumoniae*, however for other species critical errors were only detected for amoxicillin/clavulanate

The AMR dataset for *Klebsiella* spp. revealed variation between species and AMR mechanisms, hence, in order to determine whether there was variation between the computational methods, evaluation between the 4 computational methods amongst the most common species in this study (*K. pneumoniae*, *K. oxytoca* and *K. variicola*) was conducted. Figure 61 revealed critical errors were detected across all bioinformatics tools for gentamicin, ciprofloxacin, cefotaxime and amoxicillin/clavulanate against *K. pneumoniae*. No critical errors were observed with Kleborate for ciprofloxacin. Figure 61 also demonstrates the highest critical errors for amoxicillin/clavulanate, in particular for ABRicate, ResFinder with PointFinder and Kleborate. The precision was lowest for ciprofloxacin except for Kleborate. The precision for amoxicillin/clavulanate overall was high, however lowest precision of 0.2941 was associated with ARIBA (Table 36). Recall across all bioinformatics tools for all antibiotics were generally high >0.7, nevertheless, lowest recall of 0.297 was associated with both ABRicate and ResFinder with PointFinder for amoxicillin/clavulanate (Table 36) and highest recall of 1 was associated with Kleborate for ciprofloxacin. Overall, the F1 score for tools detecting resistance associated with ciprofloxacin was the lowest, however Kleborate gave the highest F1 score of 0.864. The F1 score for all tools for detecting resistance associated with gentamicin, was the highest respectively (Table 36), with Kleborate generating the highest F1 scores of amoxicillin/clavulanate and ciprofloxacin.

In comparison with *K. pneumoniae*, no critical errors were identified for gentamicin, ciprofloxacin and amoxicillin/clavulanate for *K. oxytoca* (Figure 62) and *K. variicola* (Figure 63). Critical errors were only identified with amoxicillin/clavulanate for both species. A high percentage of false positives were detected in both species for amoxicillin/clavulanate and ciprofloxacin. The vast majority (between 88.2% and 100%) were determined to be false positives for amoxicillin/clavulanate and ciprofloxacin when compared to the “true” phenotype. However there was variation observed in the computational methods with Kleborate detecting 0% FN, whereas the other tools detected 88.2% FP.

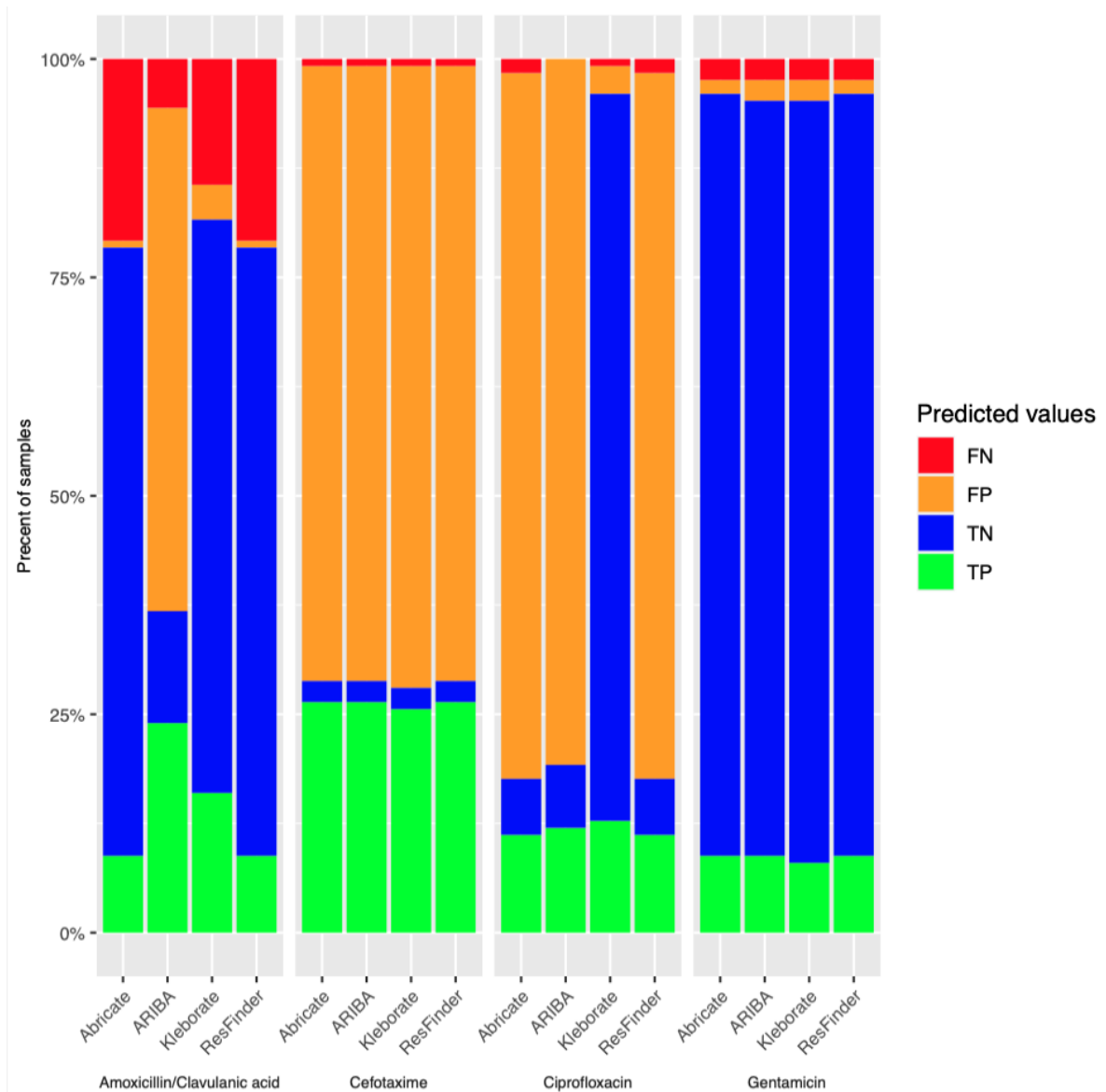


Figure 61. Graph displaying the percentage of all *K. pneumoniae* (n=125) samples producing true positives (TP), true negatives (TN), false positives (FP) (non-critical errors) and false negatives (FN) (critical errors) for ABRicate, ARIBA, ResFinder with PointFinder and Kleborate.

Table 36. Table showing the statistical comparison of precision, recall and F1 score for the detection of AMR determinants using several bioinformatics tools for *K. pneumoniae*. (Precision measures the accuracy of positive predictions of a test. Recall measures how well a test is at getting the correct result. F1 takes precision and recall into account, giving a value between 0 and 1).

Species	Antibiotic class		Precision	Recall	F1
K. pneumoniae	Cefotaxime	Abricate	0.273	0.971	0.426
		ResFinder (wth PointFinder)	0.273	0.971	0.426
		ARIBA	0.273	0.971	0.426
		Kleborate	0.264	0.970	0.416
K. pneumoniae	Amoxicillin/ Clavulanic acid	Abricate	0.917	0.297	0.449
		ResFinder (with PointFinder)	0.917	0.297	0.449
		ARIBA	0.294	0.811	0.432
		Kleborate	0.800	0.526	0.635
K. pneumoniae	Gentamicin	Abricate- Gentamicin	0.846	0.786	0.815
		ResFinder (with PointFinder)	0.846	0.786	0.815
		ARIBA	0.786	0.786	0.786
		Kleborate	0.769	0.769	0.769
K. pneumoniae	Ciprofloxacin	Abricate	0.122	0.875	0.214
		ResFinder	0.122	0.875	0.214
		ARIBA	0.129	1	0.229
		Klebroate	0.800	0.941	0.865

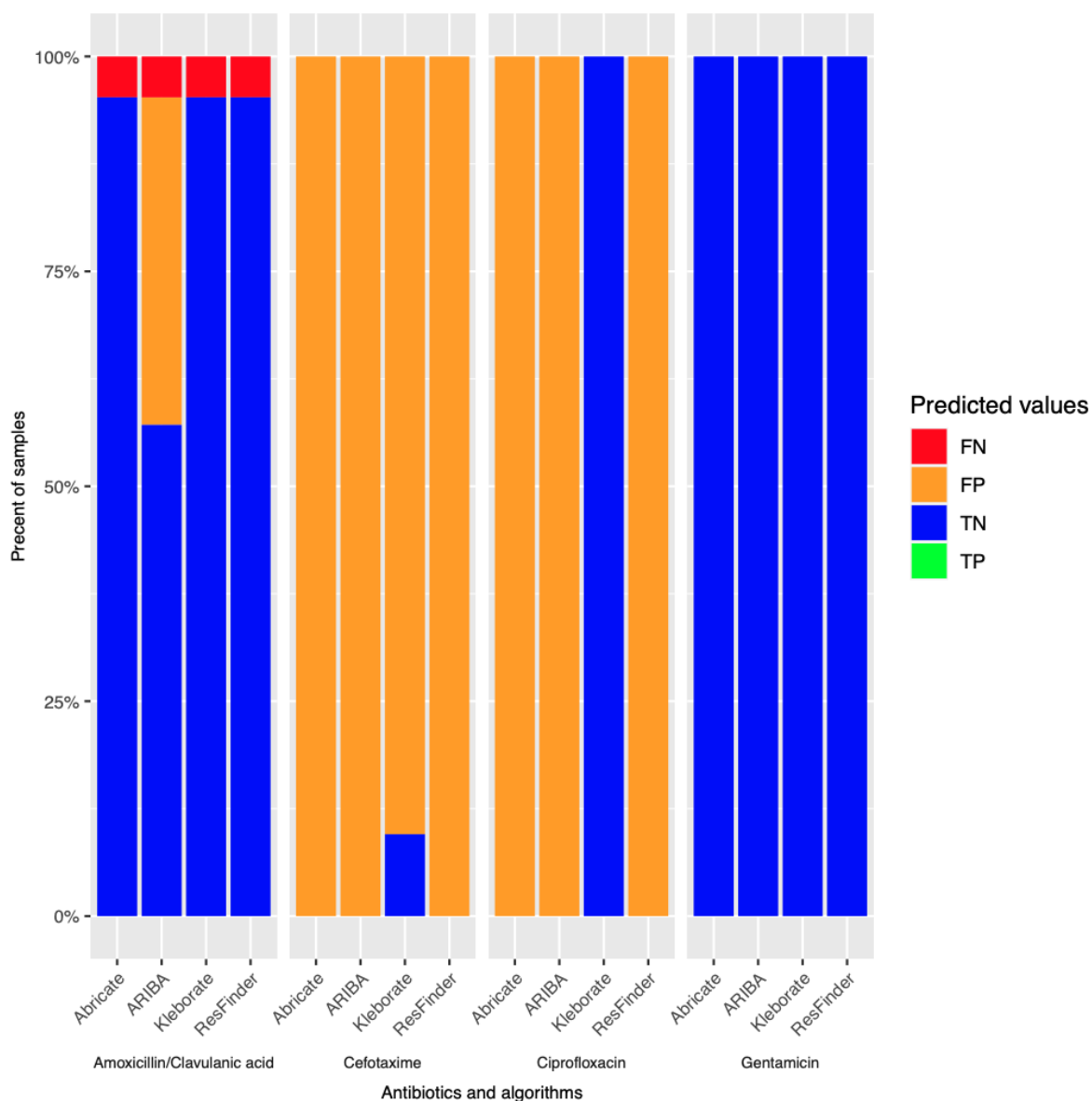


Figure 62. Graph displaying the percentage of all *K. oxytoca* (n=21) samples producing true positives (TP), true negatives (TN), false positives (FP) (non-critical errors) and false negatives (FN) (critical errors) for ABRicate, ARIBA, ResFinder with PointFinder and Kleborate.

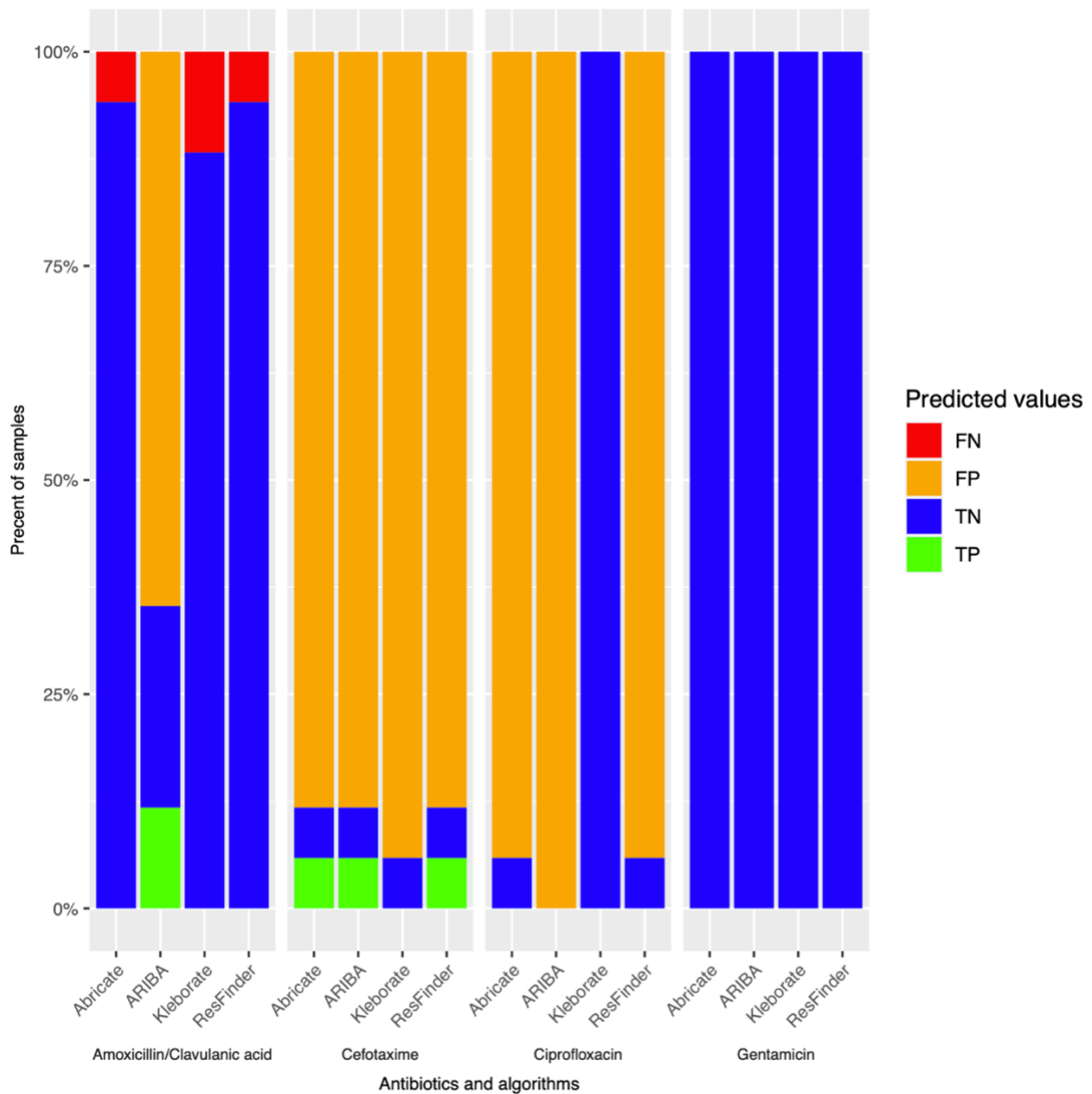


Figure 63. Graph displaying the percentage of all *K. variicola* (n=17) samples producing true positives (TP), true negatives (TN), false positives (FP) (non-critical errors) and false negatives (FN) (critical errors) for ABRicate, ARIBA, ResFinder with PointFinder and Kleborate.

6.2.5 Investigation reasons for critical errors between 3GC-R phenotype and genotype in *E. coli* and *Klebsiella* spp.

It was considered possible that in some rare cases, the bacterium sequenced (and so producing the WGS data used to predict resistance) might not be identical to the bacterium analysed in the clinical lab to provide the “true” phenotypic resistance data. This could explain seeming differences between genotypic prediction and “true” phenotype. Hence for all 3GC-R isolates where there was a critical error (false negative), antimicrobial susceptibility was retested phenotypically using the bacterium that had been sequenced. Matches describe the concordance between results from phenotypic testing and phenotype in the lab. Given time constraints this analysis was done only for 3GCs. Figure 64 displays the number of isolates retested phenotypically for both *E. coli* and *Klebsiella* spp.

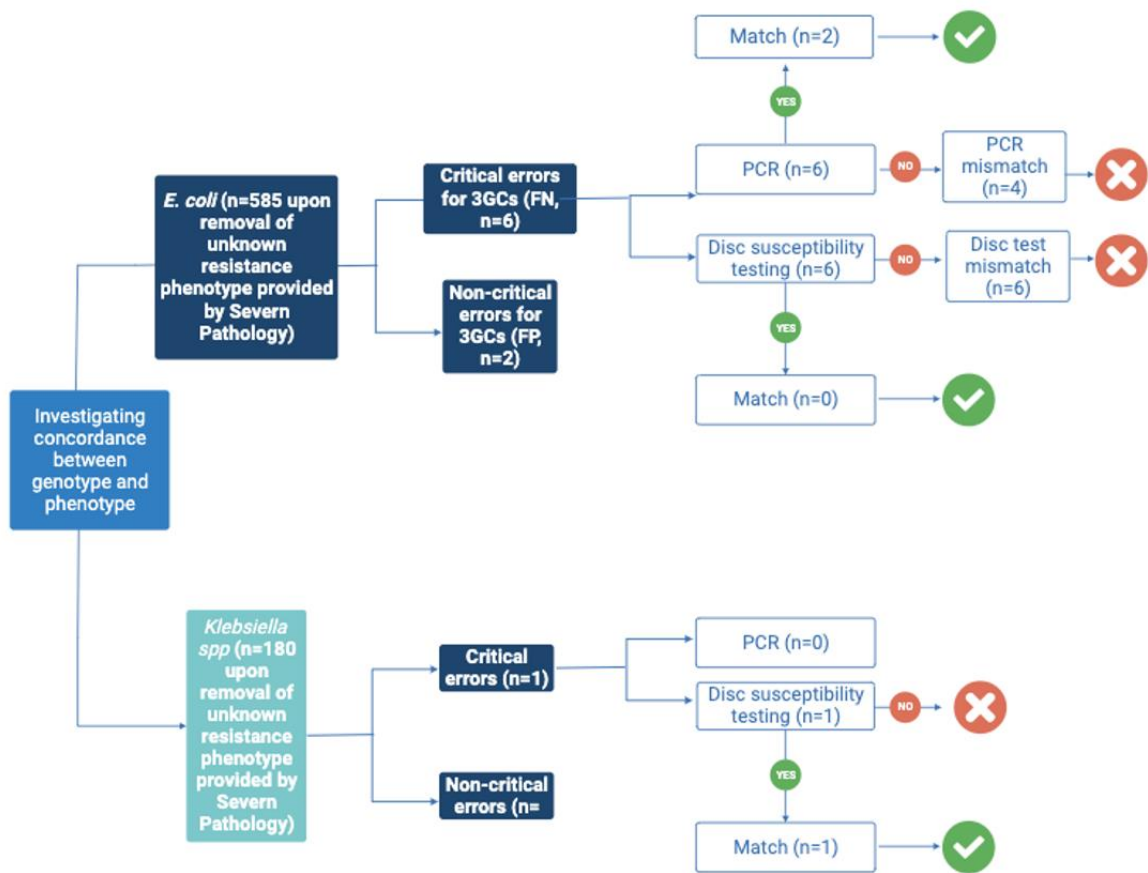


Figure 64. Flowchart displaying a summary of the number of isolates tested for concordance and the numbers of isolates retested phenotypically with disc susceptibility and PCR. Created using Biorender.

All isolates displaying critical errors for 3GC-R (defined using cefotaxime) in *E. coli* (n=6) and *Klebsiella* (n=1) were taken forwards for analysis. Disc testing revealed all *E. coli* isolates were 3GC-R, confirming the data provided by Severn Pathology (Table 37). These isolates were taken forwards for PCR to further identify whether they do possess a known 3GC-R gene that had for some reason been missed in the WGS analysis (Table 37). Upon re-testing 1 *Klebsiella* spp. isolate with a critical error was found to be susceptible so in this case, the isolate has been switched or lost resistance (lost a plasmid for example) following phenotypic testing by Severn Pathology and there is therefore no genuine critical error in this case.

Upon retesting the six 3GC-R *E. coli* with remaining critical errors plus using a CTX-M multiplex PCR (since CTX-M is the most common mechanism for 3GC-R), *bla*_{CTX-M} genes were identified in 3 out of 6 isolates. Isolates 361, 103 and 331 displayed 414bp fragments, suggesting the presence of a CTX-M group 1 genes (Figure 65) by reference to the positive controls, Hence, in these three cases the WGS data had missed the 3GC-R gene, for reasons that are not clear. However, for the other three 3GC-R isolates no mechanism could be identified using PCR or the existing bioinformatic tools. However, using a new tool (The Hound) developed in the group by Carlos Reding, wholesale changes, suggestive of the insertion of a piece of DNA upstream of the *E. coli* chromosomal *ampC* gene was identified in these three isolates. (Table 37). It is possible that this insertion includes a strong promoter, that might drive the expression of *ampC*, conferring 3GC-R in the absence of any acquired resistance gene.

Table 37. Table showing discordance of *E. coli* isolates resistant to cefotaxime with the associated disc testing results after re-testing phenotypically.

Isolate No.	Organism Identification	Cefotaxime (3rd generation cephalosporin)				CTXM multiplex PCR		AMPC promoter regions and copy numbers		
		Phenotypic	Genotypic	Match (V/N)	Disk testing measurements	Disk testing results	PCR	PCR Gene found (y/n)	AMPC promoter copy number detected by The Hound (Roman et al 2023)	AMPC promoter mutations detected by The Hound (Roman et al 2023)
361	<i>Escherichia coli</i>	r	-	n	18mm	r	Yes	y	NA	NA
103	<i>Escherichia coli</i>	r	-	n	16mm	r	Yes	y	NA	NA
255	<i>Escherichia coli</i>	r	-	n	18mm	r	No	n	0.488	-82G->A;-81G->T;-78T->G;-77C->T;-76G->A;-74T->C;-73A->G;-72C->T;-71A->T;-69T->C;-68C->A;-67T->A;-66A->T;-65A->C;-64C->T;-63G->A;-62C->A;-61A->C;-60T->G;-104C->T;-103C->A;-101G->C;-100A->C;-99C->T;-98A->G;-97G->A;-96T->A;-95T->C;-92C->T;-91A->G;-90C->T;-89A->C;-88C->A;-87T->C;-85A->C;-83T->G;-82G->A
240	<i>Escherichia coli</i>	r	-	n	20mm	s	Yes	n	1.269	-82G->A;-81G->T;-78T->G;-77C->T;-74T->C;-73A->G;-72C->T;-71A->T;-69T->C;-68C->A;-67T->A;-66A->T;-65A->C;-64C->T;-63G->A;-62C->A;-61A->C;-60T->G;-104C->T;-103C->A;-101G->C;-100A->C;-99C->T;-98A->G;-97G->A;-96T->C;-95T->A;-92C->T;-91A->G;-90C->T;-89A->C;-88C->A;-87T->C;-85A->C;-83T->G;-82G->A
262	<i>Escherichia coli</i>	r	-	n	15mm	r	Yes	n	0.831	71A->T;-69T->C;-68C->A;-67T->A;-66A->T;-65A->C;-64C->T;-63G->A;-62C->A;-61A->C;-60T->G;-104C->T;-103C->A;-101G->C;-100A->T;-99C->T;-98A->G;-97G->A;-96T->C;-95T->A;-92C->T;-91A->G;-90C->T;-89A->C;-88C->A;-87T->C;-85A->C;-83T->G;-82G->A
331	<i>Escherichia coli</i>	r	-	n	9mm	r	No	y	NA	NA
39663	<i>Klebsiella pneumoniae</i>	r	-	n	21mm	s	No	NA	NA	NA

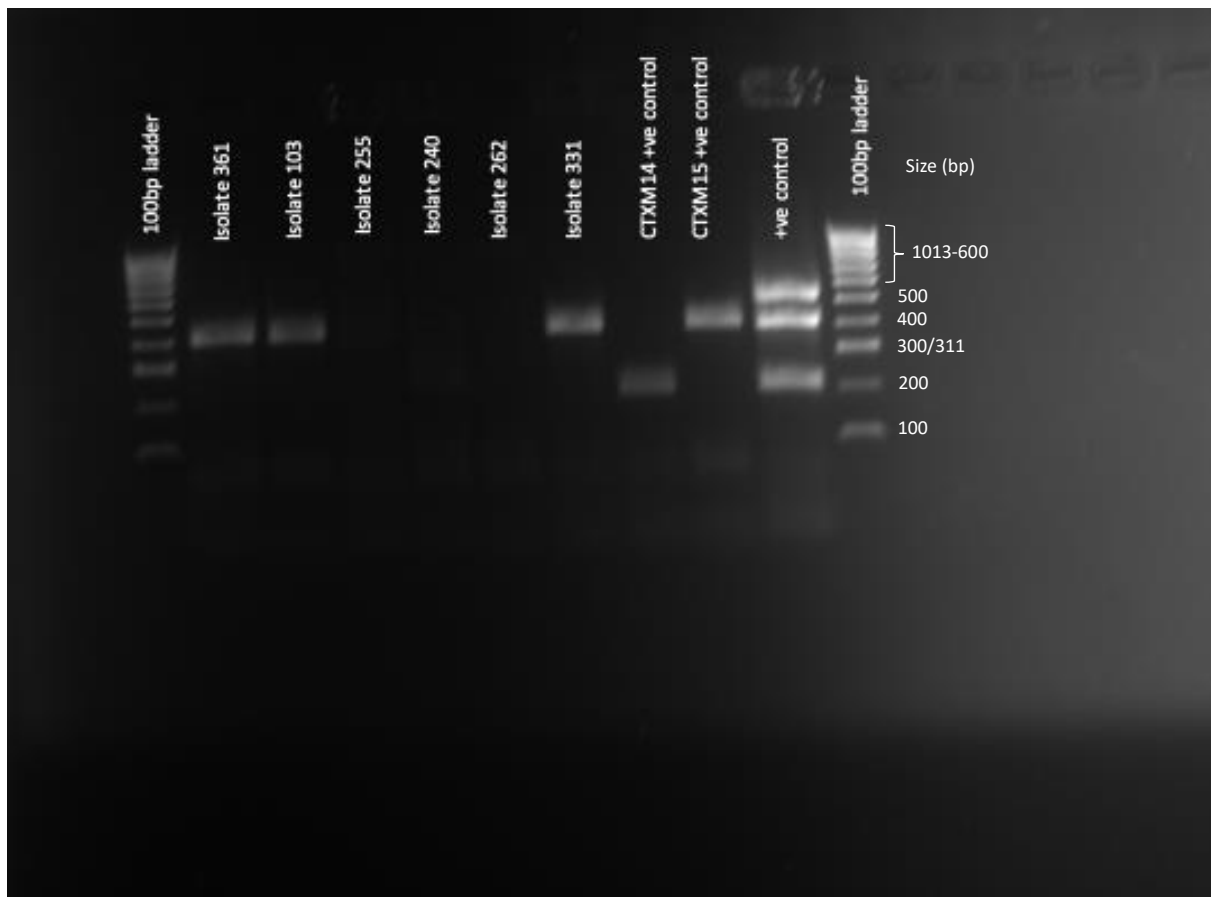


Figure 65. A gel from CTX-M multiplex PCR displaying the presence and absence of CTX-M gene. The products in the positive control as displayed relate to the primer pairs as detailed in Table 10.

6.3 Discussion and Conclusion

Revolutionary updates to WGS technology are changing the field of clinical microbiology (Chan et al, 2012; Monk, 2018) by providing far more rapid and accurate determination of AMR genotype in *Enterobacterales* including *Shigella sonnei* and *E. coli* (Sadouki et al, 2017; Tyson et al, 2015). However, Tyson *et al.* (2015) found the most discrepant results for aminoglycosides, whereas the most discordant results in this study of BSI *E. coli* and *Klebsiella* spp. were for amoxicillin/clavulanate (Figure 58, Figure 60). Other studies also reported poor genotype/phenotype prediction accuracy for other BL/BLIs such as piperacillin/tazobactam (Shelburne et al, 2017). A study conducted by Davies *et al.* (2020) demonstrated the discrepancy in results for amoxicillin/clavulanate was due to poor interpretation of the effect of genetic mechanisms on expression of phenotype such as gene promoter mutations, gene copy number. The presence of SNPs in AmpD play a role in the increased production of AmpC in *Enterobacter* spp and *Citrobacter* spp, contributing towards resistance to 3GCs and BL/BLI combinations (Lister et al, 2009; Flury et al, 2016), but not in *E. coli* (where *ampC* is not inducible) and not in *Klebsiella* spp. (which do not have an *ampC*).

In terms of false positives when predicting AMR from genotype, numerous studies have reported a high prevalence of “silent” AMR genes in *E. coli*. For example, Lanz *et al.* (2003) reported the detection of a silent streptomycin resistance gene *aadA1* in 28.49% of *E. coli* displaying susceptibility to streptomycin and Walsh reported 25% of *K. pneumoniae* harbouring silent IMP genes whilst remaining susceptible to carbapenems, shown in a study by Cheung *et al.* (2021). Another study reported susceptibility to chloramphenicol despite harbouring *catA1* in 40% of *Salmonella* spp. (Deekshit et al, 2012). Silent AMR genes may be a common phenomenon which can result in therapeutic failure when therapy is based on phenotypic resistance status,

since silencing of resistance can be reversible. The designs of molecular assays including PCR and WGS revolve around the identification of AMR genes, and so here, silent genes result in a “false positive” that means a particular agent would be avoided, and this might be best if phenotypic silencing can be reversed. This might therefore be a benefit of genotypic versus phenotypic resistance. Another would be identification of “pre-resistance” where a gene or mutation is present that increases the MIC of an antimicrobial but not to the point of resistance. Current phenotypic tests would not identify this, except for those set up to survey last resort carbapenem resistance, but it may be best to avoid an antimicrobial if an infection is caused by a bacterium that is “nearly” resistant, as opposed to one which is several genetic changes away.

The study reported in this chapter analyses the variation at AMR gene/mutation detection between several bioinformatics tools utilised widely for *E. coli* and *Klebsiella* spp. For species, highest critical errors were observed with amoxicillin/clavulanate, with ARIBA demonstrating the least critical errors (but most false positives) amongst the computational methods tested (Figure 59, Figure 60, Figure 61, Figure 62, Figure 63). One explanation for this could be the complexity of the variation of AMR gene nomenclature across the different computational methods, especially for *Enterobacterales*, therefore single SNPs in similar gene families such as *bla*_{CTX-M} can give rise to contrasting resistance profiles. An example of this is *bla*_{TEM-1} (Genbank: AY458016.1) and *bla*_{TEM-30} (Genbank: AJ437107.1) are almost identical, however *bla*_{TEM-30} contributes to BL/BLI resistance more than *bla*_{TEM-1} because TEM-30 has a mutation that reduces the efficiency of clavulanate as an inhibitor for TEM. Resistance can also arise by mutations that a limited number of bioinformatics tools can identify. A recent study revealed that mutation in both *ramR* and *ompK36* contribute to BL/BLI resistance including newly released agents ceftazidime/avibactam and

meropenem/vaborbactam (Satapoomin et al, 2022). ResFinder alone at the time this study was conducted was not able to identify, this because it does not consider mutations in *ramR*, and its database of relevant mutations in *ompK36* is limited. Hence, the inability of ResFinder, ABRicate and ARIBA to identify *ompK* mutations in *Klebsiella* spp. may have contributed to the single critical error identified in *K. pneumoniae* (Figure 61). Nevertheless, Kleborate, a specific tool used for AMR gene detection for *Klebsiella* spp. was able to detect *ompK* mutations. Further explanations regarding the false negatives found when using these computational methods could also involve the variation in reference databases bioinformatics tools utilised play a role in the limitations for the detection of novel, unknown resistance genes. Discrepancies in the nomenclature of AMR gene variants were found across the bioinformatics tools used in this study. For example *strB* was also identified by *aph(6)*-Id with some tools. Furthermore, different tools used different databases, giving rise to increased variation of different AMR gene detection. In this study, ARIBA identified mutations involved with ciprofloxacin resistance in addition to *ampC* and *ampH*, a PBP involved in peptidoglycan synthesis. This could be an explanation for the lowest critical errors and higher F1 scores compared to other tools (Table 34, Table 35, Table 36) associated with the use of ARIBA for detection in resistance to amoxicillin/clavulanate. However, since AmpH has no actual role in resistance, it may be that this also explains the high false positive rate. Essentially, tools need to be developed with reference to our actual biological understanding of AMR. However, it is important to emphasise that the one of the key reasons for failure is the lack of consideration for tools to consider gene expression.

This study also revealed that 100% of *K. oxytoca* isolates were false positive across all bioinformatics tools tested for cefotaxime (Figure 62). Furthermore, false positives

were only detected by ARIBA for amoxicillin/clavulanic acid (Figure 62). This is due to the *bla_{OXY}* gene groups, known for constitutively low expression levels, resulting in the susceptibility to β -lactams and cephalosporins. Nonetheless, hyperproduction of OXY as a consequence of mutations in the promoter regions confers resistance (González-López et al, 2009), therefore isolates predicted resistant by the bioinformatics tools tested may not necessarily be resistant. Three *bla_{OXY}* derivatives with amino acid substitutions have also been reported in the literature to give rise to resistance to BL/BLI combinations and ceftazidime (Mammeri et al, 2003; Rodríguez-Martínez et al, 2008).

One of the limitations of this study involves the evaluation of the impact of different reference databases in AMR gene detection. The comparison of these databases would increase the complexity and emphasise the significance of the outputs from computational methods. Currently, novel pipelines such as hAMRoaster, a tool are being developed to compare a range of AMR gene detection tools which emphasises the variation yielded by different computational methods (Wissel et al, 2023).

Plasmid loss over time can occur if sequencing is not performed subsequent to initial culturing. Moreover, contamination of isolates whilst subculturing due to human error can also contribute towards the discrepancies observed between phenotype and genotype (Smith & Bidochka, 1998). This can be a possible explanation for the 3GC sensitive *Klebsiella* spp. isolate from disc diffusion, compared to the detection of 3GC-R by initial laboratory tests conducted by Severn Pathology (Table 37). Possibilities of diversity in the VITEK used by Severn Pathology initially and disc diffusion assays conducted here may also affect the result. Isolates with critical errors that displayed phenotypic resistance after retesting by disc diffusion were subjected to CTX-M

multiplex PCR for detection of CTXM group genes. This study revealed that CTX-M genes were identified in 3 out of 6 3GC-R *E. coli* isolates having critical errors based on WGS data (Figure 64, Figure 65). Mutations in the promoter region of *ampC* are responsible for its overexpression, resulting in reduced susceptibility to cephalosporins and BL/BLIs (Peter-Getzlaff et al, 2018). Currently, no bioinformatics tool tested in this study is able to detect the copy number and mutation in the promoter region of *ampC* accurately. However, this can be identified accurately with The Hound, a novel tool developed by Carlos Reding Roman in the Avison Lab, therefore resolving the discrepancies in the critical errors displayed in the *E. coli* isolates. As discussed above, silent genes may also contribute to the failure in detection of AMR genes. To aid the resolution of these limitations, more effective sample processing and better purification of the isolates prior to amplification would be a strategy to employ for future work. However, a study has shown WGS has advantages in AMR gene detection compared with targeted PCR, with only 65% of bacterial strains detected by PCR (Shelburne et al, 2017). This study also revealed significantly higher positive predictive values associated with WGS compared with using traditional phenotyping methods for AMR prediction (Shelburne et al, 2017).

In conclusion, current knowledge in research utilising both genomics and phenotypic methods in addition to findings from this study, indicate phenotypic methods are currently more suitable for defining antimicrobial treatment for patients. However, this only provides limited epidemiological information and there is a delay between collecting a blood sample, isolation of bacteria from blood cultures and characterisation of their AMR profiles. WGS provides quicker turnaround times and improves species identification, and in parallel can provide information useful when considering IPC. So WGS has many potential advantages for AMR prediction as a clinical tool, but optimisation of these bioinformatic tools to be more in tune with the biological realities of AMR is still required to provide results with accuracy sufficient for use as a diagnostic tool. In the meantime, regional WGS-based AMR surveys are important for guiding clinicians to providing more accurate empiric treatment for BSIs by considering AMR patterns within bacteria associated with specific patient groups.

7.0 General Discussion and Conclusion

7.1 Discussion

Research conducted in this study investigates the incidence of resistant pathogens causing BSIs and UTIs in Bristol, Bath, North Somerset and South Gloucestershire, an NHS care board serving a population of 1.5 million people, through surveillance across 2020 and comparisons with 2018. This is the first study conducting surveillance, comparisons and characterisations of resistant pathogens causing BSIs in a pandemic year compared with a non-pandemic year in Bristol and surrounding regions. Furthermore, this research aims to determine whether the interplay of plasmids, AMR and virulence factors, in addition to *in silico* based AMR detection and its associations with source of infection, can optimise empiric therapy.

Whilst all Gram-negative bacterial isolates from BSIs were collected, *E. coli* and *Klebsiella* spp. formed the focus for this research as these pathogens were two of the most common pathogens isolated from BSIs. In literature, *E. coli* and *Klebsiella* spp. causing BSIs are an increasing public health concern and associated with high morbidity and mortality (Vihta et al, 2018; UKHSA, 2022). Analysis with *Klebsiella* spp. for UTIs could not be conducted as only *E. coli* from UTIs were provided by Severn Pathology in 2020.

The associations between phylogroups, source of infection and resistance formed most of the focus for results Chapter 1. As discussed in results Chapter 1, BSIs originate from a source, most commonly urinary source, which is a complicated UTI. This is where the pathogen has entered the bloodstream and GI source, which involves the (often micro-) perforation of the bowel, resulting in increased intestinal permeability, enabling pathogens entry to the bloodstream. Results revealed

significant associations between phylogroup A and B1 *E. coli* BSI and a GI source. Moreover, work conducted in collaboration with Dr Jordan Sealey revealed there was a strong association ($p < 0.0001$) between carriage of “farm-animal specific resistance genes”, when comparing *E. coli* phylogroups B2 to phylogroups A/B1 (Unpublished, 2023). Those AMR genes encode mechanisms of resistance to streptomycin, neomycin and florfenicol, used in the UK to treat farmed animals, in phylogroup A/B1 isolates. These findings indicate that isolates of phylogroup A/B1 have a farmed animal origin, which has not previously been reported in the Southwest, UK. Results in this chapter also revealed significant associations between phylogroup B2 ST131 and urinary source of infection. Additionally, these ST131 were highly MDR, especially 3GC-R, extensively used as empiric treatment in recent years. These findings are important and contribute towards improving empiric therapy. For example, if an ST131 *E. coli* was isolated from a patient with BSI from urinary source, information from this study can inform other treatment options excluding 3GCs, which assists with choice of antibiotic therapy. Surveillance of AMR patterns between different years can also assist with choice of antibiotic administered as empiric therapy. From the results in Chapter 1, significant increases have been observed with genes associated with resistance to BL/BLIs, suggesting this particular antimicrobial class may become increasingly ineffective as treatment for BSIs in future. This emphasizes the necessity for continuous surveillance of AMR patterns.

In results Chapter 2, significant associations were revealed with *E. coli* BSI and urinary and GI source of infection. In comparison, there were no significant associations between *K. pneumoniae* with urinary or GI source of infection, however, significant associations were identified between *K. pneumoniae* with non-line infections. The sample sizes for other non-line sources of infection, excluding urinary and GI source

in this study were too low for comparison. There is a paucity of research examining the associations between source of infection and *Klebsiella* spp. causing BSIs. One recent study reported GI source accounted for 34% of *K. pneumoniae* causing BSIs, nevertheless, 4% of *K. pneumoniae* causing BSIs were associated with respiratory source and caused higher mortality rates in comparison to other sources ($p < 0.0001$) (Roach et al, 2023). Phylogenetics in combination with AMR profiling, has enabled the identification of MDR ST307 in addition to NDM-positive ST15 *K. pneumoniae* from patients in the same ward in results Chapter 2. Initial characterisation with Illumina data revealed NDM-positive ST15 *K. pneumoniae* harbour the same AMR genes present in 5 separate regions of the genome. There have been reports of NDM-positive ST15 *K. pneumoniae* identified on plasmids (Martins et al, 2020; Sacco et al, 2022), however, the reconstruction of plasmids from Illumina data to investigate whether these ST15s identified from the same ward harboured plasmids containing MDR was a limitation. An evaluation of 4 programmes used for prediction of plasmids from short-read data in one study reported a recall and precision of 0.76 and 0.62 respectively for the prediction of small plasmids < 10 kbp, however there was a failure in the prediction of plasmids > 50 kbp (Arredondo-Alonso et al, 2017). Therefore, in order to mitigate this, NDM-positive ST15 *K. pneumoniae* causing BSIs isolated from the same ward were subjected to long read sequencing by Microbes NG. This analysis was detailed in results Chapter 3. Analysis from long read data revealed 100% identity in plasmids IncFIB, IncR and Col440 harbouring a myriad of genes associated with heavy metal resistance and AMR and virulence between two different patients from the same ward. In keeping with this, a study reported up to 18 samples from different patients in separate wards within an Ethiopian hospital, harboured identical plasmids or highly homologous plasmids containing insertions and deletions (Lin et al, 2020).

The transmission of bacteria between patients in the same ward occurring through interactions with healthcare workers and movement of patients between wards, in an environment of high levels of antimicrobial prescribing has accelerated the transmission of resistant bacteria. A study has demonstrated modelling antimicrobial usage and patient transfers between different wards using a metapopulation framework enables the prediction of the burden of AMR (Shapiro et al, 2020). Understanding the relationships between bacterial species, mechanisms of AMR and sources of infection can provide insight into severity of infection and transmission of AMR. Both of these are integral in improving choice of empiric therapy and infection control.

In results Chapter 3, strong significant associations were identified with the main virulence factors associated with ExPEC (detailed in Table 27) causing BSIs from a urinary source of infection versus all other sources ($p < 0.00001$). Comparisons between virulence factors in Table 29 individually with urinary source of infection revealed significant associations with all the main BSI-associated virulence factors, excluding brain microvascular endothelium invasion (*ibeA*) and urinary source. Furthermore, significant associations were identified between ST131 and urinary source for virulence genes *hlyF*, *iutA*, *gyuA*, *iroN* and *kpsmt*. These results align with the hypothesis that *E. coli* causing BSIs with urinary source harbour more virulence genes than other sources as high pathogenicity is required for ascension in the urinary tract and entry into the bloodstream. This is even observed for ST131, which was shown in results chapter 1 to be biased towards urinary source than other sources. Analysis on associations between virulence and source of infection can guide appropriate use of antimicrobial therapy and may provide a more comprehensive understanding of the severity of infection.

In results chapter 4, comparisons between *in silico* based and phenotypic detection of AMR were conducted. The overall genotypic-phenotypic concordance for BL/BLIs were 65%, nevertheless, a range from 95%-98% was observed for 3GCs. The concordance was diverse across different bioinformatics tools, with the greatest F1 score observed for the detection of resistance to cefotaxime in *E. coli*. In contrast with this, findings in results Chapter 4 revealed no detection of critical errors using ARIBA for the detection of resistance to ciprofloxacin. Evaluation of the current bioinformatics tools used in understanding AMR mechanisms in bacterial genomics is imperative and highlights the importance of monitoring the accuracy metrics. This data will provide insight into specific improvements that are required, in order for WGS to be used exclusively in clinical settings in the future. Investigations into the critical errors observed in key antimicrobials can contribute towards better empiric antimicrobial therapy. Findings from Chapter 4 demonstrate the majority of critical errors for 3GC-R solved through PCR and utilising the new tool (The Hound) developed in the group by Carlos Reding Roman (Reding et al, 2023). Current knowledge in research utilising both genomics and phenotypic methods in addition to findings from Results Chapter 4, indicate phenotypic methods are more suitable for determining empiric antimicrobial treatment for patients. However, this does not provide useful epidemiological information and there is a delay between collecting a blood sample, isolation of bacteria from blood cultures (if the culture is positive) and characterisation of the AMR profiles. WGS provides quicker turnaround times and improves species identification, nevertheless, optimisation of sequencing data using bioinformatic tools is still required to provide results with great accuracy. It is essential for consistent updates to databases utilised by bioinformatics tools in AMR detection. Time is required for identification of particular SNPs causing resistance and detection novel phenotypes

contributing to the detection of false positives, resulting in constant curation of databases. Thus, development of novel computational methodologies to detect novel phenotypes will continually be indeterminable. Lastly, the variety of annotation tools available, some with their own reference databases can also contribute towards the discrepancies observed in genotypes. This emphasises the need for the development of one global reference database as reference to reduce the diversity in discrepancies reported in literature.

This study has several limitations, one of which involves the collection of all Gram-negative BSI in 2020 from Severn Pathology, however, funding limitations resulted in sequencing the most common bacterial species responsible for BSIs. For comparisons in population dynamics and resistance between 2018 and 2020 for BSIs, only 3GC-R isolates in 2020 were taken forwards for analysis. This was due to the fact that prior to starting this study in 2020, isolates in 2018 were collected based on 3GC-R. The comparisons in population dynamics and resistance between 2018 and 2020 UTI could only be carried out between September and October as collection for UTI in 2020 occurred between this time period. Another limitation involves the sparsity of clinical data provided detailing the number of deaths from infection and antibiotic history. This data, in combination with genomic analysis may have provided insight into how AMR mechanisms developed overtime and understand the linkage between first and second line empiric antimicrobial therapy.

Future work involves investigating how the combination of incidence, source of infection, AMR and virulence influence mortality rates and affect patient outcomes. Additionally, due to the increased accessibility to genomic datasets, machine learning techniques can be applied to investigate reemerging resistant pathogens and prediction

of the convergence of virulence and AMR plasmids. Lastly, whilst this study focused on de-duplicated isolates, future work could involve focusing on isolates from same patients with BSIs over a range of time periods, in order to investigate the genetic basis behind the persistence in infection.

7.2 Conclusion

As antibiotic efficacy and treatment options decrease, the implementation of WGS is important for the mitigation and monitoring of AMR, which is inextricably associated with antibiotic prescribing. This study demonstrates that *in silico* detection and characterisation of AMR via WGS to inform empiric therapy is still in its infancy. The wealth of genomic data has enabled the development of multiple computational methodologies for the identification and prediction of emerging and existing MDR bacteria. However, as shown in this study, there will always be limitations causing a reduction in accuracy metrics for these computational methodologies. Nevertheless, this study emphasises the importance for genomic surveillance of resistant UTI or BSI pathogens and their association with source of infection, as this study demonstrated linkage between resistance to first line empiric antimicrobial choices and urinary source of infection. Moreover, understanding the interplay between virulence, AMR and plasmids provides further clarity on mechanisms by which resistance can spread between wards. All these factors facilitate better IPC and enable clinicians to tailor empiric choices to the circulating AMR patterns in each specific patient group.

8.0 References

- Abdulkareem, M., Abdulrahman, M. & Yassin, N. (2023). Molecular detection of plasmid-mediated quinolone resistance genes among clinical isolates of *Klebsiella pneumoniae* during COVID-19 pandemic. *Pharmacia*, 70(1), 225-231.
- Adams-Sapper, S., Diep, B. A., Perdreau-Remington, F., & Riley, L. W. (2013). Clonal composition and community clustering of drug-susceptible and -resistant *Escherichia coli* isolates from bloodstream infections. *Antimicrobial agents and chemotherapy*, 57(1), 490–497.
- Advani, S., Reich, N. G., Sengupta, A., Gosey, L., & Milstone, A. M. (2011). Central line-associated bloodstream infection in hospitalized children with peripherally inserted central venous catheters: extending risk analyses outside the intensive care unit. *Clinical infectious diseases : an official publication of the Infectious Diseases Society of America*, 52(9), 1108–1115.
- Ahmed, H. *et al.* (2019) 'Choice of empirical antibiotic therapy and adverse outcomes in older adults with suspected urinary tract infection: Cohort study', *Open Forum Infectious Diseases*, 6(3). 1-6
- Alcock, B. P., Raphenya, A. R., Lau, T. T. Y., Tsang, K. K., Bouchard, M., Edalatmand, A., *et al.* (2020). CARD 2020: antibiotic resistome surveillance with the comprehensive antibiotic resistance database. *Nucleic acids research*, 48(D1), D517–D525.
- Al-Baloushi, A. E., Pál, T., Ghazawi, A., & Sonnevend, A. (2018). Genetic support of carbapenemases in double carbapenemase producer *Klebsiella pneumoniae* isolated in the Arabian Peninsula. *Acta microbiologica et immunologica Hungarica*, 65(2), 135–150.
- Al-Hasan, M. N., Lahr, B. D., Eckel-Passow, J. E., & Baddour, L. M. (2010). Epidemiology and outcome of *Klebsiella* species bloodstream infection: a population-based study. *Mayo Clinic proceedings*, 85(2), 139–144.
- Al-Sheboul, S. A., Al-Madi, G. S., Brown, B., & Hayajneh, W. A. (2023). Prevalence of Extended-Spectrum β -Lactamases in Multidrug-Resistant *Klebsiella pneumoniae* Isolates in Jordanian Hospitals. *Journal of epidemiology and global health*, 13(2), 180–190.
- Aldawood, E., & Roberts, I. S. (2022). Regulation of *Escherichia coli* Group 2 Capsule Gene Expression: A Mini Review and Update. *Frontiers in microbiology*, 13, 858767.
- Alhashash, F., Wang, X., Paszkiewicz, K., Diggle, M., Zong, Z., & McNally, A. (2016). Increase in bacteraemia cases in the East Midlands region of the UK due to MDR *Escherichia coli* ST73: high levels of genomic and plasmid diversity in causative isolates. *The Journal of antimicrobial chemotherapy*, 71(2), 339–343.
- Ali, I., Rafeque, Z., Ahmed, I., Tariq, F., Graham, S. E., Salzman, E., *et al.* (2019). Phylogeny, sequence-typing and virulence profile of uropathogenic *Escherichia coli* (UPEC) strains from Pakistan. *BMC infectious diseases*, 19(1), 620.
- Alikhan, N. F., Petty, N. K., Ben Zakour, N. L., & Beatson, S. A. (2011). BLAST Ring Image Generator (BRIG): simple prokaryote genome comparisons. *BMC genomics*, 12, 402.

- Alghoribi, M. F., Gibreel, T. M., Farnham, G., Al Johani, S. M., Balkhy, H. H., & Upton, M. (2015). Antibiotic-resistant ST38, ST131 and ST405 strains are the leading uropathogenic *Escherichia coli* clones in Riyadh, Saudi Arabia. *The Journal of antimicrobial chemotherapy*, 70(10), 2757–2762.
- Allegretti, Y., Yamaji, R., Adams-Sapper, S. & Riley, L. (2022). Genetic features of antimicrobial drug-susceptible extraintestinal pathogenic *Escherichia coli* pandemic sequence type 95. Available from: <https://doi.org/10.1101/2021.10.28.466352>. Accessed 29.03.2023
- Alzayn, M., Dulyayangkul, P., Satapoomin, N., Heesom, K. J., & Avison, M. B. (2021). OmpF Downregulation Mediated by Sigma E or OmpR Activation Confers Cefalexin Resistance in *Escherichia coli* in the Absence of Acquired β -Lactamases. *Antimicrobial agents and chemotherapy*, 65(11), e0100421.
- Amabile de Campos, T. A., de Almeida, F. M., de Almeida, A. P. C., Nakamura-Silva, R., Oliveira-Silva, M., de Sousa, I. F. A., Cerdeira, L., et al. (2021). Multidrug-Resistant (MDR) *Klebsiella variicola* Strains Isolated in a Brazilian Hospital Belong to New Clones. *Frontiers in microbiology*, 12, 604031.
- Anderson, D. J., Richet, H., Chen, L. F., Spelman, D. W., Hung, Y. J., Huang, A. Tet al. (2008). Seasonal variation in *Klebsiella pneumoniae* bloodstream infection on 4 continents. *The Journal of infectious diseases*, 197(5), 752–756
- Andriole V. T. (2005). The quinolones: past, present, and future. *Clinical infectious diseases : an official publication of the Infectious Diseases Society of America*, 41 Suppl 2, S113–S119.
- Arca-Suárez, J., Rodiño-Janeiro, B. K., Pérez, A., Guijarro-Sánchez, P., Vázquez-Ucha, J. C., Cruz, F., et al. (2022). Emergence of 16S rRNA methyltransferases among carbapenemase-producing Enterobacterales in Spain studied by whole-genome sequencing. *International journal of antimicrobial agents*, 59(1), 106456.
- Arredondo-Alonso, S., Willems, R. J., van Schaik, W., & Schürch, A. C. (2017). On the (im)possibility of reconstructing plasmids from whole-genome short-read sequencing data. *Microbial genomics*, 3(10), e000128.
- Ashurst, J. V., & Dawson, A. (2023). *Klebsiella Pneumonia*. In *StatPearls*. StatPearls Publishing.
- Bader, M., Loeb, M., Leto, D. & Brooks, A. (2019). Treatment of urinary tract infections in the era of antimicrobial resistance and new antimicrobial agents. *Postgraduate Medicine*, 24, 1-17.
- Bankevich, A., Nurk, S., Antipov, D., Gurevich, A., Dvorkin, M., Kulikov, A. et al. 2012. SPAdes: A New Genome Assembly Algorithm and Its Applications to Single-Cell Sequencing. *Journal of Computational Biology*, 19(5), 455-477.
- Bartoletti, R. et al. (2016) Treatment of urinary tract infections and antibiotic stewardship. *European Urology Supplements*, 15(4), 81–87.

- Beghain, J., Bridier-Nahmias, A., Le Nagard, H., Denamur, E., & Clermont, O. (2018). ClermonTyping: an easy-to-use and accurate in silico method for Escherichia genus strain phylotyping. *Microbial genomics*, 4(7), e000192.
- Berbers, B., Saltykova, A., Garcia-Graells, C., Philipp, P., Arella F., Marchal, K. et al. (2020). Combining short and long read sequencing to characterise antimicrobial resistance genes on plasmids applied to an unauthorized genetically modified Bacillus. *Scientific Reports*, 10(4310), 1-13.
- Bevan, E., Jones, A. & Hawkey, P. (2017). Global epidemiology of CTX-M- β -lactamases: temporal and geographical shifts in genotype. *Journal of Antimicrobial Chemotherapy*, 72(8),2145-2155.
- Bialek-Davenet, S., Criscuolo, A., Ailloud, F., Passet, V., Jones, L., et al. (2014). Genomic definition of hypervirulent and multidrug-resistant Klebsiella pneumoniae clonal groups. *Emerging infectious diseases*, 20(11), 1812–1820.
- Biggel, M., Moons, P., Nguyen, M. N., Goossens, H., & Van Puyvelde, S. (2022). Convergence of virulence and antimicrobial resistance in increasingly prevalent Escherichia coli ST131 papGII+ sublineages. *Communications biology*, 5(1), 752.
- Birgy, A., Madhi, F., Jung, C., Levy, C., Cointe, A., Bidet, P. et al. (2020). Diversity and trends in population structure of ESBL-producing Enterobacteriaceae in febrile urinary tract infections in children in France from 2014 to 2017. *The Journal of antimicrobial chemotherapy*, 75(1), 96–105.
- Bischoff, S., Walter, T., Gerigk, M., Ebert, M. & Vogelmann, R. (2018). Empirical antibiotic therapy in urinary tract infection in patients with risk factors for antibiotic resistance in a German emergency department. *BMC Infectious Disease*, 18(1), 56
- Blanco, J., Mora, A., Mamani, R., López, C., Blanco, M., Dahbi, G., et al. (2011). National survey of Escherichia coli causing extraintestinal infections reveals the spread of drug-resistant clonal groups O25b:H4-B2-ST131, O15:H1-D-ST393 and CGA-D-ST69 with high virulence gene content in Spain. *The Journal of antimicrobial chemotherapy*, 66(9), 2011–2021.
- Blot, K., Hammami, N., Blot, S., Vogelaers, D., & Lambert, M. L. (2022). Seasonal variation of hospital-acquired bloodstream infections: A national cohort study. *Infection control and hospital epidemiology*, 43(2), 205–211.
- Blunt, I. 2013. Focus on preventable admissions. Trends in emergency admissions for ambulatory care sensitive conditions, 2001 to 2013. Available from: https://www.health.org.uk/sites/default/files/QualityWatch_FocusOnPreventableAdmissions.pdf. Accessed 17/01/2022
- Bodendoerfer, E., Marchesi, M., Imkamp, F., Courvalin, P., Böttger, E. C., & Mancini, S. (2020). Co-occurrence of aminoglycoside and β -lactam resistance mechanisms in aminoglycoside-non-susceptible Escherichia coli isolated in the Zurich area, Switzerland. *International journal of antimicrobial agents*, 56(1), 106019.
- Bolger, A., Lohse, M. & Usadel, B. (2014). Trimmomatic: a flexible trimmer for Illumina sequencing data. *Bioinformatics*, 30(15), 2114-2120.

Bonacorsi, S. & Bingen, E. (2005). Molecular epidemiology of escherichia coli causing neonatal meningitis. *International Journal of Medical Microbiology*, 295(6–7), 373–381.

Bonkat G, Pickard R, Bartoletti R, Bruyère F, Geerlings SE, Wagenlehner F, Wullt B. 2017. *Guidelines on urological infections [Internet]*. Arnhem (The Netherlands): European Association of Urology; Available from <https://uroweb.org/wp-content/uploads/Urological-Infections-2017-pocket.pdf>. Accessed 28.03.2022

Bortolaia, V., Kaas, R. S., Ruppe, E., Roberts, M. C., Schwarz, S., Cattoir, V., et al. (2020). ResFinder 4.0 for predictions of phenotypes from genotypes. *The Journal of antimicrobial chemotherapy*, 75(12), 3491–3500.

Boucher, H. W., Talbot, G. H., Bradley, J. S., Edwards, J. E., Gilbert, D., Rice, L. B., et al. (2009). Bad bugs, no drugs: no ESKAPE! An update from the Infectious Diseases Society of America. *Clinical infectious diseases : an official publication of the Infectious Diseases Society of America*, 48(1), 1–12.

Bowers, J. R., Kitchel, B., Driebe, E. M., MacCannell, D. R., Roe, C., Lemmer, D., et al. (2015). Genomic Analysis of the Emergence and Rapid Global Dissemination of the Clonal Group 258 *Klebsiella pneumoniae* Pandemic. *PloS one*, 10(7), e0133727.

Bozcal, E., Eldem, V., Aydemir, S., & Skurnik, M. (2018). The relationship between phylogenetic classification, virulence and antibiotic resistance of extraintestinal pathogenic *Escherichia coli* in İzmir province, Turkey. *PeerJ*, 6, e5470.

Breurec, S., Guessennd, N., Timinouni, M., Le, T. A., Cao, V., Ngandjio, A., et al. (2013). *Klebsiella pneumoniae* resistant to third-generation cephalosporins in five African and two Vietnamese major towns: multiclonal population structure with two major international clonal groups, CG15 and CG258. *Clinical microbiology and infection : the official publication of the European Society of Clinical Microbiology and Infectious Diseases*, 19(4), 349–355.

Brighty KE, Gootz TD. Andriole VT. Chemistry and mechanism of action of the quinolone antibacterials, *The quinolones*, 20003rd ed. San Diego Academic Press(33-97)

Brisse, S., Passet, V., & Grimont, P. A. D. (2014). Description of *Klebsiella quasipneumoniae* sp. nov., isolated from human infections, with two subspecies, *Klebsiella quasipneumoniae* subsp. *quasipneumoniae* subsp. nov. and *Klebsiella quasipneumoniae* subsp. *similipneumoniae* subsp. nov., and demonstration that *Klebsiella singaporensis* is a junior heterotypic synonym of *Klebsiella variicola*. *International journal of systematic and evolutionary microbiology*, 64(Pt 9), 3146–3152.

Brouwer, M. S. M., Zandbergen Van Essen, A., Kant, A., Rapallini, M., Harders, F., Bossers, A. et al. (2023). Implementation of WGS analysis of ESBL-producing *Escherichia coli* within EU AMR monitoring in livestock and meat. *The Journal of antimicrobial chemotherapy*, 78(7), 1701–1704.

Brumwell, A., Sutton, G., Lantos, P. M., Hoffman, K., Ruffin, F., Brinkac, L., et al. (2023). *Escherichia coli* ST131 Associated with Increased Mortality in Bloodstream Infections from Urinary Tract Source. *Journal of clinical microbiology*, 61(7), e0019923.

Bush, K., & Jacoby, G. A. (2010). Updated functional classification of beta-lactamases. *Antimicrobial agents and chemotherapy*, 54(3), 969–976.

- Campos-Madueno, E. I., Moser, A. I., Risch, M., Bodmer, T., & Endimiani, A. (2021). Exploring the Global Spread of *Klebsiella grimontii* Isolates Possessing *bla*_{VIM-1} and *mcr-9*. *Antimicrobial agents and chemotherapy*, *65*(9), e0072421.
- Carattoli, A., Zankari, E., Garcia-Fernandez, A., Voldby, M., Lund, O., Villa, L. et al. (2014). PlasmidFinder and pMLST: in silico detection and typing of plasmids. *Antimicrobial Agents Chemotherapy*, *58*(7), 3895-3903.
- CDC. 2019. Antibiotic resistance threats in the United States. Available from: <https://www.cdc.gov/drugresistance/pdf/threats-report/2019-ar-threats-report-508.pdf>. Accessed 23.03.2023
- Chan, J., Pallen, M., Oppenheim, B. & Constantinidou, C. (2012). Genome sequencing in clinical microbiology. *Nature Biotechnology*, *30*(11), 1068-1071
- Chattaway, M. A., Jenkins, C., Ciesielczuk, H., Day, M., DoNascimento, V., Day, M., et al. (2014). Evidence of evolving extraintestinal enteroaggregative *Escherichia coli* ST38 clone. *Emerging infectious diseases*, *20*(11), 1935–1937.
- Chetri, S., Bhowmik, D., Paul, D., Pandey, P., Chanda, D. D., Chakravarty, A., et al. (2019). AcrAB-TolC efflux pump system plays a role in carbapenem non-susceptibility in *Escherichia coli*. *BMC microbiology*, *19*(1), 210.
- Cheung, C. H. P., Alorabi, M., Hamilton, F., Takebayashi, Y., Mounsey, O., Heesom, K. J., Williams, P. B., Williams, O. M., Albur, M., MacGowan, A. P., & Avison, M. B. (2021). Trade-Offs between Antibacterial Resistance and Fitness Cost in the Production of Metallo-β-Lactamases by Enteric Bacteria Manifest as Sporadic Emergence of Carbapenem Resistance in a Clinical Setting. *Antimicrobial agents and chemotherapy*, *65*(8), e0241220.
- Chi, X., Meng, X., Xiong, L., Chen, T., Zhou, Y., Ji, J., et al. (2022). Small wards in the ICU: a favorable measure for controlling the transmission of carbapenem-resistant *Klebsiella pneumoniae*. *Intensive care medicine*, *48*(11), 1573–1581.
- Chin, T. L., MacGowan, A. P., Bowker, K. E., Elder, F., Beck, C. R., & McNulty, C. (2015). Prevalence of antibiotic resistance in *Escherichia coli* isolated from urine samples routinely referred by general practitioners in a large urban centre in south-west England. *The Journal of antimicrobial chemotherapy*, *70*(7), 2167–2169.
- Clinical and Laboratory Standards Institute. *M07: Methods for Dilution Antimicrobial Susceptibility Tests for Bacteria that Grow Aerobically*, 11th ed.; Clinical and Laboratory Standards Institute: Wayne, PA, USA, 2018; ISBN 1562388363.
- CLSI. *Performance standards for antimicrobial susceptibility testing, 31st edition: M100, 2021*.
- Cortes-Penfield, N. W., Trautner, B. W., & Jump, R. L. P. (2017). Urinary tract infection and asymptomatic bacteriuria in older adults. *Infectious Disease Clinics of North America*, *31*(4), 673–688.
- Croucher, N., Page, A., Connor, T., Delaney, A., Keane, J., Bentley, S. et al. (2015). Rapid phylogenetic analysis of large samples of recombinant bacterial whole genome sequences using Gubbins. *Nucleic Acids Research*, *43*(3), 15.
- Cummins, M. L., Reid, C. J., & Djordjevic, S. P. (2022). F Plasmid Lineages in *Escherichia coli* ST95: Implications for Host Range, Antibiotic Resistance, and Zoonoses. *mSystems*, *7*(1), e0121221.

Cunha, M. P. V., Saldenberg, A. B., Moreno, A. M., Ferreira, A. J. P., Vieira, M. A. M., Gomes, T. A. T. et al. (2017). Pandemic extra-intestinal pathogenic *Escherichia coli* (ExPEC) clonal group O6-B2-ST73 as a cause of avian colibacillosis in Brazil. *PloS one*, 12(6), e0178970.

Daga, A.P. et al. (2019). *Escherichia coli* bloodstream infections in patients at a university hospital: Virulence factors and clinical characteristics, *Frontiers in Cellular and Infection Microbiology*, 9.

Dahbi, G., Mora, A., López, C., Alonso, M. P., Mamani, R., Marzoa, J., Coira, A., García-Garrote, F., Pita, J. M., Velasco, D., Herrera, A., Viso, S., Blanco, J. E., Blanco, M., & Blanco, J. (2013). Emergence of new variants of ST131 clonal group among extraintestinal pathogenic *Escherichia coli* producing extended-spectrum β -lactamases. *International journal of antimicrobial agents*, 42(4), 347–351.

Dale, A. P., & Woodford, N. (2015). Extra-intestinal pathogenic *Escherichia coli* (ExPEC): Disease, carriage and clones. *The Journal of infection*, 71(6), 615–626.

Darling, A. C., Mau, B., Blattner, F. R., & Perna, N. T. (2004). Mauve: multiple alignment of conserved genomic sequence with rearrangements. *Genome research*, 14(7), 1394–1403.

Das, N., Madhavan, J., Selvi, A., & Das, D. (2019). An overview of cephalosporin antibiotics as emerging contaminants: a serious environmental concern. *3 Biotech*, 9(6), 231

Davido, B., Noussair, L., Saleh-Mghir, Salomon, E., Bouchand, F., Matt, M., et al. (2020). Case series of carbapenemase-producing Enterobacteriaceae osteomyelitis: Feel it in your bones. *Journal of Global Antimicrobial Resistance*, 23, 74-78.

Davies, T. J., Stoesser, N., Sheppard, A. E., Abuoun, M., Fowler, P., Swann, J., et al. (2020). Reconciling the Potentially Irreconcilable? Genotypic and Phenotypic Amoxicillin-Clavulanate Resistance in *Escherichia coli*. *Antimicrobial agents and chemotherapy*, 64(6), e02026-19.

Day, M. J., Doumith, M., Abernethy, J., Hope, R., Reynolds, R., Wain, J., et al. (2016). Population structure of *Escherichia coli* causing bacteraemia in the UK and Ireland between 2001 and 2010. *The Journal of antimicrobial chemotherapy*, 71(8), 2139–2142.

Deekshit, V. K., Kumar, B. K., Rai, P., Srikumar, S., Karunasagar, I., & Karunasagar, I. (2012). Detection of class 1 integrons in *Salmonella* Weltevreden and silent antibiotic resistance genes in some seafood-associated nontyphoidal isolates of *Salmonella* in south-west coast of India. *Journal of applied microbiology*, 112(6), 1113–1122.

Deen, J., Von Seidlein, L., Andersen, F., Elle, N., White, J. & Lubell, Y. (2012). Community-acquired bacterial bloodstream infections in developing countries in South and Southeast Asia: a systematic review. *Lancet Infectious Diseases*, 12(6), 480-487.

Deeny, S. R., van Kleef, E., Bou-Antoun, S., Hope, R. J., & Robotham, J. V. (2015). Seasonal changes in the incidence of *Escherichia coli* bloodstream infection: variation with region and place of onset. *Clinical microbiology and infection : the official publication of the European Society of Clinical Microbiology and Infectious Diseases*, 21(10), 924–929.

Deltourbe, L., Lacerda Mariano, L., Hreha, T.N., Hunstad, D. & Ingersoll, M. (2022) The impact of biological sex on diseases of the urinary tract. *0Mucosal Immunology*, 15(5), pp. 857–866.

- Denamur, E., Condamine, B., Esposito-Farèse, M., Royer, G., Clermon, O., Laouenan, C. *et al.* (2022). Genome wide association study of escherichia coli bloodstream infection isolates identifies genetic determinants for the portal of entry but not fatal outcome. *PLOS Genetics*, 18(3).
- Denamur, E., Clermont, O., Bonacorsi, S., & Gordon, D. (2021). The population genetics of pathogenic Escherichia coli. *Nature reviews. Microbiology*, 19(1), 37–54.
- Dhanji, H., Doumith, M., Rooney, P. J., O'Leary, M. C., Loughrey, A. C., Hope, R., Woodford, N., & Livermore, D. M. (2011). Molecular epidemiology of fluoroquinolone-resistant ST131 Escherichia coli producing CTX-M extended-spectrum beta-lactamases in nursing homes in Belfast, UK. *The Journal of antimicrobial chemotherapy*, 66(2), 297–303.
- Diancourt, L., Passet, V., Verhoef, J., Grimont, P. A., & Brisse, S. (2005). Multilocus sequence typing of Klebsiella pneumoniae nosocomial isolates. *Journal of clinical microbiology*, 43(8), 4178–4182.
- Diestra, K., Juan, C., Curiao, T., Moyá, B., Miró, E., Oteo, J., *et al.* (2009). Characterization of plasmids encoding blaESBL and surrounding genes in Spanish clinical isolates of Escherichia coli and Klebsiella pneumoniae. *The Journal of antimicrobial chemotherapy*, 63(1), 60–66.
- Din, A. a. M. N. E., Harfoush, R. a. H., Okasha, H., & Kholeif, D. a. E. S. (2016). Study of OmpK35 and OmpK36 Expression in Carbapenem Resistant ESBL Producing Clinical Isolates of Klebsiella pneumoniae. *Advances in Microbiology*, 06(09), 662–670.
- D'Onofrio, V., Cartuyvels, R., Messiaen, P. E. A., Barišić, I., & Gyssens, I. C. (2023). Virulence Factor Genes in Invasive *Escherichia coli* Are Associated with Clinical Outcomes and Disease Severity in Patients with Sepsis: A Prospective Observational Cohort Study. *Microorganisms*, 11(7), 1827.
- Dong, N., Yang, X., Chan, E. W., Zhang, R., & Chen, S. (2022). Klebsiella species: Taxonomy, hypervirulence and multidrug resistance. *EBioMedicine*, 79, 103998.
- Dong, N., Zhang, R., Liu, L., Li, R., Lin, D., Chan, E. W., & Chen, S. (2018). Genome analysis of clinical multilocus sequence Type 11 Klebsiella pneumoniae from China. *Microbial genomics*, 4(2), e000149.
- Doumith, M., Day, M., Ciesielczuk, H., Hope, R., Underwood, A., Reynolds, R. *et al.* (2015). Rapid identification of major Escherichia coli sequence types causing urinary tract and bloodstream infections. *Journal of Clinical Microbiology*, 53(1), 160-166.
- Dropa, M., Lincopan, N., Balsalobre, L. C., Oliveira, D. E., Moura, R. A., Fernandes, M. R., *et al.* (2016). Genetic background of novel sequence types of CTX-M-8-and CTX-M-15-producing Escherichia coli and Klebsiella pneumoniae from public wastewater treatment plants in São Paulo, Brazil. *Environmental science and pollution research international*, 23(5), 4953–4958.
- Dulyayangkul, P., Douglas, E. J. A., Lastovka, F., & Avison, M. B. (2020). Resistance to Ceftazidime/Avibactam plus Meropenem/Vaborbactam When Both Are Used Together Is Achieved in Four Steps in Metallo- β -Lactamase-Negative Klebsiella pneumoniae. *Antimicrobial agents and chemotherapy*, 64(10), e00409-20.

Effah, C. Y., Sun, T., Liu, S., & Wu, Y. (2020). *Klebsiella pneumoniae*: an increasing threat to public health. *Annals of clinical microbiology and antimicrobials*, 19(1), 1.

Elankumaran, P., Browning, G. F., Marendra, M. S., Reid, C. J., & Djordjevic, S. P. (2022). Close genetic linkage between human and companion animal extraintestinal pathogenic *Escherichia coli* ST127. *Current research in microbial sciences*, 3, 100106.

Ellington, M.J., Ekelund, O., Aarestrup, F.M., Canton, R., Doumith, M., Giske, C. et al. (2017). The role of whole genome sequencing in antimicrobial susceptibility testing of bacteria: report from the EUCAST Subcommittee. *Clinical Microbiology and Infection*, 23(1), 2-22.

El-Shaboury, S. R., Saleh, G. A., Mohamed, F. A., & Rageh, A. H. (2007). Analysis of cephalosporin antibiotics. *Journal of pharmaceutical and biomedical analysis*, 45(1), 1–19.

Ejaz H. (2022). Analysis of diverse β -lactamases presenting high-level resistance in association with OmpK35 and OmpK36 porins in ESBL-producing *Klebsiella pneumoniae*. *Saudi journal of biological sciences*, 29(5), 3440–3447.

Espinal, P., Nucleo, E., Caltagirone, M., Mattioni Marchetti, V., Fernandes, M. R., Biscaro, V., et al. (2019). Genomics of *Klebsiella pneumoniae* ST16 producing NDM-1, CTX-M-15, and OXA-232. *Clinical microbiology and infection : the official publication of the European Society of Clinical Microbiology and Infectious Diseases*, 25(3), 385.e1–385.e5.

EUCAST (The European Committee on Antimicrobial Susceptibility Testing). Breakpoint Tables for Interpretation of MICs and Zone Diameters, Version 12.0. Available online: http://www.eucast.org/clinical_breakpoints/ (accessed on 23 February 2022).

European Centre for Disease Prevention and Control. (2019). Surveillance of antimicrobial resistance in Europe 2018. *Stockholm: ECDC*

FarajzadehSheikh, A., Veisi, H., Shahin, M., Getso, M., & Farahani, A. (2019). Frequency of quinolone resistance genes among extended-spectrum β -lactamase (ESBL)-producing *Escherichia coli* strains isolated from urinary tract infections. *Tropical medicine and health*, 47, 19.

Feil, E. J., Li, B. C., Aanensen, D. M., Hanage, W. P., & Spratt, B. G. (2004). eBURST: inferring patterns of evolutionary descent among clusters of related bacterial genotypes from multilocus sequence typing data. *Journal of bacteriology*, 186(5), 1518–1530.

Feldgarden, M., Brover, V., Haft, D. H., Prasad, A. B., Slotta, D. J., Tolstoy, I., et al. (2019). Validating the AMRFinder Tool and Resistance Gene Database by Using Antimicrobial Resistance Genotype-Phenotype Correlations in a Collection of Isolates. *Antimicrobial agents and chemotherapy*, 63(11), e00483-19.

Felman, S., Temkin, E., Wulffhart, L., Nutman, A., Schechner, V., Shitrit, P. et al. (2022). Effect of temperature on *Escherichia coli* bloodstream infection in a nationwide population-based study of incidence and resistance. *Antimicrobial Resistance and Infection Control*, 11(1), 144.

Findlay, J., Gould, V. C., North, P., Bowker, K. E., Williams, M. O., MacGowan, A. P., & Avison, M. B. (2020). Characterization of cefotaxime-resistant urinary *Escherichia coli* from primary care in South-West England 2017-18. *The Journal of antimicrobial chemotherapy*, 75(1), 65–71.

- Findlay, J., Hopkins, K. L., Loy, R., Doumith, M., Meunier, D., Hill, R., Pike, R., Mustafa, N., Livermore, D. M., & Woodford, N. (2017). OXA-48-like carbapenemases in the UK: an analysis of isolates and cases from 2007 to 2014. *The Journal of antimicrobial chemotherapy*, *72*(5), 1340–1349.
- Flament-Simon, S. C., García, V., Duprilot, M., Mayer, N., Alonso, M. P., García-Meniño, I., Blanco, J. E., Blanco, M., Nicolas-Chanoine, M. H., & Blanco, J. (2020). High Prevalence of ST131 Subclades C2-H30Rx and C1-M27 Among Extended-Spectrum β -Lactamase-Producing *Escherichia coli* Causing Human Extraintestinal Infections in Patients From Two Hospitals of Spain and France During 2015. *Frontiers in cellular and infection microbiology*, *10*, 125.
- Flores-Mireles, A., Walker, J., Caparon, M. & Hultgren, S. (2015). Urinary tract infections: epidemiology, mechanisms of infection and treatment options. *Nature Reviews Microbiology*, *13*(5), 269-284.
- Flury, B., Ellington, M., Hopkins, K., Turton, J., Doumith, M., Loy, R. et al. (2016). Association of Novel nonsynonymous Single Nucleotide Polymorphisms in *ampD* with Cephalosporin Resistance and Phylogenetic Variations in *ampC*, *ampR*, *ompF*, and *ompC* in *Enterobacteria cloacae* isolates that are highly resistant to carbapenems. *Antimicrobial Agents Chemotherapy*, *60*(4), 2383-2390.
- Foxman, B. (2002). Epidemiology of urinary tract infections: incidence, morbidity and economic costs. *The American Journal of Medicine*, *113*(1), 5-13
- Fröhlich, C., Sørum, V., Thomassen, A. M., Johnsen, P. J., Leiros, H. S., & Samuelsen, Ø. (2019). OXA-48-Mediated Ceftazidime-Avibactam Resistance Is Associated with Evolutionary Trade-Offs. *mSphere*, *4*(2), e00024-19.
- Gajic, I., Kabic, J., Kekic, D., Jovicevic, M., Milenkovic, M. et al. (2022). Antimicrobial Susceptibility Testing: A Comprehensive Review of Currently Used Methods. *Antibiotics (Basel, Switzerland)*, *11*(4), 427.
- García-Meniño, I., Lumbreras, P., Lestón, L., Álvarez-Álvarez, M., García, V., Hammerl, J. A., Fernández, J., & Mora, A. (2022). Occurrence and Genomic Characterization of Clone ST1193 Clonotype 14-64 in Uncomplicated Urinary Tract Infections Caused by *Escherichia coli* in Spain. *Microbiology spectrum*, *10*(3), e0004122.
- Garofalo, C. K., Hooton, T. M., Martin, S. M., Stamm, W. E., Palermo, J. J., Gordon, J. I., et al. (2007). *Escherichia coli* from urine of female patients with urinary tract infections is competent for intracellular bacterial community formation. *Infection and immunity*, *75*(1), 52–60.
- Gibreel, T., Dodgson, A., Cheesbrough, J., Fox, A., Bolton, F., & Upton, M. (2012). Population structure, virulence potential and antibiotic susceptibility of uropathogenic *Escherichia coli* from Northwest England. *Journal of Antimicrobial Chemotherapy*, *67*(2) 346-356
- Gilchrist, C. L. M., & Chooi, Y. H. (2021). clinker & clustermap.js: automatic generation of gene cluster comparison figures. *Bioinformatics (Oxford, England)*, *37*(16), 2473–2475.
- Global Burden of Disease Study 2013 Collaborators. 2015. Global, regional, and national incidence, prevalence, and years lived with disability for 301 acute and chronic diseases and injuries in 188 countries, 1990-2013: a systemic analysis for the Global Burden of Disease Study 2013. *The Lancet*, *386*(9995), 743-800.

- Gonullu, N., Aktas, Z., Kayacan, C. B., Salcioglu, M., Carattoli, A., Yong, D. E., et al. (2008). Dissemination of CTX-M-15 beta-lactamase genes carried on Inc FI and FII plasmids among clinical isolates of *Escherichia coli* in a university hospital in Istanbul, Turkey. *Journal of clinical microbiology*, 46(3), 1110–1112.
- González-López, J. J., Coelho, A., Larrosa, M. N., Lavilla, S., Bartolomé, R., & Prats, G. (2009). First detection of plasmid-encoded bla_{OXY} beta-lactamase. *Antimicrobial agents and chemotherapy*, 53(7), 3143–3146.
- Goto, M. & Al-Hasan, M. (2013). Overall burden of bloodstream infection and nosocomial bloodstream infection in North America and Europe. *Clinical Microbiology and Infection*, 19(6), 501-509.
- Grabe, M., Bartoletti, R., Bjerklund Johansen, E., Cai, T., Cek, M., Koves, B. et al. (2015). Urological infections. European Association of Urology: Elsevier: 641-646.
- Gradel, K. O., Nielsen, S. L., Pedersen, C., Knudsen, J. D., Østergaard, C., Arpi, M., et al. (2016). Seasonal Variation of *Escherichia coli*, *Staphylococcus aureus*, and *Streptococcus pneumoniae* Bacteremia According to Acquisition and Patient Characteristics: A Population-Based Study. *Infection control and hospital epidemiology*, 37(8), 946–953.
- Greig, D. R., Dallman, T. J., Hopkins, K. L., & Jenkins, C. (2018). MinION nanopore sequencing identifies the position and structure of bacterial antibiotic resistance determinants in a multidrug-resistant strain of enteroaggregative *Escherichia coli*. *Microbial genomics*, 4(10), e000213.
- Grubaugh, N. D., Faria, N. R., Andersen, K. G., & Pybus, O. G. (2018). Genomic Insights into Zika Virus Emergence and Spread. *Cell*, 172(6), 1160–1162.
- Guo, Q., Spychala, C. N., McElheny, C. L., & Doi, Y. (2016). Comparative analysis of an IncR plasmid carrying armA, bla_{DHA-1} and qnrB4 from *Klebsiella pneumoniae* ST37 isolates. *The Journal of antimicrobial chemotherapy*, 71(4), 882–886.
- Gupta K, Sahm D, Mayfield D & Stamm W. 2001. Antimicrobial resistance among uropathogens that cause community-acquired urinary tract infections in women: a nationwide analysis. *Clinical Infectious Diseases*, 33(1), 89-94.
- Hagan, E.C. & Mobley, H.L. (2007). Uropathogenic *escherichia coli* outer membrane antigens expressed during urinary tract infection. *Infection and Immunity*, 75(8), 3941–3949. doi:10.1128/iai.00337-07.
- Hansen, D. S., Aucken, H. M., Abiola, T., & Podschun, R. (2004). Recommended test panel for differentiation of *Klebsiella* species on the basis of a trilateral interlaboratory evaluation of 18 biochemical tests. *Journal of clinical microbiology*, 42(8), 3665–3669.
- Harada, K., Shimizu, T., Mukai, Y., Kuwajima, K., Sato, T., Usui, M., et al. (2016). Phenotypic and Molecular Characterization of Antimicrobial Resistance in *Klebsiella* spp. Isolates from Companion Animals in Japan: Clonal Dissemination of Multidrug-Resistant Extended-Spectrum β -Lactamase-Producing *Klebsiella pneumoniae*. *Frontiers in microbiology*, 7, 1021.
- Harmer, C. J., Pong, C. H., & Hall, R. M. (2020). Structures bounded by directly-oriented members of the IS26 family are pseudo-compound transposons. *Plasmid*, 111, 102530.
- Hawkey, J. et al. (2022) 'ESBL plasmids in *Klebsiella pneumoniae*: Diversity, transmission and contribution to infection burden in the hospital setting', *Genome Medicine*, 14(1).

- He, R., Yang, Y., Wu, Y., Zhong, L. L., Yang, Y., Chen, G., et al. (2021). Characterization of a Plasmid-Encoded Resistance-Nodulation-Division Efflux Pump in *Klebsiella pneumoniae* and *Klebsiella quasipneumoniae* from Patients in China. *Antimicrobial agents and chemotherapy*, 65(2), e02075-20
- Heiden, S. E., Hübner, N. O., Bohnert, J. A., Heidecke, C. D., Kramer, A., Balau, V., et al. (2020). A *Klebsiella pneumoniae* ST307 outbreak clone from Germany demonstrates features of extensive drug resistance, hypermucoviscosity, and enhanced iron acquisition. *Genome medicine*, 12(1), 113.
- Hernández, M., López-Urrutia, L., Abad, D., De Frutos Serna, M., Ocampo-Sosa, A. A., et al. (2021). First Report of an Extensively Drug-Resistant ST23 *Klebsiella pneumoniae* of Capsular Serotype K1 Co-Producing CTX-M-15, OXA-48 and ArmA in Spain. *Antibiotics (Basel, Switzerland)*, 10(2), 157.
- Hooper D. C. (2001). Mechanisms of action of antimicrobials: focus on fluoroquinolones. *Clinical infectious diseases : an official publication of the Infectious Diseases Society of America*, 32 Suppl 1, S9–S15.
- Hooper, D. C., & Jacoby, G. A. (2015). Mechanisms of drug resistance: quinolone resistance. *Annals of the New York Academy of Sciences*, 1354(1), 12–31.
- Hornsey, M., Phee, L., & Wareham, D. W. (2011). A novel variant, NDM-5, of the New Delhi metallo- β -lactamase in a multidrug-resistant *Escherichia coli* ST648 isolate recovered from a patient in the United Kingdom. *Antimicrobial agents and chemotherapy*, 55(12), 5952–5954.
- Horowitz, D. S., & Wang, J. C. (1987). Mapping the active site tyrosine of *Escherichia coli* DNA gyrase. *The Journal of biological chemistry*, 262(11), 5339–5344.
- Hoyos-Mallecot, Y., Riazco, C., Miranda-Casas, C., Rojo-Martín, M. D., Gutiérrez-Fernández, J., & Navarro-Marí, J. M. (2014). Rapid detection and identification of strains carrying carbapenemases directly from positive blood cultures using MALDI-TOF MS. *Journal of microbiological methods*, 105, 98–101.
- Huang, S.H., Wass, C., Prasadarao, N, Stins, M. & Kim, K. (1995). *Escherichia coli* invasion of brain microvascular endothelial cells in vitro and in vivo: Molecular cloning and characterization of invasion gene IBE10. *Infection and Immunity*, 63(11), 4470–4475.
- Huang, J., Zhang, S., Zhang, S., Zhao, Z., Cao, Y., Chen, M., et al. (2020). A Comparative Study of Fluoroquinolone-Resistant *Escherichia coli* Lineages Portrays Indistinguishable Pathogenicity- and Survivability-Associated Phenotypic Characteristics Between ST1193 and ST131. *Infection and drug resistance*, 13, 4167–4175.
- Hughes, J.M., Murad, F., Chang, B. & Guerrant, R.. (1978) 'Role of cyclic GMP in the action of heat-stable enterotoxin of *Escherichia coli*', *Nature*, 271(5647), 755–756.
- Hung, W. T., Cheng, M. F., Tseng, F. C., Chen, Y. S., Shin-Jung Lee, S., Chang, T. H., et al. (2019). Bloodstream infection with extended-spectrum beta-lactamase-producing *Escherichia coli*: The role of virulence genes. *Journal of microbiology, immunology, and infection = Wei mian yu gan ran za zhi*, 52(6), 947–955.

Illiaquer, M., Caroff, N., Bémer, P., Aubin, G. G., Juvin, M. E., Lepelletier, D., et al. (2012). Occurrence and molecular characterization of *Klebsiella pneumoniae* ST37 clinical isolates producing plasmid-mediated AmpC recovered over a 3-year period. *Diagnostic microbiology and infectious disease*, 74(1), 95–97.

Imai, K., Ishibashi, N., Kodana, M., Tarumoto, N., Sakai, J., Kawamura, T. et al. (2019). Clinical characteristics in blood stream infections caused by *Klebsiella pneumoniae*, *Klebsiella variicola*, and *Klebsiella quasipneumoniae*: a comparative study, Japan, 2014–2017. *BMC infectious diseases*, 19(1), 946.

Jacoby G. A. (2009). AmpC beta-lactamases. *Clinical microbiology reviews*, 22(1), 161–182.

Jacoby, G. A. (2005). Mechanisms of Resistance to Quinolones. *Clinical Infectious Diseases*, 41, S120–S126.

Jain, M., Koren, S., Miga, K., Quick, J., Rand, A., Sasani, T. et al. (2018). Nanopore Sequencing and assembly of a human genome with ultra-long reads. *Nature Biotechnology*, 36(4), 338–345.

Jauneikaite, E., Honeyford, K., Blandy, O., Mosavie, M., Pearson, M., Ramzan, F. A. et al. (2022). Bacterial genotypic and patient risk factors for adverse outcomes in *Escherichia coli* bloodstream infections: a prospective molecular epidemiological study. *The Journal of antimicrobial chemotherapy*, 77(6), 1753–1761.

Jauréguy, F., Carbonnelle, E., Bonacorsi, S., Clec'h, C., Casassus, P., Bingen, E., et al. (2007). Host and bacterial determinants of initial severity and outcome of *Escherichia coli* sepsis. *Clinical microbiology and infection : the official publication of the European Society of Clinical Microbiology and Infectious Diseases*, 13(9), 854–862.

Jaureguy, F., Landraud, L., Passet, V., Diancourt, L., Frapy, E., Guigon, G., et al. (2008). Phylogenetic and genomic diversity of human bacteremic *Escherichia coli* strains. *BMC genomics*, 9, 560.

Jia, P., Jia, X., Zhu, Y., Liu, X., Yu, W., Li, R., et al. (2022). Emergence of a Novel NDM-5-Producing Sequence Type 4523 *Klebsiella pneumoniae* Strain Causing Bloodstream Infection in China. *Microbiology spectrum*, 10(5), e0084222.

Johansson, M. H. K., Bortolaia, V., Tansirichaiya, S., Aarestrup, F. M., Roberts, A. P., & Petersen, T. N. (2021). Detection of mobile genetic elements associated with antibiotic resistance in *Salmonella enterica* using a newly developed web tool: MobileElementFinder. *The Journal of antimicrobial chemotherapy*, 76(1), 101–109.

Johnson, J. (2017). Definitions of complicated urinary tract infection and pyelonephritis. *Clinical Infectious Diseases*, 64(3), 390

Johnson, J. R., & Stell, A. L. (2000). Extended virulence genotypes of *Escherichia coli* strains from patients with urosepsis in relation to phylogeny and host compromise. *The Journal of infectious diseases*, 181(1), 261–272.

Johnson, J. R., Johnston, B., Clabots, C. R., Kuskowski, M. A., Roberts, E., & DebRoy, C. (2008). Virulence genotypes and phylogenetic background of *Escherichia coli* serogroup O6 isolates from humans, dogs, and cats. *Journal of clinical microbiology*, 46(2), 417–422.

- Jolley, K. A., Hill, D. M., Bratcher, H. B., Harrison, O. B., Feavers, I. M., Parkhill, J. et al. (2012). Resolution of a meningococcal disease outbreak from whole-genome sequence data with rapid Web-based analysis methods. *Journal of clinical microbiology*, 50(9), 3046–3053.
- Joseph, A., Cointe, A., Mariani Kurkdjian, P., Rafat, C., & Hertig, A. (2020). Shiga Toxin-Associated Hemolytic Uremic Syndrome: A Narrative Review. *Toxins*, 12(2), 67.
- Kadri, S. S., Lai, Y. L., Warner, S., Strich, J. R., Babiker, A., Ricotta, E. E., Demirkale, C. Y. et al. (2021). Inappropriate empirical antibiotic therapy for bloodstream infections based on discordant in-vitro susceptibilities: a retrospective cohort analysis of prevalence, predictors, and mortality risk in US hospitals. *The Lancet. Infectious diseases*, 21(2), 241–251.
- Källman, O., Motakefi, A., Wretling, B., Kalin, M., Olsson-Liljequist B. & Giske, CG. (2008). Cefuroxime non-susceptibility in multidrug-resistant *Klebsiella pneumoniae* overexpressing *ramA* and *acrA* and expressing *ompK35* at reduced levels. *Journal of Antimicrobial Chemotherapy*, 62(5), 986-990.
- Källman, O., Giske, CG., Samuelsen, O., Wretling B., Kalin, M. & Olsson-Liljequist, B. (2009). Interplay of efflux, impermeability, and AmpC activity contributes to cefuroxime resistance in clinical, non-ESBL-producing isolates of *Escherichia coli*. *Microbial Drug resistance*, 15(2), 91-95.
- Kallonen, T., Brodrick, H. J., Harris, S. R., Corander, J., Brown, N. M., Martin, V., et al. (2017). Systematic longitudinal survey of invasive *Escherichia coli* in England demonstrates a stable population structure only transiently disturbed by the emergence of ST131. *Genome research*, 27(8), 1437–1449.
- Kalra, O. & Raizada, A. (2009). Approach to a patient with urosepsis. *Journal of Global Infectious Diseases*, 1(1), 57-63.
- Kaper, J.B., Nataro, J.P. & Mobley, H.L. (2004). Pathogenic escherichia coli. *Nature Reviews Microbiology*, 2(2), 123–140
- Kaprou, G. D., Bergšpica, I., Alexa, E. A., Alvarez-Ordóñez, A., & Prieto, M. (2021). Rapid Methods for Antimicrobial Resistance Diagnostics. *Antibiotics (Basel, Switzerland)*, 10(2), 209.
- Kariuki, K., Diakhate, M. M., Musembi, S., Tornberg-Belanger, S. N., Rwigy, D., Mutuma, T., et al. (2023). Plasmid-mediated quinolone resistance genes detected in Ciprofloxacin non-susceptible *Escherichia coli* and *Klebsiella* isolated from children under five years at hospital discharge, Kenya. *BMC microbiology*, 23(1), 129.
- Karlsson, S., Varpula, M., Ruokonen, E., Pettilä, V., Parviainen, I., Ala-Kokko, T. I., et al. (2007). Incidence, treatment, and outcome of severe sepsis in ICU-treated adults in Finland: the Finnsepsis study. *Intensive care medicine*, 33(3), 435–443
- Khalifa, S. M., Abd El-Aziz, A. M., Hassan, R., & Abdelmegeed, E. S. (2021). β -lactam resistance associated with β -lactamase production and porin alteration in clinical isolates of *E. coli* and *K. pneumoniae*. *PloS one*, 16(5), e0251594.
- Kim, B., Kim, J. H., & Lee, Y. (2022). Virulence Factors Associated With *Escherichia coli* Bacteremia and Urinary Tract Infection. *Annals of laboratory medicine*, 42(2), 203–212.

Kim, D., Park, B. Y., Choi, M. H., Yoon, E. J., Lee, H., Lee, K. J., et al. (2019). Antimicrobial resistance and virulence factors of *Klebsiella pneumoniae* affecting 30 day mortality in patients with bloodstream infection. *The Journal of antimicrobial chemotherapy*, 74(1), 190–199.

Kim, J. S., Hong, C. K., Park, S. H., Jin, Y. H., Han, S., Kim, H. S., et al. (2020). Emergence of NDM-4 and OXA-181 carbapenemase-producing *Klebsiella pneumoniae*. *Journal of global antimicrobial resistance*, 20, 332–333.

Kim, B., Kim, J., Jo, H. U., Kwon, K. T., Ryu, S. Y., Wie, S. H., et al. (2022). Changes in the characteristics of community-onset fluoroquinolone-resistant *Escherichia coli* isolates causing community-acquired acute pyelonephritis in South Korea. *Journal of microbiology, immunology, and infection = Wei mian yu gan ran za zhi*, 55(4), 678–685.

Kim, J. S., Yu, J. K., Jeon, S. J., Park, S. H., Han, S., Park, S. H., et al. (2021). Dissemination of an international high-risk clone of *Escherichia coli* ST410 co-producing NDM-5 and OXA-181 carbapenemases in Seoul, Republic of Korea. *International journal of antimicrobial agents*, 58(6), 106448.

Kitchel, B., Rasheed, J. K., Patel, J. B., Srinivasan, A., Navon-Venezia, S., Carmeli, Y., et al. (2009). Molecular epidemiology of KPC-producing *Klebsiella pneumoniae* isolates in the United States: clonal expansion of multilocus sequence type 258. *Antimicrobial agents and chemotherapy*, 53(8), 3365–3370.

Kirtikliene, T., Mierauskaitė, A., Razmienė, I., & Kuisiene, N. (2022). Genetic Characterization of Multidrug-Resistant *E. coli* Isolates from Bloodstream Infections in Lithuania. *Microorganisms*, 10(2), 449.

Kito, Y., Kuwabara, K., Ono, K., Kato, K., Yokoi, T., Horiguchi, K., Kato, K., Hirose, M., Ohara, T., Goto, K., Nakamura, Y., Koike, Y., & Horiguchi, T. (2022). Seasonal variation in the prevalence of Gram-negative bacilli in sputum and urine specimens from outpatients and inpatients. *Fujita medical journal*, 8(2), 46–51.

Koga, V. L., Tomazetto, G., Cyويا, P. S., Neves, M. S., Vidotto, M. C., Nakazato, G., et al. (2014). Molecular screening of virulence genes in extraintestinal pathogenic *Escherichia coli* isolated from human blood culture in Brazil. *BioMed research international*, 2014, 465054.

Kolmogorov, M., Yuan, J., Lin, Y., & Pevzner, P. A. (2019). Assembly of long, error-prone reads using repeat graphs. *Nature biotechnology*, 37(5), 540–546.

Kutob, L., Justo, J., Bookstaver, P., Kohn, J., Albrecht, H. & Al-Hasan, M. (2016). Effectiveness of oral antibiotics for definitive therapy of Gram-negative bloodstream infections. *International Journal of Antimicrobial Agents*, 48(5), 498-503.

Lam, M. M. C., Wick, R. R., Watts, S. C., Cerdeira, L. T., Wyres, K. L., & Holt, K. E. (2021). A genomic surveillance framework and genotyping tool for *Klebsiella pneumoniae* and its related species complex. *Nature communications*, 12(1), 4188.

Langford, B. J., Brown, K. A., Diong, C., Marchand-Austin, A., Adomako, K., Saedi, A., et al. (2021). The Benefits and Harms of Antibiotic Prophylaxis for Urinary Tract Infection in Older Adults. *Clinical infectious diseases : an official publication of the Infectious Diseases Society of America*, 73(3), e782–e791.

- Lanz, R., Kuhnert, P., & Boerlin, P. (2003). Antimicrobial resistance and resistance gene determinants in clinical *Escherichia coli* from different animal species in Switzerland. *Veterinary microbiology*, 91(1), 73–84.
- Lark, L., Saint, S., Chenoweth, C., Zemencuk, K., Lipsky, A. & Plorde, J. (2001). Four-year perspective evaluation of community-acquired bacteremia: epidemiology, microbiology and patient outcome. *Diagnostic Microbiology and Infectious Disease*, 41(1-2), 15-22.
- Laupland, K. (2013). Incidence of bloodstream infection: a review of population-based studies. *Clinical Microbiology and Infection*, 19(6), 492-500.
- Laupland, K. & Church, D. (2014). Population-Based Epidemiology and Microbiology of Community-Onset Bloodstream Infections. *Clinical Microbiology Reviews*, 27(4), 647-664.
- Lazareva, I. V., Ageevets, V. A., Ershova, T. A., Zueva, L. P., Goncharov, A. E., Darina, M. G., et al. (2016). Prevalence and Antibiotic Resistance of Carbapenemase-Producing Gram-Negative Bacteria in Saint Petersburg and Some Other Regions of the Russian Federation. *Antibiotiki i khimioterapiia = Antibiotics and chemotherapy [sic]*, 61(11-12), 28–38.
- Lean, K., Nawaz, R. F., Jawad, S., & Vincent, C. (2019). Reducing urinary tract infections in care homes by improving hydration. *BMJ open quality*, 8(3), e000563.
- Lee, C., Lee, C., Hong, M., Tong, H. & Ko, W. (2017). Timing of appropriate empirical antimicrobial administration and outcome of adults with community-onset bacteremia. *Critical Care*, 21(1), 119.
- Lefort, A. et al. (2011) 'Host factors and portal of entry outweigh bacterial determinants to predict the severity of escherichia coli bacteremia', *Journal of Clinical Microbiology*, 49(3), pp. 777–783. doi:10.1128/jcm.01902-10.
- Leshner, G. Y., Froelich, E. J., Gruett, M. D., Baily, J. H., & Brundage, R. P. (1962). 1,8-Naphthyridine derivatives. A new class of chemotherapeutic agents. *Journal of medicinal and pharmaceutical chemistry*, 5, 1063–1065.
- Letunic, I., & Bork, P. (2021). Interactive Tree Of Life (iTOL) v5: an online tool for phylogenetic tree display and annotation. *Nucleic acids research*, 49(W1), W293–W296.
- Levy, M., Artigas, A., Philips, G., Rhodes, A., Beale, R., Osborn, T. et al. (2012). Outcomes of the surviving sepsis campaign in intensive care units in USA and Europe: a prospective cohort study. *The Lancet Infectious Disease*, 12(12), 919-924.
- Li H, Durbin R. 2009. Fast and accurate short read alignment with Burrows-Wheeler transform. *Bioinformatics*,25:1754-1760.
- Li H, Handsaker B, Wysoker A, Fennell T, Ruan J, Homer N, Marth G, Abecasis G, Durbin R. 2009. The sequence alignment/Map format and SAMtools. *Bioinformatics*. 25:2978-2079
- Li, L., & Huang, H. (2017). Risk factors of mortality in bloodstream infections caused by *Klebsiella pneumoniae*: A single-center retrospective study in China. *Medicine*, 96(35), e7924.
- Li, X. Z., Plésiat, P., & Nikaido, H. (2015). The challenge of efflux-mediated antibiotic resistance in Gram-negative bacteria. *Clinical microbiology reviews*, 28(2), 337–418.

- Lim, J. Y., Yoon, J., & Hovde, C. J. (2010). A brief overview of *Escherichia coli* O157:H7 and its plasmid O157. *Journal of microbiology and biotechnology*, 20(1), 5–14.
- Lin, W., Huang, Y., Wang, J., Chen, Y. & Chang, S. (2019). Prevalence of and risk factor for community-onset third generation cephalosporin resistant *Escherichia coli* bacteremia at a medical center in Taiwan. *BMC Infectious Diseases*, 19(245), 1-11.
- Lin, Y. L., Sewunet, T., Kk, S., Giske, C. G., & Westerlund, F. (2020). Optical maps of plasmids as a proxy for clonal spread of MDR bacteria: a case study of an outbreak in a rural Ethiopian hospital. *The Journal of antimicrobial chemotherapy*, 75(10), 2804–2811.
- Lister, P., Wolter, D. & Hanson, N. (2009). Antibacterial-Resistant *Pseudomonas aeruginosa*: Clinical Impact an Complex Regulation of Chromosomally Encoded Resistance Mechanisms. *Clinical Microbiology Reviews*, 22(4), 582-610.
- Livermore, D., Hope, R., Reynolds, R., Blackburn, R., Johnson, A. & Woodford, N. (2013). Declining cephalosporin and fluoroquinolone non-susceptibility among bloodstream Enterobacteriaceae from the UK: links to prescribing change? *Journal of Antimicrobial Chemotherapy*, 68(11), 2667-2674
- Loman, J., Quick, J., Simpson, T. (2015). A complete bacterial genome assembled de novo using only nanopore sequencing data. *Nature methods*, 12(8), 733-735.
- Long, S. W., Linson, S. E., Ojeda Saavedra, M., Cantu, C., Davis, J. J., Brettin, T., et al. (2017). Whole-Genome Sequencing of Human Clinical *Klebsiella pneumoniae* Isolates Reveals Misidentification and Misunderstandings of *Klebsiella pneumoniae*, *Klebsiella variicola*, and *Klebsiella quasipneumoniae*. *mSphere*, 2(4), e00290-17.
- Lozer, D. M., Souza, T. B., Monfardini, M. V., Vicentini, F., Kitagawa, S. S., Scaletsky, I. C., & Spano, L. C. (2013). Genotypic and phenotypic analysis of diarrheagenic *Escherichia coli* strains isolated from Brazilian children living in low socioeconomic level communities. *BMC infectious diseases*, 13, 418.
- Mahamat, O., Lounnas, M., Hide, M., Tidjani, A., Benavides, J., Diack, A., et al. (2019). Spread of NDM-5 and OXA-181 Carbapenemase-Producing *Escherichia coli* in Chad. *Antimicrobial agents and chemotherapy*, 63(11), e00646-19.
- Mahfouz, N., Ferreira, I., Beisken, S., von Haeseler, A., & Posch, A. E. (2020). Large-scale assessment of antimicrobial resistance marker databases for genetic phenotype prediction: a systematic review. *The Journal of antimicrobial chemotherapy*, 75(11), 3099–3108.
- Mahjoub-Messai, F., Bidet, P., Caro, V., Diancourt, L., Biran, V., Aujard, Y., et al. (2011). *Escherichia coli* isolates causing bacteremia via gut translocation and urinary tract infection in young infants exhibit different virulence genotypes. *The Journal of infectious diseases*, 203(12), 1844–1849.
- Maiden M. C. (2006). Multilocus sequence typing of bacteria. *Annual review of microbiology*, 60, 561–588.
- Maiden, M. C., Bygraves, J. A., Feil, E., Morelli, G., Russell, J. E., Urwin, R., Zhang, Q., Zhou, J., Zurth, K., Caugant, D. A., Feavers, I. M., Achtman, M., & Spratt, B. G. (1998). Multilocus sequence typing: a portable approach to the identification of clones within populations of pathogenic microorganisms. *Proceedings of the National Academy of Sciences of the United States of America*, 95(6), 3140–3145.

- Maiden, M. C., Jansen van Rensburg, M. J., Bray, J. E., Earle, S. G., Ford, S. A., Jolley, K. A., & McCarthy, N. D. (2013). MLST revisited: the gene-by-gene approach to bacterial genomics. *Nature reviews. Microbiology*, 11(10), 728–736.
- Mairi, A., Pantel, A., Sotto, A., Lavigne, J. P., & Touati, A. (2018). OXA-48-like carbapenemases producing Enterobacteriaceae in different niches. *European journal of clinical microbiology & infectious diseases : official publication of the European Society of Clinical Microbiology*, 37(4), 587–604.
- Mammeri, H., Poirel, L., & Nordmann, P. (2003). In vivo selection of a chromosomally encoded beta-lactamase variant conferring ceftazidime resistance in *Klebsiella oxytoca*. *Antimicrobial agents and chemotherapy*, 47(12), 3739–3742.
- Manges, A. R., Geum, H. M., Guo, A., Edens, T. J., Fibke, C. D., & Pitout, J. D. D. (2019). Global Extraintestinal Pathogenic *Escherichia coli* (ExPEC) Lineages. *Clinical microbiology reviews*, 32(3), e00135-18.
- Martins, W. M. B. S., Nicolas, M. F., Yu, Y., Li, M., Dantas, P., Sands, K., et al. (2020). Clinical and Molecular Description of a High-Copy IncQ1 KPC-2 Plasmid Harbored by the International ST15 *Klebsiella pneumoniae* Clone. *mSphere*, 5(5), e00756-20.
- Matsui, Y., Hu, Y., Rubin, J., de Assis, R. S., Suh, J., & Riley, L. W. (2020). Multilocus sequence typing of *Escherichia coli* isolates from urinary tract infection patients and from fecal samples of healthy subjects in a college community. *MicrobiologyOpen*, 9(6), 1225–1233.
- Matsumura, Y., Yamamoto, M., Nagao, M., Hotta, G., Matsushima, A., Ito, Y., Takakura, S., Ichiyama, S., & Kyoto-Shiga Clinical Microbiology Study Group (2012). Emergence and spread of B2-ST131-O25b, B2-ST131-O16 and D-ST405 clonal groups among extended-spectrum- β -lactamase-producing *Escherichia coli* in Japan. *The Journal of antimicrobial chemotherapy*, 67(11), 2612–2620.
- Maurya, N., Jangra, M., Tambat, R., & Nandanwar, H. (2019). Alliance of Efflux Pumps with β -Lactamases in Multidrug-Resistant *Klebsiella pneumoniae* Isolates. *Microbial drug resistance (Larchmont, N.Y.)*, 25(8), 1155–1163.
- Meatherall, B. L., Gregson, D., Ross, T., Pitout, J. D., & Laupland, K. B. (2009). Incidence, risk factors, and outcomes of *Klebsiella pneumoniae* bacteremia. *The American journal of medicine*, 122(9), 866–873.
- Medina, Martha, and Edgardo Castillo-Pino. (2019) "An Introduction to the Epidemiology and Burden of Urinary Tract Infections." *Therapeutic Advances in Urology*, 11., p. 175628721983217.0
- Mercuro, N.J., Stogsdill, P. & Wungwattana, M. (2018). Retrospective analysis comparing oral stepdown therapy for Enterobacteriaceae bloodstream infections: Fluoroquinolones versus β -lactams. *International Journal of Antimicrobial Agents*, 51(5), 687–692.
- Méric, G., Hitchings, M., Pascoe, B & Sheppard, S. (2016). From escherich to the escherichia coli genome. *The Lancet Infectious Diseases*, 16(6),634–636.
- Miajlovic, H., Mac Aogáin, M., Collins, C. J., Rogers, T. R., & Smith, S. G. J. (2016). Characterization of *Escherichia coli* bloodstream isolates associated with mortality. *Journal of medical microbiology*, 65(1), 71–79.

- Micenková, L., Beňová, A., Frankovičová, L., Bosák, J., Vrba, M., Ševčíková, A., et al. (2017). Human *Escherichia coli* isolates from hemocultures: Septicemia linked to urogenital tract infections is caused by isolates harboring more virulence genes than bacteraemia linked to other conditions. *International journal of medical microbiology : IJMM*, 307(3), 182–189.
- Minino, M., Murphy, L., Xu, J. & Kochanek, D. (2011). Deaths: final data for 2008. *National Vital Statistics Report*, 59(10), 1-126.
- Moon H. W. (1978). Mechanisms in the pathogenesis of diarrhea: a review. *Journal of the American Veterinary Medical Association*, 172(4), 443–448.
- Mohapatra, S., Ghosh, D., Vivekanandan, P., Chunchanur, S., Venugopal, S., Tak, V., et al. (2023). Genome profiling of uropathogenic *E. coli* from strictly defined community-acquired UTI in paediatric patients: a multicentric study. *Antimicrobial resistance and infection control*, 12(1), 36.
- Monk, J. (2018). Predicting Antimicrobial Resistance and Associated Genomic Features from Whole Genome Sequencing. *Journal of Clinical Microbiology*, 57(2), 1610-1618.
- Mora-Rillo, M., Fernández-Romero, N., Navarro-San Francisco, C., Díez-Sebastián, J., Romero-Gómez, M., Fernández, F. et al. (2015). Impact of virulence genes on sepsis severity and survival in *Escherichia coli* bacteremia. *Virulence*, 6(1), 93-100
- Moradigaravand, D., Martin, V., Peacock, S. J., & Parkhill, J. (2017). Population structure of multidrug resistant *Klebsiella oxytoca* within hospitals across the UK and Ireland identifies sharing of virulence and resistance genes with *K. pneumoniae*. *Genome biology and evolution*, 9(3), 574–587.
- Morin, N., Santiago, A., Ernst, R., Guillot, S & Nataro, J. (2013). Characterization of the aggr regulon in enteroaggregative *Escherichia coli*. *Infection and Immunity*, 81(1), 122–132.
- Moss, E., Maghini, D. & Bhatt, A. (2020). Complete, closed bacterial genomes from microbiomes using nanopore sequencing. *Nature biotechnology*. 38, 701-707.
- Munnink, B. B., Nieuwenhuijse, D. F., Stein, M., O'Toole, Á., Haverkate, M., Mollers, M., et al. (2020). Rapid SARS-CoV-2 whole-genome sequencing and analysis for informed public health decision-making in the Netherlands. *Nature medicine*, 26(9), 1405–1410.
- Murphy CN, Mortensen MS, Krogfelt KA, Clegg S. Role of *Klebsiella pneumoniae* type 1 and type 3 fimbriae in colonizing silicone tubes implanted into the bladders of mice as a model of catheter-associated urinary tract infections. *Infect Immun*. 2013 Aug;81(8):3009-17.
- Najar MS, Saldanha CL, Banday KA. Approach to urinary tract infections. *Indian J Nephrol*. 2009 Oct;19(4):129-39.
- Nataro, J.P, Yikang, D, YingKang, D. & Walker K. (1994). Aggr, a transcriptional activator of aggregative adherence fimbria I expression in enteroaggregative *Escherichia coli*. *Journal of Bacteriology*, 176(15), 4691–4699.
- National Institute for Health and Care Excellence. (2016). Sepsis: Recognition, Assessment and Early Management. Available from: <https://www.ncbi.nlm.nih.gov/books/NBK385343/> [Accessed 3rd February 2020].

National Institute for Health and Care Excellence. (2018). Urinary tract infection (lower): antimicrobial prescribing NICE guideline [NG109]. Available from <https://www.nice.org.uk/guidance/ng109/chapter/Recommendations> [Accessed 5th February 2020].

Navon-Venezia, S., Kondratyeva, K., & Carattoli, A. (2017). *Klebsiella pneumoniae*: a major worldwide source and shuttle for antibiotic resistance. *FEMS microbiology reviews*, 41(3), 252–275.

Nguyen, M. N., Hoang, H. T. T., Xavier, B. B., Lammens, C., Le, H. T., Hoang, N. T. B., et al. (2021). Prospective One Health genetic surveillance in Vietnam identifies distinct bla_{CTX-M}-harbouring *Escherichia coli* in food-chain and human-derived samples. *Clinical microbiology and infection : the official publication of the European Society of Clinical Microbiology and Infectious Diseases*, 27(10), 1515.e1–1515.e8.

Nicole, E. & ANNU Canada Guidelines Committee. (2005). Complicated urinary tract infections in adults. *The Canadian Journal of Infectious Diseases and Medical Microbiology*, 16(6), 349-360.

Nicolle, L.E. (2014) 'Catheter associated urinary tract infections', *Antimicrobial Resistance and Infection Control*, 3(1).

Nielubowicz, G.R. & Mobley, H.L. (2010). Host–pathogen interactions in urinary tract infection. *Nature Reviews Urology*, 7(8), 430–441.

Nisly, S., McClain, D., Fillius, A. & Davis, K. (2020). Oral antibiotics for the treatment of Gram-negative bloodstream infections: A retrospective comparison of three antibiotic classes. *Journal of Global Antimicrobial Resistance*, 20(1), 74-77.

Nordmann, P., Dortet, L., & Poirel, L. (2012). Carbapenem resistance in Enterobacteriaceae: here is the storm!. *Trends in molecular medicine*, 18(5), 263–272.

Nouws, S., Bogaerts, B., Verhaegen, B., Denayer, S., Crombé, F., De Rauw, K., et al. (2020). The Benefits of Whole Genome Sequencing for Foodborne Outbreak Investigation from the Perspective of a National Reference Laboratory in a Smaller Country. *Foods (Basel, Switzerland)*, 9(8), 1030.

Olesen, B., Hansen, D. S., Nilsson, F., Frimodt-Møller, J., Leihof, R. F., Struve, C. et al. (2013). Prevalence and characteristics of the epidemic multiresistant *Escherichia coli* ST131 clonal group among extended-spectrum beta-lactamase-producing *E. coli* isolates in Copenhagen, Denmark. *Journal of clinical microbiology*, 51(6), 1779–1785.

O'Neill, J. (2016). The Review On Antimicrobial Resistance, from https://amr-review.org/sites/default/files/160518_Final%20paper_with%20cover.pdf [Accessed 6th February 2020]

Partridge, S. R., Kwong, S. M., Firth, N., & Jensen, S. O. (2018). Mobile Genetic Elements Associated with Antimicrobial Resistance. *Clinical microbiology reviews*, 31(4), e00088-17.

Paula de Souza da-Silva, A. P., de Sousa, V. S., de Araújo Longo, L. G., Caldera, S., Baltazar, I. C. L., Bonelli, R. R., Santoro-Lopes, G. et al. (2020). Prevalence of fluoroquinolone-resistant and broad-spectrum cephalosporin-resistant community-acquired urinary tract infections in Rio de Janeiro: Impact of *Escherichia coli* genotypes ST69 and ST131. *Infection, genetics and evolution : journal of molecular epidemiology and evolutionary genetics in infectious diseases*, 85, 104452.

Pammi M., Zhong, D., Johnson, Y., Revell, P. & Versalovic, J. (2014). Polymicrobial bloodstream infections in the neonatal intensive care unit are associated with increased mortality: a case-control study. *BMC Infectious Diseases*, 14(1), 1-8.

Peirano, G., & Pitout, J. D. (2010). Molecular epidemiology of Escherichia coli producing CTX-M beta-lactamases: the worldwide emergence of clone ST131 O25:H4. *International journal of antimicrobial agents*, 35(4), 316–321.

Peirano, G., Sang, J. H., Pitondo-Silva, A., Laupland, K. B., & Pitout, J. D. (2012). Molecular epidemiology of extended-spectrum- β -lactamase-producing Klebsiella pneumoniae over a 10 year period in Calgary, Canada. *The Journal of antimicrobial chemotherapy*, 67(5), 1114–1120.

Peter-Getzlaff, S., Polsfuss, S., Poledica, M., Hombach, M., Giger, J., Böttger, E. C. et al. (2011). Detection of AmpC beta-lactamase in Escherichia coli: comparison of three phenotypic confirmation assays and genetic analysis. *Journal of clinical microbiology*, 49(8), 2924–2932.

Perez, F., Rudin, S. D., Marshall, S. H., Coakley, P., Chen, L., Kreiswirth, B. N., Rather, P. N., Hujer, A. M., Toltzis, P., van Duin, D., Paterson, D. L., & Bonomo, R. A. (2013). OqxAB, a quinolone and olaquinox efflux pump, is widely distributed among multidrug-resistant Klebsiella pneumoniae isolates of human origin. *Antimicrobial agents and chemotherapy*, 57(9), 4602–4603.

Pitout, J. D. D., & Chen, L. (2023). The Significance of Epidemic Plasmids in the Success of Multidrug-Resistant Drug Pandemic Extraintestinal Pathogenic Escherichia coli. *Infectious diseases and therapy*, 12(4), 1029–1041.

Pitout, J. D. D., Peirano, G., Chen, L., DeVinney, R., & Matsumura, Y. (2022). Escherichia coli ST1193: Following in the Footsteps of E. coli ST131. *Antimicrobial agents and chemotherapy*, 66(7), e0051122.

Pitout, J. D. D., Peirano, G., Kock, M. M., Strydom, K. A., & Matsumura, Y. (2019). The Global Ascendancy of OXA-48-Type Carbapenemases. *Clinical microbiology reviews*, 33(1), e00102-19.

Podewils, L. J., Mintz, E. D., Nataro, J. P., & Parashar, U. D. (2004). Acute, infectious diarrhea among children in developing countries. *Seminars in pediatric infectious diseases*, 15(3), 155–168.

Podschun, R., & Ullmann, U. (1998). Klebsiella spp. as nosocomial pathogens: epidemiology, taxonomy, typing methods, and pathogenicity factors. *Clinical microbiology reviews*, 11(4), 589–603.

Poirel, L., Potron, A., & Nordmann, P. (2012). OXA-48-like carbapenemases: the phantom menace. *The Journal of antimicrobial chemotherapy*, 67(7), 1597–1606.

Potron, A., Nordmann, P., Lafeuille, E., Al Maskari, Z., Al Rashdi, F., & Poirel, L. (2011). Characterization of OXA-181, a carbapenem-hydrolyzing class D beta-lactamase from Klebsiella pneumoniae. *Antimicrobial agents and chemotherapy*, 55(10), 4896–4899.

Prestinaci, F., Pezzotti, P., & Pantosti, A. (2015). Antimicrobial resistance: a global multifaceted phenomenon. *Pathogens and global health*, 109(7), 309–318.

Public Health England. (2019). Laboratory Surveillance of *Escherichia coli* bacteraemia in England, Wales and Northern Island: 2018. *Health Protection Report*, 13(37), 1-15

Public Health England. (2020). AMR local indicators. Available from: <https://fingertips.phe.org.uk/profile/amr-local-indicators> [Accessed 12th October 2020].

Pupo, G. M., Lan, R., & Reeves, P. R. (2000). Multiple independent origins of Shigella clones of Escherichia coli and convergent evolution of many of their characteristics. *Proceedings of the National Academy of Sciences of the United States of America*, 97(19), 10567–10572.

Queenan, A. M., & Bush, K. (2007). Carbapenemases: the versatile beta-lactamases. *Clinical microbiology reviews*, 20(3), 440–458.

Quick, J., Loman, N. J., Duraffour, S., Simpson, J. T., Severi, E., Cowley, L., et al. (2016). Real-time, portable genome sequencing for Ebola surveillance. *Nature*, 530(7589), 228–232.

Radha, S., Warriar, A. R., Wilson, A., & Prakash, S. (2023). Use of Ceftazidime-Avibactam in the Treatment of Clinical Syndromes With Limited Treatment Options: A Retrospective Study. *Cureus*, 15(1), e33623.

Reding, C., Satapoomin, N. & Avison, M. Hound: A novel tool for automated mapping of genotype to phenotype in bacterial genomes assembled *de novo*. Available from: <https://www.biorxiv.org/content/10.1101/2023.09.15.557405v1.article-info>. Accessed 20.09.2023

Reid, R. & Samarasinghe, S. (2018). The development and evaluation of a multiplex real-time PCR assay for the detection of ESBL genes in urinary tract infections. *International Journal of Clinical Microbiology*, 1(1), 16-24

Riley L. W. (2014). Pandemic lineages of extraintestinal pathogenic Escherichia coli. *Clinical microbiology and infection : the official publication of the European Society of Clinical Microbiology and Infectious Diseases*, 20(5), 380–390.

Roach, D. J., Sridhar, S., Oliver, E., Rao, S. R., Slater, D. M., Hwang, W., et al. (2023). Clinical and genomic characterization of a cohort of patients with Klebsiella pneumoniae bloodstream infection. *Clinical infectious diseases : an official publication of the Infectious Diseases Society of America*, ciad507.

Robicsek, A., Strahilevitz, J., Jacoby, G. A., Macielag, M., Abbanat, D., Park, C. H., et al. (2006). Fluoroquinolone-modifying enzyme: a new adaptation of a common aminoglycoside acetyltransferase. *Nature medicine*, 12(1), 83–88.

Rodríguez-Medina, N., Barrios-Camacho, H., Duran-Bedolla, J., & Garza-Ramos, U. (2019). *Klebsiella variicola*: an emerging pathogen in humans. *Emerging microbes & infections*, 8(1), 973–988.

Rodríguez, I., Figueiredo, A. S., Sousa, M., Aracil-Gisbert, S., Fernández-de-Bobadilla, M. D., Lanza, V. F., et al. (2021). A 21-Year Survey of Escherichia coli from Bloodstream Infections (BSI) in a Tertiary Hospital Reveals How Community-Hospital Dynamics of B2 Phylogroup Clones Influence Local BSI Rates. *mSphere*, 6(6), e0086821.

Rodríguez-Martínez, J. M., Poirel, L., Nordmann, P., Fankhauser, C., Francois, P., & Schrenzel, J. (2008). Ceftazidime-resistant Klebsiella oxytoca producing an OXY-2-type variant from Switzerland. *International journal of antimicrobial agents*, 32(3), 278–279.

Rodríguez-Martínez, J. M., Machuca, J., Cano, M. E., Calvo, J., Martínez-Martínez, L., & Pascual, A. (2016). Plasmid-mediated quinolone resistance: Two decades on. *Drug resistance updates : reviews and commentaries in antimicrobial and anticancer chemotherapy*, 29, 13–29.

- Rodrigues, C., Lanza, V. F., Peixe, L., Coque, T. M., & Novais, Â. (2023). Phylogenomics of Globally Spread Clonal Groups 14 and 15 of *Klebsiella pneumoniae*. *Microbiology spectrum*, 11(3), e0339522.
- Rooney, P. J., O'Leary, M. C., Loughrey, A. C., McCalmont, M., Smyth, B., Donaghy, P., Badri, M., Woodford, N., Karisik, E., & Livermore, D. M. (2009). Nursing homes as a reservoir of extended-spectrum beta-lactamase (ESBL)-producing ciprofloxacin-resistant *Escherichia coli*. *The Journal of antimicrobial chemotherapy*, 64(3), 635–641.
- Rose, D., Sordillo, P., Gini, S., Cerva, C., Boros, S., Rezza, G., et al. (2015). Microbiologic characteristics and predictors of mortality in bloodstream infections in intensive care unit patients: A 1-year, large, prospective surveillance study in 5 Italian hospitals. *American journal of infection control*, 43(11), 1178–1183.
- Rosen, D. A., Pinkner, J. S., Walker, J. N., Elam, J. S., Jones, J. M., & Hultgren, S. J. (2008). Molecular variations in *Klebsiella pneumoniae* and *Escherichia coli* FimH affect function and pathogenesis in the urinary tract. *Infection and immunity*, 76(7), 3346–3356.
- Rosenblueth, M., Martínez, L., Silva, J., & Martínez-Romero, E. (2004). *Klebsiella variicola*, a novel species with clinical and plant-associated isolates. *Systematic and applied microbiology*, 27(1), 27–35.
- Ruben, L., Dearwater, T. & Norden W. (1995). Clinical infections in the noninstitutionalised geriatric age group: methods utilized and incidence of infections. *American Journal of Epidemiology*, 141(1), 145-157
- Ruiz-Garbajosa, P., Hernández-García, M., Beatobe, L., Tato, M., Méndez, M. I., Grandal, M., et al. (2016). A single-day point-prevalence study of faecal carriers in long-term care hospitals in Madrid (Spain) depicts a complex clonal and polyclonal dissemination of carbapenemase-producing Enterobacteriaceae. *The Journal of antimicrobial chemotherapy*, 71(2), 348–352
- Russo, T., Olson, R., Fang, C., Stoesser, N., Miller, M., MacDonald, U., et al. (2018). Identification of biomarkers for differentiation of hypervirulent *Klebsiella pneumoniae* from classical *K. pneumoniae*. *Journal of Clinical Microbiology*, 56(9), 10-1128.
- Rutherford, K., Parkhill, J., Crook, J., Horsnell, T., Rice, P., Rajandream, M. et al. (2000). Artemis: sequence visualisation and annotation. *Bioinformatics*, 16(1), 944-945.
- Sabih A, Leslie SW. Complicated Urinary Tract Infections. [Updated 2023 Jan 18]. In: StatPearls [Internet]. Treasure Island (FL): StatPearls Publishing; 2023 Jan-. Available from: <https://www.ncbi.nlm.nih.gov/books/NBK436013/>. Accessed 17.01.2022
- Sacco, F., Raponi, G., Oliva, A., Bibbolino, G., Mauro, V., Di Lella, F. M., et al. (2022). An outbreak sustained by ST15 *Klebsiella pneumoniae* carrying 16S rRNA methyltransferases and bla_{NDM}: evaluation of the global dissemination of these resistance determinants. *International journal of antimicrobial agents*, 60(2), 106615.
- Sadouki, Z., Day, M., Doumith, M., Chattaway, M., Dallman, T., Hopkins, K. et al. (2017). Comparison of phenotypic and WGS-derived antimicrobial resistance profiles of *Shigella sonnei* isolates from cases of diarrhoeal disease in England and Wales, 2015. *Journal of Antimicrobial Chemotherapy*, 72(9), 2496-2502.

Saidenberg, A., van Vliet, A. H. M., Stegger, M., Johannesen, T. B., Semmler, T., Cunha, M., et al. (2022). Genomic analysis of the zoonotic ST73 lineage containing avian and human extraintestinal pathogenic *Escherichia coli* (ExPEC). *Veterinary microbiology*, 267, 109372.

Salah, F. D., Soubeiga, S. T., Ouattara, A. K., Sadjji, A. Y., Metuor-Dabire, A., Obiri-Yeboah, et al. (2019). Distribution of quinolone resistance gene (*qnr*) in *ESBL*-producing *Escherichia coli* and *Klebsiella spp.* in Lomé, Togo. *Antimicrobial resistance and infection control*, 8, 104.

Satapoomin, N., Dulyayangkul, P., & Avison, M. B. (2022). *Klebsiella pneumoniae* Mutants Resistant to Ceftazidime-Avibactam Plus Aztreonam, Imipenem-Relebactam, Meropenem-Vaborbactam, and Cefepime-Taniborbactam. *Antimicrobial agents and chemotherapy*, 66(4), e0217921.

Seemann T, *Abriicate*, **GitHub** <https://github.com/tseemann/abriicate>

Seemann T. 2014. Prokka: rapid prokaryotic genome annotation. *Bioinformatics*; 30(14), 2068-9

Seki, M., Gotoh, K., Nakamura, S., Akeda, Y., Yoshii, T., Miyaguchi, S., et al. (2013). Fatal sepsis caused by an unusual *Klebsiella* species that was misidentified by an automated identification system. *Journal of medical microbiology*, 62(Pt 5), 801–803.

Shaidullina, E. R., Schwabe, M., Rohde, T., Shapovalova, V. V., Dyachkova, M. S., Matsvay, A. D., et al. (2023). Genomic analysis of the international high-risk clonal lineage *Klebsiella pneumoniae* sequence type 395. *Genome medicine*, 15(1), 9.

Shankar, C., Veeraraghavan, B., Nabarro, L. E. B., Ravi, R., Ragupathi, N. K. D., & Rupali, P. (2018). Whole genome analysis of hypervirulent *Klebsiella pneumoniae* isolates from community and hospital acquired bloodstream infection. *BMC microbiology*, 18(1), 6.

Shankar, C., Jacob, J. J., Vasudevan, K., Biswas, R., Manesh, A., Sethuvel, D. P. M., et al. (2020). Emergence of Multidrug Resistant Hypervirulent ST23 *Klebsiella pneumoniae*: Multidrug Resistant Plasmid Acquisition Drives Evolution. *Frontiers in cellular and infection microbiology*, 10, 575289.

Shankar, C., Vasudevan, K., Jacob, J. J., Baker, S., Isaac, B. J., Neeravi, A. R., et al. (2022). Hybrid Plasmids Encoding Antimicrobial Resistance and Virulence Traits Among Hypervirulent *Klebsiella pneumoniae* ST2096 in India. *Frontiers in cellular and infection microbiology*, 12, 875116.

Shapiro, J. T., Leboucher, G., Myard-Dury, A. F., Girardo, P., Luzzati, A., Mary, M., et al. (2020). Metapopulation ecology links antibiotic resistance, consumption, and patient transfers in a network of hospital wards. *eLife*, 9, e54795.

Sharma, A., Gupta, V. K., & Pathania, R. (2019). Efflux pump inhibitors for bacterial pathogens: From bench to bedside. *The Indian journal of medical research*, 149(2), 129–145.

Shelburne S., Kim J., Munita, J., Sahasrabhojane, P., Shields, R., Press, E. et al. (2017). WGS accurately predicts antimicrobial resistance in *Escherichia coli*. *Journal of Antimicrobial Chemotherapy*, 70, 2763-2769.

Sherry, N. L., Gorrie, C. L., Kwong, J. C., Higgs, C., Stuart, R. L., Marshall, C., et al. (2022). Multi-site implementation of whole genome sequencing for hospital infection control: A prospective genomic epidemiological analysis. *The Lancet regional health. Western Pacific*, 23, 100446.

Sherry, N. L., Horan, K. A., Ballard, S. A., Gonçalves da Silva, A., Gorrie, C. L., Schultz, M. B., et al. (2023). An ISO-certified genomics workflow for identification and surveillance of antimicrobial resistance. *Nature communications*, 14(1), 60.

Shinu, P., Bareja, R., Nair, A. B., Mishra, V., Hussain, S., Venugopala, K. N., Sreeharsha, N., Attimarad, M., & Rasool, S. T. (2020). Monitoring of Non- β -Lactam Antibiotic Resistance-Associated Genes in ESBL Producing *Enterobacterales* Isolates. *Antibiotics (Basel, Switzerland)*, 9(12), 884.

Sikkema, R. S., Schrama, M., van den Berg, T., Morren, J., Munger, E., Krol, L., van der Beek, J. G., et al. (2020). Detection of West Nile virus in a common whitethroat (*Curruca communis*) and *Culex* mosquitoes in the Netherlands, 2020. *Euro surveillance : bulletin Europeen sur les maladies transmissibles = European communicable disease bulletin*, 25(40), 2001704.

Singh, A., Turner, J. M., Tomberg, J., Fedarovich, A., Unemo, M., Nicholas, R. A. et al.. (2020). Mutations in penicillin-binding protein 2 from cephalosporin-resistant *Neisseria gonorrhoeae* hinder ceftriaxone acylation by restricting protein dynamics. *The Journal of biological chemistry*, 295(21), 7529–7543.

Skjøt-Rasmussen, L., Olsen, S. S., Jakobsen, L., Ejrnaes, K., Scheutz, F., Lundgren, B., Frimodt-Møller, N., & Hammerum, A. M. (2013). Escherichia coli clonal group A causing bacteraemia of urinary tract origin. *Clinical microbiology and infection : the official publication of the European Society of Clinical Microbiology and Infectious Diseases*, 19(7), 656–661.

Smith, M. A., & Bidochka, M. J. (1998). Bacterial fitness and plasmid loss: the importance of culture conditions and plasmid size. *Canadian journal of microbiology*, 44(4), 351–355.

Smith, M., Pouwels, B., Hopkins, S., Naylor, R., Smieszek, T. & Robotham V. (2019). Epidemiology and health-economic burden of urinary-cather-associated infection in English NHS hospitals: a probabilistic modelling study. *Journal of Hospital Infections*, 103(1), 44-54.

Smyth, ET., McIlvenny, G., Enstone, J., Emmerson, AM., Humphreys, H., Fitzpatrick, F. et al. (2008). Four Country healthcare association infection prevalence survey 2006: overview of the results. *Journal of Hospital Infections*, 69(3), 230-248

Sora, V.M., Meroni, G., Martino, P., Soggiu, A., Bonizzi, L. & Zecconi, A. (2021). Extraintestinal pathogenic escherichia coli: Virulence factors and antibiotic resistance. *Pathogens*, 10(11)1355.

Soundararajan, N., Shanmugam, P., Devanbu, C., & Sattar, S. B. (2016). A study on the aac-(6¹)-lb-cr gene prevalence among ciprofloxacin-resistant strains of uropathogenic *Enterobacteriaceae*. *International journal of applied & basic medical research*, 6(4), 258–261.

Stamatakis, A. (2014). RAxML version 8: a tool for phylogenetic analysis and post-analysis of large phylogenies. *Bioinformatics*, 30(9), 1312-1313.

Stapleton, A. E., Wagenlehner, F. M. E., Mulgirigama, A., & Twynholm, M. (2020). Escherichia coli Resistance to Fluoroquinolones in Community-Acquired Uncomplicated Urinary Tract Infection in Women: a Systematic Review. *Antimicrobial agents and chemotherapy*, 64(10), e00862-20.

Stoesser, N., Batty, E. M., Eyre, D. W., Morgan, M., Wyllie, D. H., Del Ojo Elias, C., et al. (2013). Predicting antimicrobial susceptibilities for Escherichia coli and Klebsiella pneumoniae isolates using whole genomic sequence data. *The Journal of antimicrobial chemotherapy*, 68(10), 2234–2244.

Stoesser, N., Sheppard, A. E., Pankhurst, L., De Maio, N., Moore, C. E., Sebra, R., Turner, P., Anson, L. W., Kasarskis, A., Batty, E. M., Kos, V., Wilson, D. J., Phetsouvanh, R., Wyllie, D., Sokurenko, E., Manges, A. R., Johnson, T. J., Price, L. B., Peto, T. E., Johnson, J. R., ... Modernizing Medical Microbiology Informatics Group (MMMIG) (2016). Evolutionary History of the Global Emergence of the Escherichia coli Epidemic Clone ST131. *mBio*, 7(2), e02162.

Subashchandrabose, S., & Mobley, H. L. T. (2015). Virulence and Fitness Determinants of Uropathogenic Escherichia coli. *Microbiology spectrum*, 3(4), 10.1128/microbiolspec.UTI-0015-2012.

Sullivan, M., Petty, N. & Beatson, S. (2011). EasFig: a genome comparison visualiser. *Bioinformatics*, 27(7), 1009-1010

Sun, S., Selmer, M., & Andersson, D. I. (2014). Resistance to β -lactam antibiotics conferred by point mutations in penicillin-binding proteins PBP3, PBP4 and PBP6 in Salmonella enterica. *PLoS one*, 9(5), e97202.

Takatsuka, Y., & Nikaido, H. (2009). Covalently linked trimer of the AcrB multidrug efflux pump provides support for the functional rotating mechanism. *Journal of bacteriology*, 191(6), 1729–1737.

Tang, M., Kong, X., Hao, J., & Liu, J. (2020). Epidemiological Characteristics and Formation Mechanisms of Multidrug-Resistant Hypervirulent *Klebsiella pneumoniae*. *Frontiers in microbiology*, 11, 581543.

Tedwolde, R., Dallman, T., Schaefer, U., Shappard, C., Ashton, P., Pichon, B. et al. (2016). MOST: a modified MLST typing tool based on short read sequencing. *Peer-Reviewed and Open Access*, 4, 2308. DOI:

Treangen, T. J., Ondov, B. D., Koren, S., & Phillippy, A. M. (2014). The Harvest suite for rapid core-genome alignment and visualization of thousands of intraspecific microbial genomes. *Genome biology*, 15(11), 524.

Tseng, C. H., Huang, Y. T., Mao, Y. C., Lai, C. H., Yeh, T. K., et al. (2023). Insight into the Mechanisms of Carbapenem Resistance in *Klebsiella pneumoniae*: A Study on IS26 Integrons, Beta-Lactamases, Porin Modifications, and Plasmidome Analysis. *Antibiotics (Basel, Switzerland)*, 12(4), 749.

Tyson, H., McDermott, F., Li, C., Chen, Y., Tadesse, D., Mukherjee, S. et al. (2015). WGS accurately predicts antimicrobial resistance in *Escherichia coli*. *Journal of Antimicrobial Chemotherapy*, 70(10), 2763-2769.

Ugboko, H. U., Nwinyi, O. C., Oranusi, S. U., & Oyewale, J. O. (2020). Childhood diarrhoeal diseases in developing countries. *Heliyon*, 6(4), e03690.

UKHSA (2021). English surveillance programme for antimicrobial utilisation and resistance (ESPAUR) report. Available from: <https://www.gov.uk/government/publications/english-surveillance-programme-antimicrobial-utilisation-and-resistance-espaur-report> Accessed 18/01/21

Usein, C. R., Papagheorghe, R., Oprea, M., Condei, M., & Străuț, M. (2016). Molecular characterization of bacteremic *Escherichia coli* isolates in Romania. *Folia microbiologica*, 61(3), 221–226.

Valenza, G., Werner, M., Eisenberger, D., Nickel, S., Lehner-Reindl, V., Höller, C., & Bogdan, C. (2019). First report of the new emerging global clone ST1193 among clinical isolates of extended-spectrum β -lactamase (ESBL)-producing *Escherichia coli* from Germany. *Journal of global antimicrobial resistance*, 17, 305–308.

Varani, A., He, S., Siguier, P., Ross, K. & Chandler, M. (2021). The IS6 family, a clinically important group of insertion sequences including IS26. *Mobile DNA* 12(11).

Vélez, J. R., Cameron, M., Rodríguez-Lecompte, J. C., Xia, F., Heider, L. C., Saab, M. et al. (2017). Whole-Genome Sequence Analysis of Antimicrobial Resistance Genes in *Streptococcus uberis* and *Streptococcus dysgalactiae* Isolates from Canadian Dairy Herds. *Frontiers in veterinary science*, 4, 63.

Verschuuren, T., Bosch, T., Mascaro, V., Willems, R., & Kluytmans, J. (2022). External validation of WGS-based antimicrobial susceptibility prediction tools, KOVER-AMR and ResFinder 4.1, for *Escherichia coli* clinical isolates. *Clinical microbiology and infection: the official publication of the European Society of Clinical Microbiology and Infectious Diseases*, 28(11), 1465–1470.

Vieira, A. R., Collignon, P., Aarestrup, F. M., McEwen, S. A., Hendriksen, R. S., Hald, T., & Wegener, H. C. (2011). Association between antimicrobial resistance in *Escherichia coli* isolates from food animals and blood stream isolates from humans in Europe: an ecological study. *Foodborne pathogens and disease*, 8(12), 1295–1301.

Vihta, K. D., Stoesser, N., Llewelyn, M. J., Quan, T. P., Davies, T., Fawcett, N. J., et al. (2018). Trends over time in *Escherichia coli* bloodstream infections, urinary tract infections, and antibiotic susceptibilities in Oxfordshire, UK, 1998-2016: a study of electronic health records. *The Lancet. Infectious diseases*, 18(10), 1138–1149.

Villa, L., Feudi, C., Fortini, D., Brisse, S., Passet, V., Bonura, C., et al. (2017). Diversity, virulence and antimicrobial resistance of the KPC-producing *Klebsiella pneumoniae* ST307 clone. *Microbial Genomics*, 3(4), 110.

Vincent, J. L., Rello, J., Marshall, J., Silva, E., Anzueto, A., Martin, C. D., et al. (2009). International study of the prevalence and outcomes of infection in intensive care units. *JAMA*, 302(21), 2323–2329.

Vincent, J. L., Sakr, Y., Sprung, C. L., Ranieri, V. M., Reinhart, K., Gerlach, H., et al. (2006). Sepsis in European intensive care units: results of the SOAP study. *Critical care medicine*, 34(2), 344–353.

Vracko, R., & Sherris, J. C. (1963). Indole-spot test in bacteriology. *Technical bulletin of the Registry of Medical Technologists. American Society of Clinical Pathologists. Registry of Medical Technologists*, 33, 47–50.

- Wagenlehner, F., Lichtenstern, C., Rolfes, C., Mayer, K., Uhle, F., Weidner, W. et al. (2013). Diagnosis and management for urosepsis. *International Journal of Urology*, 20(10),963-970.
- Walsh T. R. (2005). The emergence and implications of metallo-beta-lactamases in Gram-negative bacteria. *Clinical microbiology and infection : the official publication of the European Society of Clinical Microbiology and Infectious Diseases*, 11 Suppl 6, 2–9.
- Watson, J. T., Jones, R. C., Siston, A. M., Fernandez, J. R., Martin, K., Beck, E., Sokalski, S., Jensen, B. J., Arduino, M. J., Srinivasan, A., & Gerber, S. I. (2005). Outbreak of catheter-associated *Klebsiella oxytoca* and *Enterobacter cloacae* bloodstream infections in an oncology chemotherapy center. *Archives of internal medicine*, 165(22), 2639–2643.
- WHO. (2019). Implementation manual to prevent and control the spread of carbapenem-resistant organisms at the national and health care facility level. Available from: <https://iris.who.int/bitstream/handle/10665/312226/WHO-UHC-SDS-2019.6-eng.pdf?isAllowed=y&sequence=1>. Accessed 25.03.2023.
- Watts., Hancock, V., Ong, C-LY., Vejborg, R., Mabbett, A., Totsika, M., et al. (2010). *Escherichia coli* isolates causing asymptomatic bacteriuria in catheterized and noncatheterized individuals possess similar virulence properties. *Journal of Clinical Microbiology*, 48(7), 2449-2458.
- Wick, R., Schultz, B., Zobel, J. & Holt, E. (2015). Bandage: interactive visualisation of *de novo* genome assemblies. *Bioinformatics*, 31(20), 3350-3352
- Wissel, E., Talbot, B., Toyosato, N., Petit, R., Hertzberg, V., Dunlop, A. et al. (2023). hAMRoaster: a tool for comparing performance of AMR gene detection software. Available from: <https://www.biorxiv.org/content/biorxiv/early/2023/01/30/2022.01.13.476279.full.pdf>. Accessed 12.06.2023
- Wojszel, Z. B., & Toczyńska-Silkiewicz, M. (2018). Urinary tract infections in a geriatric sub-acute ward-health correlates and atypical presentations. *European Geriatric Medicine*, 9(5), 659–667.
- Wu, X., Shi, Q., Shen, S., Huang, C., & Wu, H. (2021). Clinical and Bacterial Characteristics of *Klebsiella pneumoniae* Affecting 30-Day Mortality in Patients With Bloodstream Infection. *Frontiers in cellular and infection microbiology*, 11, 688989.
- Wyres, K. L., & Holt, K. E. (2016). *Klebsiella pneumoniae* Population Genomics and Antimicrobial-Resistant Clones. *Trends in microbiology*, 24(12), 944–956.
- Wyes, K., Lam, M. Holt, K. (2020). Population genomics of *Klebsiella pneumoniae*. *Nature Reviews Microbiology*, 18, 344-259.
- Xia, P., Yi, M., Yuan, Y., Huang, J., Yang, B., Liao, J., et al. (2022). Coexistence of Multidrug Resistance and Virulence in a Single Conjugative Plasmid from a Hypervirulent *Klebsiella pneumoniae* Isolate of Sequence Type 25. *mSphere*, 7(6), e0047722.
- Xiang, T., Chen, C., Wen, J., Liu, Y., Zhang, Q., Cheng, N., Wu, X., & Zhang, W. (2020). Resistance of *klebsiella pneumoniae* strains carrying BLANDM–1 gene and the genetic environment of blandm–1. *Frontiers in Microbiology*, 11(700).

Xavier, D. E., Picão, R. C., Girardello, R., Fehlberg, L. C., & Gales, A. C. (2010). Efflux pumps expression and its association with porin down-regulation and beta-lactamase production among *Pseudomonas aeruginosa* causing bloodstream infections in Brazil. *BMC microbiology*, *10*, 217.

Yamaji, R., Rubin, J., Thys, E., Friedman, C. R., & Riley, L. W. (2018). Persistent Pandemic Lineages of Uropathogenic *Escherichia coli* in a College Community from 1999 to 2017. *Journal of clinical microbiology*, *56*(4), e01834-17.

Yamane, K., Wachino, J., Suzuki, S., & Arakawa, Y. (2008). Plasmid-mediated qepA gene among *Escherichia coli* clinical isolates from Japan. *Antimicrobial agents and chemotherapy*, *52*(4), 1564–1566.

Yang, J., Ye, L., Guo, L., Zhao, Q., Chen, R., Luo, Y., et al. (2013). A nosocomial outbreak of KPC-2-producing *Klebsiella pneumoniae* in a Chinese hospital: dissemination of ST11 and emergence of ST37, ST392 and ST395. *Clinical microbiology and infection : the official publication of the European Society of Clinical Microbiology and Infectious Diseases*, *19*(11), E509–E515.

Yoon, E. J., Choi, M. H., Park, Y. S., Lee, H. S., Kim, D., Lee, H., et al (2018). Impact of host-pathogen-treatment tripartite components on early mortality of patients with *Escherichia coli* bloodstream infection: Prospective observational study. *EBioMedicine*, *35*, 76–86.

York, M. K., Baron, E. J., Clarridge, J. E., Thomson, R. B., & Weinstein, M. P. (2000). Multilaboratory validation of rapid spot tests for identification of *Escherichia coli*. *Journal of clinical microbiology*, *38*(9), 3394–3398.

Yu, W. L., Ko, W. C., Cheng, K. C., Lee, C. C., Lai, C. C., & Chuang, Y. C. (2008). Comparison of prevalence of virulence factors for *Klebsiella pneumoniae* liver abscesses between isolates with capsular K1/K2 and non-K1/K2 serotypes. *Diagnostic microbiology and infectious disease*, *62*(1), 1–6.

Zankari, E., Hasman, H., Cosentino, S., Vestergaard, M., Rasmussen, S., Lund, O., et al. (2012). Identification of acquired antimicrobial resistance genes. *Journal of Antimicrobial Chemotherapy*. *67*, 2640–2644.

Zapun, A., Contreras-Martel, C., & Vernet, T. (2008). Penicillin-binding proteins and beta-lactam resistance. *FEMS microbiology reviews*, *32*(2), 361–385.

Zhang, Y., Kashikar, A., Brown, C. A., Denys, G., & Bush, K. (2017). Unusual *Escherichia coli* PBP 3 Insertion Sequence Identified from a Collection of Carbapenem-Resistant Enterobacteriaceae Tested *In Vitro* with a Combination of Ceftazidime-, Ceftaroline-, or Aztreonam-Avibactam. *Antimicrobial agents and chemotherapy*, *61*(8), e00389-17.

Zhang, F., Li, Z., Liu, X., Luo, G., Wu, Y., Li, C., et al. (2023). Molecular Characteristics of an NDM-4 and OXA-181 Co-Producing K51-ST16 Carbapenem-Resistant *Klebsiella pneumoniae*: Study of Its Potential Dissemination Mediated by Conjugative Plasmids and Insertion Sequences. *Antimicrobial agents and chemotherapy*, *67*(1), e0135422.

Zhao, W. H., & Hu, Z. Q. (2013). Epidemiology and genetics of CTX-M extended-spectrum β -lactamases in Gram-negative bacteria. *Critical reviews in microbiology*, *39*(1), 79–101.